Chemical Classification of Gem Garnets

Deepti Maharaj

29183376

GLY 890 Dissertation

November 2015

Department of Geology

University of Pretoria

© University of Pretoria

ABSTRACT

Gem garnet chemistry is described using the end-members pyrope, almandine, spessartine, andradite, grossular, and uvarovite. The large variation in garnets makes classification difficult. Garnet gemstones are typically classified by means of their refractive indices, together with specific gravity. However, the range of refractive indices for gem garnets can be restrictive and unreliable in gemstone classification. Chemical classification is generally the most accurate means of classification and was used in this thesis by means of a portable XRF for the non-destructive chemical analyses of 1513 garnet gemstones. Colour, refractive index and magnetic susceptibility were also determined. The garnets were divided into two species: ugrandite (uvarovite, grossular and andradite) and pyralspite (pyrope, spessartine and almandine). The chemistry of the pyralspite species was very diverse with a large range in end-member proportions producing extensive solid solutions between end-members. A diverse range in colour, refractive index, and magnetic susceptibility was also observed in the pyralspite species. However, no distinction based on refractive index and magnetic susceptibility could be made in the pyralspite species. Distinctive chemistries were observed in the ugrandite species, which correlates with the magnetic susceptibility and refractive index. Colour was the excepton as no relationship between colour and chemistry was observed. The samples with unusual compositions were reported such as pyrope-andradite, spessartine-grossular, and almandine-grossular. This study concluded that refractive index, magnetic susceptibility and colour should not be used in isolation because this can lead to misinterpretation. Rather, analytical techniques, if available, should be used.

© University of Pretoria

TABLE OF CONTENTS

1. Introduction 1
2. Literature Review 3
2.1. Garnet 3
2.1.1. Garnet production 10
2.2. Gem Classification Schemes 10
2.2.1. Webster 10
2.2.2. Anderson 12
2.2.3. Stockton and Manson 12
2.3. Colour in Gem Garnets 14
2.3.1. Colour in garnets gemstones as a means of classification 14
2.3.2. Colour change 14
2.4. Magnetic Susceptibility 15
2.4.1. Previous uses of magnets in gemology 16
2.4.2. Garnet magnetism 17
2.5. Gem Garnets 17
2.5.1. Uvarovite 17
2.5.2. Almandine 17
2.5.2.1. Localities 18
2.5.2.1.1. Tanzania 18
2.5.2.1.2. America 18
2.5.2.1.3. Canada 18
2.5.2.1.4. Other localities 19
2.5.3. Andradite 19
2.5.3.1. Demantoid 19
2.5.3.1.1. History 20
2.5.3.1.2. Localities 20
2.5.3.1.2.1. Russia 20
2.5.3.1.2.2. Val Malenco, Italy 21
2.5.3.1.2.3. Kerman Province, Iran and Kaghan Valley, Pakistan 22
2.5.3.1.2.4. Erongo Province, Namibia 22
2.5.3.1.2.5. Antetezambato, Madagascar 22
2.5.3.1.2.6. Other localities 23
2.5.3.1.2.7. Comparison of different localities 24
2.5.4. Grossular 25
2.5.4.1. Tsavorite 26
2.5.4.1.1. Localities 27

© University of Pretoria

2.5.4.1.1.1. Kenya 27
2.5.4.1.1.2. Tanzania 27
2.5.4.1.1.3. Madagascar 28
2.5.4.1.1.4. Pakistan 28
2.5.4.1.1.5. East Antarctica 28
2.5.4.1.1.6. Other localities 28
2.5.4.1.2. Tsavorite geochemistry 29
2.5.4.2. Hessonite 29
2.5.4.2.1. Localities 30
2.5.5. Grossular-andradite 30
2.5.5.1. Mali garnet 30
2.5.5.1.1. Localities 30
2.5.6. Pyrope 31
2.5.6.1. History 31
2.5.6.2. Properties 32
2.5.6.3. Localities 32
2.5.6.3.1. Czechoslovakia 32
2.5.6.3.2. Italy 33
2.5.6.3.3. East Africa 33
2.5.6.3.4. Canada 33
2.5.6.3.5. China 33
2.5.6.3.6. America 34
2.5.7. Pyrope-almandine 34
2.5.7.1. Rhodolite 34
2.5.7.1.1. History 34
2.5.7.1.2. Properties 34
2.5.7.1.3. Localities 35
2.5.7.1.3.1. East Africa 35
2.5.7.1.3.2. Canada 35
2.5.7.1.3.3. China 36
2.5.8. Spessartine 36
2.5.8.1. History and Properties 36
2.5.8.2. Occurrence 36
2.5.8.3. Localities 36
2.5.8.3.1. America 36
2.5.8.3.2. China 37
2.5.8.3.3. England 38

© University of Pretoria

2.5.8.3.4. Pakistan 38
2.5.8.3.5. Canada 38
2.5.8.3.6. Africa 38
2.5.9. Pyrope-spessartine 39
2.5.9.1. Malaya garnet 39
2.5.9.1.1. Localities 40
2.5.9.1.1.1. Tanzania and Kenya 40
2.5.9.1.1.2. Bekily, Madagascar 40
2.5.9.2. Colour change garnet 41
2.5.9.2.1. Properties 41
2.5.9.2.2. Localities 42
2.5.9.2.2.1. Tanzania 42
2.5.9.2.2.2. Madagascar 42
2.5.9.2.2.3. Tranoroa, Madagascar 44
2.5.9.3. Conflict 44
3. Methodology 45
3.1. Weighing of Stones 45
3.2. R.I. 45
3.3. Colour 46
3.4. Sample Acquisition 46
3.5. Magnetic Susceptibility 47
3.6. Chemistry 47
3.7. Calculation Sequence 48
4. Results 52
4.1. Classification 52
4.1.1. Classification of the pyralspite species by trade name 55
4.1.1.1. Classification Based on Refractive Index 57
4.1.1.2. Classification based on magnetic susceptibility 58
4.1.1.3. Colour change occurrence 59
4.1.2. Classification of the ugrandite species 60
4.1.2.1. Classification based on refractive index 62
4.1.2.2. Classification based on magnetic susceptibility 63
4.2. Pyralspite Species 64
4.2.1. Chemistry 64
4.2.1.1. Almandine 64
4.2.1.2. Almandine grossular 71
4.2.1.3. Almandine-pyrope 73

© University of Pretoria

4.2.1.4. Almandine-spessartine 73
4.2.1.5. Pyrope 74
4.2.1.6. Pyrope-almandine and rhodolite 77
4.2.1.7. Pyrope-spessartine I and II 78
4.2.1.8. Spessartine 79
4.2.1.9. Spessartine-almandine 79
4.2.1.10. Spessartine-grossular 80
4.2.1.11. Spessartine-pyrope I and II 80
4.2.2. Magnetic susceptibility 81
4.2.3. Refractive index 84
4.2.4. Colour 86
4.2.4.1. Orange and red varieties 86
4.2.4.2. Pink and purple varieties 90
4.2.4.3. Orange pink varieties 96
4.2.4.4. Brown and yellow varieties 99
4.2.4.5. Colour change 101
4.3. Ugrandite Species 109
4.3.1. Chemistry 109
4.3.1.1. Almandine-grossular 109
4.3.1.2. Mali garnet and CC Mali garnet 110
4.3.1.3. Demantoid 117
4.3.1.4. Hessonite 118
4.3.1.5. Spessartine-grossular 118
4.3.1.6. Tsavorite 119
4.3.2. Magnetic susceptibility 122
4.3.3. Refractive Index 123
4.3.4. Colour 123
4.3.4.1. Colour change 123
5. Discussion 124
5.1. Colour 124
5.1.1. Pyralspite 124
5.1.2. Ugrandite 126
5.2. Colour Change 126
5.2.1. Pyralspite 126
5.2.1.1. Colour change chemistry 127
5.2.1.1.1. Pyralspite 127
5.2.1.1.2. Ugrandite 130

© University of Pretoria

5.3. Colour Change Terms 130
5.4. Refractive Index 130
5.4.1. Pyralspite 130
5.4.2. Ugrandite 130
5.5. Magnetic Susceptibility 131
5.5.1. Pyralspite 131
5.5.2. Ugrandite 132
5.6. Use of Magnetic Susceptibly with RI 132
5.7. Chemistry of the Pyralspite and Ugrandite Species 133
5.7.1. Pyralspite 133
5.7.2. Ugrandite 133
5.8. End-member Proportions and Variability 133
5.8.1. Pyralspite 133
5.8.2. Ugrandite 134
5.9. Comparison with the Literature 135
5.9.1. Pyralspite 135
5.9.1.1. Almandine-grossular 135
5.9.1.2. Almandine 140
5.9.1.3. Almandine-pyrope 141
5.9.1.4. Almandine-spessartine 141
5.9.1.5. Pyrope 141
5.9.1.6. Pyrope-almandine and rhodolite 141
5.9.1.7. Spessartine 141
5.9.1.8. Spessartine-almandine 142
5.9.1.9. Spessartine-grossular 142
5.9.1.10. Pyrope-spessartine (I and II) and spessartine-pyrope (I and II) 142
5.9.2. Ugrandite 142
5.9.2.1. Almandine-grossular 143
5.9.2.2. CC Mali and Mali garnets 147
5.9.2.3. Demantoid 147
5.9.2.4. Hessonite 147
5.9.2.5. Spessartine-grossular 148
5.9.2.6. Tsavorite 148
5.9.3. Garnets of similar composition 148
5.10. Classification Schemes 152
5.10.1. Traditional gem classification schemes in gemology 152

© University of Pretoria

5.10.2. Modification of past gem classification schemes 153
5.11. Concluding Remarks on Chemistry 159
5.12. Seperation of the Pyralspite and Ugrandite Species 159
5.13. Terms 159
5.14. Effect on the Price of Gem Garnets 160
6. Conclusions 161
7. Acknowledgements 164
8. References 165
9. Appendix 172
9.1. Magnetic susceptibility 172
9.1.1. Calibration of magnetic pull using $CuSO_4$. $5H_2O$ 174
9.2. Chemistry 177
9.2.1. Recalibration 178
9.2.2. Reproducibility 187
9.2.3. Limitations of the XRF 187

LIST OF FIGURES

Figure 1. A map of the world and the countries producing garnet (Maps of World, 2012). ... 10
Figure 2. Diagram from Webster (1962) with some modification (Grew *et al*., 2013). 11
Figure 3. Malaya garnets from Bekily, Madagascar (Schmetzer *et al*., 2001).. 41
Figure 4. Colour change pyrope-spessartine garnets from Tranoroa (Schmetzer *et al*., 2002) 44
Figure 5. a) and b) Pie graph showing the classification of pyralspite garnets 56
Figure 6. a) and b) Pie charts showing classification of pyralspite garnets based on RI 57
Figure 7. a) and b) Pie chart showing the classification pyralspite garnets based on magnetic susceptibility. 58
Figure 8. Type of colour change of the pyralspite garnets. 59
Figure 9. a) and b) Pie graph showing classification of the ugrandite species. 61
Figure 10. a) and b) Pie graph showing classification of ugrandite garnets based on RI.. ... 62
Figure 11. a) and b) Pie graph showing classification of ugrandite garnets based on magnetic susceptibility.. 63
Figure 12. FeO_{total} vs. MgO concentrations in wt. % of the pyralspite garnets. 65
Figure 13. FeO_{total} (wt. %) vs. MnO (wt. %) of the pyralspite garnets. 66
Figure 14. CaO (wt. %) of the different garnets from the pyralspite species. 66
Figure 15. Cr_2O_3 (wt. %) boxplot for garnet samples from the pyralspite species. 67
Figure 16. V_2O_3 (wt. %) content for the garnet samples from the pyralspite species 67
Figure 17. The almandine and andradite components for the different types of garnets from the pyralspite species 68
Figure 18. The almandine and pyrope components of the garnets from the pyralspite species 69
Figure 19. The spessartine and almandine components of the different garnets from the pyralspite species.. 70

© University of Pretoria

Figure 20. Ternary diagram of the different garnet types from the pyralspite species. 71
Figure 21. The grossular and andradite components of the different garnet types from the pyralspite species. 72
Figure 22. The pyrope and spessartine components of the different types of garnets from the pyralspite species. 75
Figure 23. The MgO vs MnO concentrations in wt. % for the pyralspite species. 76
Figure 24. a) and b) Magnetic volume susceptibility vs. Fe_{total} + Mn (mol. %) of the garnets from the pyralspite species. 82
Figure 25. Boxplot showing RI values of the different types of garnets from the pyralspite species. 84
Figure 26. The RI of the different garnets from the pyralspite species plotted against the pyrope component. 85
Figure 27. The almandine and spessartine components for the orange and red varieties of the pyralspite garnets. 86
Figure 28. The pyrope and spessartine components of the orange and red samples from the pyralspite species. 88
Figure 29. The almandine and pyrope components of the dark red and very dark red samples from the pyralspite species. 89
Figure 30. The almandine and spessartine components of the pink and purple samples from the pyralspite species. 90
Figure 31. The almandine and pyrope components of the pink and purple samples from the pyralspite species. 92
Figure 32. The pyrope and spessartine components of the pink samples from the pyralspite species. 93
Figure 33. The almandine and pyrope components of the purple samples from the pyralspite species. 94
Figure 34. The pyrope and spessartine components of the purple samples from the pyralspite species. 95
Figure 35. The almandine and spessartine components for dark pink and pink orange samples of the pyralspite garnets. 96
Figure 36. The almandine and pyrope components of the pink orange samples together with the pink varieties from the pyralspite species. 98
Figure 37. The pyrope and spessartine components of the pink orange samples from the pyralspite species. 99
Figure 38. The pyrope and spessartine components of the brown and yellow samples from the pyralspite species. 100
Figure 39. The grossular and andradite components of the yellow and gold garnets from the pyralspite species. 101
Figure 40. The different types of colour change and the V_2O_3 (wt. %) and Cr_2O_3 (wt. %) of the pyralspite species. 102
Figure 41. a) and b) Boxplot of Cr_2O_3 content for different types of garnets from the pyralspite species and their colour change. 103
Figure 42. Ternary diagram showing the uvarovite component * 50 for the garnet samples from the pyralspite species based on their type of colour change. 105
Figure 43. Ternary diagram showing the pyrope, almandine and spessartine components of the pyralspite garnets with their type of colour change. 106
Figure 44. The pyrope and spessartine components of the pyralspite garnets together with the type of colour change. 107

© University of Pretoria

Figure 45. The MnO (wt. %) content and the RI values of the pyralspite garnets together with their type of colour change. 108
Figure 46. The FeO_{total} (wt. %) content for the ugrandite species. 109
Figure 47. Ternary diagram of the grossular, andradite and spessartine components for the ugrandite species. 110
Figure 48. The CaO and FeO_{total} contents in wt. % of the garnets from the ugrandite species 111
Figure 49. The TiO_2 (wt. %) content for the ugrandite species. 112
Figure 50. The CaO and MnO contents in wt. % of the garnets from the ugrandite species. 113
Figure 51. The Cr_2O_3 (wt. %) content for the ugrandite garnets. 114
Figure 52. The V_2O_3 (wt. %) content for the ugrandite species. 115
Figure 53. a) and b) Ternary diagram of the grossular, andradite and pyrope components for the ugrandite species. 116
Figure 54. The uvarovite component for the garnets from the ugrandite species. 117
Figure 55. a) and b) The spessartine and grossular components of the ugrandite species. 119
Figure 56. The andradite component for the garnets from the ugrandite species. 121
Figure 57. The magnetic susceptibility and Fe_{total} + Mn (mol. %) content for the garnets from the ugrandite species. 122
Figure 58. The RI values for the garnets from the ugrandite species. 123
Figure 59. A summary of the composition of the different coloured samples in the pyralspite species excluding the red samples. 126
Figure 60. a) and b) The V_2O_3 and MnO contents of the colour change garnets from the thesis and Krzemnicki *et al*. (2001). 128
Figure 61. The almandine and andradite components for the garnets from the pyralspite species in this study compared with those from the gemological literature and the petrological literature. 136
Figure 62. The almandine and pyrope components of the garnets from the pyralspite species in this study compared with those from Georoc (2015) and the gemological and the petrological literature. 137
Figure 63. The pyrope and spessartine components of the garnets from the pyralspite species in this study compared with those from Georoc (2015), the gemological and the petrological literature. 138
Figure 64. The spessartine and almandine components of the garnets from the pyralspite species in this study compared with those from Georoc (2015), the gemological and the petrological literature. 139
Figure 65. Ternary diagram of the different garnet types from the pyralspite species in this study with data from Georoc (2015), the petrological and the gemological literature.. 140
Figure 66. The grossular and andradite components of the samples from the ugrandite species in this study with the data from Georoc (2015), the petrological and the gemological literature. 143
Figure 67. The grossular and pyrope components of the samples from the ugrandite species in this study with the data from Georoc (2015), the petrological and the gemological literature. 144
Figure 68. The grossular and spessartine components of the samples from the ugrandite species in this study with the data from Georoc (2015), the petrological and the gemological literature. 145

© University of Pretoria

Figure 69. a) and b) The grossular, andradite and pyrope components of the ugrandite species in this study with data from Georoc (2015), the petrological literature and the gemological literature. 146
Figure 70. Apparatus used to measure magnetic susceptibly. 173
Figure 71. Copper sulphate calibration curve. 175
Figure 72. Average pull vs. weight of copper sulphate crystals. 177
Figure 73. a), b), c) and d) Graph on which calibration is based. 179
Figure 74. a), b), c), d) and e) Graphs for the various standards after recalibration. 183

LIST OF TABLES

Table 1. A classification of the 32 approved species for garnets. 4

Table 2. List of the 15 naturally occurring and 14 hypothetical end-members from Locock (2008). 6

Table 3. The end-members of garnets and their properties from Anderson (1976). 12

Table 4. Refractive indices and other properties of garnet gemstones from Hanneman (2000). 13

Table 5. The end-member proportions of a rhodolite, spessartine-grossular and Mali garnet are calculated according to Grew *et al*. (2013).. 48

Table 6. The end-member proportions of a rhodolite, spessartine-grossular and Mali garnet are calculated according to Locock (2008). 49

Table 7. The end-member proportions of a rhodolite, spessartine-grossular and Mali garnet are calculated according to Rickwood (1968).. 50

Table 8. Summary of garnet samples and their subdivision. 53

Table 9. The list of terms used in the thesis with the approved mineral names by Grew *et al*. (2013) and gem trade names by Stockton and Manson (1985). 54

Table 10. Summary of the orange and red varieties and their composition from the pyralspite garnets. 87

Table 11. Summary of the purple and pink varieties and their composition for the pyralspite garnets. 91

Table 12. Summary of the orange pink varieties and their composition for the pyralspite garnets. 97

Table 13. Properties of the three ‘pyrope-spessartine’ samples from the pyralspite species with very low RI when compared to the ranges proposed by Stockton and Manson (1985). 130

Table 14. Summary of the different garnet compositions reported in literature presented in this thesis. 149

Table 15. Summary of properties of the ‘pyrope’ samples from the thesis. 150

Table 16. Summary of properties of the ‘spessartine-grossular’ samples from the thesis.. 150

Table 17. Summary of properties of the gemstones reported by Howie (1965) and Lee *et al*. (1963). 151

© University of Pretoria

Table 18. Summary of ‘spessartine-grossular’ samples from petrological literature..... 151

Table 19. Summary of the properties of the ‘almandine-grossular’ and ‘grossular-almandine’ samples reported in petrological literature..... 152

Table 20. The colour of the gem garnets from the thesis compared to those from Stockton and Manson (1985). The words in italics represent colours that were not commonly observed in the samples from the thesis..... 154

Table 21. A modified classification scheme using RI values and colour from Stockton and Manson (1985) and magnetic susceptibility values from Gemstone Magnetism (2014) combined with data from this thesis.. 156

Table 22. Summary of the properties of the different gem garnets with a RI from Stockton and Manson (1985) and magnetic susceptibility from Gemstone Magnetism (2014). 158

Table 23. Repeat measurements of copper sulphate crystals. 176

Table 24. a) and b) Compositions of the manganese and iron ore standards from Europe and Canada. 178

Table 25. The results of the multiple analyses of a garnet gemstone at different points on the sample together with arithmetic mean and standard deviation. 187

© University of Pretoria

1. Introduction

Garnets are one of the oldest known gemstones, having adorned many a neck of royalty in the past. It is still considered a beautiful and highly desired gemstone (Howard, 1933). Traditionally, garnets refer to red gemstones, but in recent times, gem quality garnets have been found to occur in a diverse range of colours from red to orange, to green, to blue, with prices that can exceed that of some sapphires (Anderson, 1976; Webster, 1962; Stockton and Manson, 1985).

Garnet refers to the name for a complex group of minerals that share a common crystal structure and a general chemical-structural formula $\{X_3\}[Y_2](Z_3)\ \varphi_{12}$ where X is Na^{1+}, Mg^{2+}, Ca^{2+}, Mn^{2+}, Fe^{2+} or Y^{3+}, Y is Al^{3+}, V^{3+}, Ti^{3+}, Fe^{3+},Cr^{3+}, Mg, Si^{3+}, Sc^{3+}, Mn^{3+}, Fe^{2+}, Zr or Zn and Z is Si^{4+}, Ti^{4+}, Al^{3+} or Fe^{3+}. φ is O, OH or F (Grew *et al*., 2013; Stockton and Manson, 1985; Locock, 2008; Webster, 1962). Garnets have great chemical variability as the constituent metallic cations possess similar dimensions, charges and chemical affinities, and can substitute for one another, producing extensive solid solutions. Nomenclature problems have arisen due to this chemical variability in the garnet structure (Stockton and Manson, 1985; Anderson, 1976; Grew *et al.*, 2013; Locock, 2008).

The chemical composition of garnets is described by recasting the analysis into the molar proportion of the end-member components (Stockton and Manson, 1985; Rickwood, 1968; Locock, 2008). Grew *et al.* (2013) recognise 32 approved end-member species to describe garnet composition. These are katoite, cryolithionite, yafsoanite, holtstamite, henritiermite, bitikleite, usturite, dzhuluite, elbrusite, kimzeyite, irinarassite, schorlomite, kerimasite, toturite, menzerite-(Y), pyrope, grossular, spessartine, almandine, eringate, goldmanite, momoiite, knorringite, uvarovite, andradite, calderite, majorite, morimotoite, schäferite, palenzonaite, berzeliite and manganerzeliite (Grew *et al*., 2013).

Various methods for the recasting of garnet analyses into molar proportions of end-member components have been put forward to provide simplification and a rapid assessment of complex compositions (Grew *et al*., 2013; Locock, 2008; Rickwood, 1968). The calculation sequence in the recasting is very important as different calculation sequences produce different results (Rickwood, 1968; Locock, 2008). A standard procedure is necessary to recast garnet analyses into the molar proportions of end-member components to ensure consistency. In this thesis, the method of garnet recasting by Locock (2008) and Rickwood (1968) has been tested. The method by Rickwood (1968) is the most commonly used today and the author emphasises the importance of the calculation sequence, which greatly influences the resulting end-members (Rickwood, 1968). Different

© University of Pretoria

calculatio sequences can produce different results for the same garnet analysis (Locock, 2008; Rickwood, 1968).

The different calculation sequences for the recasting of garnet analyses and the inherent problems are discussed in this thesis, however, it was not the objective of this thesis to solve the calculation problems (Grew *et al*., 2013; Locock, 2008; Rickwood, 1968). Nevertheless, the calculation procedures by Grew *et al*. (2013), Locock (2008) and Rickwood (1968) and their problems were highlighted to emphasise the uncertainty surrounding garnet end-member calculation and classification.

In gemmology, pyrope, almandine, spessartine, andradite, grossular and uvarovite are the traditionally recognised end-members. The other nine end-members have been disregarded, as they do not produce gem quality minerals (Hanneman, 2000). Gem garnets with compositions between these six end-members are more common than a pure end-member, resulting in variable compositions and difficulties in garnet classification (Stockton and Manson, 1985; Anderson, 1976; Webster, 1962).

Refractive index (R.I.) and specific gravity (S.G.) are generally used to classify gem garnets because these are the easiest characteristics to measure. However, the R.I. and S.G. are too general a means, as the characteristics of the different garnets tend to overlap. Colour, in conjunction with R.I. and S.G., is also used to identify gem garnets, although this method is unreliable as garnets of similar colour can have different compositions (Stockton and Manson, 1985; Serov *et al*., 2011). Hoover and Williams (2007) have developed a new method of classification using the magnetic susceptibility of garnets and this was considered an important characteristic to measure when classifying garnet gems in this thesis.

Further complications in classification have arisen due to the lack of consensus between different gemstone societies on the use of garnet trade names as well as the lack of a universal rule being applicable in the classification of garnets. The repeated use of different trade names for garnet gems that are based on colour and source (not on chemistry) further complicates the matter (Stockton and Manson, 1985; Anderson, 1976; Webster, 1962; Hanneman, 2000). The rhodolite garnet, for example, was named due to its ‘delicate rose-like color’ by Hidden and Pratt (1898) and not according to its chemistry or other scientific means. One may then wonder whether the gemstones being sold to the public are actually what they are paying for. In addition, the lack of distinction between colour change and colour shift, and the absence of a definable meaning of the two terms has also added to the confusion of garnet gemstone classification, especially when referring to the colour change garnets.

© University of Pretoria

Traditional gem garnet classification schemes are available (Webster, 1962; Anderson, 1976; Stockton and Manson, 1985) and are discussed further in this thesis. However, these classification schemes have proven to be outdated and inadequate when dealing with newly discovered gem garnets (Seifert and Hyrsl, 1999; Dirlam *et al*., 1992; Crowningshield, 1970; Shigley *et al*., 2000; Schmetzer *et al*., 2001). This prompts the need for an updated classification scheme that includes recently discovered gem garnets and is based on quantifiable criteria (i.e. chemistry).

Chemical analysis is the preferred means of classification, but it is not readily available. Chemical analysis is expensive and may involve the destruction of samples (Stockton and Manson, 1985).

The aim of this thesis was to classify gem garnets using the non-destructive chemical analyses of a large number of gem garnets. The objective of this study was to describe the chemistry and chemical variability of garnet gemstones; to check for consistency and accuracy in the classification of gem garnets; to evaluate past chemical classification schemes for garnet gemstones in the literature (including those gem garnets that have recently been discovered); to compare past gemological and petrological literature data with the data from this thesis; and to examine the influence of chemistry on the colour of a gem garnet. The Niton Model FXL from Thermo Scientific provided a quick and non-destructive analysis of garnet gemstones and was used in this thesis to provide the chemical data for classification.

2. Literature Review

2.1. Garnet

The general image of a garnet is typically red in colour, for example, most of the famous Bohemian garnets used in Victorian jewellery. The word ‘garnet’ is derived from the Latin word ‘granatus’ meaning a pomegranate. Garnet is a popular stone appearing in a diverse range of colours from red to orange to green with prices that can exceed that of sapphires (Anderson, 1976; Webster, 1962).

Garnet refers to the name for a complex group of minerals that share a common crystal structure (rhombic dodecahedra, icositetrahedra or a combination of the two) and a general chemical-structural formula $\{X_3\}[Y_2](Z_3)\ \varphi_{12}$ where X is a divalent metal (Na^{1+}, Mg^{2+}, Ca^{2+}, Mn^{2+}, Fe^{2+} or Y^{3+}) bonded to eight oxygen atoms in a dodecahedral formation, Y is a trivalent metal, (Al^{3+}, V^{3+}, Ti^{3+}, Fe^{3+},Cr^{3+}, Mg, Si^{3+}, Sc, Mn^{3+}, Fe^{2+}, Zr or Zn) bonded to six atoms in an octahedral formation, and Z (Si^{4+} , Ti^{4+}, Al^{3+} or Fe^{3+}) is bonded to four atoms (O,

© University of Pretoria

OH or F) in a tetrahedral formation (Grew *et al*., 2013; Deer *et al*., 1982; Locock, 2008; Webster, 1962). When only one type of ion occupies each site, this is referred to as an end-member of the garnet mineral group. The molar proportion of these end-members is used to describe the composition of garnets (Rickwood, 1968; Locock, 2008).

Grew *et al*. (2013) refer to the garnet supergroup, which includes several chemical classes; this is shown in Table 1**.**

Table 1. A classification of the 32 approved species for garnets. Those given in capitals are group names (Grew *et al*., 2013).

Z charge	Group	Class	X	Y	Z	φ
0	Katoite	Hydroxide	Ca_3	Al_2	□	$(OH)_{12}$
3	Cryolitionite	Halide	Na_3	Al_2	Li_3	F_{12}
6	Yafsoanite	Oxide	Ca_3	Te_2^{6+}	Zn_3	O_{12}
8	HENRITERMIERITE	Silicate				
	Holtstamite		Ca_3	Al_2	$Si_2 \mid □ O_8$	$(OH)_4$
	Henritemiertie		Ca_3	Mn_2^{3+}	$Si_2 \mid □O_8$	$(OH)_4$
9	BITIKLEITE	Oxide				
	Bitikleite		Ca_3	$Sb^{5+}Sn^{4+}$	Al_3	O_{12}
	Usturite		Ca_3	$Sb^{5+}Zr$	Fe_3^{3+}	O_{12}
	Dzhuluite		Ca_3	$Sb^{5+}Sn^{4+}$	Fe_3^{3+}	O_{12}
	Elbrusite		Ca_3	$U_{0.5}^{6+}Zr_{1.5}$	Fe_3^{3+}	O_{12}
10	SCHORLOMITE	Silicate				
	Kimzeyite		Ca_3	Zr_2	$SiAl_2$	O_{12}
	Irinarassite		Ca_3	Sn_2^{4+}	$SiAl_2$	O_{12}
	Schorlomite		Ca_3	Ti_2	$SiFe_2^{3+}$	O_{12}
	Kerimasite		Ca_3	Zr_2	$SiFe_2^{3+}$	O_{12}
	Toturite		Ca_3	Sn_2^{4+}	$SiFe_23+$	O_{12}
12	GARNET	Silicate				
	Menzerite-(Y)		Y_2Ca	Mg_2	Si_3	O_{12}

© University of Pretoria

	Pyrope		Mg_3	Al_2	Si_3	O_{12}
	Grossular		Ca_3	Al_2	Si_3	O_{12}
	Spessartine		Mn_32+	Al_2	Si_3	O_{12}
	Almandine		Fe_32+	Al_2	Si_3	O_{12}
	Eringaite		Ca_3	Sc_2	Si_3	O_{12}
	Goldmanite		Ca_3	V_2^{3+}	Si_3	O_{12}
	Momoiite		Mn_32+	V_2^{3+}	Si_3	O_{12}
	Knorringite		Mg_3	Cr_2^{3+}	Si_3	O_{12}
	Uvarovite		Ca_3	C_2^{3+}	Si_3	O_{12}
	Andradite		Ca_3	Fe_2^{3+}	Si_3	O_{12}
	Calderite		Mn_32+	Fe_2^{3+}	Si_3	O_{12}
	Majorite		Mg_3	SiMg	Si_3	O_{12}
	Morimotoite		Ca_3	$TiFe^{2+}$	Si_3	O_{12}
15	BERZELIITE	Vanadate, arsenate				
	Schäferite		Ca_2Na	Mg_2	V_3^{5+}	O_{12}
	Palenzonaite		Ca_2Na	Mn_2^{2+}	V_3^{5+}	O_{12}
	Berzeliite		Ca_2Na	Mg_2	As_3^{5+}	O_{12}
	Manganberzeliite		Ca_2Na	Mn_2^{2+}	As_3^{5+}	O_{12}

Locock (2008) recognises 15 end-member mineral species for garnet with another 14 end-members being hypothetical (Table 2). Hypothetical end-members are “those end-members that have not been shown to form individually a majority of any natural garnet specimen” and hence, are not regarded as a mineral species (Locock, 2008; p. 1769). The end-members are summarised in the Table 2 below.

© University of Pretoria

Table 2. List of the 15 naturally occurring and 14 hypothetical end-members from Locock (2008).

Naturally occurring end-members				
End-members	**Dodecahedral**	**Octahedral**	**Tetrahedral**	**Anion**
Henritermierite	Ca_3	Mn^{3+}_2	$Si_2(H_4)$	O_{12}
Katoite	Ca_3	Al_2	$(H_4)_3$	O_{12}
Kimzeyite	Ca_3	Zr_2	$SiAl_2$	O_{12}
Schorlomite	Ca_3	Ti_2	$SiFe^{3+}_2$	O_{12}
Morimotoite	Ca_3	$TiFe^{2+}$	Si_3	O_{12}
Majorite	Mg_3	MgSi	Si_3	O_{12}
Goldmanite	Ca_3	V_2	Si_3	O_{12}
Uvarovite	Ca_3	Cr_2	Si_3	O_{12}
Knorringite	Mg_3	Cr_2	Si_3	O_{12}
Spessartine	Mn^{2+}_3	Al_2	Si_3	O_{12}
Pyrope	Mg_3	Al_2	Si_3	O_{12}
Almandine	Fe^{2+}_3	Al_2	Si_3	O_{12}
Grossular	Ca_3	Al_2	Si_3	O_{12}
Andradite	Ca_3	Fe^{3+}_2	Si_3	O_{12}
Calderite	Mn^{2+}_3	Fe^{3+}_2	Si_3	O_{12}
Hypothetical end-members				
Blythite	Mn^{2+}_3	Mn^{3+}_2	Si_3	O_{12}
FCa garnet	Ca_3	Al_2	$()_3$	F_{12}
FMn garnet	Mn_3	Al_2	$()_3$	F_{12}
Yttrogarnet	Y_3	Al_2	Al_3	O_{12}
Kimzeyite-Fe	Ca_3	Zr_2	$SiFe^{3+}_2$	O_{12}
Tin garnet	Ca_3	$SnFe^{2+}$	Si_3	O_{12}
Schorlomite-Al	Ca_3	Ti_2	$SiAl_2$	O_{12}
NaTi garnet	Na_2Ca	Ti_2	Si_3	O_{12}
Morimotoite-Mg	Ca_3	TiMg	Si_3	O_{12}
Morimotoite-Fe	Fe^{2+}_3	$TiFe^{2+}$	Si_3	O_{12}
Sc garnet	Ca_3	Sc_2	Si_3	O_{12}
Yamatoite	$Mn2+_3$	V_2	Si_3	O_{12}
Skiagite	Fe^{2+}_3	Fe^{3+}_2	Si_3	O_{12}
Khoharite	Mg_3	Fe^{3+}_2	Si_3	O_{12}

The mineral species listed in Tables 1 and 2 are generally used to describe the chemical composition of garnets. Mineral species are defined in accordance with the dominance principle of the Commission on New Minerals, Nomenclature and Classification (CNMNC) of the International Mineralogical Association. An end-member formula requires that 1) the chemical formula be fixed, 2) the formula and the crystal structure are compatible and 3) the chemical composition at each structural site is fixed. Two cations or anions at more than one site are not allowed (Locock, 2008; Grew *et al*., 2013).

There is large variability in the chemistry of garnets as the constituent metallic ions possess similar dimensions, charges and chemical affinities, and can interchange with one another, producing extensive solid solutions (Anderson, 1976). Hence, nomenclature

© University of Pretoria

problems in garnet classification have arisen due to this large chemical variability in its structure (Grew *et al*., 2013).

Various procedures have been put forward for the recalculation of the analysis of garnets into molar proportions of end-members (Rickwood, 1968; Grew *et al*., 2013; Locock, 2008). This recasting of garnets into end-member components provides simplification and allows for a quick evaluation of complex minerals (Rickwood, 1968). The calculation sequence is of great importance in determining the molar proportion of end-members as different sequences greatly influence the resulting molar proportions of the end-member components (Rickwood, 1968). When calculating the molar proportions of garnet end-members from analyses, a common procedure must be used to ensure that the results are consistent. This emphasises the need for a standard procedure to recast garnet analyses into molar proportions of end-member components (Locock, 2008; Grew *et al*., 2013; Rickwood 1968).

The most commonly used method is that of Rickwood (1968), who discusses the inherent problems in the calculation of end-members. Rickwood (1968) noted that titanium and manganese in trivalent states are unlikely to occur in silicate crystal structures and that titanium is tetravalent and present as a schorlomite component. In the calculation sequence, yttrogarnet ($Y_3Al_2Al_3O_{12}$), yamatoite ($Mn_3V_2Si_3O_{12}$), goldmanite, kimzeyite, and ferric-kimzeyite ($Ca_3Zr_2Fe_2SiO_{12}$) are calculated first. This is followed by uvarovite and andradite with almandine being calculated last of the six common aluminous silicates (pyrope, almandine, spessartine, grossular, andradite and uvarovite). Schorlomite is then calculated from the remaining quantities of Fe^{3+}, Ti and Ca (Rickwood, 1968).

Hanléite, khoharite, calderite, yttrogarent, blythite, goldmanite, yamatoite, skiagite, hydroandradite, ferric-kimzeyite and kimzeyite are rarely encountered and rarely considered in the calculation of end-members. Thus, almandine, pyropoe, spessartine, grossular, andradite, Uvarovite, and hydrogrossular are the most common end-member components. Rickwood (1968) also noted that the discarding of an analysis is not appropriate as almost all the elements in the periodic table can be accommodated in the garnet structure. Rickwood's (1968) method, however, has been criticised by Muhling and Griffin (1991) due to the incorrect treatment of Ti.

Locock (2008) developed a calculation procedure for the recasting of garnet analyses into molar proportions of end-member components using an Excel spreadsheet. This differed from Rickwood's (1968) in its calculation sequence and its treatment of Ti. Locock's (2008) spreadsheet uses 29 possible end-members (15 mineral species and 14 hypothetical

© University of Pretoria

end-members, as mentioned in Table 2). The advantage of this method is the accommodation of a wider compositional range. Locock (2008) concluded that Ti^{3+} is unlikely to occur in natural garnets, as supported by the results from synthesis experiments and X-ray absorption spectroscopy. In Ti-rich garnets, the presence of both Ti^{4+} and Ti^{3+} has been suggested to achieve charge balance. However, due to recent studies on the crystal chemistry of Ti-bearing garnets conducted Armbruster *et al*., (2001) and Chakhmouradian and McCammon, (2005), Locock (2008) suggests that Ti^{3+} is less likely to occur in natural garnets, as the reducing conditions required for Ti^{3+} to occur in garnets is not common in terrestrial garnet-forming environments. Locock (2008) argues that the recasting of Ti-rich garnet analyses can require up to six Ti-bearing end-members to describe their chemical composition adequately. The calculation sequence of Locock's (2008) method varies from that of Rickwood (1968) due to the different treatment of Ti, H, Mn^{3+} and octahedral Si, as well as the inclusion of more hypothetical end-members in the calculation sequence that do not occur in Rickwood's (1968) method. Blythite is calculated much earlier and andradite is calculated later with the schorlomite component being calculated earlier in the sequence when compared to Rickwood's (1968) method.

A definitive paper on the end-members of garnets by Grew *et al*. (2013) for garnet classification is available with a spreadsheet for the calculation sequence of molar proportions.

The different calculation procedures from Rickwood (1968), Locock (2008) and Grew *et al*. (2013) are compared in this thesis together with the problems encountered by each (see Section 3.7). However, solving these calculation problems is not the objective of this report. The various calculation procedures and their problems have been highlighted to emphasise the uncertainty surrounding garnet end-member calculation and classification.

In gemology, pyrope, almandine, spessartine, andradite, grossular and uvarovite (the latter occurring in insufficient sizes to be of gem-quality) are the traditionally recognised end-members with the other nine end-members being disregarded, as they do not produce gem quality minerals (Hanneman, 2000). Garnets of compositions between these six end-members are more common than a pure end-member, resulting in compositions that make it difficult to classify garnets. This, together with the presence of trace, but chemically important, amounts of Cr^{3+}, Ti^{4+} and/or V^{3+} further adds to the complexity of garnet chemistry. Gemstones with compositions close to an end-member are given that end-member's name. For example, a gemstone with a composition of 80 mol. % grossular is termed grossular (Stockton and Manson, 1985; Anderson, 1976; Webster, 1962).

© University of Pretoria

Generally, the refractive index (R.I.) and specific gravity (S.G.) are used to classify garnet gemstones, as these are the easiest characteristics to routinely measure, whereas chemical analysis is rarely available. The R.I. and S.G. depend on the proportion of end-members present in the garnet gemstone (Stockton and Manson, 1985; Anderson, 1976; Webster, 1962).

Colour is also used, in conjunction with R.I. and S.G., to identify a garnet gemstone, but this method is sometimes unreliable because garnets of similar colour can contain different chromophores and, hence, have different compositions (Stockton and Manson, 1985 and Serov *et al*., 2011). The absorption spectra observed from a hand spectroscope supports gemstone classification because spectral absorption bands caused by chromophores are a characteristic of certain garnets. However, these methods have proved inefficient with the recently discovered new types of garnets, which are complex mixtures of several end-members that transcend the chemical solid solution series. A modified classification system is required that includes chemical analysis.

The traditional classification systems include works by Webster (1962) and Anderson (1976). A more recent classification system for garnets, as devised by Stockton and Manson (1985), is based on chemical data and requires the determination of only the R.I., colour and spectral features to classify a garnet (Stockton and Manson, 1985; Anderson, 1976; Webster, 1962).

© University of Pretoria

2.1.1. Garnet production

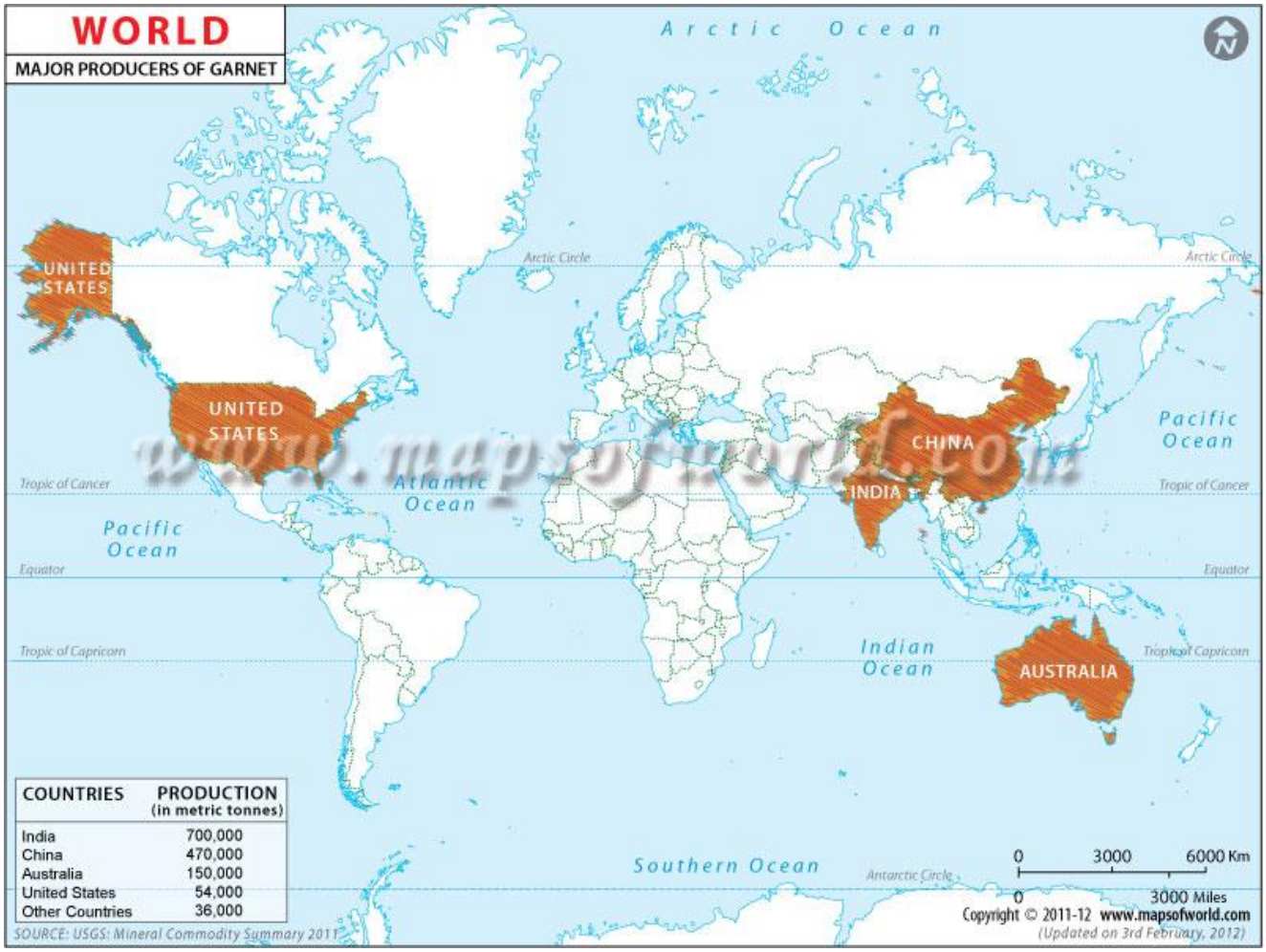

Figure 1. A map of the world and the countries producing garnet (Maps of World, 2012).

The total world industrial garnet production was estimated 440 000 tons. As can be seen in Figure 1, the United States, India, China, and Australia are the leading producers of garnets. Small mining operations are also found in Canada, Chile, Pakistan, South Africa, Thailand, the Ukraine, Chile, and the Czech Republic, and are primarily for domestic use (Olson, 2015).

2.2. Gem Classification Schemes

2.2.1. Webster

Webster (1962) used six end-members, namely almandite = almandine, pyrope, spessartite = spessartine, grossular, melanite andradite and Uvarovite, although the latter is not utilised in jewellery. Webster (1962) used the term melanite, however, the correct term according to the International Mineralogical Association (IMA) is a Ti-rich andradite called

© University of Pretoria

morimotoite (Grew *et al*., 2013). The ions in each end-member can interchange between the end-members, depending on the limited sold solutions, producing an isomorphous series. Garnets consist of two isomorphous series: the pyrope-almandine-spessartine (also known as pyralspite) series and the uvarovite-grossular-andradite (also known as ugrandite) series. These two series are slightly miscibile with each other. Webster (1962) uses the diagram in Figure 2 to better explain the complex miscibility between the different garnet end-members (Webster, 1962).

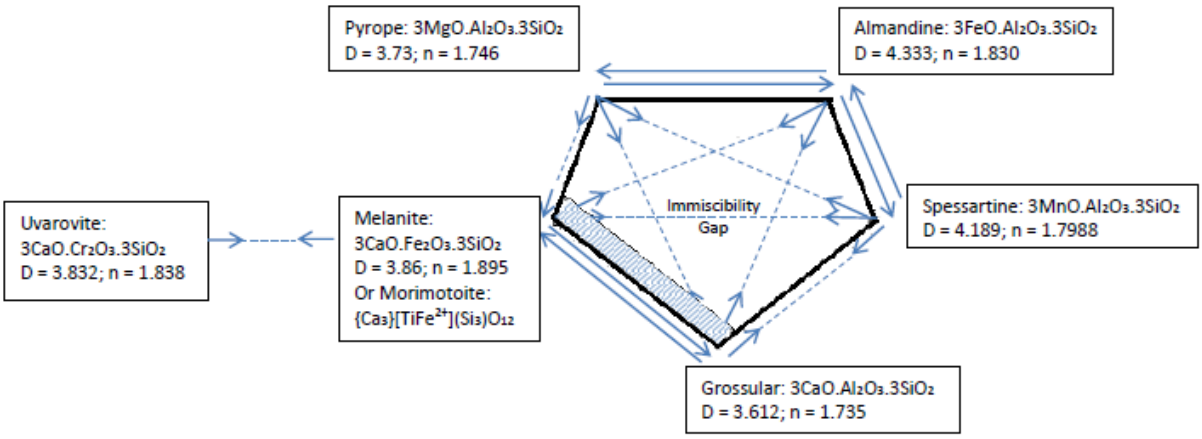

Figure 2. Diagram from Webster (1962) with some modification according the IMA (Grew *et al*., 2013).

In Figure 2, the arrows that extend unbroken between two end-members, e.g. pyrope and almandine, represent a complete solid solution and both the exchangeable end-members (Mg^{2+} and Fe^{2+}) can occur in any proportions. A complete solid solution exists between:

- Pyrope and almandine;
- Almandine and spessartine; and
- Andradite and grossular.

In the first two solid solutions, the divalent constituent is always interchangeable in all proportions. In the andradite-grossular solid solution, the trivalent constituent is interchangeable. Where the partly extended arrows link each type of garnet (except for uvarovite which occupies a separate position), a certain proportion of the other constituent is present but not as a complete solid solution, as mentioned above. This is due to the fact that after a certain percentage (~10%) the miscibility ends and there is an immiscibility gap. A garnet that plots in the shaded portion of the diagram would contain primarily grossular and andradite, but would also contain a mixture of pyrope, almandine and spessartine (Webster, 1962).

© University of Pretoria

2.2.2. Anderson

Anderson (1976) also used the same six garnet species as those of Webster (1962).

Anderson (1976) theorised that the properties of the end-members, i.e. R.I. and S.G. could enable us to estimate the composition of any garnet. The end-members of the garnet and their various properties as recognised by Anderson (1976) are summarised in the table below (Anderson, 1976).

Table 3. The end-members of garnets and their properties from Anderson (1976).

Name	Formula	S.G.	R.I.	Colour
Almandine	$Fe_3Al_2Si_3O_{12}$	4.32	1.830	Red
Pyrope	$Mg_3Al_2Si_3O_{12}$	3.58	1.714	Red
Spessartine	$Mn_3Al_2Si_3O_{12}$	4.18	1.800	Orange
Andradite	$Ca_3Fe_2Si_3O_{12}$	3.86	1.887	Green
Grossular	$Ca_3Al_2Si_3O_{12}$	3.59	1.734	Green
Uvarovite	$Ca_3Cr_2Si_3O_{12}$	3.9	1.860	Green

2.2.3. Stockton and Manson

Stockton and Manson (1985) are the most recent to have devised a new classification system for garnet gemstones based on chemical data that also includes garnets of intermediate compositions. They noted that the old classification systems designed by Anderson (1976) had to be revised due to the discovery of new garnets from East Africa (Carstens, 1973; Crowningshield, 1970; Gübelin and Schmetzer, 1982; Manson and Stockton, 1984; Manson and Stockton, 1981; Manson and Stockton, 1982). Examples of new gemstones that do not fit into the traditional garnet categories include

- Malaya (yellow-orange to red-orange variety of pyrope-spessartine) (Stockton and Manson, 1985),
- Colour-change pyrope-spessartine (displays a distinct change in colour between daylight and incandescent light) (Crowningshield, 1970),
- Chrome pyrope (orange-red variety of pyrope) (Stockton and Manson, 1985) and
- Tsavorite (green to yellowish-green variety of grossular) (Manson and Stockton, 1982).

This discovery of new garnets further spurred the debate on the terminology of gem garnets. The availability of the electron microprobe since the 1960s enabled accurate, non-destructive and rapid analysis of gemstones, allowing for a definite and rigorous characterisation of the new garnet varieties. Stockton and Manson (1985) also noted that the

© University of Pretoria

presence of Cr^{3+}, Ti^{4+} and/or V^{3+}, even though of minor quantities, in garnets cannot be ignored as they have a large influence on garnet properties, such as colour (Stockton and Manson, 1985).

Stockton and Manson (1985) distinguished eight types of garnet gemstones based on their chemistry: grossular, andradite, pyrope, pyrope-almandine, almandine, almandine-spessartine, spessartine and pyrope-spessartine. This can be summarised in the table below (Hanneman, 2000).

Table 4. Refractive indices and other properties of garnet gemstones from Hanneman (2000).

Species	Refractive index	Hues	Varieties
Grossular	1.730-1.760	Green through reddish-orange, colorless	Tsavorite, hessonite
Andradite	1.880-1.895	Very slightly yellowish green through orangy yellow	Demantoid, topazolite
Pyrope	1.714-1.742	Purplish red through reddish orange, colorless	Chrome pyrope
Pyrope-almandine	1.742-1.785	reddish orange through red-purple	Rhodolite
Almandine	1.785-1.830	Orange red through purplish red	
Almandine-spessartine	1.810-1.820	Reddish orange through orange-red	
Spessartine	1.780-1.810	Yellowish orange through reddish orange	
Pyrope-spessartine	1.742-1.780	Greenish yellow through purple	Malaia, color change

Some of the varietal terms used today in gemology, such as tsavorite, hessonite, demantoid, chrome pyrope, rhodolite, Malaya, and colour-change garnets, are based on colour and appearance. Stockton and Manson (1985) suggest that these names remain; for example, a pyrope-almandine appearing purplish-red may be called rhodolite but a red stone with similar R.I. and S.G. values may be called pyrope-almandine (Stockton and Manson, 1985). They also suggest discarding the use of S.G. as a means of classification as there is an overlap in the S.G. ranges for the different types of garnets as well as the strong influence of inclusions on S.G. values (Stockton and Manson, 1985).

© University of Pretoria

2.3. Colour in Gem Garnets

2.3.1. Colour in garnets gemstones as a means of classification

Looking at the chemical formula of a garnet ($\{X_3\}[Y_2](Z_3)\ \varphi_{12}$) and the possible variations in which ions can bond with silicon and oxygen gives us a wide range of colour in gem garnets (Grew *et al*., 2013; Stockton and Manson, 1985). The colour of garnets is caused by chromophores, which usually occupy the X and Y sites (Serov *et al*., 2011); these include iron, manganese, chromium, and vanadium. Titanium, even present in small amounts, can strongly affect the colour of garnets (Gemstone Magnetism, 2014; Stockton and Manson, 1985; Schmetzer *et al*., 2009; Krzemnicki *et al*., 2001).

Garnet gemstones occur in a wide variety of colour; therefore this cannot be solely relied upon as a means of classification (Stockton and Manson, 1985; Serov *et al*., 2011). Certain colours can be distinctive, although these generalities should be avoided, as there are exceptions; for example, intense green colours usually occur in grossulars, uvarovite and andradites; however, this colour can also be found in colour change garnets (Stockton and Manson, 1985). Serov *et al*. (2011) note that colour is not a reliable means of classifying gem garnets, especially when using the absorption spectra, as the same chromophores can give different absorption patterns and colours. With the recent discovery of colour change pyrope-spessartine garnets, the ranges of colours noted for garnets has expanded, which brought confusion to gem garnet identification. The confusion in distinguishing between Malaya and colour change garnets based on colour is a noted problem amongst gem traders due to both garnets having similar physical and chemical properties (Dirlam *et al*., 1992; Stockton and Manson, 1985; Schmetzer *et al*., 2009; Schmetzer *et al*., 2001; Schmetzer *et al*., 2002; Krzemnicki *et al*., 2001). Schmetzer *et al*. (2009) note that there is no simple parameter that can be used to predict the colour and colour change amongst colour change garnets. Malaya garnets are also similar to hessonite in colour, with both having similar R.I. and S.G. ranges. Krzemnicki *et al*. (2001) also note that the relationship between chemistry and colour and colour change is very complex. Malaya garnets also display similar colours to those observed in rhodolites, pyrope-almandines and pyropes. Gem garnets of the pyrope-almandine series have similar R.I. values and observed colours to those from the pyrope-spessartine series (Stockton and Manson, 1985; Schmetzer *et al*., 2001; Dirlam *et al*., 1992; Zwaan, 1974; Seifert and Hyrsl, 1999).

2.3.2. Colour change

© University of Pretoria

Colour change is a phenomenon that has attracted the attention of gemmologists in recent years. The term was first used for alexandrite from the Urals region in Russia. The stone appears green in daylight and red in incandescent light. This change in colour (green to red) was then termed the 'alexandrite effect'. Other colour changes, i.e. blue green under daylight to purplish red or violet under incandescent light, were not as common then. Today, the term 'alexandrite effect' is no longer applied to stones that display the traditional colour change, but has become a general term to describe all types of colour change between different types of illumination. This adds confusion to the colour change phenomenon considering the inherent diversity in the factors influencing colour change. Oddly enough, the alexandrite effect is not used to describe colour change garnets; rather, the term 'colour shift' is more commonly employed. The term colour change was traditionally used to describe stones displaying a change in colour under different illuminations that were not commonly observed in that gem variety as a whole.

The term 'colour shift' was applied to a gem variety where all the samples display various colours under different illumination. To add to the confusion, the term 'colour shift' was employed by Stockton and Manson (1985) to describe garnets showing different colours under transmitted and reflected light (Stockton and Manson, 1985; Schmetzer *et al*., 2009; Krzemnicki *et al*., 2001). Schmetzer *et al*. (2009) employed the term 'colour change' only for stones that show different colours under various illuminations, which has not been produced by heat treatment or irradiation, as this would then be termed colour alteration. This variety in expressions for colour change, alongside the large influx of different types of light sources in the market today has placed the different terms for colour change under scrutiny. Various authors (Schmetzer *et al*., 2009; Krzemnicki *et al*., 2001) have investigated the cause of colour change. Schmetzer *et al*. (2009) maintained the use of the term 'colour change' for stones showing moderate, strong or very strong colour change and the term 'colour variation' for those with only a faint change in colour. They then abandoned the term 'colour shift' altogether.

2.4. Magnetic Susceptibility

The existing methods used for the classification of garnets have proven to be insufficient in classifying some of the new varieties of garnets that have been discovered in recent times (Stockton and Manson, 1985). Hoover and Williams (2007) have developed a new technique involving magnetic susceptibility, which is both viable and cost effective for the classification of garnets and specifically Malaya garnets (Hoover and Williams, 2007).

© University of Pretoria

In gemology, the few quantitative measurements that are employed are birefringence, refractive index and density. The most recent measurement that can be added to this list is magnetic susceptibility. Gemstones have been known for their magnetic properties, but this property has not been taken advantage of in the classification of gem garnets until recently. Different gemstones have different magnetic susceptibilities and this can be employed for the purpose of gemstone discrimination. The application of a rare earth element magnet to a gemstone provides an approximate measure of the total content of magnetic ions present. These magnetic ions, when dealing with gemstones, are mostly iron and manganese (Hoover and Williams, 2007).

Magnetism results due to the motion of electrons in atoms and is analogous to the magnetic field that is created about a wire as a result of an electric current being run through the wire. Within the atoms, electrons spin and move within the orbits about the nucleus and it is these two types of motions that create small magnetic dipole fields. Hence, these electrons serve as small permanent magnets within an atom (Hoover and Williams, 2007).

When applying magnetic susceptibility to gemstones, it is only the magnetic susceptibility per unit volume that is concerned, as this is what is directly measured. Magnetic volume susceptibility is expressed by the letter '*k*' and is dimensionless. However, there are two systems of units that are employed when comparing results namely: 1) the older emu/cgs (centimetre-gram-second) and 2) the more commonly used SI (metre-kilogram-second). The SI system is preferably chosen when dealing with gemstones and is done so in this report. It is predominantly the iron- and manganese-bearing gemstones that will possess the highest magnetic volume susceptibility and the testing of the gemstones will show the presence or absence of iron and manganese (Hoover and Williams, 2007).

The magnetic volume susceptibility of an unknown gemstone can be given by Equation 1:

Equation 1: $k = C \times Pull$

Where C = k (of standard)/ pull (of standard),

Pull = measured pull of the test stone,

k is expressed as SI, and

Pull is expressed as carat (Hoover *et al.*, 2008).

2.4.1. Previous uses of magnets in gemology

© University of Pretoria

Magnets have been used in gemmology since the 1980s. Koivula and Fryer (1984) developed a number of techniques of varying sensitivity that were used to determine the magnetic attraction in synthetic diamonds (Koivula and Fryer, 1984). Gumpesberger (2006) performed a number of qualitative tests by floating a specimen or hanging it as a pendulum to determine whether there was any magnetic attraction and whether the material was strongly magnetic, then by lifting it. Anderson (1980) was one of the first researchers to utilise semi-quantitative measurements of magnetic attraction, and in the 1990s, Haralyi (1993) performed a quantitative measurement of magnetic susceptibility on gemstones (Hoover and William, 2007).

2.4.2. Garnet magnetism

Garnets tend to be more magnetic than other gems due to their high concentration of iron and/or manganese. Hoover *et al*. (2008) suggests that chemistry can be inferred by the determination of the iron and manganese concentrations in garnets. Hoover *et al*.'s (2008) method provides a more accurate means of determining garnet chemistry than that proposed by Stockton and Manson (1985) as it takes into account an additional variable apart from R.I., for example, magnetic susceptibility.

2.5. Gem Garnets

2.5.1. Uvarovite

Uvarovite is a calcium-chromium silicate that appears rich green in colour. It is primarily coloured by intrinsic chromium and has an R.I. of 1.87, S.G. of 3.77 and a hardness of 7.5 on Mohs scale. Uvarovite occurs in association with chromite in serpentine or within granular limestone in the Ural Mountains of Russia, the Himalayan Mountains and California, America. However, this stone does not occur in sufficient quantity or size to be of commercial gem-quality (Anderson, 1976; Webster, 1962).

2.5.2. Almandine

Almandine is an iron-aluminium silicate that appears orange-red to purplish red in colour and generally occurs together with pyrope (Anderson, 1976; Stockton and Manson, 1985). The word almandine comes from the word 'Alabanda' in Asia Minor (Anderson, 1976). Theoretically, pure almandine should have an R.I. of 1.83, nevertheless, as mentioned above, pure almandine is rare and it is more common to find almandine with lesser amounts of pyrope in a gem garnet, so their R.I. ranges from 1.785 to 1.830 (Webster, 1962; Stockton and Manson, 1985). In practise, a garnet is referred to as an almandine if it

© University of Pretoria

has an R.I. higher than 1.78 and an S.G. higher than 3.95 (Webster, 1962). Due to the dark red colour sometimes evidenced in almandines, they are usually cut in the cabochon form called 'carbuncles' (Webster, 1962; Anderson, 1976). Titanium (from the shorlomite species) tends to mix with almandine and pyrope, which alters the colour towards blackish undertones (Gemstone Magnetism, 2014). It is the hardest garnet gemstone with a 7.5 on the Mohs scale and a dispersion similar to that of pyrope (0.027) (Webster, 1962; Anderson, 1976). Almandine generally occurs in schists and are found worldwide, but with gem-quality almandine being scarcer (Webster, 1962).

2.5.2.1. Localities

2.5.2.1.1. Tanzania

Zwaan (1974) analysed almandine garnets from Umba, Tanzania, which ranged in colour from red to brownish red in colour with most of the stones being of gem-quality. It was noted that of the four stones chemically analysed, only two were almandines, with the other two being pyrope-almandines but not rhodolites. The andradite component in the samples was very low and the iron present was primarily Fe^{2+}. Inclusions included apatite and prismatic rutile crystals, although these inclusions are not characteristic of Umba since similar inclusions occur in almandines from Ceylon (Zwaan, 1974).

2.5.2.1.2. America

Almandine deposits have been found in North Carolina that appear pink to scarlet red, to brownish red, to deep red in colour. They occur in the mica mines in the Avery, Mitchell and Yancey Counties and are crystallised in blocks and sheets of mica (Pratt, 1933).

2.5.2.1.3. Canada

Almandine has also been found in Canada in metamorphic rocks. Almandine is quite common in Canada and appears dark red to reddish-brown in colour. Almandines weighing less than 1 ct. have been found in Ontario, Quebec, the Northwest Territories, Nunavut, Manitoba and Yukon. Almandine was first discovered in the south coast of Baffin Island of Nunavut in 1915 appearing dark red with a brownish overtone. However, the exact vicinity of this stone has yet to be located despite several attempts. Gem-quality almandine is also found in British Columbia in vugs that also contain aquamarine. The almandine appears dark red in colour and is usually attached to pocket walls. The crystals can be as wide as 4 cm with the largest weighing in at 4.04 ct. (Wilson, 2009).

© University of Pretoria

2.5.2.1.4. Other localities

India is one of the more famous localities of almandine where it occurs in mica schist of Rajmahal of Rajasthan. Another Indian locality is the Warangal district (Webster, 1962). Very purple almandine, dubbed grape garnet, can be found in the state of Orissa, India (Gemstone Magnetism, 2014). Some of the almandines from India display asterism. Almandine is also found at Trincomalee on the northeast coast of Ceylon and also occurs in South America in Brazil and in Rio de Janeiro near Minas Gerais (Webster, 1962).

2.5.3. Andradite

Andradite is a species of the garnet group with a chemical formula of $Ca_3Fe_2Si_3O_{12}$ and ranges in colour from faint yellowish green to an orangy yellow. It has a refractive index from 1.880 to 1.895 and typically occurs in metamorphic rocks such as skarns and serpentinites (Adamo *et al*., 2011; Stockton and Manson, 1985). Andradite forms a complete solid solution with grossular, with intermediate compositions being common but gem-quality stones of both grossular and andradite usually occur with compositions close to their ideal end-member. Andradite is coloured by the intrinsic ferric iron present, producing the yellow colour observed in andradite crystals (Phillips and Talantsev, 1996). Three varieties of andradite are recognised today: topazolite, melanite and demantoid, with only the latter being important in gemology (Stockton and Manson, 1985). Note that term ‘demantoid’ is not approved by the Interanational Mineralogical Association, however, for the sake of gemological convention, it will be used in this report (Adamo *et al*., 2009).

2.5.3.1. Demantoid

Demantoid is a green andradite garnet, where the green colour is caused by the presence of chromium with the yellow overtone being caused by the presence of intrinsic ferric iron (Adamo *et al*., 2011; Phillips and Talantsev, 1996). It is usually near the ideal andradite composition with minor amounts of chromium, titanium, vanadium, aluminium, and occasionally manganese present. Demantoid results from the substitution of Cr^{3+} from solid solution with uvarovite for Fe^{3+} , producing the green colour that superimposes over the intrinsic yellow colour (Phillips and Talantsev, 1996). It is one of the most appreciated garnet gemstones today due to its brilliance, rarity and colour. However, its hardness of less than 7 makes it difficult to employ as a ring stone, but it can be used in other jewellery (Adamo *et al*., 2011; Phillips and Talantsev, 1996). The crystals are generally small with gems larger than 2-3 ct being quite rare and those with a vivid, intense colour being more sought after (Adamo *et al*., 2011). Demantoid usually possesses some distinct characteristics that make

© University of Pretoria

it easy to identify: a strong dispersion of 0.057 and high R.I. (1.89), which is not found in other garnets, together with the presence of 'horsetail' inclusions (Stockton and Manson, 1983; Phillips and Talantsev, 1996).

Demantoid is typically found in the Central Ural Mountains of Russia, Val Malenco of Italy, the Kerman Province of Iran, the Kaghan Valley of Pakistan, the Erongo Province of Namibia, and Antetezambato of Madagasca with the latter four being more recent discoveries (Adamo *et al*., 2011; Phillips and Talantsev, 1996; Adamo *et al*., 2009; Pezzotta *et al*., 2011).

2.5.3.1.1. History

Demantoid was first discovered in Russia in 1875 (Adamo *et al*., 2009). In 1853, children from the Elizavetinskoye settlement of the Central Urals region found grass-green pebbles in the runoff from the Bobrovka River. Demantoid was initially identified incorrectly as chrysolite and became popular amongst the nobility of 19th century Czarist Russia. Nil von Nordensheld was the first to recognise the stone as a new mineral and not a chrysolite. In 1864, he described the stone as a green andradite garnet coloured by a small amount of chromium and due to its unusual brilliance and fire, he proposed the name demantoid i.e. 'diamond-like' (Phillips and Talantsev, 1996). With the onset of the Bolshevik Revolution in 1917, priorities in Russia shifted and the production of demantoid was no longer a primary necessity. However, since the start of the 21st century, demantoid has become more popular and seen an increase in demand (Phillipa and Talantsev, 1996; Adamo *et al*., 2009).

2.5.3.1.2. Localities

2.5.3.1.2.1. Russia

Two major districts in the Central Urals region of Russia are recognised as a source of demantoids: the Nizhniy Tagil and Sissertsk regions.

The Nizhniy Tagil region contains two deposits:

- A placer deposit of alluvial demantoids on the Bobrovka River and
- A primary, *in situ*, deposit located at the head of the Bobrovka River (Phillips and Talantsev, 1996).

A very distinctive internal feature found in the demantoids from Russia, and in demantoids from other regions, is the presence of the 'horsetail' inclusion; an indicative feature for demantoids (Phillips and Talantsev, 1996; Adamo *et al*., 2011). This feature is

© University of Pretoria

present in almost all of the Russian demantoids and occurs in no other green gemstone. 'Horsetail' usually refers to hair-like asbestiform amphibole of actinolite-tremolite composition fibres that generally diverge from a focal point. In other recent literature, randomly orientated acicular inclusions have been found that are not related to the horsetail fibres (Phillips and Talantsev, 1996; Krzemnicki, 1999). Krzemnicki (1999) analysed 11 demantoid samples from the Ural Mountains of Russia in order to further understand the inclusions that occur within Russian demantoids. All the samples contained the characteristic Russian horsetail inclusions as well as some colourless acicular inclusions in some samples. The acicular inclusions were identified as diopside (Krzemnicki, 1999).

2.5.3.1.2.2. Val Malenco, Italy

Another locality for demantoids is Val Malenco of Italy. It is located in the Sondrio Province of northern Italy with the demantoid occurring as well-formed rhombic dodecahedral crystals. Gemstones from this region are rarely bigger than 2-3 ct. (Adamo *et al*., 2009). The demantoid occurs in the asbestos mines found between Dossi di Franscia and Coston d'Acquanegra that are not easily accessible. Towards the end of the 1970s, the mines closed down (Adamo *et al*., 2009). The demantoid occurs in foliated serpentinites within asbestos (chrysotile)-filled fractures. Demantoid is often associated with Cr-bearing magnetite, hydromagnestie, magnetite, brucite, clinochlore, calcite and rarely forsterite (Adamo *et al*., 2009).

The stones range in colour from yellowish green to green to intense green with colour being generally homogenously distributed. The R.I. is higher than 1.81 and a S.G. between 3.81 and 3.88 (Adamo *et al*., 2009).

The composition of the demantoids is near the end-member composition of andradite similar to demantoids from Russia with the green colour correlating with the Cr^{3+} content, the primary chromophore (Adamo *et al*., 2009; Phillips and Talantsev, 1996). The yellow demantoids from Val Malenco are coloured by the presence of instrinsic iron and possess lower chromium content, usually close to the detection limit, than their green counterparts (Adamo *et al*., 2009).

The demantoids from Val Malenco usually contain horsetail inclusions of chrysotile as well as fractures. This horsetail feature is typical of demantoids hosted within serpentinites (Adamo *et al*., 2009).

© University of Pretoria

2.5.3.1.2.3. Kerman Province, Iran and Kaghan Valley, Pakistan

Demantoids were discovered in the Soghan region of the Kerman Province in October 2001. The Soghan region consists of ultramafic-mafic complexes, with demantoids occurring as clusters of well-formed single crystals inside regionally metamorphosed asbestiform rocks within serpentinite (Adamo *et al*., 2011).

The Kaghan Valley is in northern Pakistan, the same region known for producing gem-quality olivine. This region consists of ultramafic rocks with demantoid occurring in serpentine, which is associated with ludwigite and magnetite (Adamo *et al*., 2011).

A chemical analysis of the demantoids from both Iran and Pakistan shows a near end-member composition of andradite with trace amounts of magnesium, manganese, titanium, chromium and aluminium. Chromium is believed to be the cause of the green colour in these samples (Adamo *et al*., 2011).

2.5.3.1.2.4. Erongo Province, Namibia

Demantoid deposits have been found in the forelands of the Erongo Mountains of Namibia during the 1990s. The demantoid garnets of the Green Dragon Mine in the Erongo Province are associated with a Neoproterozoic metasedimentary sequence of amphibolite, schist, marble and calc-silicate rock. This sequence was intruded by granitic dykes and is believed to be the cause of contact metamorphism of the marble producing calc-silicate rock and andradite garnet. The demantoid is located in both marble and calc-silicated rocks along the contact to the granitic veins and plugs. The calc-silicate rocks host a zone of large green garnet crystals in a calcite matrix with quartz and minor silicates. The garnets possess a near end-member andradite composition with low Ti, Mg, Mn and Cr. A more brown garnet occurs in the marble and massive calc-silicate rocks with a near grossular composition (Koller *et al*., 2012).

Andradite is also produced in the Namgar mine of the Erongo Province within calc-silicate skarn. The garnet results from crystallisation in dolomitic marbles. The samples have a near andradite end-member composition with low to almost no chromium, similar to that of Madagascar and Canada (Adamo *et al*., 2011, Pezzotta *et al*., 2011; Wilson, 2009).

2.5.3.1.2.5. Antetezambato, Madagascar

The village of Antetezambato is located in northern Madagascar, where the mining of demantoid has occurred since 2009. The colour of the samples ranges from yellow-green to bluish-green, and it has R.I. values higher than 1.81. The demantoids occur within skarns

© University of Pretoria

and lack the typical horsetail inclusions found in demantoids hosted within serpentinites (Pezzotta *et al*., 2011).

Production of the gem-quality andradite decreased significantly from 2009, as mining became difficult and dangerous due to the need for deeper pits and the lack of drainage systems for infiltrated seawater during high tide. Most of the demantoid production occurred in 2009 with production halting since November 2010 (Pezzotta *et al*., 2011).

The garnet occurs in the northwestern side of the magmatic area within tilted blocks of layered sediments intruded by lamprophyric dykes. The lack of titanium produced brown demantoid. (Pezzotta *et al*., 2011)

A chemical analysis of Antetezambato demantoids shows an almost pure andradite component (>98 mol. %), with trace amounts of Na, K, Al, Mn, and Ti (Pezzotta *et al*., 2011). The Cr and V content were below the detection limit in these samples from Pezzotta *et al*. (2011), contrary to what is observed in samples from Russia, Italy, Iran, and Pakistan. This corresponds to that observed by Adamo *et al*. (2011). In addition, these demantoids from Antetezambato lack the presence of horsetail inclusions typical for serpentinite-hosted demantoids from Russia, Italy, Iran and Pakistan. The Antetezambato demantoids are similar to the skarn-hosted demantoids from Namibia, and display a high total REE content (higher than serpentinite-hosted demantoids) due to the mobility and enrichment of these elements in skarn (Pezzotta *et al*., 2011; Phillips and Talantsev, 1996; Adamo *et al*., 2009; Adamo *et al*., 2011). No chormophores are present in significant amounts, except for intrinsic ferric iron, and there is no correlation observed between colour and composition in the Antetezambato demantoids. Some of the demantoids displayed a colour-shift, believed to be caused by the trace amounts of cerium and neodymium present, similar to that observed in demantoids from Quebec, Canada (Pezzotta *et al*., 2011).

2.5.3.1.2.6. Other localities

Gem-quality demantoid was discovered in the asbestos mines in Black Lake, Quebec, Canada in the 1990s. The demantoid ranges in size with the largest being 21 mm. Most appeared opaque to translucent and less intense green than those observed in other localities. These demantoids differ from those in Russia, Italy, Iran, and Pakistan in that they do not contain any chromium or vanadium. This suggests that the colour of these garnets from Canada is not caused by chromium and/or vandium (Wilson, 2009; Phillips and Talantsev, 1996; Adamo *et al*., 2009; Adamo *et al*., 2011). Two main colour groups were observed in these demantoids: yellowish green with greyish overtones and a truer green with

© University of Pretoria

a slight bluish overtone without any grey. A higher dispersion is observed in these demantoids than those from Russia (Wilson, 2009).

A colour-shift can be observed in the Canadian samples between incandescent light and daylight, appearing faded with overtones of grey under incandescent light, and richer bluish green under daylight (Wilson, 2009).

Skarn-hosted demantoid was also found near Swift River, southern Yukon, in 1997, with colours ranging from yellowish brown to yellow green. These demantoids also displayed a colour-shift between daylight and incandescent light appearing bright yellowish green under daylight and faded with brownish or greyish overtones under incandescent light, similar to those observed in Black Lake, Canada and Antetezambato, Madagascar (Wilson, 2009; Pezzotta *et al*., 2011).

Gem-quality demantoids have been recovered from the Xinjiang Uygur Autonomous Region of China appearing jade green to yellow-green in colour. The demantoid occurs in serpentinised pyroxene-peridotites and is associated with chrome spinel and asbestos. Stones are generally less than 3 mm in diameter (Keller and Faquan, 1986).

Very recently, deposits of andradite displaying iridescence were found in Japan and Mexico (Shigley *et al*., 2010)

2.5.3.1.2.7. Comparison of different localities

Demantoid from different localities display different characteristics, mainly those observed between serpentinite- and skarn-hosted demantoids. Serpentinite-hosted demantoids occur in the Central Ural Mountains of Russia, Val Malenco of Italy, the Kerman Province of Iran, and the Kaghan Valley of Pakistan. These Russain, Italian, Iranian, and Pakistani demantoids display the characteristic horsetail inclusions. Their green colour is due to the presence of minor amounts of Cr^{3+} that substitute for Fe^{3+} in the octahedral sites, superimposing the green colour over the yellow overtone. Both chromium and intrinsic ferric iron are present as chromophores. Furthermore, no colour shift effect was observed in any demantoids from these localities (Adamo *et al*., 2011; Adamo *et al*., 2009; Pezzotta *et al*., 2011; Phillips and Talantsev, 1996; Wilson, 2009).

Skarn-hosted demantoids from the Erongo Province of Namibia, Antetezambato of Madagascar, and Black Lake in Canada display different characteristics, specifically the absence of horsetail inclusions. Although their chemical composition is similar to serpentinite-hosted demantoids (near end-member andradite composition), the absence or

© University of Pretoria

very low amounts of chromium are observed. Hence, chromium is not the cause of the colour in these skarn-hosted demantoids. Moreover, the demantoids from Canada and Madagascar displayed a subtle shift in colour between daylight and incandescent light, a phenomenon not observed in the serpentinite-hosted demantoids (Adamo *et al*., 2011; Adamo *et al*., 2009; Pezzotta *et al*., 2011; Phillips and Talantsev, 1996; Wilson, 2009).

2.5.4. Grossular

Grossular garnet has a chemical formula of $Ca_3Al_2Si_3O_{12}$, and displays a variety of colours including yellow, orange, and green. This garnet received little recognition as a popular gemstone and the little fame that it received was only for hessonite. However, in the 1970s and 1980s, economic deposits of intense green grossular were discovered in east Africa, and were given the trade name ‘tsavorite’. The introduction of tsavorite to the gem market made grossular a popular gem-quality garnet across the world. Unfortunately, a precise definition of hessonite and tsavorite has yet to be formulated, making it difficult to distinguish between the two varieties except by the traditional difference of colour (Manson and Stockton, 1982).

For the sake of gemological convention, in this report, hessonite will be regarded as grossular with an orange, yellow, brown, or red colour and tsavorite as pale to intense green in colour.

Hessonite is traditionally a brown, yellow or orange variety of grossular but colour descriptions vary with some reporting it as yellowish and brownish red and orange-brown, (Manson and Stockton, 1982). Manson and Stockton (1982) also reported that there was no mention of saturation of colour when referring to the colours reported in these stones. Tsavorite is described as appearing similar to emerald, although this is a poor description (Manson and Stockton, 1982).

Manson and Stockton (1982) analysed 105 grossular garnets, which ranged in colour from pale to intense yellow, orange and green. The R.I. ranged from 1.731 to 1.754 and the S.G. from 3.57 to 3.67. Pure grossular appears colourless, but this is rarely seen in nature. Manson and Stockton (1982) reported observing two colour trends in the 105 grossular garnets examined: a yellow-green to a pure, vivid green, and a yellow and orange to a vivid red-orange with saturation increasing towards one extreme. A chemical analysis of the stones showed that grossular was the dominant component (>70%) with lesser amounts of andradite and uvarovite. Evidence has shown that the andradite component is primarily responsible for the departure of the gemstone properties away from the properties of

© University of Pretoria

grossular, but the influence of other end-member components cannot be ruled out. A correlation was observed to exist between the V_2O_3 content and the green colour in the stones with V increasing with a greener colour. Cr_2O_3 also caused the green colour in the grossular samples. The Fe_2O_3 content increased with stones changing from yellow and orange to red-orange with the green colour decreasing. The high grossular component makes it easy to identify from other gem species (Manson and Stockton, 1982).

It is thought that grossular is chemically continuous with andradite and uvarovite and forms a subgroup with them, but recent evidence from Manson and Stockton (1982) suggests otherwise, i.e. appears to be a gap in this series when dealing with gem-quality grossular. They suggest that gem grossulars be regarded as discrete with regard to any other garnet species (Manson and Stockton, 1982).

2.5.4.1. Tsavorite

Tsavorite is the vanadian variety of grossular with a saturated green colour and a chemical formula of Ca_3 $(Al,V)_2Si_3O_{12}$ (Feneyrol *et al*., 2010; Adamo *et al*., 2012). Material that is less saturated is referred to as green grossular or mint green grossular (Adamo *et al*., 2012). It was first discovered in 1967 by the Scottish geologist C. Bridges in north-eastern Tanzania, with discoveries subsequently being made in the Taita Hilla of south-eastern Kenya (Feneyrol *et al*., 2013; Feneyrol *et al*., 2010). The first economic deposit was discovered in 1970 close to the Tsavo National Park in south-eastern Kenya, hence the name tsavorite. More recent occurrences of tsavorite have been discovered in the Sør Rondane Mountains of Antarctica, in Gogogogo and Behara of Madagascar, in the Swat Valley of Pakistan, in the Coat-an-Noz basin of France, in the Mogok area of Myanmar, in the Malé Karpaty mountains of Slovakia, and in the Hemlo gold mine of Canada with the latter four deposits being uneconomical (Feneyrol *et al*., 2013; Feneyrol *et al*., 2010).

Although the name tsavorite is not accepted by the International Mineralogical Association (IMA) it will be used in this report to be consistent with gemological convention (Feneyrol *et al*., 2013; Adamo *et al*., 2012).

Tsavorite has now become a highly valued economic gemstone that is primarily used in jewellery. It is highly valued due to its durability and hardness, its lack of cleavage and its chemical resistance, it's beautiful green colour (that is considered to be more vivid that emerald), its high refractive index (1.74), dispersion (0.028), brilliance, saturation, and transparency. The fact that it is also rare with only a few economic deposits worldwide further adds to its value. All the economic deposits worldwide belong to the Neoproterozoic

© University of Pretoria

Metamorphic Mozambique Belt (NMMB), with the garnets being primarily mined from south-eastern Kenya, south- and north-eastern Tanzania, and southern Madagascar (Feneyrol *et al*., 2013). The Mozambique Belt forms part of Gondwana and was formed by the deformation of crustal segments between the Neoproterozoic and Cambrian times. The deformation occurred due to a 'Himalayan type' continental collision between western and eastern Gondwanaland after the closure of the Mozambique Ocean. Most of the gems are located in the 'Gemstone Belt of East Africa' i.e. the north-south high-grade metamorphic Mozambique Belt. These gems include ruby, tanzanite (vanadian zoisite), sapphire, kyanite, tourmaline, scapolite, diopside, and garnet (tsavorite, pyrope-spessartine also known as colour change garnet, and rhodolite) (Feneyrol *et al*., 2010). The NMMB extends from Kenya through to Tanzania and also occurs in Madagascar. Mining has been more sporadic in the Swat Valley of Pakistan and the Sør Rondane Mountains of East Antarctica (Feneyrol *et al*., 2010)

2.5.4.1.1. Localities

2.5.4.1.1.1. Kenya

The first tsavorites to be discovered in Kenya occurred in 1970 in the south-eastern Mwatate area at the Mindi Range with mining beginning in 1973 in the Mgama Ridge (Feneyrol *et al*., 2013; Suwa *et al*., 1996). This area lies within the Mozambique Belt and is composed of metamorphosed politic, psammitic and calcareous sediments with intercalated thin bands of amphibolite (Suwa *et al*., 1996). All the tsavorite deposits are hosted by graphitic gneiss and is sometimes associated with ultramafic rocks that extends into the Umba district of north-eastern Tanzania. The primary mining areas are the Mgama Ridge, the Mindi Range, Mangare with the Aqua-Tsavorite-Nadan II mines, and Kuranze (Feneyrol *et al*., 2013).

2.5.4.1.1.2. Tanzania

Tsavorite was first discovered in Tanzania during the late 1960s, today, most of the commercial mining occurs in the area south of the Taita Hills. The tsavorite occurs in metamorphic rocks composed of graphite-bearing gneisses and marbles. Tsavorite occurs as rounded forms up to fist size 'potatoes' (Kane *et al*., 1990). The area occurs within the NMMB and four main economic tsavorite mining regions are found within the metasedimentary sequence, namely Umba-Kalalani and Lelatema Fold Belt situated in the north-eastern part of Tanzania, and Ruangwa and Tunduru in south-eastern Tanzania (Feneyrol *et al*., 2013).

© University of Pretoria

2.5.4.1.1.3. Madagascar

Tsavorite was first mined in southern Madagascar in the Gogogogo and Behara regions in 1991 and 1997 respectively. The tsavorite from Gogogogo occur as fractured nodules within graphitic gneiss associated with marble, and range in colour from dark green to pale yellowish green (Feneyrol *et al*., 2013). Adamo *et al*. (2012) reported some tsavorite from the village of Itrafo in central Madagascar in 2002, with the tsavorite being hosted by brecciated veins of fine-grained graphite-rich rock. The stones range in colour from greenish brown to brown-green to brownish, and yellowish green, to pure green, and are similar in terms of R.I. and S.G. to tsavorites from Gogogogo (Adamo *et al*., 2012).

2.5.4.1.1.4. Pakistan

Tsavorite is found in the Swat Valley of north-western Pakistan. It was first discovered in 1966 and later identified as vanadian grossular in the 1990s. The tsavorite is hosted in graphitic schist and occurs in pockets and as disseminated grains in graphitic schist and quartz veins (Feneyrol *et al*., 2013).

2.5.4.1.1.5. East Antarctica

Tsavorite deposits were found in the Søn Rondane Mountains of East Antarctica with the tsavorite occurring in nodules within calcareous metapelites. The nodules display zoning with the vanadium content of tsavorite increasing from the core to the rim together with manganese, iron and chromium contents. These deposits in East Antarctica, however, are uneconomic (Feneyrol *et al*., 2013).

2.5.4.1.1.6. Other localities

Tsavorite deposits have been known to occur in other regions of the world, but these deposits are uneconomical. Yellow to green vanadium-rich grossular-goldmanite has been found in calcareous metapelites and skarns in the Coat-an-Noz basin of France. This grossular-golmanite occurs as zoned porphyroblasts with a green vanadium-rich core and a yellow vanadium-poor rim (Feneyrol *et al*., 2013).

Tsavorite also occurs in skarns and amphibolites of the Nevoria gold deposit in Australia. The tsavorite occurs as goldmanite-rich grossular within skarn veins that crosscut hornblende-plagioclase amphibolites (Feneyrol *et al*., 2013).

In Myanmar, pale green grossular is hosted within the marbles of the Mogok area together with sapphire and ruby (the primary gemstone deposit within the region). These

© University of Pretoria

tsavorites are almost pure grossular with trace amounts of pyrope, goldmanite and uvarovite (Feneyrol *et al*., 2013).

Green grossulars that are both vanadium- and chromium-rich have been found in the Malé Karpaty Mountains in the Pezinok-Pernek Complex of Slovakia. The grossular occurs as porphyroblasts hosted within schists (Feneyrol *et al*., 2013).

Vandadium- and chromium-rich grossular also occurs within mica-rich schist in the Hemlo gold mine in Ontario, Canada. The grossular occurs within lenses of green mica schist with the fine-grained garnets displaying zoning of a V-rich rim and a V-poor core (Feneyrol *et al*., 2013).

2.5.4.1.2. Tsavorite geochemistry

The vanadium content is reported to be higher in the Pakistani deposits than that of the Tanzania deposits with the Mn, Ti, and Mg contents being small, but not negligible, in both localities (Feneyrol *et al*., 2013). The green to yellow and brown grossulars reported by Adamo *et al*. (2012) are characterised by a high iron content with the Fe_2O_3 content increasing in samples with a yellow or brown colour. This iron content in the samples from Itrafo, Madagascar, are considerably higher than those reported in Kenya, Tanzania, Gogogogo, and Pakistan together with a much lower vanadium content (Adamo *et al*., 2012).

2.5.4.2. Hessonite

Hessonite is the brownish orange variety of grossular named primarily based on its colour. It is applied to grossular gems that appear brownish orange in colour. Yellow-orange to reddish orange colours are also observed in hessonite gem garnets (Manson and Stockton, 1982; Stockton and Manson, 1985). Hessonite is also known as cinnamon garnet or hyacinth (Pratt, 1933; Manson and Stockton, 1982). However, little is mentioned about the degree of saturation observed in these stones (Manson and Stockton, 1982). Additionally, not much is documented about hessonite apart from its colour and identification; hence, it lacks a clear definition (Stockton and Manson, 1985). Manson and Stockton (1982) noted that there is no relationship between the V content and the strength of the yellow or orange colour. The increase in Fe_2O_3 is believed to be responsible for the yellow to orange to red-orange colour. It is inferred from the evidence in Manson and Stockton (1982) that hessonite is primarily composed of grossular (>70%).

© University of Pretoria

2.5.4.2.1. Localities

Hessonite has been found in the mica mines near Bakersville, North Carolina in America with a few of the stones being cut into gems weighing a carat or more (Pratt, 1933). Hessonite deposits also occur in Sri Lanka as alluvial deposits with the original source still unknown. However, it is known that the hessonite occurs in the Highland group in Sri Lanka. The alluvial hessonite deposit occurs in horizontal layers consisting of sand and gravel near Okkampitiya and Kataragarna (Zwaan, 1982; Mathavan *et al*., 2000).

Hessonite is also found in Quebec, Canada. It is one of the most famous of Canadian gemstones and is mined from the Jeffery mine in Asbestos. Production of asbestos started in 1881 with hessonite being discovered around 1950. The hessonites vary in colour from orange to orange brown with gems weighing more than 5 ct. being rare. Dark brown orange hessonite has also been found in the York River skarn zone of Ontario with the hessonite appearing opaque to translucent. Small amounts of hessonite were recovered from garnet-vesuvianite skarns adjacent to the Horserance Range near McDame in British Columbia. The stones possess a rich orange colour, finer than that found at Jeffery mine, and are opaque to translucent. Small, dark orange brown hessonite was found near the Horn Mountain of Yukon with the largest weighing 0.24 ct. (Wilson, 2009).

2.5.5. Grossular-andradite

2.5.5.1. Mali garnet

A relatively new garnet was discovered in the 1990s in the Republic of Mali, West Africa. These gems usually appear yellow-green to brown in colour and are composed of grossular and andradite. It first appeared in the market in 1994 and appeared yellow to green to brown in colour with properties that were similar, but not the same as grossular. These garnets are typically found in Mali, as the name suggests, but have recently also been discovered in Madagascar, Brazil, Nigeria, Namibia, Kenya, Pakistan, and Afghanistan (Johnson *et al*., 1995).

2.5.5.1.1. Localities

Mali garnets are found in the Zone of Sangafe in the Kayes region of Mali. The garnets occur in contact metamorphic zones, which consist of clay and feldspar-bearing sandstones and marbles that are intruded by diabase. Although intense green Mali garnets do occur, they are rare and yellow-green and brown varieties are more common. The brown varieties include brownish greenish yellow, dark orangy brown and brown-orange (Johnson

© University of Pretoria

et al., 1995). The R.I. ranges from 1.752-1.769 for yellow green and green stones and 1.773-1.779 for orangy brown varieties in Johnson *et al*.'s (1995) study.

All the stones examined in the paper by Johnson *et al*. (1995) were grossular-andradite with compositions of roughly $Gr_{80}And_{18}Py_2$ and Fe present as Fe^{3+}. Grossular was the dominant component followed by andradite and minor amounts of pyrope. It is believed that the Fe^{3+} colours the stones except in the intense green varieties, where chromium and vanadium possibly influence the colour. The characteristics of the Mali garnets studied by Johnson *et al*. (1995) are what one would expect from a stone between the end-members of grossular and andradite, with slight deviations corresponding to the minor amounts of pyrope, spessartine, or uvarovite that is sometimes present. Although the proper mineralogical name for Mali garnets is grossular due to the high grossular component (>50 mol. %), in the gem trade, it is always referred to as Mali garnet. However, the GIA Gem Trade Laboratory refers to it as grossular andradite as it lies between the two end-members (Johnson *et al*., 1995). In this report, the term Mali garnet is used to avoid confusion with other grossular gemstones.

2.5.6. Pyrope

Pyrope is a purplish red through to reddish orange and colourless variety of garnet with the chemical formula of $Mg_3Al_2Si_3O_{12}$ (Stockton and Manson, 1985; Stockton, 1988). Pure pyrope appears colourless but does not occur in nature. However, almost-pure colourless pyrope (98 mol. %) has been found in the western Alps but is too fractured or too small to be of gem-quality (Stockton, 1988). The colour of pyrope gems varies considerably with some displaying characteristics similar to almandine, spessartine or both. However, dark red pyrope stones of gem-quality more commonly occur in nature (Stockton and Manson, 1985). The pure red to orange-red colours are due to the presence of trace amounts of chromium with some iron (Gemstone Magnetism, 2014).

2.5.6.1. History

The name 'pyrope' is derived from the Greek word 'pyropos' meaning fiery red (Stockton, 1988). Pyrope was first mined in Czechoslovakia during the 16th century. It was initially mined in Bohemia (now a province of Czechoslovakia) giving rise to the common term 'Bohemian Garnet'. Today, only one deposit in Czechoslovakia is mined in the Bohemian Hills. During the Middle Ages, pyrope was initially recovered from the surface after heavy rainfall or sifted and washed out of material dug from relatively shallow pits. Bohemian garnets became popular in Victorian jewellery in the 1880s, but production began

© University of Pretoria

to decrease at the beginning of the1900s due to a change in fashion and the economic depression in the 1920s. It ws not until recently that pyrope became popular once again in western Europe and the rest of the world (Schlüter and Weitschat, 1991).

2.5.6.2. Properties

The R.I. of pyrope ranges from 1.714 to 1.74 (Stockton and Manson, 1985). The colouring agents in pyrope are Fe^{2+} and/or Mn^{2+} with an increase in Mn producing a deeper orange colour. Pyrope that appears lighter will have a refractive index that is closer to that of the pure end-member with high S.G. values correlating with high iron content present in the stone (Stockton, 1988; Guastoni *et al*., 2001). Pink pyrope is due to the presence of trace amounts of chromium with small amounts of Mn^{2+} and/or Fe^{2+} (Stockton, 1988). Pyrope garnets are predominantly composed of Mg with small amounts of Fe^{2+}, Mn^{2+} and trace amounts of chromium (Stockton, 1988; Schlüter and Weitschat, 1991). Chromium-rich pyrope gems from Czechoslovakia have shown a change in colour from daylight to incandescent light changing from green to red-violet. The colour change is similar to that observed in alexandrite and is termed the alexandrite effect. Pyropes from Norway have also been reported to display an alexandrite effect appearing violet in daylight and wine-red in incandescent light. This change in colour generally occurs in pyrope gems with a Cr_2O_3 content between 6% and 7%, depending on the total composition of the garnet (Carstens, 1973).

2.5.6.3. Localities

2.5.6.3.1. Czechoslovakia

As mentioned above, pyrope is still mined in the Bohemian Hills of Czechoslovakia outside the village of Podsedice. The pyrope occurs as alluvial deposits in garnetiferous gravels along the southern slope of the Bohemian Hills. The original host rocks are serpentinised garnet peridotite formed in the mantle that has been emplaced in the upper crust. At the Linhorka pipe, serpentinised garnetiferous peridotites can be found that are rich in gem-quality pyrope. Since the Miocene, much of this rock has been eroded away with the volcanic components being decomposed and the resistant components being transported to the alluvial gravels where the pryope is mined today (Schlüter and Weitschat, 1991).

A chemical analysis of the Bohemian pyropes shows little variability with high amounts of Mg and Al and small amounts of Fe^{2+} and Cr^{3+}; similar to that observed for chrome pyrope from other localities. The pyropes appear predominantly red in colour with fire-red samples containing relatively high amounts of Cr_2O_3 between 1.5 and 2.5 wt. %. Cut

© University of Pretoria

stones are small, approximately 0.1 ct. The R.I. of the pyropes is between 1.748 and 1.75 with no inclusions and impurities present (Schlüter and Weitschat, 1991).

2.5.6.3.2. Italy

From the 1990s, large pyrope crystals have been recovered from the Varaita Valley in the Dora Maira Massif in the Western Alps of Italy. The stones are of gem-quality but are smaller than 1 ct. The deposit is extensive, although large-scale mining is not possible due to environmental restrictions. The pyrope is hosted in a light coloured phengitic-schist-quartzite layer, with the quartzite layer containing the pyrope crystals. These pyrope stones appear pale purplish pink in colour and have near end-member composition (87.8-97.5 mol. % pyrope) with darker stones corresponding to higher ferrous iron content. The R.I. values range from 1.717 to 1.730 and correlate with the iron content. The S.G. values range from 3.58 to 3.67, with the lowest values corresponding with the palest stones, and the highest values corresponding with high iron concentrations. Inclusions of ellenbergerite (a silicate of magnesium, titanium, zirconium and aluminium) have also been found, which is indicative of this locality (Guastoni *et al*., 2001).

2.5.6.3.3. East Africa

Chromium- and iron-poor pyrope (70 mol. %) has been found in east Africa together with grossular and Malaya garnet. The pyrope appears orange to pink in colour and ranges in size from 2 to 5 ct. (Stockton, 1988).

2.5.6.3.4. Canada

Bright red pyrope has been found in Canada as an accessory mineral of kimerlites being analysed for their diamond potential. Some of these stones may be large enough to yield gem-quality pyrope. Small pyrope stones were recovered from the Ekati diamond mine and, when cut, produced gems weighing up to 0.10 ct. (Wilson, 2009).

2.5.6.3.5. China

Chrome-rich pyrope has been found in the Quaternary alluvial deposits near Donghai in eastern China. The garnets originated from diamond-bearing kimberlites 130 km northwest of Donghai. The stones appear dark red in colour and are small (<1 cm in diameter). They are transparent and display a change in colour from purple to red between daylight and incandescent light due to the chromium content. Pyrope was also found together with sapphire and zircon, in the Fujian Province (Keller and Fuquan, 1986).

© University of Pretoria

2.5.6.3.6. America

Pyrope appearing blood-red in colour occurs in the sands of the gold washing of the Burke, McDowell and Alexander Counties of North Carolina, America (Pratt, 1933)

2.5.7. Pyrope-almandine

2.5.7.1. Rhodolite

Rhodolite is a member of the pyrope-almandine series and appears slightly purplish red to red purple in colour (Dirlam *et al*., 1992; Stockton and Manson, 1985). It was assigned the name 'rhodolite' owing to its 'delicate rose-like color' by Hidden and Pratt (1898) who noted a new variety of garnet in western North Carolina that was both beautiful and unique. A chemical analysis of the stone showed a 2:1 ratio of MgO to FeO suggesting that the stone is not almandine or completely a pyrope (Hidden and Pratt, 1898). However, the name rhodolite has come under scrutiny in recent times (Martin, 1970) as more rhodolite deposits have been discovered in Africa, and its similarity in sound and spelling to rhodonite (a silicate mineral) has produced further debate on the terminology and definition of the different garnet varieties (Stockton and Manson, 1985; Zwaan, 1974). Stockton and Manson (1985) suggest that rhodolite refer to purplish-red pyrope-almandine whereas red stones possessing similar properties are referred to as pyrope-almandine (Stockton and Manson, 1985). Nontheless, it will be difficult to remove the name rhodolite from the industry as it has been thoroughly incorporated into the gemology world (Zwaan, 1974). For the sake of convenience, the term 'rhodolite' will be used in this report.

2.5.7.1.1. History

Martin (1970) reported rhodolite gems from unknown localities with an average R.I. of 1.747, lower than the R.I. of 1.758 for the rhodolite gems from North Carolina. Stockton and Manson (1985) noted that the only difference between rhodolite and other varieties from the pyrope-almandine series is the colour of the stone (Zwaan, 1974).

2.5.7.1.2. Properties

Rhodolite appears generally rose-red in colour as well as purplish red (Zwaan, 1974; Stockton and Manson, 1985). The chemical composition usually lies between pyrope and almandine, but tends to have a higher pyrope component. Rhodolite with low R.I. and S.G. corresponds with low Fe and high Mg content and *vice versa.* The Ti and Cr contents are generally low for rhodolite. Rhodolite gems are generally clean similar to that of pyrope gems, with rutile appearing as an inclusion (sometimes). Rhodolite shares the same

© University of Pretoria

properties as pyrope and almandine with the only difference being its rose-red colour (Zwaan, 1974).

2.5.7.1.3. Localities

2.5.7.1.3.1. East Africa

Rhodolite has become popular in recent times and occurs in various localities with the most recent being Tanzania (Stockton and Manson, 1985; Seifert and Hyrsl, 1999). The rhodolite occurs in the Precambrian metamorphic rocks of Tanzania with the Umba deposits being alluvial in nature along the Umba River. Tanzania possesses economic deposits of rhodolite that have been mined since 1964 in the Umba region. Rhodolite ranges in colour from dark red to purplish red to reddish purple. Rhodolite has also been found in Komolo and Kangala, with the latter producing raspberry red stones. Stones with a darker hue, occurring as pebbles are recovered from Tiriri in northeast Tanzania. Rhodolite also occurs in Nyorinyori and Nyamberera with *in situ* material recovered from Handeni appearing light reddish purple in colour (Dirlam *et al*., 1992).

Rhodolite deposits were also found in the Landaban Rhodolite mines near Mt. Kilimanjaro with the rhodolite hosted in granitic pegmatite (Berg and Cooney, 2006).

Rhodolite has been recovered from the Kalalani area of Tanzania in the Peter A. claim. The colour of the stones ranges from dark red to purplish red. The R.I. ranged from 1.763 to 1.770 with the purple red stones being regarded as rhodolite (Seifert and Hyrsl, 1999).

The Umba deposits contain pink-purple rhodolite in alluvial deposits whereas the deposits of Kalalani are mined from primary deposits. The rhodolite gems from Umba are pink purple in colour, while the Kalalani deposits contain both pyrope-almandine and rhodolite with the former being dark red to brownish red to dark red in colour (Seifert and Hyrsl, 1999).

2.5.7.1.3.2. Canada

Rhodolite deposits have been found near Passmore in Canada with the garnets occurring as placer and primary deposits. The stones appear medium red to pinkish red in colour with the largest stones weighing up to 3 ct. and are cranberry red to intense pink in colour (Wilson, 2009).

© University of Pretoria

2.5.7.1.3.3. China

Rhodolite has also been reported in China (Kellar and Fuquan, 1986).

2.5.8. Spessartine

Spessartine, also known as spessartite, is a manganese-aluminium garnet ranging in colour from yellowish orange to aurora red or brownish red appearing similar to and often being mistaken for hessonite (Anderson, 1976; Webster, 1962). The formula is $Mn_3Al_2Si_3O_{12}$ but the substitution of some of the Mn^{2+} by Fe^{2+} often occurs (Webster, 1962).

2.5.8.1. History and Properties

It was first discovered in Aschaffenburg in the Spessart district of Bavaria, hence the name spessartine (Webster, 1962). Spessartine was not known before the 19th century but has become popular in recent times due to its colour (Laurs and Knox, 2001; Anderson, 1976). Typically, its composition lies close to its theoretical composition, although spessartine can often mix with almandine causing its yellow-orange colour to become more red (Anderson, 1976). Its hardness is just above 7 on the Mohs's scale and its refractive index lies between 1.79 and 1.81 (Anderson, 1976; Webster, 1962). Its refractive index has since been revised by Stockton and Manson (1985) to be between 1.78 and 1.81. Crystals often display an etched pattern, making this a characteristic of spessartines (Anderson, 1976; Webster, 1962).

2.5.8.2. Occurrence

Spessartine is usually recovered from granitic pegmatites and not metamorphic rocks (Anderson, 1976). Famous localities include Madagascar, Brazil, and the United States of America. Spessartine is also found in Norway and Italy, but the stones from the latter are too small to be cut into gemstones (Webster, 1962).

2.5.8.3. Localities

2.5.8.3.1. America

Intense orange spessartine has been sourced from the Little Three Mine in Ramona, San Diego County, California. The stones from Ramona appear bright orange yellow to yellow orange in colour and were the primary source of gem-quality spessartine until the 1990s, when gem-quality spessartine was discovered in Namibia and Nigeria.

© University of Pretoria

The Little Three Mine is a pegmatite mine that was first discovered in 1903 with mining halting for the next forty years after 1912 due to the collapse of the Chinese tourmaline market. Intensive mining began in 1955 with the best gem-quality spessartine coming from the Hercules-Spessartite and Spaulding mines. The largest cut spessartine recovered from the Ramona district was a 39.63 ct gemstone. Since 1997, no significant mining has occurred within the area and approximately 40 000 carats of gem-quality spessartine have been collected from the Ramona region (Laurs and Knox, 2001).

Spessartine also occurs in Alto Mirador in north-eastern Brazil (Laurs and Knox, 2001). The stones appear light yellow-orange to medium brown-orange and have the etched pattern common in spessartine (Laurs and Knox, 2001, Anderson, 1976; Webster, 1962). No eye-visible zoning occurrs and few inclusions are found. The R.I. ranged from 1.799 to 1.808 with the lightest stones having the lowest R.I. values. It was noted that the manganese content decreased and the ferrous iron content increased with a change in colour from light orange-yellow to medium yellow-orange. The composition of the spessartine was close to the spessartine end-member composition with trace amounts of titanium and calcium and very low to no magnesium, which is typical of granitic pegmatites. The Ramona spessartine can be differentiated from the spessartine of other localities by its intense orange yellow to yellow orange colour (Laurs and Knox, 2001).

2.5.8.3.2. China

Spessartine is also found in the Altay Mountain Range of China, and appears similar to those found in Brazil and Virginia, America (Wang and Liu, 1993; Keller and Fuquan, 1986). Gem-quality spessartine was first discovered in China in 1950 in the Qibeiling mine (Wang and Liu, 1993).

The spessartine occurs in the replacement zones within the inner part of pegmatite. Two different generations of spessartine occur, with the first being small, heavily included and not of gem-quality. The second generation is of gem-quality and is sourced from the first generation, which was dissolved and redeposited (Wang and Liu, 1993).

The spessartine appears brown to red-brown in colour with R.I. values between 1.805 and 1.811 and S.G. values between 4.20 and 4.25. The composition of the spessartine is close to the end-member composition with the almandine component being the second most dominant component. The iron present is predominantly Fe^{2+} with the colour changing from orange to orange-red as Fe^{2+} increases together with the R.I. and S.G (Wang and Liu, 1993).

© University of Pretoria

2.5.8.3.3. England

Spessartine was discovered in the Calcareous Group of Devonshire appearing as small golden yellow spessartine crystals. The stones occur in the basal bed of the Calcereous Group. A chemical analysis of the spessartine showed predominantly spessartine (74.7 %) with lesser amounts of grossular (11.2%) and pyrope (7.9%) (Howie, 1965).

Redder spessartine was found in the Meldon B.R. Quarry in quartz-garnet veins and is a rare mix of spessartine and grossular. This type of spessartine occurs in metasomatic calc-silicate assemblages and garnet-quartz rocks. This is the first recorded occurrence of spessartine to be discovered in England (Howie, 1965).

2.5.8.3.4. Pakistan

Spessartine has been found the Himalayan region of Pakistan in granitic pegmatites (Jan *et al*., 1995). The garnet is found in the Neelum Valley in Azad Kashmir where pegamatites intrude the Precambrian basement and the cover rocks. Spessartine occurs in potash feldspar and is well developed. It has been estimated that, since 1994, up to 40 kg of gem-quality garnets have been recovered. The crystals range in colour from yellow-red, to tangerine to intense crimson red with no fractures, inclusions or alteration. The average R.I. is 1.80 and the dominant end-member component is spessartine with lesser amounts of almandine and grossular. No pyrope or andradite component was reported (Jan *et al*., 1995).

2.5.8.3.5. Canada

An undisclosed location in Yukon has yielded a bright orange spessartine that, when faceted, weighed 0.34 ct. and is moderately included. There is a potential for spessartine gems in Canada, possibly of gem-quality, but more research needs to be performed (Wilson, 2009).

2.5.8.3.6. Africa

Orange spessartine garnet deposits occur in Namibia and Zambia. Production from the Kunene area of Namibia declined at the end of the 1990s, however, new deposits of larger and cleaner spessartine were discovered in Nigeria (Shigley *et al*. 2000; Shigley *et al*., 2010). Recently, a new discovery of significant spessartine was found in Tanzania near the Kenyan border at Loliondo (Shigley *et al*., 2010).

© University of Pretoria

2.5.9. Pyrope-spessartine

Pyrope-spessartine garnets contain, as the name suggests, pyrope and spessartine. The R.I. lies between 1.742 and 1.78 and the gems can appear anywhere from greenish yellow to purple in colour (Stockton and Manson, 1985). Some can display a distinct change in colour between daylight and incandescent light (Schmetzer *et al*., 2001; Crowningshield, 1970). However, whether pyrope is actually the dominant component in this species is still uncertain (Dirlam *et al*., 1992, Schmetzer *et al*., 2001, Schmetzer *et al*., 2002).

Pyrope-spessartine can be divided into two types: Malaya garnets and colour change garnets. Malaya garnets appear yellowish orange to red orange in colour, while colour change garnets display a distinct change in colour between daylight and incandescent light (Stockton and Manson, 1985). The exact differences that separate Malaya garnets from colour change garnets are hard to pin point as Malaya garnets can also display a distinct change in colour between daylight and incandescent light (Schmetzer *et al*., 2001). Their R.I. and chemical composition are similar and their colour is too variable to make a distinction between the two. There are also pyrope-spessartine gems that do not display any difference in colour between daylight and incandescent light; making the matter even more complicated (Schmetzer *et al*., 2001). Further confusion arises as the exact definition of colour change and colour shift are not specified and various literature sources are inconsistent in what they classify as colour change and colour shift.

2.5.9.1. Malaya garnet

Malaya garnets are of the pyrope-spessartine solid solution series with significant amounts of almandine and grossular and appear red, pink, pinkish red, orange, brownish pink, orangey red, brownish orange and near-colourless in colour (Gemstone Magnetism, 2014; Dirlam *et al*., 1992; Stockton and Manson, 1985). It is named Malaya after the Swahili language of Tanzania meaning ‘outcast’ or ‘out of the family’ as the properties of this stone do not fit into the traditional garnet categories. It was first discovered in the mid-1960s in the Umba River, Tanzania, where it was initially thought to be a spessartine when miners were mining rhodolite (Dirlam *et al*., 1992). The chemistry of Malaya garnets is highly variable with many disputes arising as to its exact composition (Stockton and Manson, 1985; Schmetzer *et al*., 2001; Schmetzer *et al*., 2002). Stockton and Manson (1985) considered Malaya garnets to be pyrope-spessartine.

© University of Pretoria

2.5.9.1.1. Localities

2.5.9.1.1.1. Tanzania and Kenya

Malaya garnets were first discovered in the Umba Valley, Tanzania and were termed 'Umbalite' owing to the location. These garnets appear red-orange to yellow-orange in colour under daylight. It is found in alluvial deposits along the Umba River, as well as several plains along the border between Tanzania and Kenya (Dirlam *et al*., 1992).

2.5.9.1.1.2. Bekily, Madagascar

Malaya garnets were also found in Bekily, Madagascar in 1997. These garnets are generally pink to pinkish orange in colour under daylight with the less common orange red variety and displays a distinct colour-change to a reddish-orange or reddish-pink in incandescent light. These garnets are pyrope-spessartine with smaller amounts of almandine component and trace amounts of vanadium and chromium. It was observed that the andradite component in most of these garnets was very small or absent due to the small amounts of iron in the trivalent state present in the samples (Schmetzer *et al*., 2001).

It was noted by Schmetzer *et al*. (2001) that an increase in the Fe^{2+} content (almandine component) intensified the colour of the samples from very light pink to an intense pink or almost red colour. The trace amounts of chromium and vanadium are also attributed to the pink colour in the garnets. Higher manganese content, together with low iron, has resulted in a deeper orange colour and can appear similar to the colour of the end-member spessartine. The lack of manganese in garnets leads to a purplish-pink to purplish-red colour in the stones, however, much of the Bekily Malaya garnets contain small amounts of MnO, thus giving the samples an intense red colour rather than purple. Two other mechanisms are known that can cause the colour change from purplish-red or purplish-pink to orange-red or red: 1) when the chromium spectrum is superimposed over the iron-related absorption bands and 2) when Fe^{3+}-related absorption bands are superimposed over the Fe^{2+}-related spectrum. The refractive index of the Bekily garnets ranges from 1.739 to 1.782 (Schmetzer *et al*., 2001). Some garnets from Bekily are shown in Figure 3.

© University of Pretoria

Figure 3. Malaya garnets from Bekily, Madagascar (Schmetzer *et al*., 2001).

2.5.9.1.1.1. Comparison of Malaya garnets from Tanzania with those from Madagascar

The Malaya garnets from East Africa possess a more intense orange, yellowish-orange or pinkish-orange colour when compared to those from Bekily, Madagascar, which are more pinkish-orange with the yellowish-orange and orange varieties being less common. The Bekily garnets have a smaller variation in chemistry compared to the Malaya garnets from Tanzania. According to Schmetzer *et al*., (2001) only a small portion of the garnets from the Umba Valley actually conform to the composition that represents the Bekily garnets, with the Umba Valley samples containing significantly higher amounts of manganese than those from Bekily. In addition, the Umba Valley Malaya garnets lack negative crystals and graphite platelets as inclusions that are commonly observed in the Bekily garnets (Schmetzer *et al*., 2001).

2.5.9.2. Colour change garnet

2.5.9.2.1. Properties

Colour change garnet gemstones were discovered in the Umba valley and Tunduru-Songea, Tanzania; Athiliwewa and Embilipitiya, Sri Lanka; Nigeria; Afghanistan, and Ilakaka and Bekily, Madagascar with the latter containing commercial quantities. These garnets, with a typical refractive index of 1.742 to 1.78, are a special case of pyrope-spessartine with minor amounts of iron, vanadium and chromium, which shows a distinct change in colour between different illuminations. It is believed that the vanadium and/or chromium contents play a major role in the colour change phenomenon, but manganese and iron should not be discounted. The change in colour observed in garnets varies with localities with those from Madagascar appearing blue green, yellowish green or greenish yellow in daylight, and purple and intense pink under incandescent light. Other colour changes from different localities reported include pink to purple, orange to pink, orange to yellow and red to orange (Dirlam *et al*., 1992; Stockton and Manson, 1985; Schmetzer *et al*., 2009; Gemstone Magnetism, 2014; Krzemnicki *et al*., 2001). Most colour change stones from Madagascar

© University of Pretoria

reported a higher vanadium than chromium content with only a few being chromium-rich (Schmetzer *et al*., 2009; Krzemnicki *et al*., 2001). Those samples that were chromium-rich were analysed by Schmetzer *et al*. (2002) and appeared brownish purple red in daylight and purplish red under incandescent light (Schmetzer *et al*., 2002; Schmetzer *et al*., 2009).

The spessartine component can vary, Krzemnicki *et al*. (2001) have reported spessartine from 30.5% to 80.1% and Schmetzer *et al*. (2009) reporting spessartine from 22.96% to 73.83%, highlighting the variability in chemistry observed in colour change garnets (Schmetzer *et al*., 2009; Krzemnicki *et al*., 2001).

2.5.9.2.2. Localities

2.5.9.2.2.1. Tanzania

Crowningshield (1970) examined a colour change garnet from northern Tanzania. It had a refractive index of 1.765 and appeared blue-green in daylight and purple-red in incandescent light. It tested as an isomorphous mixture of pyrope and spessartine, with vanadium and/or chromium believed to be the cause of the distinct colour change in the stone. However, Crowningshield (1970) concluded that the relationship is too complex and not well understood, thus requiring further research.

Jobbin *et al*. (1975) also reported a colour change garnet that displayed a distinct colour change between daylight and incandescent light. It appeared greenish blue in daylight and magenta by tungsten illumination. It was also a pyrope-spessartine with trace amounts of vanadium, but no chromium, present (Manson and Stockton, 1984).

2.5.9.2.2.2. Madagascar

Schmetzer *et al*. (2009) looked at colour change garnets from Madagascar with an emphasis on the chemical, spectroscopic, and colorimetric properties thereof. A total of 52 garnets were investigated with most of the garnets coming from Bekily and only a few coming from Ilakaka. They also included four vanadium- and chromium-free pyrope spessartine Malaya garnets from Bekily (Schmetzer *et al*., 2009).

All the stones were members of the pyrope-spessartine solid solution series with the iron content ranging from minor to major, and trace amounts of chromium (uvarovite) and vanadium (goldmanite) being present. No direct correlation was observed between the different colours of the groups and their chemistry, especially referring to the Mn (spessartine) content. However, it was noted that samples appearing green, bluish green, and greenish blue in daylight had higher vanadium and chromium contents than the yellow

© University of Pretoria

to reddish orange samples in daylight. Violet, purplish red and purple samples in daylight had relatively high vanadium and chromium contents, but also high iron contents. The red samples in daylight had the lowest vanadium and chromium contents and very high iron content. Schmetzer *et al*. (2009) observed that the replacement of magnesium by calcium in garnet influences the colour of the garnet even though magnesium and calcium are not colour-causing agents. Schmetzer *et al*. (2009) concluded that there are no simple parameters that can be used to predict colour and colour change in garnets. It was deduced that vanadium and chromium were primarily responsible for the colour difference observed between different illuminations, but a large range of minor elements in garnets can also cause a change in colour and therefore need to be accounted for (Schmetzer *et al*., 2009).

Krzemnicki *et al*. (2001) looked at 24 colour change garnets from Madagascar in terms of their chemistry and colorimetric properties. They noted that the variation in RI was due to the replacement of magnesium by manganese and a correlation was observed between the chemistry and RI. All of the samples were members of the pyrope-spessartine solid solution series with minor, but significant, amounts of grossular and smaller iron contents. All the iron was present as Fe^{2+} but small amounts of Fe^{3+} are possible. All of the samples contained vanadium and chromium with vanadium being higher than chromium by a factor of 2 to 5. Krzemnicki *et al*. (2001) concluded that the relationship between chemistry and colour, and colour change is very complex, although vanadium and some chromium were believed to be the main influence. Some vanadium-poor samples displayed large degrees of colour change, whereas some vanadium-rich samples displayed a slight colour change. Garnets with no vanadium and/or chromium show no colour change. Samples with an MgO/MnO ratio of ~ 1 are potential colour change garnets. When they possess low vanadium and/or chromium contents, only a slight to moderate colour change (green to pink) is observed. Vanadium contents higher than 0.5 wt. % produce a moderate to distinct colour change from blue in daylight to purple in tungsten light. However, there is a threshold where, if the vanadium content increases above 1.60 wt. %, slight or no colour change is observed. This could explain the absence of colour change in vanadium-rich pyrope-spessartine, as the lattice parameters are slightly modified by the goldmanite when the vanadium is above the critical value. As Mn increases, the potential for colour change decreases (Krzemnicki *et al*., 2001).

Furthermore, pyrope-spessartine garnets with a distinct colour change from blue-green to purple are known to occur in Bekily. These garnets possess similar features to the Bekily Malaya garnets, with the only difference being the higher chromium and vanadium contents in the samples as compared to the Malaya garnets. This is also attributed to the

© University of Pretoria

distinct colour change observed in these special colour-change garnets (Schmetzer *et al*., 2001).

2.5.9.2.2.3. Tranoroa, Madagascar

Schmetzer *et al*., (2002) tested pyrope-spessartine garnets from Tranoroa, located some 60km southwest of Bekily, Madagascar. These samples displayed a colour change from brownish-purple in daylight light to purplish-red in incandescent light. The refractive indices ranged from 1.768 to 1.773, which falls within the range for Malaya garnets from the same locality. The specific gravity of these samples had a small range indicating a very narrow range of chemical composition between the end-members pyrope, almandine and spessartie. It was noted that these samples have relatively high vanadium and chromium contents with Fe^{3+} content being very low or absent. These samples showed features similar to those of the V>Cr-bearing colour-change garnets from Bekily. However, there were some samples that possessed a higher Cr-content relative to V-content and these samples displayed a different colour behaviour compared to the rest of the samples. The Tranoroa samples also had a relatively high Mn content and this, together with the vanadium and chromium content differences, explains the difference in colour behaviour of the Tranoroa samples compared to the Bekily samples. Some of the garnets from Tranoroa are shown in Figure 4 (Schmetzer *et al*., 2002).

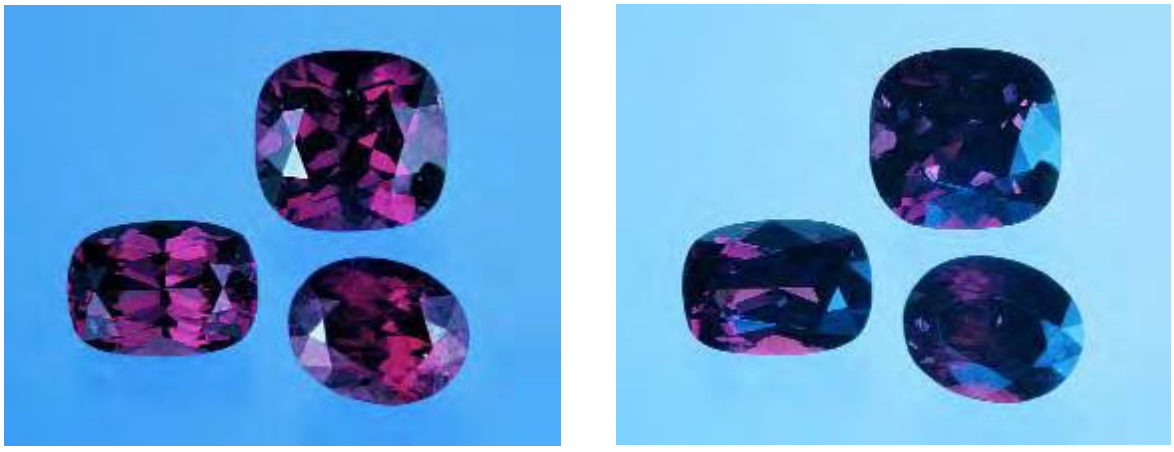

Figure 4. Colour change pyrope-spessartines occurring in a metamorphic belt consisting of high-grade Precambrian metamorphic rocks in Tranoroa, Madagascar. Left shows the stones under fluorescent light and right under incandescent light (Schmetzer *et al*., 2002)

2.5.9.3. Conflict

As can be seen from the above-mentioned sources, the classification of Malaya and colour change garnets is still a problem today (Stockton and Manson, 1985). Although

© University of Pretoria

Malaya garnets are recognised as predominantly pyorope-spessartine garnets of the garnet solid-solution series, their large variation in chemistry, together with variable and strange colour behaviour, makes it difficult to classify these gemstones (Dirlam *et al*., 1992, Schmetzer *et al*., 2001; Schmetzer *et al*., 2002). This, together with the similarities observed in colour change garnets makes it almost difficult at times to distinguish between the two. Another question that should be asked is, "What is the difference between Malaya garnets and colour change garnets?" Both Malaya garnets and colour change garnets have a similar composition, similar refractive indices, and both display strange colour behaviours and colour changes. Hence, what really is the difference between the two, apart from the observed difference in colour? (Manson and Stockton, 1984)

The Malaya garnet samples in this thesis were classified based on their chemistry as either pyrope-spessartine (pyrope dominant) or spessartine-pyrope (spessartine dominant). Stones that displayed a change in colour were assigned 'II' after their name and those that did not display a colour change were assigned a 'I' after their name.

3. Methodology

A total of 1513 faceted garnet gemstones including pyrope, almandine, spessartine, spessartine-almandine, pyrope-almandine, rhodolite, Malaya garnets, colour-change garnets, Mali garnets, demantoid, tsavorite, and hessonite were analysed. The colour of the stones were observed under daylight as well as incandescent light (a filament torch). A digital scale was used to weigh the gemstones and to measure the magnetic susceptibility (see below).

3.1. Weighing of Stones

A Diamond scale was used to weigh the stones. It was calibrated against the 50 ct. and 25 ct. weights supplied with the scale.

3.2. R.I.

A refractometer with a 1.81 liquid was used to measure the refractive index of the stones. It is accurate to two decimal places with the third decimal place interpolated by eye. The R.I. was checked against minerals with R.I. values that show little variation e.g. quartz (R.I. of 1.544 to 1.553), apatite (R.I. of 1.628 to 1.650), beryl (R.I. of 1.563 to 1.620), chrysoberyl (R.I. from 1.740 to 1.777), danburite (R.I. from 1.627 to 1.639), sillimanite (R.I. from 1.654 to 1.683), topaz (R.I. from 1.609 to 1.643), corundum (R.I. from 1.762 to 1.770) and fluourite (R.I. from 1.432 to 1.434).

© University of Pretoria

3.3. Colour

When the colour of a sample was determined, the equipment required to measure colour quantitatively was not available. It was originally planned to be used, but the instrument became unavailable. Colour was then identified subjectively. The Munsell colour system was not used as the attempt of colour identification was beyond the scope of this thesis. Just a general indication of colour was needed. In the present gem trade, except for a small selection of sellers and gem labs, the Munsell colour system is not used and only an approximate colour is given.

When looking at colour change and colour shift, a systematic approach was used. Despite Schmetzer *et al*. (2009) deeming that the term 'colour shift' be abandoned, it was used in this thesis because the term 'colour shift' is often used to describe gemstones in the literature (Stockton and Manson, 1985; Krzemnicki *et al*., 2001) and trade. Garnets that displayed only a slight change or shift in hue e.g. red to red-purple were considered colour shift garnets. Garnets that displayed a complete change in colour between different lighting, e.g. purple to green, were considered colour change garnets.

When describing the colour of a sample, the following method was used. All samples were viewed in daylight, as well as in a well lit room. If a stone showed a colour that could not be defined by a single colour, e.g. a colour between purple and pink, then the stone would be named purple pink. Purple would be placed first in the name if the stone appeared more purple than pink. If the stone appeared more pink than purple, then the stone would be pink purple in colour. Samples were also viewed under incandescent light (torch light; both LED and a filament torch) to observe colour change or colour shift.

3.4. Sample Acquisition

A collector provided the gem samples for this study. In referring to whether the sample set was representative as a valid statistical sample, various factors had to be observed. All of the garnets were cut and polished and bought through sellers listed on eBay between 2008 and 2014. Only a few of the stones were certified by a range of commercial laboratories in Thailand before shipping (AIGS, Tokyo Lab, EMIL). This was predominant in the larger and more expensive stones. To be classified as a valid statistical sample, the garnets would have to be random, unbiased, reproducible and representative. The following criteria were used when purchasing the gemstones:

- Trustworthy sellers (eBay, 2015) with a good track record together with an evaluation of historically neutral and negative comments,

© University of Pretoria

- If the clarity was VVS or better with only a few exceptions (eye clean and if inclusions are present, they are only visible under at least 10 x magnification),
- If the quality of the cut was acceptable based on the opinion of the buyer
- With an inclination for colour change or colour shift stones and
- Bought by a price conscious buyer.

3.5. Magnetic Susceptibility

As demonstrated by Hoover and Williams (2007), the magnetic susceptibility of garnets can be easily measured. Different gemstones have different magnetic susceptibilities and this can be used as a means of characterisation. This was done in this study based on the research of Hoover *et al.* (2008) and Hoover and Williams (2007). The method of measuring magnetic susceptibility involves the use of a digital scale to weigh the cut gemstones, a rare earth element magnet and a device to lift the gemstone slowly towards the magnet to determine the force of attraction between the magnet and the sample. More detail on the technique involved for measuring magnetic susceptibility is available in the appendix (Section 9.1.).

3.6. Chemistry

The Thermo Scientific Niton FXL 959 FM-XRF analyser was used to chemically analyse the stones. The desktop model is an energy dispersive instrument with the X-ray tube SN 55658-0051, the maximum voltage and maximum power were 50 kV and 4 W respectively (Thermo Scientific, 2011).

The Niton FXL is an analytical instrument that employs X-ray fluorescence for elemental analysis of samples of various matrices. The main advantage of this instrument is its non-destructive quantitative analysis in ppm or wt. % of 40 elements (Ba, Sb, Sn, Cd, Pd, Ag, Mo, Nb, Zr, Bi, Pb, Hg, Se, Au, Pt, Zn, Cu, Ni, Co, Fe, Mn, Cr, V, Ti, Al, Sr, U, Rb, Th, As, W, Sc, Ca, K, S, Cs, Te, Nd, Pr, Ce, La, Y, Cl, P, Si and Mg) in any sample (Thermo Scientific, 2011). The instrument reported iron as Fe^{2+} and not Fe^{3+}. Calculating the Fe^{3+} content was not necessary as the spreadsheets used to calculate the end-member proportion for garnets calculates the Fe^{3+} content from the Fe^{2+} content (refer to Section 3.7.).

Details on the calibration and reproducibility are available in the appendix (Section 9.2.).

© University of Pretoria

After analyses of all the garnet gemstones were carried out, the analyses were converted to oxide concentrations and were normalised to 100 wt. % as the total percentages fell slightly short of 98-102 wt. %. The spectrum (approximately 100 %) includes background and other counts not allocated to specific elements. The sum of the counts allocated to elements falls short of 100 %. The results were normalised to 100 % to compensate for differences in unallocated counts. The results were taken as reported because, in the data recalculation software, the non-allocated counts are not considered and have no effect on proportions of elements in the analysis.

The analyses, after normalisation, were entered into an Excel spreadsheet from The Open University (2015). The spreadsheet was designed based on 12 oxygens with Fe^{2+}/Fe^{3+} calculated assuming full site occupancy and follows the calculation procedures of Rickwood (1968).

3.7. Calculation Sequence

The calculation procedures from Grew *et al*. (2013) (Table 5), Locock (2008) (Table 6), and Rickwood (1968) (Table 7) were compared and can be seen in the tables below.

Table 5. The end-member proportions of a rhodolite, spessartine-grossular and Mali garnet are calculated according to Grew *et al*. (2013). The iron and manganese were input as FeO and MnO with the spreadsheet calculating the proportions of the divalent and trivalent Fe and Mn required for charge balance.

		Grew *et al.* (2013)	
	Mali Garnet	**Rhodolite**	**Spessartine-grossular**
	050358*b	**642963a**	**860203-3**

© University of Pretoria

SiO_2	41,25	41,35	45,36
TiO_2	0,55		0,00
ZrO_2	0,01	0,01	0,01
Al_2O_3	13,86	20,05	17,05
Cr_2O_3	**Below Detection Limit**	**Below Detection Limit**	0,00
V_2O_3	**Below Detection Limit**	**Below Detection Limit**	0,30
FeO / FeO_{tot}	5,93	20,45	2,61
MnO	0,04	0,80	25,08
MgO	2,37	15,78	
CaO	35,81	1,32	8,64
Total	99,82	99,76	99,05
Group (or formula type)	Garnet	Garnet	Garnet
Species	grossular	pyrope	spessartine
Complete Formula	$\{Ca_{2.928}Mg_{0.078}\}\Sigma 3.006[Al_{1.247}FeIII_{0.378}Mg_{0.192}Si_{0.148}Ti_{0.032}MnIII_{0.002}]\Sigma 1.999(Si_3)\Sigma 3O_{12}$	$\{Mg_{1.676}Fe_{1.169}Ca_{0.105}Mn_{0.05}\}\Sigma 3[Al_{1.755}FeIII_{0.101}Mg_{0.072}Si_{0.071}]\Sigma 1.999(Si_3)\Sigma 3O_{12}$	$\{Mn_{1.656}Ca_{0.722}Fe_{0.17}\}\Sigma 2.548[Al_{1.567}Si_{0.537}V_{0.019}]\Sigma 2.123(Si_3)\Sigma 3O_{12}$

Table 6. The end-member proportions of a rhodolite, spessartine-grossular and Mali garnet are calculated according to Locock (2008). The end-members in italics are hypothetical end-members. The iron and manganese were input as FeO and MnO with the spreadsheet calculating the proportions of the divalent and trivalent Fe and Mn required for charge balance. For compositions that cannot be expressed perfectly by the 29 end-members as stated by Locock (2008), a remainded is calculated.

	Locock (2008)

© University of Pretoria

	Mali Garnet	Rhodolite	Spessartine-grossular
	050358*b	**642963a**	**860203-3**
SiO_2	41,25	41,35	45,36
TiO_2	0,55		0,00
ZrO_2	0,01	0,01	0,01
Al_2O_3	13,86	20,05	17,05
Cr_2O_3	Below Detection Limit	Below Detection Limi	Below Detection Limi
V_2O_3	Below Detection Limi	Below Detection Limi	Below Detection Limi
FeO / FeO_{tot}	5,93	20,45	2,61
MnO	0,04	0,80	25,08
MgO	2,37	15,78	
CaO	35,81	1,32	8,64
Total	99,82	99,76	99,05
End-members			
Morimotoite-Mg	3,16%		
Majorite	4,12%	7,14%	
Goldmanite			0,98%
Spessartine		1,68%	57,58%
Pyrope		48,73%	
Almandine		37,36%	5,92%
Grossular	62,29%		18,20%
Andradite	18,91%	3,50%	
Skiagite		1,56%	
Remainder	11,53%	0,04%	17,32%
Total	100,01%	100,01%	100,00%

Table 7. The end-member proportions of a rhodolite, spessartine-grossular and Mali garnet are calculated according to Rickwood (1968). The iron and manganese were input as FeO and MnO with the spreadsheet calculating the proportions of the divalent and trivalent Fe and Mn required for charge balance.

		Rickwood (1968)	
	Mali Garnet	**Rhodolite**	**Spessartine-grossular**
	050358*b	**642963a**	**860203-3**

© University of Pretoria

SiO_2	41,25	41,35	45,36
TiO_2	0,55	0,55	0
Al_2O_3	13,86	20,05	17,05
FeO / FeO_{tot}	5,93	20,45	2,61
MnO	0,04	0,8	25,08
MgO	2,37	15,78	
CaO	35,81	1,32	8,64
ZnO		0,01	0,03
Cl	0,11	0,02	0,51
Cr_2O_3	Below Detection Limit	Below Detection Limit	0
Total	99,92	100,33	99,28
Almandine	0	30,51	0
Andradite	23,29	3,84	0
Grossular	65,55	0	29,53
Pyrope	11,06	63,81	0
Spessartine	0,11	1,84	70,47
Uvarovite	0	0	0

In Tables 5, 6 and 7 the three calculation sequences and the results from Grew *et al*. (2013), Locock (2008) and Rickwood (1968) are compared. All three produce similar results for the sample 642963a (rhodolite). However, Locock's (2008) calculation sequence produces a very different result for the sample 860203-3 (spessartine-grossular). A large remainder of 17.32% is produced. For the sample 050358*b (Mali garnet), only Rickwood's (1968) calculation sequence produced acceptable results (Mali garnets are composed primarily of grossular and andradite). The calculation sequence from Grew *et al*. (2013) calculated an andradite content that is too low for a Mali garnet. The calculation sequence from Locock (2008) produced a large remainder of 11.53% for the Mali garnet. Only Rickwood's (1968) calculation sequence produced acceptable and consistent results for all three samples. It would not have been possible to use one calculation sequence for one sample and another calculation sequence for another. The large remainders seen in the calculation sequence from Locock (2008) for the two samples made it inapplicable in this thesis. The reporting of the results by Grew *et al*. (2013) in the format of $\{X_3\}[Y_2](Z_3)\ \varphi_{12}$ with only one dominant species being identified (Table 5) is not commonly applied to gemstones. Most gemologists apply Rickwood's (1968) calculation sequence when assigning end-member proportions to gem garnets. Hence, the calculation sequence of Rickwood (1968) was deemed more suitable for this thesis.

© University of Pretoria

4. Results

The results are presented in the following sequence:

- Classification,
- Chemistry,
- Magnetic susceptibility,
- Refractive Index (R.I.), and
- Colour.

The chemistry is presented before the other characteristics as all the other variables depend on it. Furthermore, chemistry is the most reliable means of classification between the different garnets while the others are less reliable.

4.1. Classification

After the recasting of the garnet analyses into molecular percentages of end-members, the garnets were named. Subdivisions were created based on the main end-members ratio followed by colour, if possible. Stones were given either a name describing their composition or their traditional gem name. The stones that were assigned their traditional gem names were ‘rhodolite’, ‘Mali garnets’, ‘demantoid’, ‘hessonite’ and ‘tsavorite’. The reason for this is explained in more detail in the following paragraphs.

The first step in naming the garnets was to determine the dominant end-member component. Where an end-member comprised more than 80 mol. % in the sample, this end-member was used as the name for the garnet sample. The only exception to this rule is the ‘Mali garnets’, as they have a grossular component from 61.07 to 88.79 mol. % and an andradite component from 7.02 mol. % to 38.07 mol. %. If two end-member components were dominant in a sample analysis e.g. almandine = 50 mol. % and pyrope = 40 mol. % and spessartine = 10 mol. %, the sample was named according to the two dominant end-members i.e. almandine-pyrope. The order in which the end-members were placed in the name depend on the amount present in the sample with the end-member of a higher molar proportion being placed first. The same rule applied if three end-members were dominant within a sample.

In the pyrope-almandine solid solution series, samples that contained primarily pyrope followed by almandine were called either ‘pyrope-almandine’ or ‘rhodolite’. The samples called ‘rhodolite’ had to display the distinctive purple red colour that is associated with these gemstones. It was deemed appropriate to use the name ‘rhodolite’ as this gem garnet is commonly referred to as ‘rhodolite’ and is regarded as separate from ‘pyrope-

© University of Pretoria

almandine'. Samples called 'pyrope-almandine' did not display the purple red colour commonly associated with 'rhodolite'.

The second step was to determine the colour change. The samples were only labelled colour change if they displayed a distinct change in colour across the colour wheel under different illuminations. Colour shift was not regarded as a complete colour change in this thesis. This rule only applied to samples from the pyrope-spessartine series and the Mali garnets.

Certain names, e.g. 'demantoid', 'tsavorite', 'hessonite' and 'Mali garnet', were kept and not changed according to their molar proportions of end-members. This was due to their distinctive compositions, which did not overlap with other types of garnets. Also, these names are commonly used when referring to that specific gem garnet in the literature (Stockton and Manson, 1985; Johnson *et al*., 1995) and it was deemed appropriate to keep these names in this thesis.

The term 'CC' in the name 'CC Mali garnets' refers to colour change and was used to distinguish between the 'Mali garnets' that displayed colour change and those that did not.

'Hessonite' and 'tsavorite' have similar compositions, i.e. > 80 mol. % grossular. However, they can be distinguished from each other based on their colour with the former appearing orange brown and the latter green in colour. This criterion was used to distinguish between the two in this thesis.

In the pyrope-spessartine solid solution series, the symbol 'II' denotes the occurrence of colour change and 'I' the absence of colour change.

The gemstones were subsequently divided into two species based on their compositions: ugrandite (uvarovite, grossular and andradite) and pyralspite (pyrope, spessartine and almandine). This was done for clarity to make the data more manageable. In addition, most of the samples had distinct compositions that did not overlap between the two groups, which made the division appropriate. However, a few samples had compositions that overlapped between the two species (e.g. almandine-grossular and spessartine-grossular). These samples were only a small number and were placed in both species.

Table 8. Summary of garnet samples and their subdivision. Colour change is only applicable to samples of the pyrope spessartine and grossular andradite solid solution series. The use of colour as a means of classification was only applicable to 'rhodolite', 'hessonite' and 'tsavorite'.

© University of Pretoria

Name	Composition according to molar proportions of end-members	Colour Change	Colour	Species	Number of samples
Almandine	Almandine > 80 mol. %	N/A	N/A	Pyralspite	3
Almandine-grossular	Almandine > grossular	N/A	N/A	Pyralspite and ugrandite	1
Almandine-pyrope	Almandine > pyrope	N/A	N/A	Pyralspite	30
Almandine-spessartine	Almandine > spessartine	N/A	N/A	Pyralspite	2
CC Mali garnet	Grossular > andradite	Yes	N/A	Ugrandite	94
Demantoid	Andradite > 80 mol. %	N/A	N/A	Ugrandite	36
Hessonite	Grossular > 80 mol. %	N/A	Orange brown	Ugrandite	14
Mali garnet	Grossular > andradite	No	N/A	Ugrandite	327
Pyrope	Pyrope > 80 mol. %	N/A	N/A	Pyralspite	32
Pyrope-almandine	Pyrope > almandine	N/A	N/A	Pyralspite	204
Pyrope-spessartine I	Pyrope > spessartine	No	N/A	Pyralspite	88
Pyrope-spessartine II	Pyrope > spessartine	Yes	N/A	Pyralspite	75
Rhodolite	Pyrope > almandine	N/A	Purple red	Pyralspite	115
Spessartine	Spessartine > 80 mol. %	N/A	N/A	Pyralspite	320
Spessartine-almandine	Spessartine > almandine	N/A	N/A	Pyralspite	9
Spessartine-grossular	Spessartine > grossular	N/A	N/A	Pyralspite and ugrandite	4
Spessartine-pyrope I	Spessartine > pyrope	No	N/A	Pyralspite	49
Spessartine-pyrope II	Spessartine > pyrope	Yes	N/A	Pyralspite	72
Tsavorite	Grossular > 80 mol. %	N/A	Green	Ugrandite	38
Total					1513

Table 9. List of terms used in the thesis with the approved mineral names from Grew *et al*. (2013) and gem trade names from Stockton and Manson (1985).

Gem names used in this thesis	Mineral names (Grew *et al*., 2013)	Gem trade names (Stockton and Manson, 1985)
Almandine	Almandine	Almandine

© University of Pretoria

Almandine-grossular	Almandine	N/A
Almandine-pyrope	Almandine	Pyrope-almandine
Almandine-spessartine	Almandine	Almandine-spessartine
Pyrope	Pyrope	Pyrope
Pyrope-almandine, rhodolite	Pyrope	Pyrope-almandine, rhodolite
Pyrope-spessartine I (pyrope dominant and displays no colour change) Pyrope-spessartine II (pyrope dominant and displays a distinct colour change)	Pyrope	Pyrope-spessartine, Malaya, colour-change pyrope-spessartine
Spessartine	Spessartine	Spessartine
Spessartine-almandine	Spessartine	Almandine-spessartine
Spessartine-grossular	Spessartine	N/A
Spessartine-pyrope I (spessartine dominant and displays no colour change) Spessartine-pyrope II (spessartine dominant and displays a distinct colour change)	Spessartine	Pyrope-spessartine, Malaya, colour-change pyrope-spessartine
CC Mali garnet (displays distinct colour change) Mali garnet (displays no colour change)	Grossular	N/A
Demantoid (composed predominantly of andradite)	Andradite	Demantoid
Hessonite (composed predominantly of grossular and appears orange brown)	Grossular	Hessonite
Tsavorite (composed predominantly of grossular and appears green)	Grossular	Tsavorite

4.1.1. Classification of the pyralspite species by trade name

Figure 5a shows a large proportion of the stones that were classified incorrectly when they were sold.

© University of Pretoria

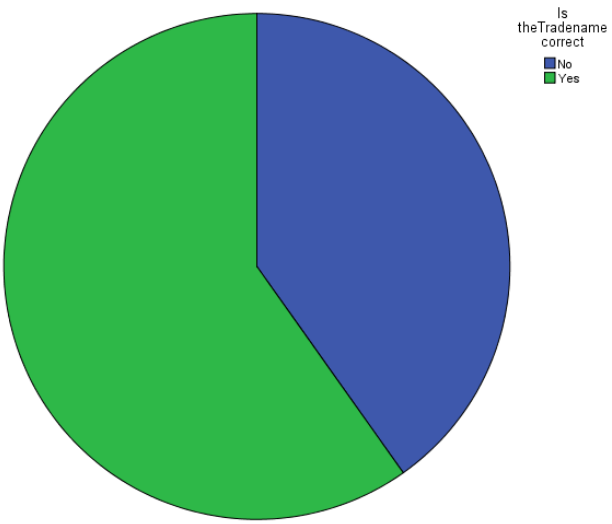

Figure 5. a) Pie graph showing whether the pyralspite garnets were classified correctly by the sellers.

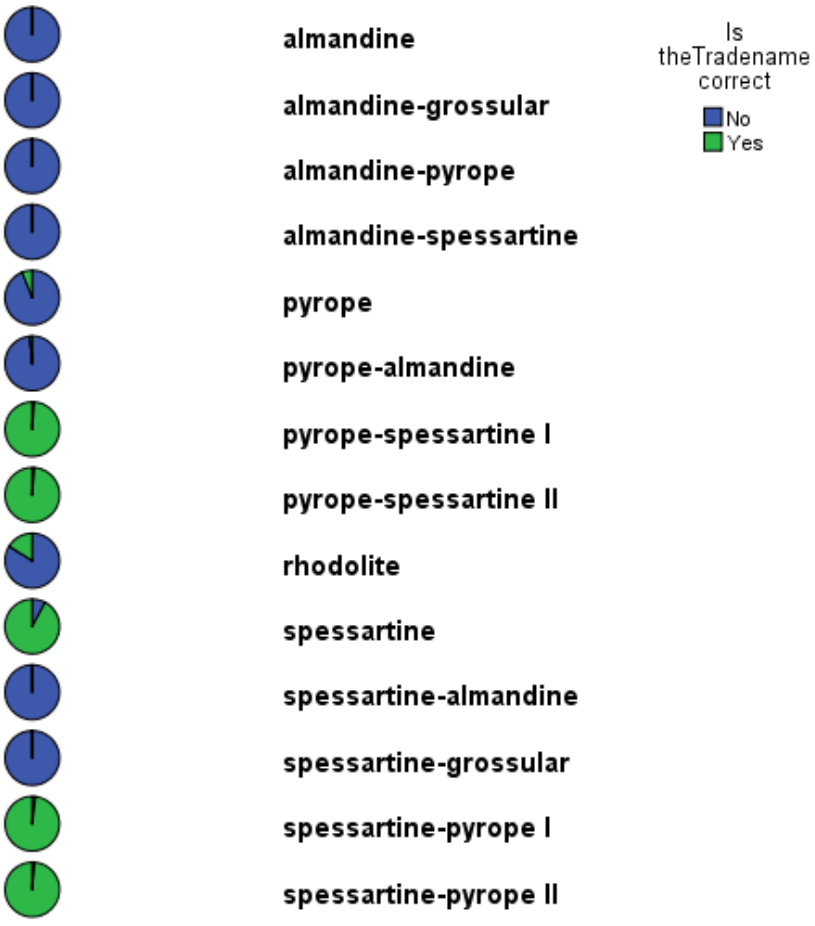

Figure 5. b) Pie graphs showing whether the pyralspite garnets are classified correctly by the sellers.

Most of the different types of garnets from the pyralspite species are incorrectly classified by sellers. Only stones from the pyrope-spessartine solid solution series and the spessartine samples have a majority that is correctly classified.

© University of Pretoria

4.1.1.1. Classification Based on Refractive Index

Traditionally, RI and colour are used to identify gem garnets. However, a large percentage of the stones in this thesis possess RI values that are not within the traditional range for that type of stone (Stockton and Manson, 1985). This shows that the use of RI as a sole means of classification of garnet gemstones is not reliable (Figure 6a).

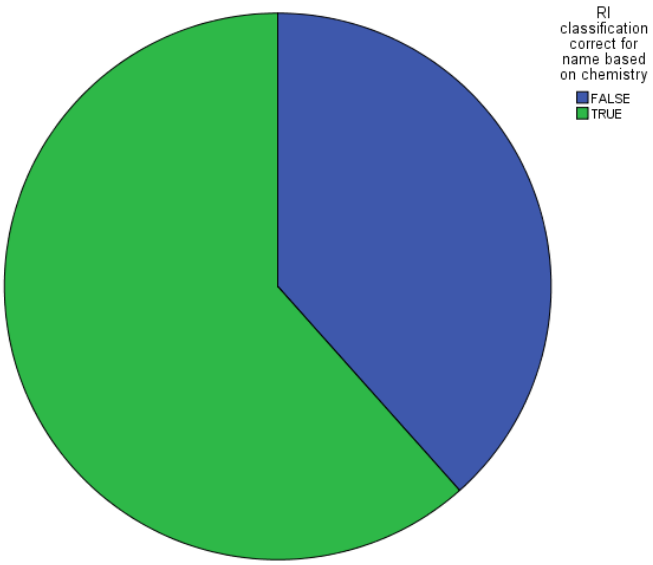

Figure 6. a) Pie chart showing how correct the seller's classification is based on RI for the pyralspite garnets.

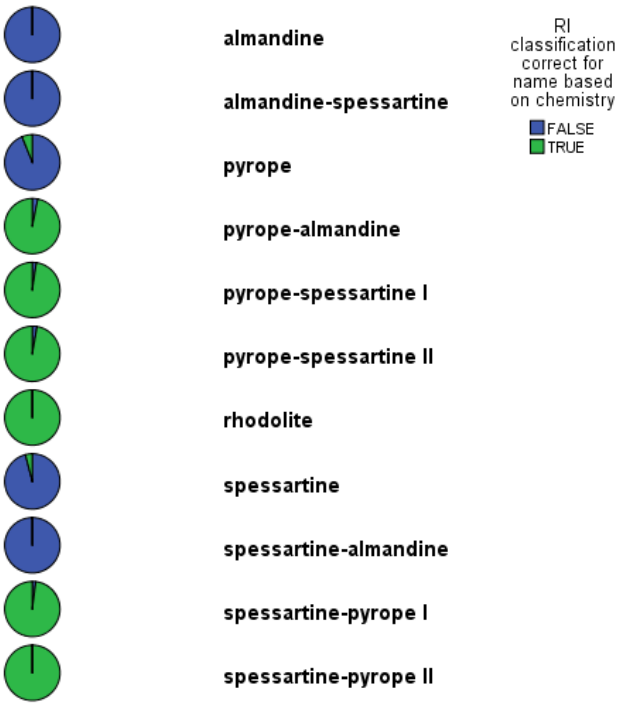

Figure 6. b) Pie charts showing how correct the seller's classification is based on the RI for the pyralspite garnets.

© University of Pretoria

4.1.1.2. Classification based on magnetic susceptibility

The magnetic susceptibility classification scheme designed by Hoover *et al*. (2008) is employed here, and, as can be seen in Figure 7a, 50% of the classifications were incorrect, making this method unreliable.

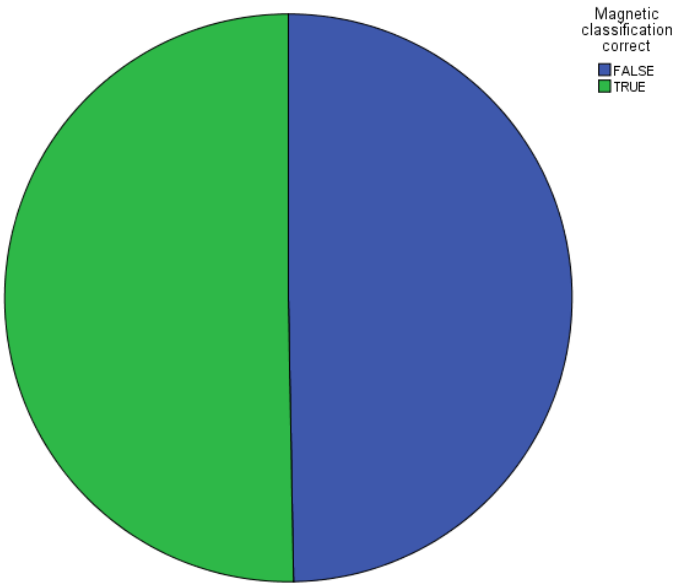

Figure 7. a) Pie chart showing how correct the classification is based on the pyralspite garnets' magnetic susceptibility. The magnetic susceptibility ranges are taken from Gemstone Magnetism (2014).

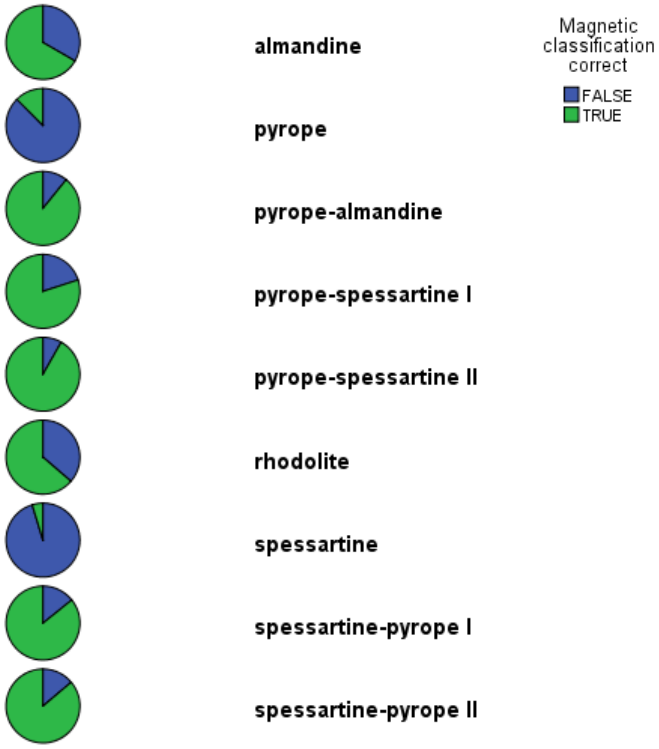

Figure 7. b) Pie charts showing how correct the classification was based on magnetic susceptibility for the pyralspite garnets.

© University of Pretoria

4.1.1.3. Colour change occurrence

Those samples approaching a pure end-member in composition show little to no colour change or shift, which indicates that colour change and shift are predominant in the samples of intermediate composition (Figure 8).

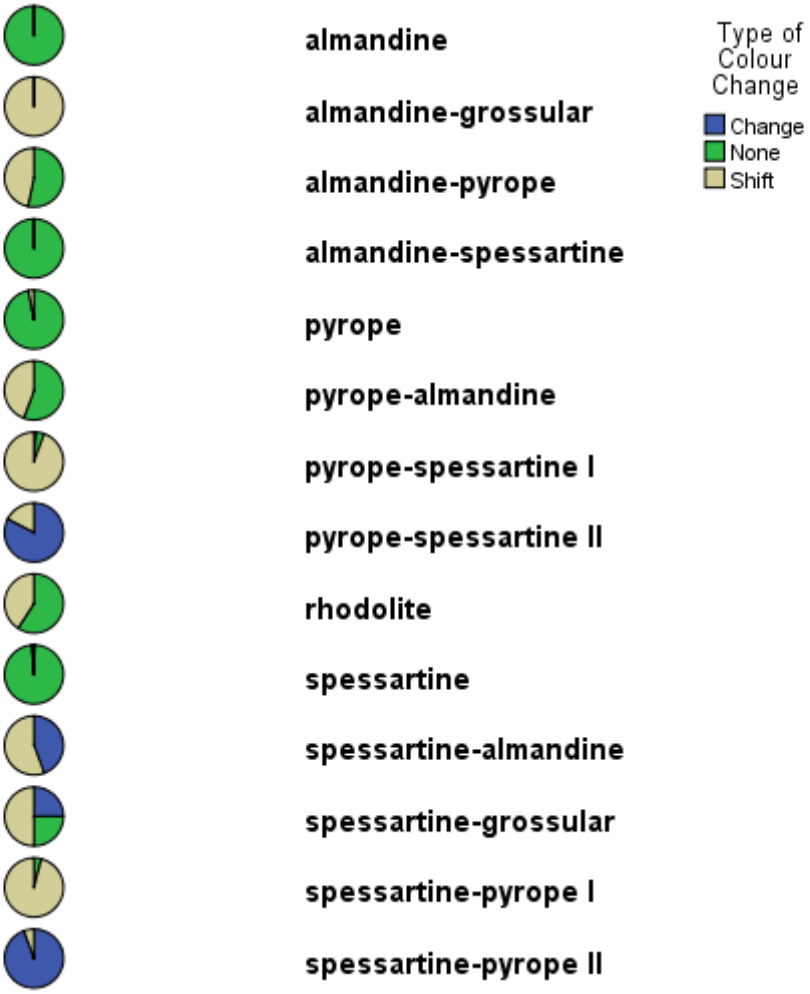

Figure 8. Type of colour change of the pyralspite garnets.

Samples that displayed no colour change or shift:

- Almandine;
- Almandine-spessartine;
- Pyrope; and
- Spessartine.

Samples that displayed a shift in colour:

- Almandine-pyrope;

© University of Pretoria

- Pyrope-almandine;
- Pyrope-spessartine;
- Spessartine-almandine;
- Spessartine-grossular; and
- Spessartine-pyrope.

Only a few samples displayed a shift in colour in the pyrope and spessartine samples.

Colour change occurred only in the:

- Pyrope-spessartine;
- Spessartine-almandine;
- Spessartine-grossular; and
- Spessartine-pyrope samples.

In the spessartine-almandine series, colour change and colour shift occurs only in spessartine-almandine samples and not in the almandine-spessartine samples.

Colour change occurs more in the spessartine-pyrope samples than in the pyrope-spessartine samples. In this series, colour change and colour shift are common.

A quarter of the spessartine-grossular samples displayed a distinct colour change between daylight and incandescent light.

4.1.2. Classification of the ugrandite species

Figure 9a shows that the majority of the stones were bought under the correct trade name with only a few being incorrect. This differs significantly from the pyralspite species, where a large number of stones were sold under the incorrect name.

© University of Pretoria

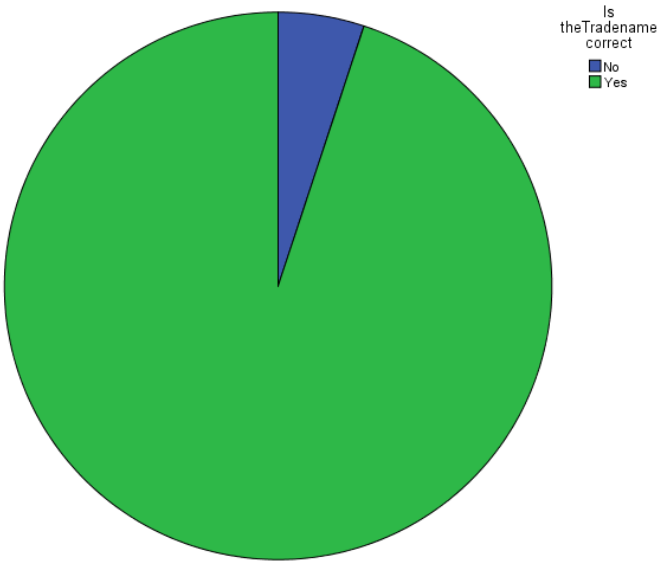

Figure 9. a) Pie graph showing the proportions of stones of the ugrandite species that were classified correctly by the seller.

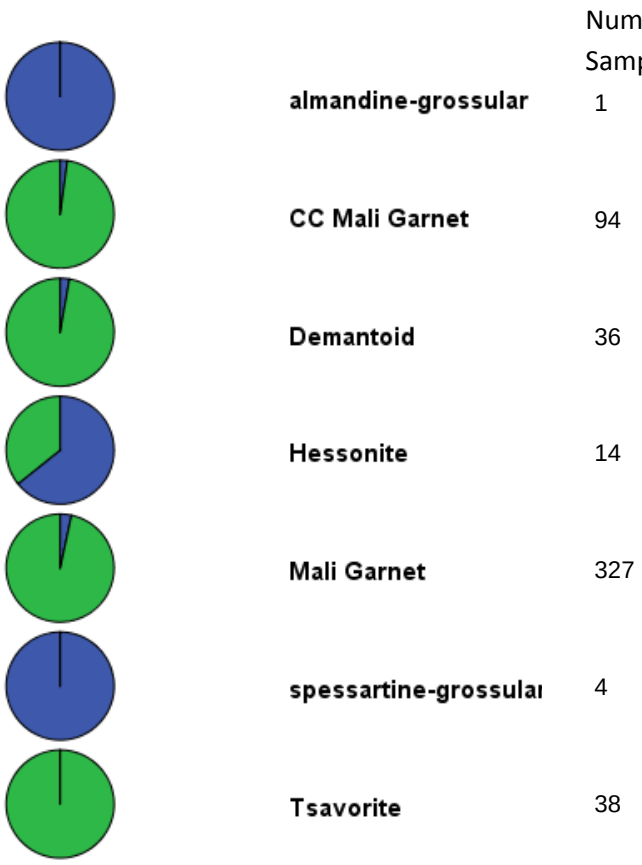

Figure 9. b) Pie graphs showing the proportion of stones of the ugrandite species that were classified correctly by the seller.

Three of the 'spessartine-grossular' samples were sold as CC garnets and one as a Malaya garnet. The 'almandine-grossular' sample was sold as a CC garnet. Ten of the

© University of Pretoria

fourteen 'hessonite' samples were classified incorrectly by the seller as Mali, Malaya, spessartine, rhodolite, and colour change garnets.

4.1.2.1. Classification based on refractive index

Again, only a small number of samples possessed RI values that do not fit within the traditional range of RI values for that type stone (Figure 10a). This differs from the pyralspite species which has a much larger number of samples whose RI does not match that of their traditional RI ranges.

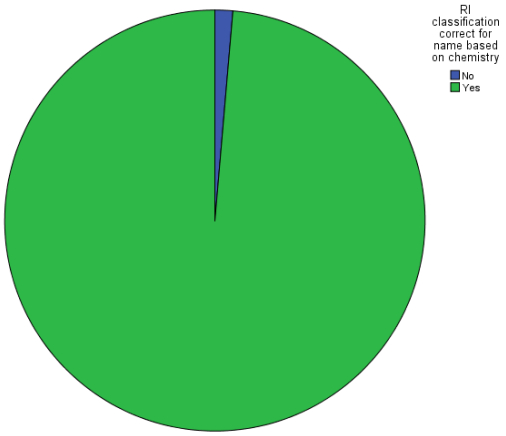

Figure 10. a) Pie graph showing the proportions of stones of the ugrandite species that were classified correctly based on their RI values.

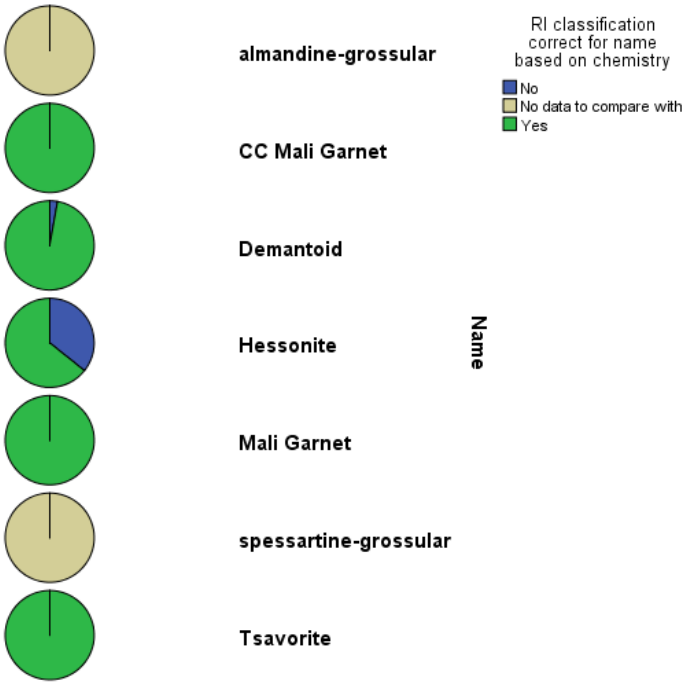

Figure 10. b) Pie graphs showing the proportions of stones of the ugrandite species that were classified correctly based on their RI values. The light brown colour indicates samples where the traditional RI values for that particular type of garnet are unknown, e.g. almandine-grossular and spessartine-grossular (Stockton and Manson, 1985).

© University of Pretoria

In Figure 10b, the hessonite samples were the only ones that had a relatively high number with RI values that did not fit into the traditional RI scheme for hessonites of Stockton and Manson (1985).

4.1.2.2. Classification based on magnetic susceptibility

The majority of the samples' magnetic susceptibilities fell within the traditional range for that particular stone, as defined by Gemstone Magnetism (2014) (Figure 11a). This method of classification, as defined by Hoover *et al*. (2008) and Gemstone Magnetism (2014), proves more reliable for the ugrandite species than the pyralspite species.

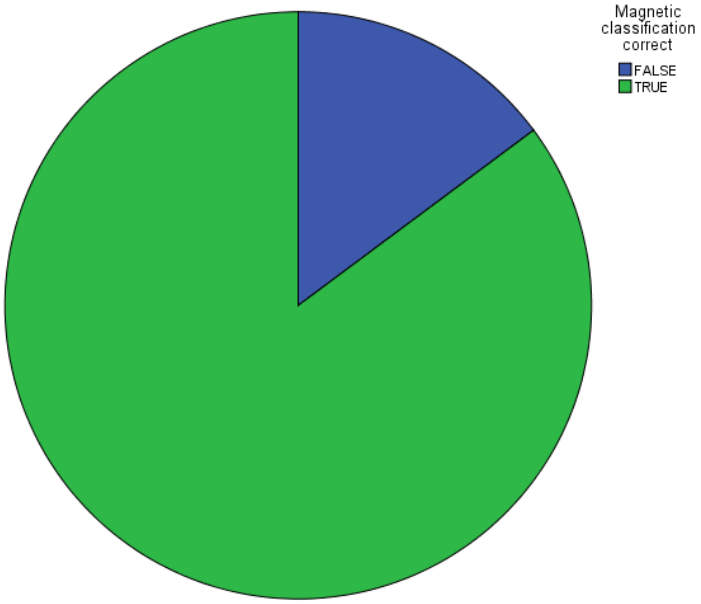

Figure 11. a) Pie graph showing the proportion of stones of the ugrandite species that were classified correctly based on their magnetic susceptibilities.

© University of Pretoria

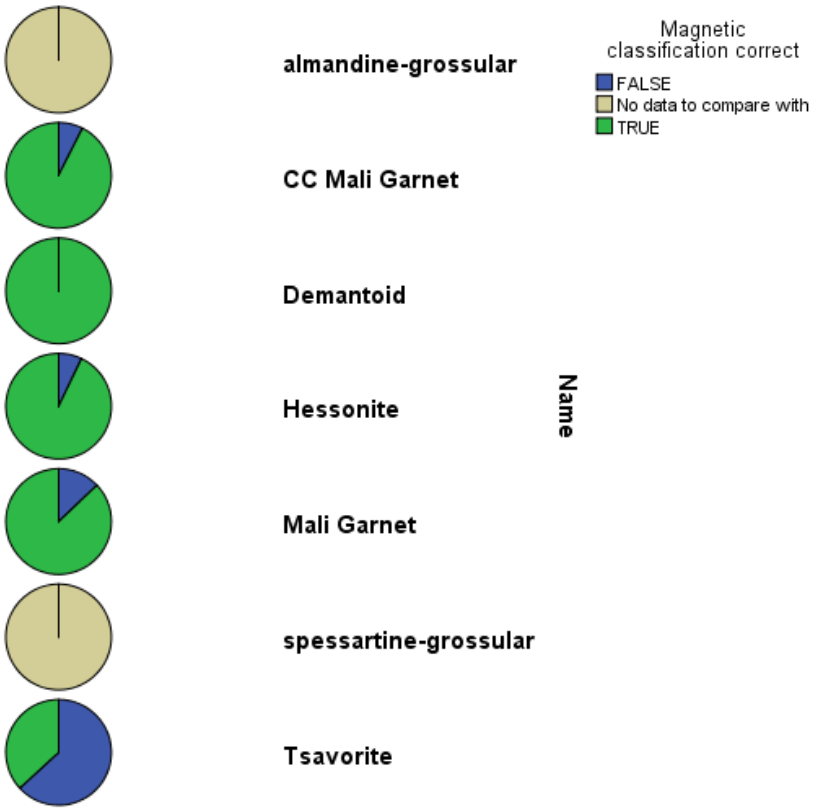

Figure 11. b) Pie graphs showing the proportion of stones of the ugrandite species that were classified correctly based on their magnetic susceptibilities. The light brown colour indicates samples where the traditional magnetic susceptibility values for that particular type of garnet are unknown, e.g. almandine-grossular and spessartine-grossular (Gemstone Magnetism, 2014).

4.2. Pyralspite Species

4.2.1. Chemistry

4.2.1.1. Almandine

Three 'almandine' samples were found in the data with the high FeO_{total} contents (37.28-40.73 wt. %) in the pyralspite species (Figure 12). The MgO contents range from 2.89 to 4.84 wt. % and the MnO content ranges from 0.92 to 2.06 wt. % (Figures 12 and 13). The CaO content is 0.54-0.61 wt. % (Figure 14). None of the 'almandine' samples had any detectable Cr_2O_3 and V_2O_3 (Figures 15 and 16).

© University of Pretoria

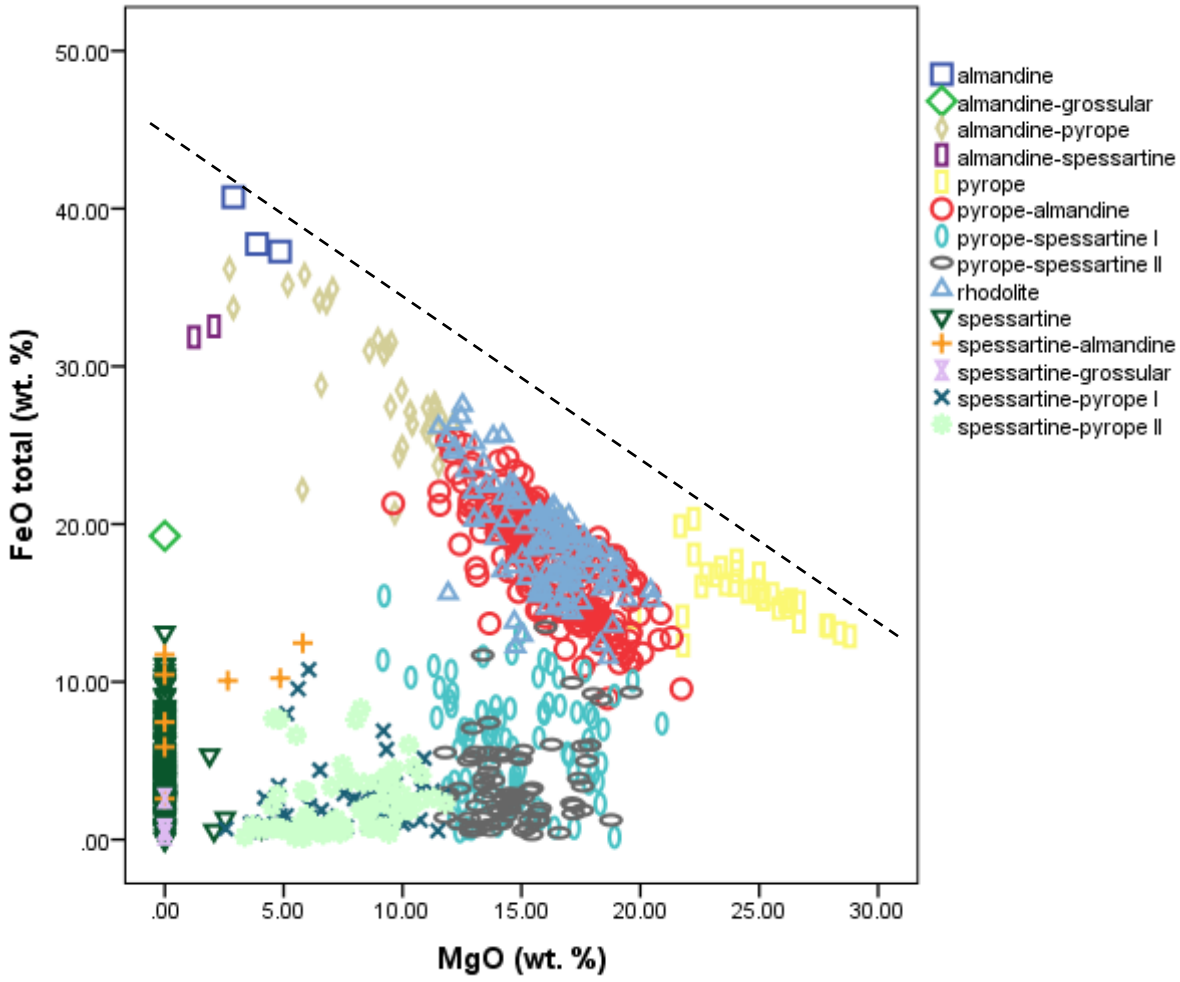

Figure 12. FeO_{total} vs. MgO concentrations in wt. %. The dashed line represents the theoretical solid solution series between almandine and pyrope.

© University of Pretoria

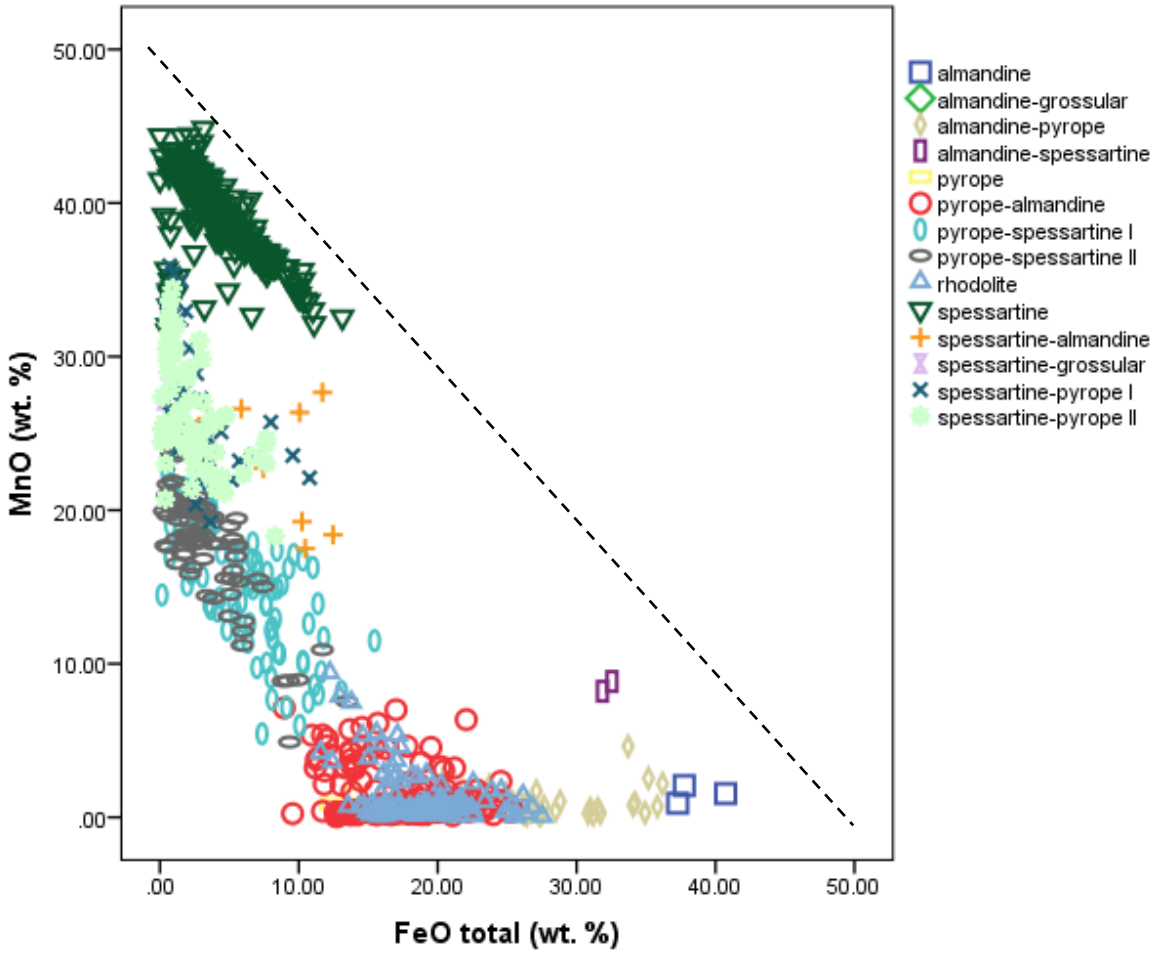

Figure 13.FeO_{total} (wt. %) vs. MnO (wt. %) of the different types of garnets from the pyralspite species. The 'pyrope' and 'almandine-grossular' samples are hidden beneath the 'pyrope-almandine' and 'rhodolite' samples.

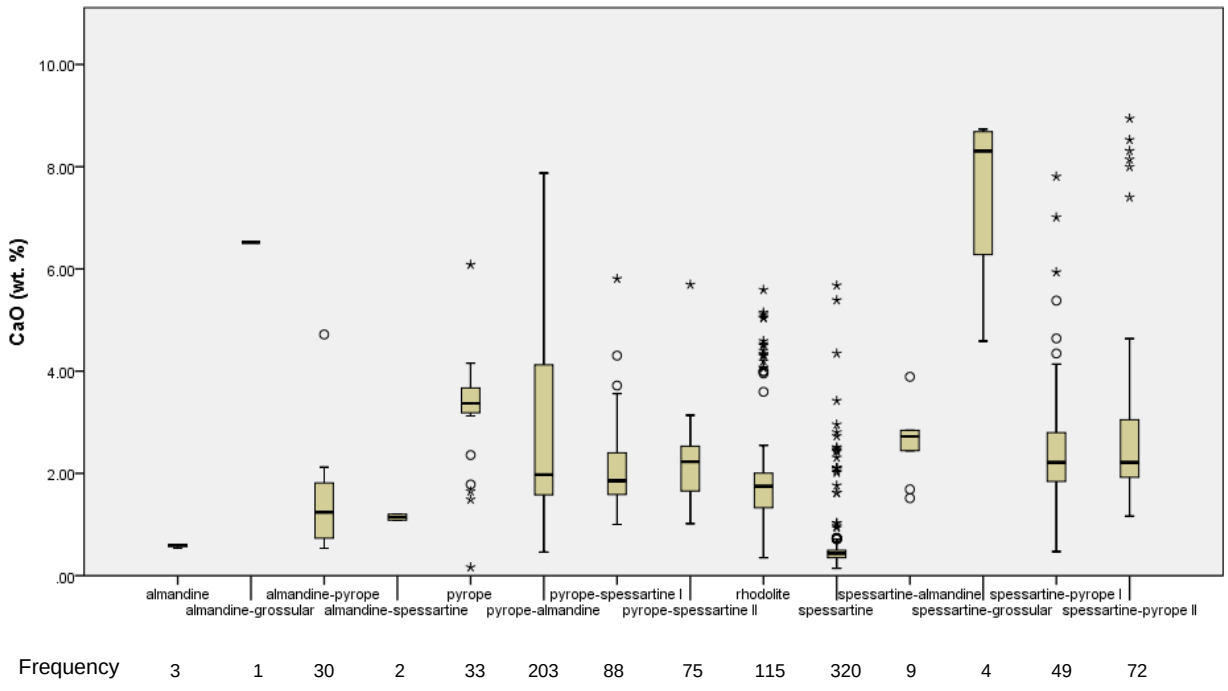

Figure 14. CaO (wt. %) of the different garnets from the pyralspite species. Below the boxplot are the frequencies for the different pyralspite garnets.

© University of Pretoria

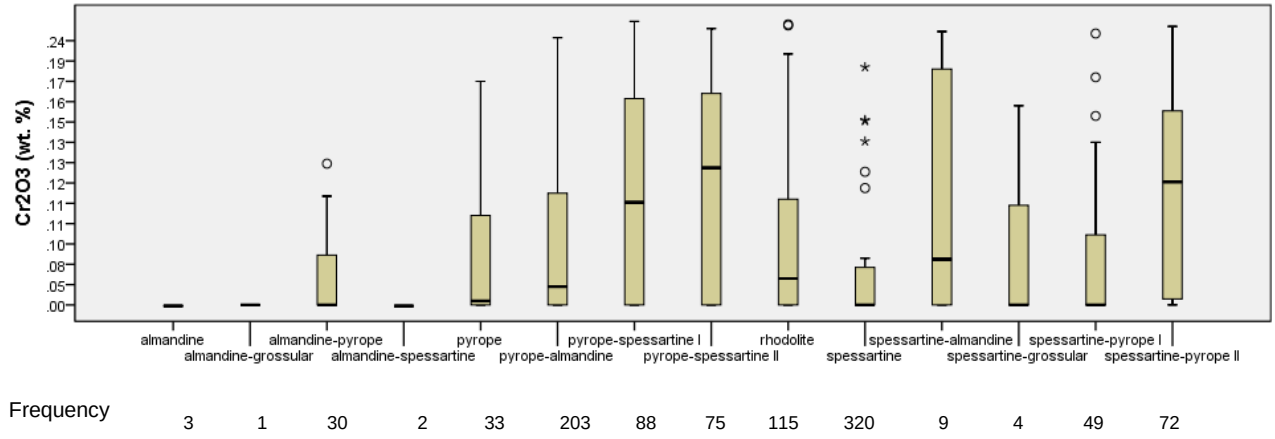

Figure 15. Cr_2O_3 (wt. %) boxplot for garnet samples from the pyralspite species. Below the boxplot are the frequencies for the different pyralspite garnets.

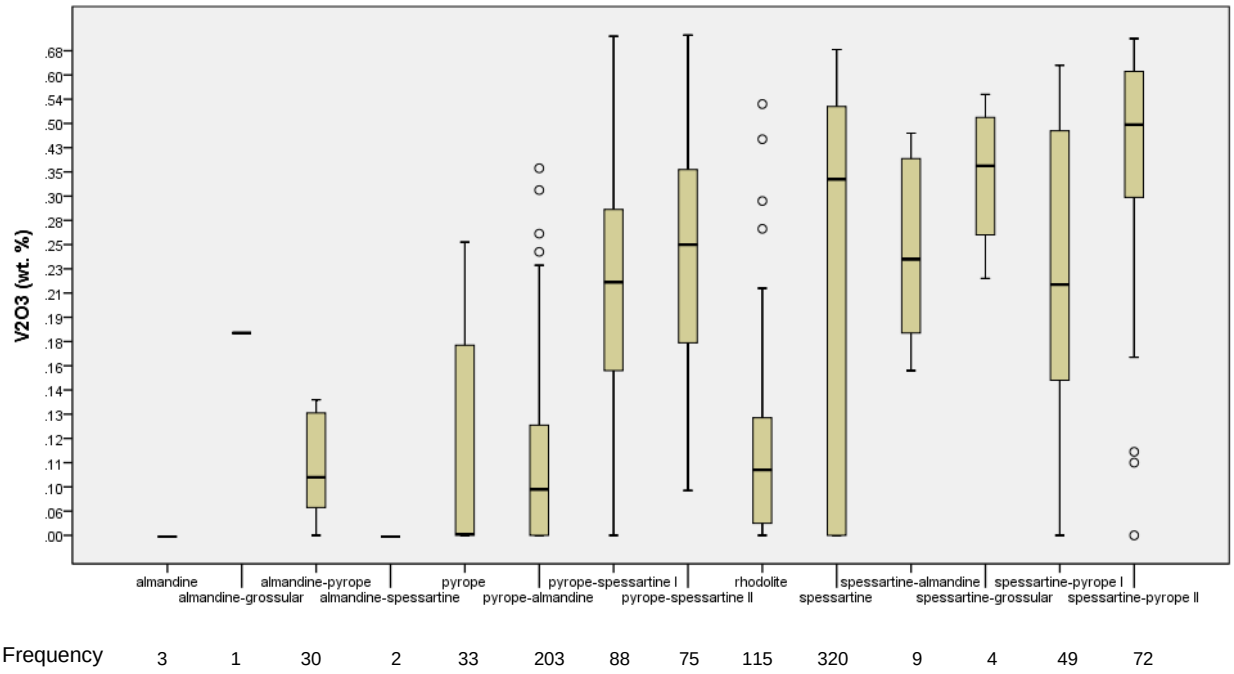

Figure 16. V_2O_3 (wt. %) content for the garnet samples from the pyralspite species. Below the boxplot are the frequencies for the different pyralspite garnets.

The high FeO_{total} content in the 'almandine' samples makes a distinguishing feature of 'almandine' gem garnets. Low amounts of MgO, MnO and CaO are present in all the 'almandine' samples. The 'almandine-pyrope' samples did show some very high FeO_{total} but this is still marginally lower than the 'almandine' samples.

The dominant end-member component in the 'almandine' samples is almandine (80.00-80.75 mol.%) with lesser amounts of pyrope (11.87-15.66 mol.%) and spessartine (2.38-5.38 mol.%) (Figures 17, 18 and 19).

© University of Pretoria

The ‘almandine’ samples could be distinguished from the other garnets based on the high almandine component (≥ 80 mol.% almandine). Some of the ‘almandine-grossular’ and ‘almandine-pyrope’ samples do plot near the ‘almandine’ samples, but their almandine component is below 80 mol.%. The ‘almandine’ samples clustered together in Figures 17, 18, 19 and 20) and are distinguished by their high almandine component with low pyrope, spessartine and andradite. The samples usually plot at the almandine end in the solid solution series between almandine and pyrope and almandine and spessartine (Figures 18 and 19). The ‘almandine’ samples plot along the solid solution series between pyrope and almandine in the almandine-rich region in Figures 18 and 20. Minor amounts of uvarovite up to 0.19 mol.% and andradite (1.77-2.00 mol.%) are also present in the ‘almandine’ samples (Figure 17).

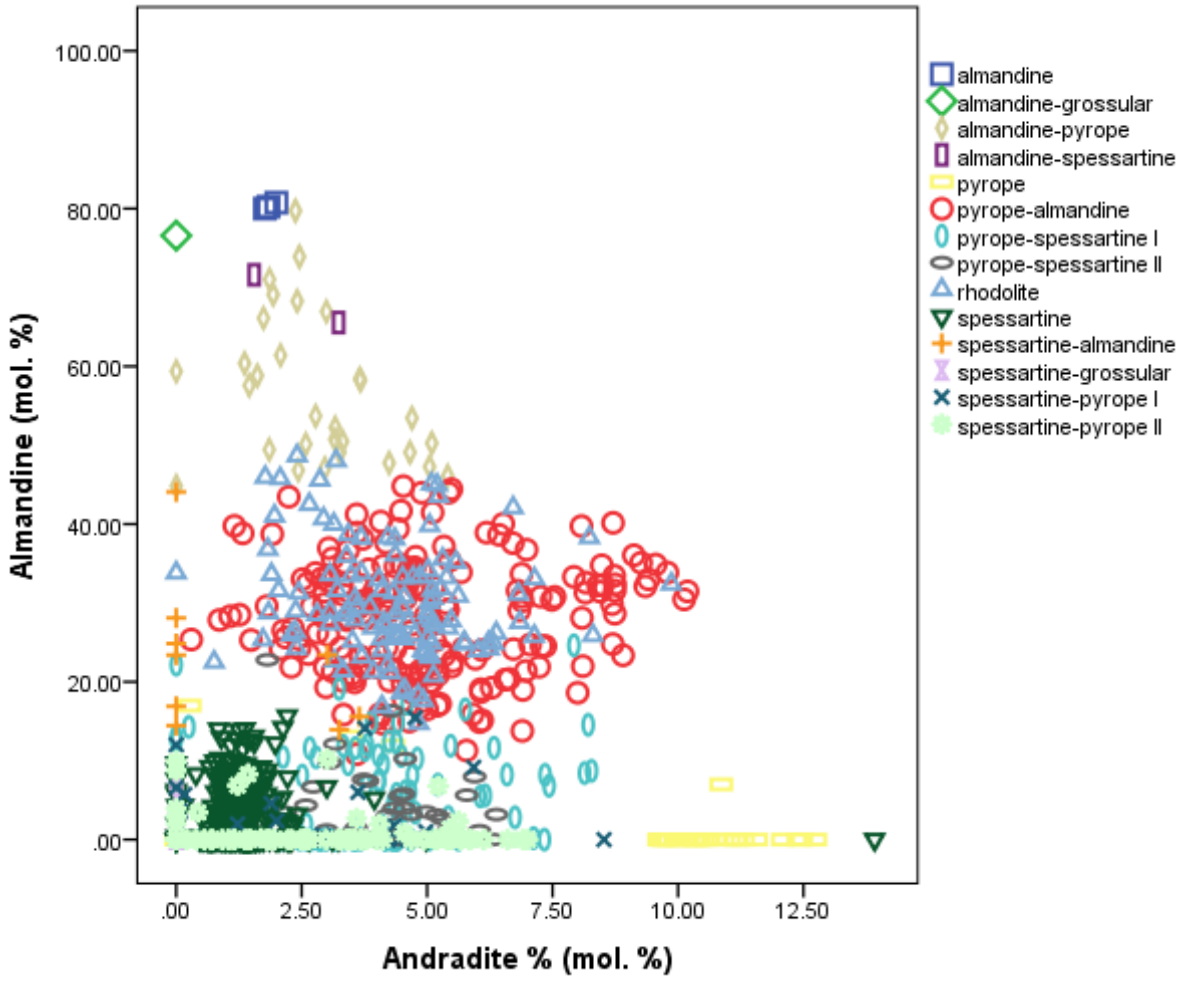

Figure 17. The proportions of almandine and andradite components for the different types of garnets from the pyralspite species.

© University of Pretoria

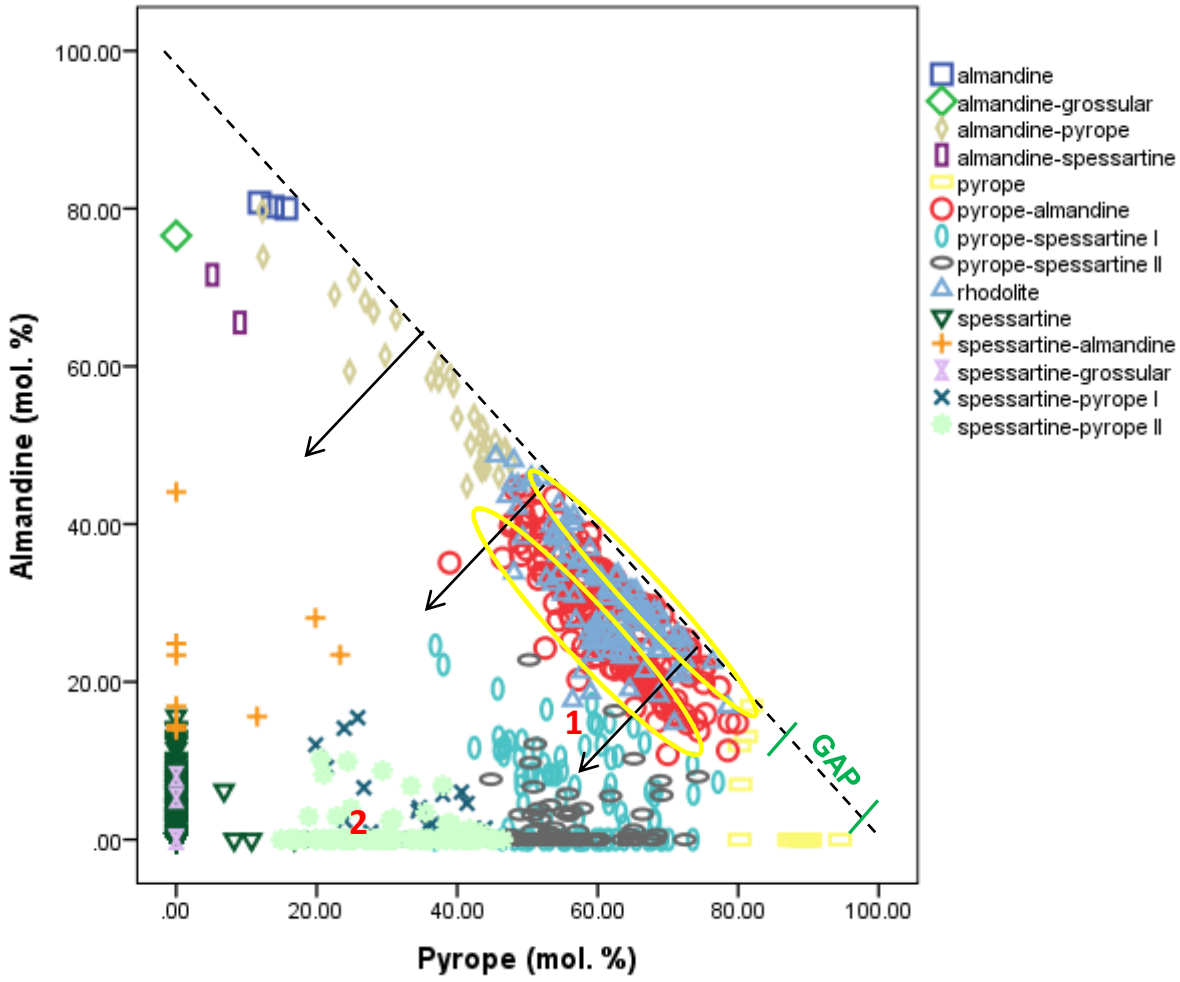

Figure 18. The proportions of almandine and pyrope components are plotted against each other for the different types of garnets from the pyralspite species. The dashed line is the trend between almandine and pyrope and represents the theoretical solid solution series between pyrope and almandine. Any deviations from this line (as indicated by the arrows) mean additional substitutions. A small gap exists, as indicated by the green lines where no samples plot. The area called '1' indicates the area where the almandine component from the pyrope-almandine solid solution series is substituted by a spessartine component and becomes part of the pyrope-spessartine series. The area called '2' is part of the pyrope-spessartine series where the spessartine component is dominant.

© University of Pretoria

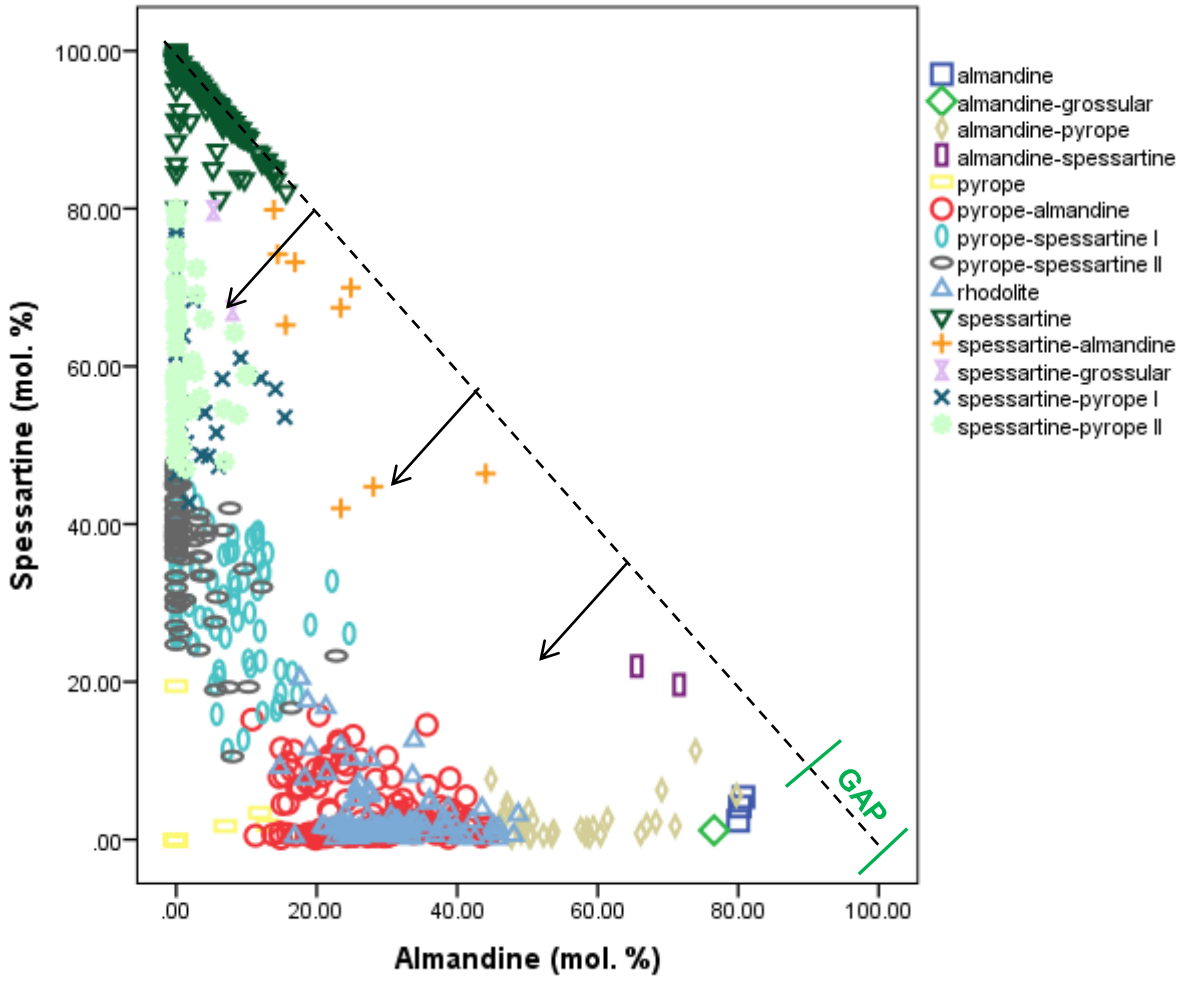

Figure 19. The spessartine and almandine components of the different garnet types from the pyralspite species. The dashed line indicates the solid solution series between spessartine and almandine. The arrows indicate deviation from the trend line. The short green lines represent a gap observed along the dashed line where no samples plot. For clarity purposes, most of the 'pyrope' samples are represented by a single yellow rectangle at the origin of the graph as most samples contained no spessartine or almandine. Only a few 'pyrope' samples plotted away from the origin and contained some spessartine and almandine.

© University of Pretoria

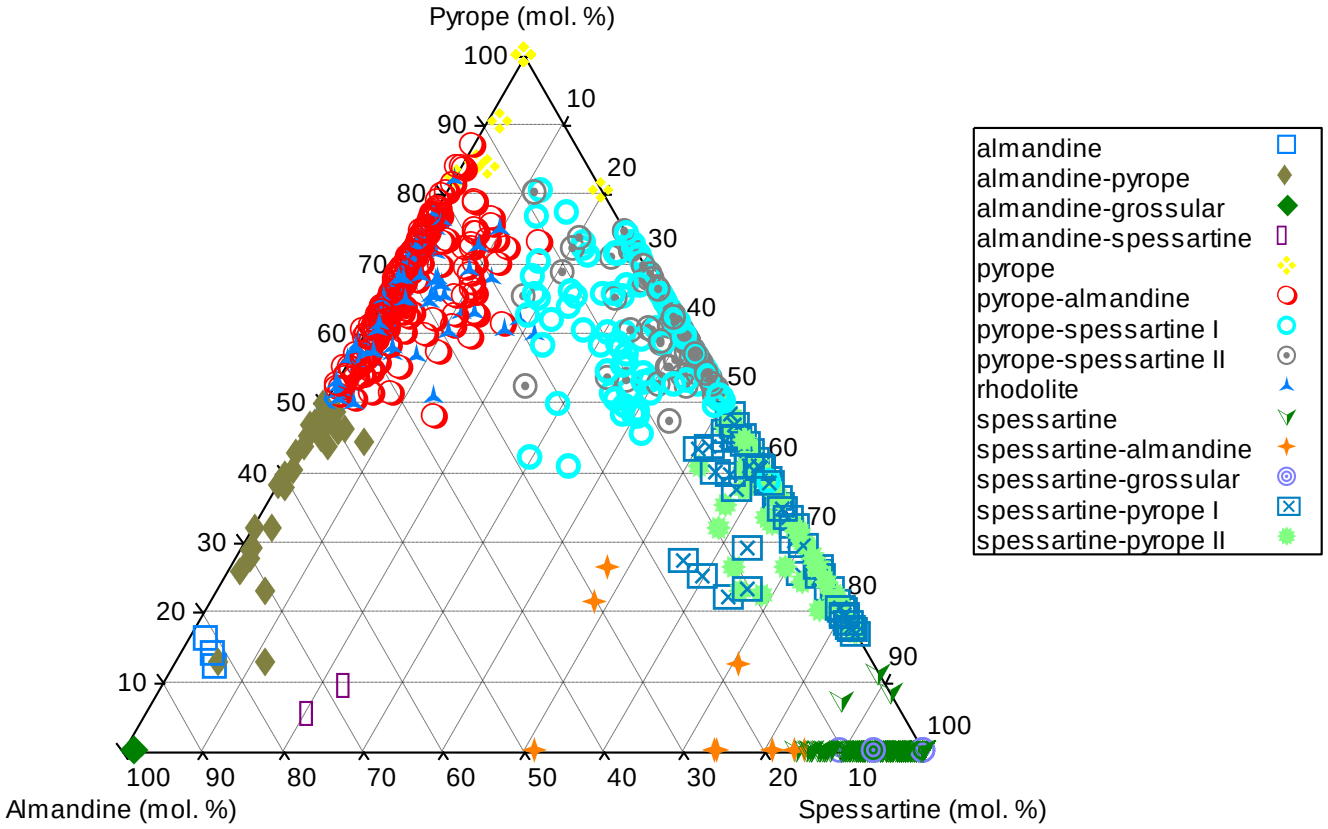

Figure 20. Ternary diagram of the different garnet types from the pyralspite species. For clarity purposes, the 'almandine-grossular' and 'spessartine-grossular' samples were removed. The chemical variability in the pyrope-almandine and pyrope-spessartine solid solution series can be seen above.

4.2.1.2. Almandine grossular

One 'almandine-grossular' sample is present in the data with a FeO_{total} content of 19.25 wt. % and CaO content of 6.52 wt. % (Figures 12 and 14). A minor amount of MnO (0.44 wt. %) is also resent (Figure 13).

© University of Pretoria

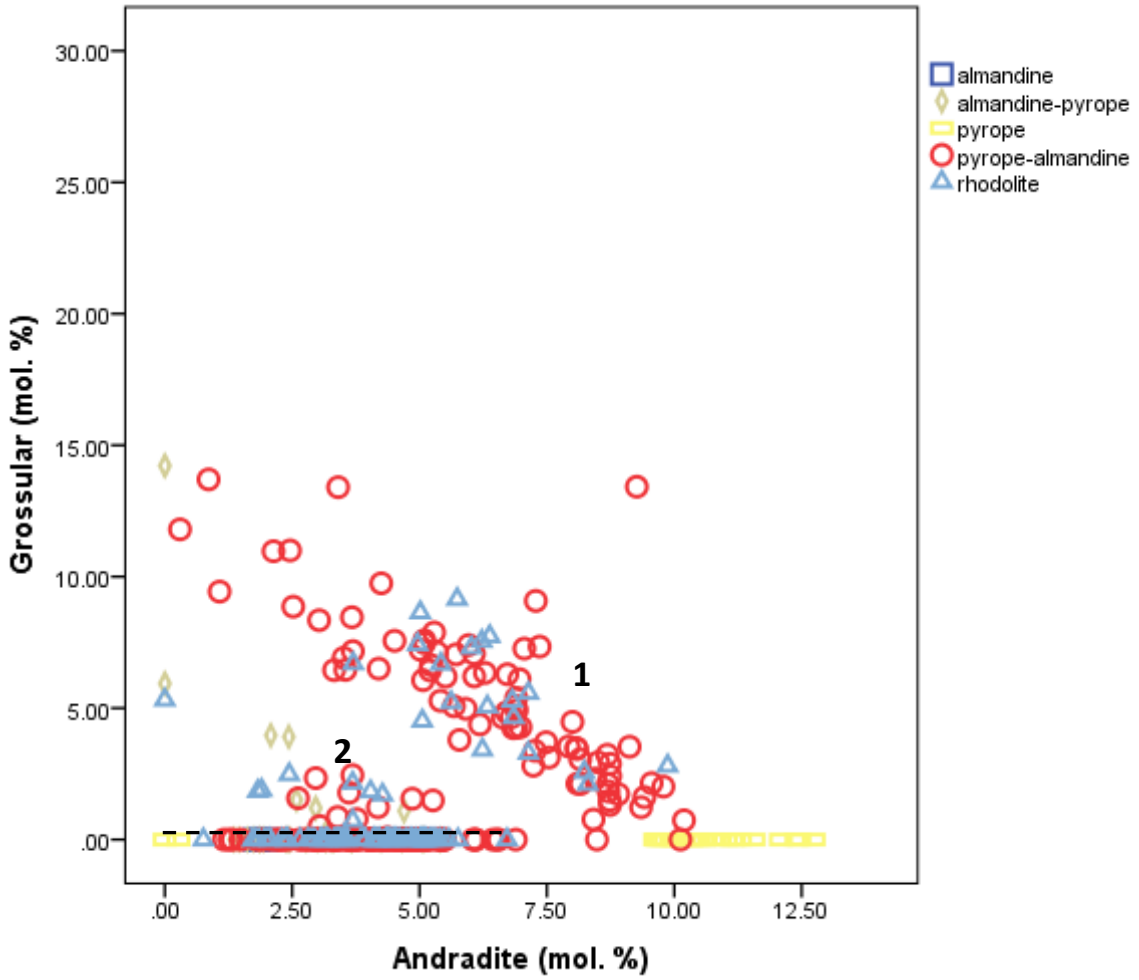

Figure 21. The grossular and andradite components of the different garnet types from the pyralspite species. For the sake of clarity, only the samples that are part of the pyrope almandine series were depicted as the other series contained very low to no grossular and andradite. The dashed line indicates the possible trends observed. The numbers '1' and '2' indicate the different clusters observed in the 'rhodolite' and 'pyrope-almandine' samples. Some plot in cluster 1 along the dashed line. Others plot at 2 where there is very little to no grossular component and a low andradite component. The 'almandine' samples are hidden beneath the 'rhodolite' and 'pyrope-almandine' samples in cluster '2'.

The almandine component is very high (76.57 mol.%) with smaller amounts of grossular (21.90 mol.%), spessartine (1.17 mol.%) and uvarovite (0.35 mol.%) present (Figures 17, 19 and 21). The 'almandine-grossular' sample could be distinguished from the other types of gem garnets by its high almandine component and significant CaO content (Figures 17 and 14), with the latter being relatively high for the pyralspite species In Figure 18, the 'almandine-grossular' samples do not plot along the trend line indicating additional substitutions of grossular.

© University of Pretoria

4.2.1.3. Almandine-pyrope

Thirty 'almandine-pyrope' samples are present with high FeO_{total} contents (44.81-79.73 wt. %) (Figure 12). Lesser amounts of MgO (2.71-12.13 wt. %) and MnO (0.12-4.63 wt. %) are also present (Figures 12 and 13). Minor amounts of CaO were present ranging from 0.53 to 4.72 wt. % (Figure 14). The Cr_2O_3 and V_2O_3 contents are present as trace amounts (≤ 0.12 and ≤ 14 wt. % respectively) (Figures 15 and 16).

The almandine component ranges from 44.81 to 79.73 mol.% with the pyrope component ranging from 12.27 to 47.58 mol.% (Figure 18). Lower amounts of spessartine (0.27-11.27 mol.%) and grossular (0.00-14.22 mol.%) are also present (Figures 19 and 21). The andradite component is relatively low (below 5.41 %) (Figure 17) and the uvarovite component is very low with the highest value being 0.42 mol.%.

These samples form a continuous trend with 'pyrope-almandine' and 'rhodolite' samples (Figures 20 and 18). The 'almandine-pyrope' samples form part of the solid solution series between pyrope and almandine, with the samples plotting in the almandine-rich region (Figure 18). The 'almandine-pyrope' samples contain a smaller range in the spessartine component than the 'pyrope-almandine' samples (Figure 19). The 'almandine-pyrope' samples also contain lower andradite and grossular components than the 'pyrope-almandine' samples (Figure 21). This suggests that the almandine dominant samples in the pyrope almandine series have less chemical variability than the pyrope dominant samples (Figure 20).

4.2.1.4. Almandine-spessartine

Two 'almandine-spessartine' samples with predominantly FeO_{total} (31.85; 32.53 wt. %) and MnO (8.21; 8.84 wt. %) contents were found (Figure 13). MgO and CaO are also present (1.23; 2.07 and 1.08; 1.20 wt. % respectively) (Figures 12 and 14). No Cr_2O_3 and V_2O_3 are detected (Figure 15 and 16).

The samples are composed primarily of almandine (65.56; 71.60 mol.%) with lesser amounts of spessartine (19.62; 21.98 mol.%) and pyrope (5.15; 9.06 mol.%) (Figure 18 and 19). The grossular and uvarovite components are low, being 0.00 and 1.95, as well as 0.12 and 0.17 mol.% respectively (Figure 21).

These samples plot near the solid solution line between almandine and spessartine (Figure 19), and contain high almandine but this is still below 80 mol.% (Figures 18 and 19). The samples fall outside of the trend line in Figure 18 and indicate additional substitutions of

© University of Pretoria

spessartine. The 'almandine-spessartine' samples contain lower pyrope than the 'spessartine-almandine' samples (Figure 18) suggesting less chemical variability.

4.2.1.5. Pyrope

Thirty 'pyrope' samples with 16.62-28.81 wt. % MgO are present (Figure 12). Lesser amounts of FeO_{total} (12.32-20.33 wt. %) and CaO (0.16-6.08 wt. %) are also present (Figures 12 and 14). Trace amounts of MnO (0.30-11.86 wt. %), Cr_2O_3 (≤ 0.17 wt. %) and V_2O_3 (≤ 0.25 wt. %) were also found. (Figures 13, 15 and 16)

The dominant end-member in these samples is pyrope (80.18-94.51 %) with andradite being the second highest (0.00-12.75 mol.%) (Figure 18 and 17). The spessartine and almandine components are relatively low except for a few samples: These samples have a spessartine component ranging up to 19.48 mol.% and an almandine component ranging up to 17.00 mol. % (Figures 19 and 18). The uvarovite component is low ranging from 0.00 to 0.51 mol.%.

© University of Pretoria

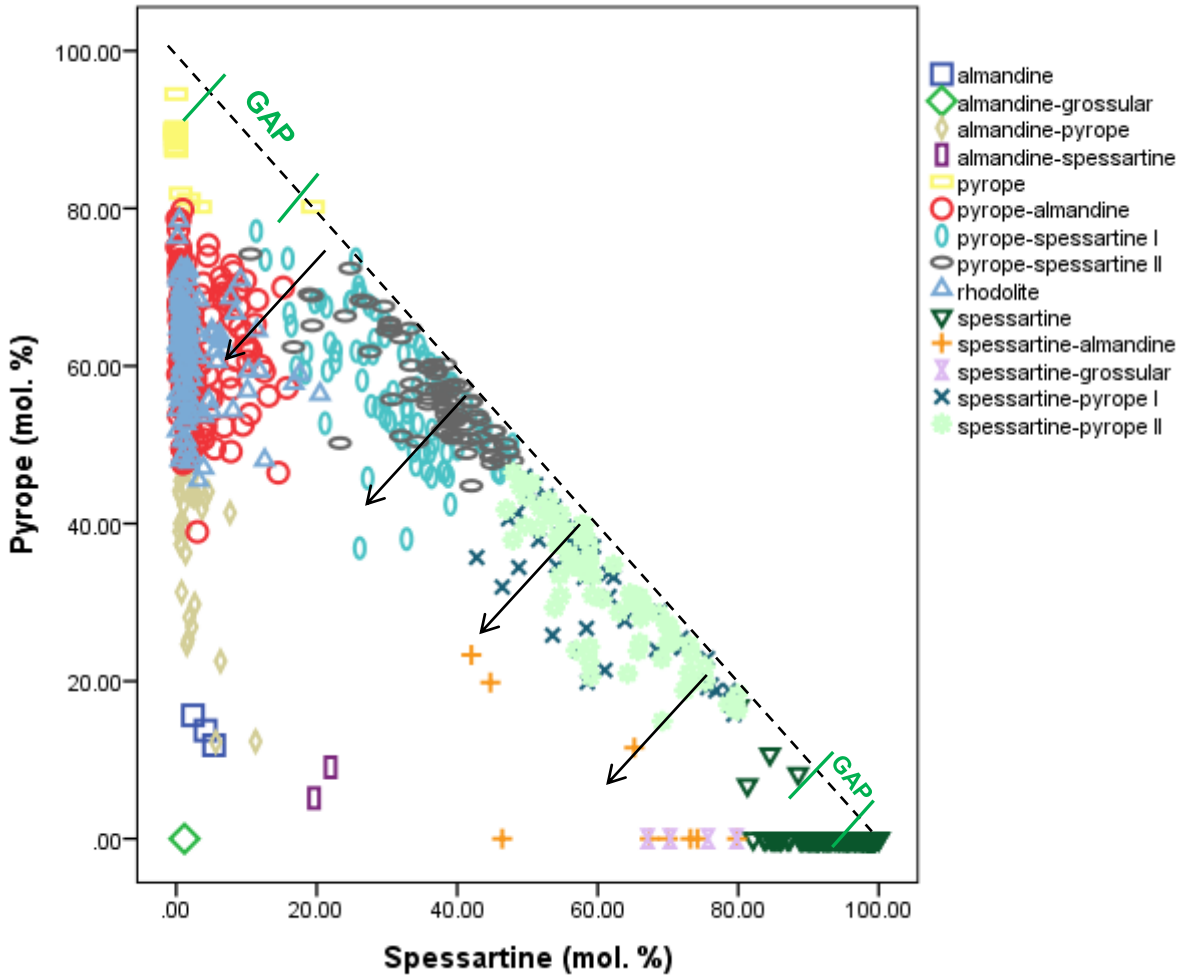

Figure 22. The pyrope and spessartine components of the different types of garnets from the pyralspite species. The dashed line indicates the pyrope spessartine solid solution series. The arrows represent deviation away from the trend line and indicate additional substitutions. The short green lines represent a gap in the series where none of the samples plot.

© University of Pretoria

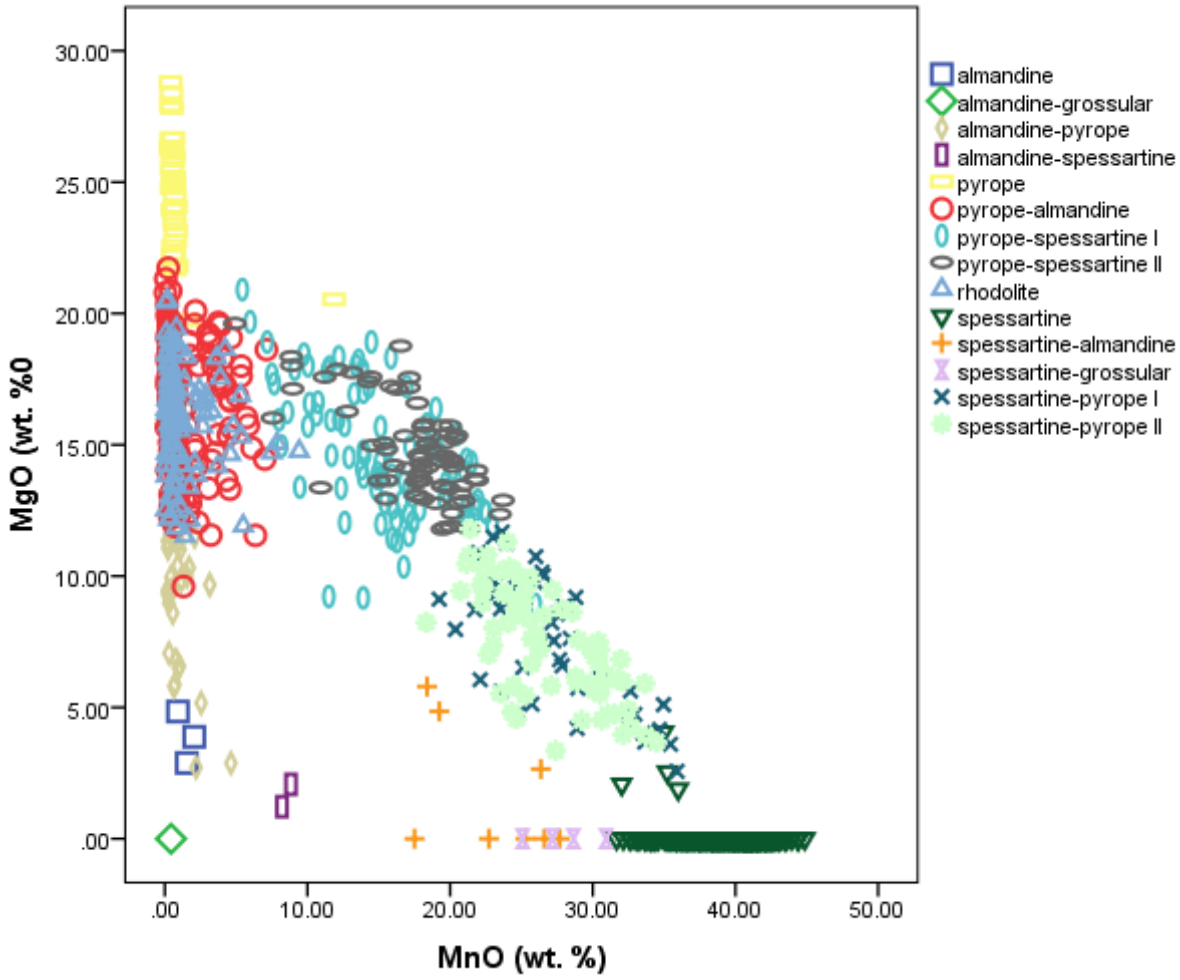

Figure 23. The MgO vs MnO concentrations in wt. % for the pyralspite species.

These 'pyrope' samples form part of the pyrope almandine solid solution series plotting in the pyrope-rich region (Figure 18). The 'pyrope' samples cluster together due to their high pyrope component (Figures 20, 18 and 22). The other end-member components are very low or absent. Most of the 'pyrope' samples possess no almandine component except for four samples with an almandine component from 7.00 mol.% to 17.00 mol.% (Figure 17). The 'pyrope' samples contain the highest andradite component in the pyralspite species with the andradite component increasing as pyrope becomes dominant (Figure 17). The high andradite component with low almandine present in the samples suggests the existence of a pyrope andradite series. This is addressed in more detail below.

Two groups amongst the 'pyrope' samples could be observed in Figures 12 and 17. One group in Figure 12 shows the FeO_{total} content decreasing as the MgO content increases. This group corresponds to the group observed in Figure 17 where the samples contain relatively high andradite and no almandine. The other group observed in Figure 12 plots near the 'pyrope-almandine' and 'rhodolite' samples and contain lower FeO_{total} and MgO than the first group (Figure 12). This latter group corresponds to the 'pyrope' samples

© University of Pretoria

in Figure 17, which contains some almandine and lower andradite. In Figure 19, the 'pyrope' samples cluster together with no almandine or spessartine, however, a few samples contain some almandine (7.00-17.00 mol.%) and some spessartine (0.64-3.40 mol.%). One sample has the highest spessartine component amongst the 'pyrope' samples with 19.48 mol.%. The two groups can also be observed in Figure 21, where one group contains andradite and the other contains little to no andradite. Neither of these groups contain grossular.

4.2.1.6. Pyrope-almandine and rhodolite

Two-hundred and four 'pyrope-almandine' and 105 'rhodolite' samples are present in the dataset, all of which are MgO dominant (9.60-21.73 wt. %) with significant amounts of FeO_{total} (8.95-27.54 wt. %) (Figure 12). CaO is also present in significant amounts (0.5-7.88 wt. %) with lower amounts of MnO (0.04-9.42 wt. %) (Figures 14 and 13). Both the 'pyrope-almandine' and 'rhodolite' samples contain below the detection limit or low Cr_2O_3 (≤ 0.47 wt. %) and below the detection limit or low V_2O_3 (≤ 0.54 wt. %) (Figures 15 and 16). The 'pyrope-almandine' samples have higher CaO than the 'rhodolite' samples (Figure 14).

The 'pyrope-almandine' and 'rhodolite' samples are pyrope dominant (38.94-79.84 mol.%) with 10.81-48.69 mol.% almandine (Figures 18 and 20). The grossular (0.00-13.70 mol.%) and spessartine (0.09-20.46 mol.%) components can be observed in Figures 21 and 19 respectively. The andradite component is variable ranging from 0.00 to 10.19 mol.% (Figure 17) and the uvarovite component is low (0.00-1.48 mol.%).

These samples plot along the solid solution series between pyrope and almandine in Figure 18, with none plotting beyond pyrope = 79.84 mol.%. The 'pyrope-almandine' and 'rhodolite' samples cluster together in Figures 19 and 20 and cannot be distinguished from each other based on their chemistry. The same can be observed in all of the graphs (Figures 17, 18, 21 and 22) where the 'pyrope-almandine' and 'rhodolite' samples cluster together. In Figure 20, the 'pyrope-almandine' and 'rhodolite' samples show larger spessartine variation than the almandine dominant samples, which suggest that pyrope-dominant samples of the pyrope almandine series has greater chemical variability. In Figure 17, the andradite component increases along the trend line from 'almandine-pyrope' to 'pyrope-almandine' and 'rhodolite'. Hence, the andradite component increases as the pyrope component increases.

Two groups of data can be seen within the 'pyrope-almandine' and 'rhodolite' samples in Figure 18 (the areas circled in yellow). These two groups are not visible in Figure 12. The group that plots away from the trend line consist of samples that contain higher

© University of Pretoria

amounts of spessartine (refer to Figures 19 and 22). The 'pyrope-almandine' and 'rhodolite' samples cluster together and plot in both groups in Figure 18. Again, two groups can be observed in Figure 21, which shows the different clusters present in the pyrope-almandine solid solution series when looking at their grossular and andradite components. Most of the samples plot at '2' with low to no grossular. The other group is represented by '1' and plot along the dashed line between grossular and andradite. In this group, the grossular component decreases as the andradite component increases. Both the 'rhodolite' and 'pyrope-almandine' samples plot in both groups.

These two groups observed in Figure 21 are different to the two groups observed in Figure 18. The former two groups refer to the substitution of grossular for andradite (Figure 21) and the latter two groups refer to the substitution of spessartine (Figure 18).

4.2.1.7. Pyrope-spessartine I and II

Eighty-eight 'pyrope-spessartine I' and 75 'pyrope-spessartine II' samples are present with MgO (8.92-20.91 wt. %) and MnO (4.90-25.98 wt. %) having the highest concentrations (Figure 23). FeO_{total} is also present in significant amounts ranging from 0.15 to 15.45 wt. % and CaO ranging from 1.00 to 5.81 wt. % (Figures 12 and 14). The Cr_2O_3 contents (≤ 0.52 wt. %) are lower than the V_2O_3 contents (≤ 1.64 wt. %) (Figures 15 and 16). The 'pyrope-spessartine II' samples contain higher V_2O_3 content (0.10-1.64 wt. %) than the 'pyrope-spessartine I' samples (0.00-1.48 wt. %) (Figure 16).

These 'pyrope-spessartine I and II' samples have Cr_2O_3 contents similar to the 'spessartine-pyrope II' samples (Figure 15). The chromium content is very similar amongst the colour change and non-colour change 'pyrope-spessartine I and II' samples and cannot be distinguished from each other based on their Cr_2O_3 content.

Pyrope is the dominant end-member ranging from 36.81 to 77.13 mol.%. Spessartine follows with 10.55 to 58.61 mol.%, while almandine is variable and ranges from 0.00 to 24.62 mol.% (Figures 22 and 18). In some cases, the almandine component almost equals the pyrope and/or spessartine components (Figure 20, 18 and 19). The grossular component ranges from 0.00-7.07 mol.% (Figure 21). Uvarovite and andradite are present in low amounts from 0.00 to 1.59 mol.% and 0.00 to 8.28 mol.% respectively (Figure 17).

The samples form part of the solid solution series between pyrope and spessartine (Figures 20 and 22). These samples plot in the pyrope-rich region of the pyrope spessartine solid solution series in Figure 20 and 22. Gaps, however, are present in the series (represented by the green lines in Figure 22). The 'pyrope-spessartine I and II' samples in

© University of Pretoria

Figures 20 and 18 show a larger range in, and higher almandine component than the 'spessartine-pyrope I and II' samples. The same can be observed in Figure 19 between the 'pyrope-spessartine I' and 'pyrope-spessartine II' samples suggesting that the presence of almandine decreases the potential for colour change.

In Figure 22, the 'spessartine-pyrope I and II' samples show less deviation from the trend line than the 'pyrope-spessartine I and II' samples.

4.2.1.8. Spessartine

Three-hundred and twenty 'spessartine' samples are present with the highest MnO (31.66-44.86 wt. %) content in the pyralspite species (Figure 23). Lesser amounts of FeO_{total} (0.17-13.13 wt. %), MgO (1.88-4.05 wt. %), and CaO (0.14-5.68 wt. %) are also present (Figures 12 and 14). The Cr_2O_3 and V_2O_3 contents are low (≤ 0.18 and ≤ 0.70 wt. % respectively) (Figures 15 and 16).

The spessartine component is dominant in the samples and ranges from 80.06-100.00 mol.%. (Figure 20 and 19). Lower amounts of almandine, pyrope and grossular are present (Figures 18 and 21). The andradite content is generally below 5 mol.% (Figure 17) except for one sample with an andradite component of 13.92 mol.%. The uvarovite component ranges from 0.00-0.68 mol.%.

The 'spessartine' samples cluster together in the spessartine dominant corner in Figures 20, 22 and 19. Little to none of the other end-member components are present in the 'spessartine' samples with the spessartine samples having very little chemical variability.

4.2.1.9. Spessartine-almandine

Nine 'spessartine-almandine' samples are present with a MnO content of 17.50-26.67 wt. % (Figure 13). The FeO_{total} (2.60-12.46 wt. %) and CaO (1.52-3.89 wt. %) contents are also present (Figures 12 and 14). The MgO content is below the detection limit or very low (≤ 5.80 wt. %). Cr_2O_3 is present in trace amounts (≤ 0.32 wt.%) (Figure 15). The V_2O_3 content in the samples is relatively high ranging from 0.16 to 0.47 wt. % (Figure 16).

The samples are spessartine dominant (42.01-79.85 mol.%) with lesser amounts of almandine (13.93-44.07 mol.%) and grossular (2.66-11.37 mol.%) (Figures 20, 19 and 21). The pyrope component is below the detection limit for most of the samples (Figure 18). A few samples, however, have relatively high pyrope with the highest being 23.32 mol.% (Figure 18). The andradite (0.00-3.65 mol.%) and uvarovite (0.00-1.17 mol.%) components are low (Figure 17).

© University of Pretoria

The samples plot below the solid solution series between almandine and spessartine in the spessartine-rich region (Figure 19). In Figure 19, a gap can be seen in the series (green lines) where no samples plot. The 'spessartine-almandine' samples show deviation from the trend line indicating additional substitutions of the pyrope component (Figures 19 and 20). The 'almandine-spessartine' samples show smaller variability in their chemistry, specifically the pyrope component, than the 'spessartine-almandine' samples (Figure 20). The 'spessartine-almandine' samples also contain higher amounts of V_2O_3 and Cr_2O_3 than the 'almandine- spessartine' samples (Figures 15 and 16), which explains the presence of colour change in the former and the absence of colour change in the latter.

4.2.1.10. Spessartine-grossular

Four 'spessartine-grossular' samples are found with the MnO ranging from 25.08 to 30.92 wt. % and CaO from 4.59 to 8.73 wt. % (Figures 13 and 14). FeO_{total} is present in minor amounts (0.28-2.61 wt. %) with MgO being undetected (Figure 12). Cr_2O_3 and V_2O_3 are present in trace amounts (≤ 0.16 wt. % and 0.22-0.56 wt. % resepectively) (Figures 15 and 16). The latter amount is relatively high for V_2O_3 content. The CaO content is relatively high for a garnet from the pyralspite species (Figure 14).

Spessartine is the dominant component with 67.09 to 79.77 mol.% with grossular being the second (14.71-29.45 mol.%) (Figures 19 and 21). Almandine ranges up to 8.01 mol.% and uvarovite up to 0.58 mol.% (Figure 17). Pyrope and andradite are not present (Figures 18 and 17).

4.2.1.11. Spessartine-pyrope I and II

Forty-nine 'spessartine-pyrope I' and 72 'spessartine-pyrope II' samples arre found. The MnO contents (18.31-35.90 wt. %) are the highest followed by MgO (2.57-11.80 wt. %), CaO (0.47-8.97 wt. %), and FeO_{total} (0.11-10.78 wt. %) (Figures 13, 12 and 14). The V_2O_3 contents (≤ 1.09 wt. %) are higher than the Cr_2O_3 contents (≤ 0.42 wt. %) (Figures 16 and 15). The V_2O_3 (≤ 1.09 wt. %) and Cr_2O_3 (≤ 0.42 wt. %) contents in 'spessartine-pyrope II' samples are higher than that in the 'spessartine-pyrope I' samples (≤ 0.62 wt. % and ≤ 0.30 wt. % respectively).

The spessartine component is the highest (42.78-79.94 mol.%) followed by pyrope (14.93-46.51 mol.%), grossular (0.00-18.48 mol.%) and andradite (≤ 8.52 mol.%) (Figures 22 and 21). In contrast to the 'pyrope-spessartine I and II' samples, very low almandine (≤ 15.46 mol.%) is present in these samples (Figures 20 and 18) with these 'spessartine-pyrope I and II' samples showing less chemical variability than their pyrope-dominant

© University of Pretoria

counterparts. Uvarovite is present in low amounts with 'spessartine-pyrope II' samples (≤ 1.55 %) containing higher maximum concentrations than the 'spessartine-pyrope I' samples (≤ 1.00 %).

The samples plot along the solid solution series between pyrope and spessartine in the spessartine-rich region (Figure 22 and 20). These samples show less deviation from the trend line (dashed line in Figure 22) when compared to the 'pyrope-spessartine I and II' samples. In Figure 22, no differences could be observed between colour change and non-colour change samples.

The 'spessartine-pyrope II' samples have much higher Cr_2O_3 than the 'spessartine-pyrope I' samples (Figure 15), and the 'spessartine-pyrope I and II' samples have higher V_2O_3 content than the 'pyrope-spessartine I and II' samples with the 'spessartine-pyrope II' samples having the highest V_2O_3 content (Figure 16). The chromium contents in Figure 15 show similar trends. This indicates that colour change is more likely to occur in spessartine dominant samples with high Cr_2O_3 and V_2O_3 content than in pyrope dominant samples. A few 'spessartine-pyrope I and II' samples have high CaO (4.35-8.94 wt. %) (Figure 14).

4.2.2. Magnetic susceptibility

Two 'spessartine' samples had very high magnetic volume susceptibility at 0.036 and 0.012 SI. These values are considered too high and irregular for 'spessartine' gem garnets and is thus not further considered. The cause of this high magnetic susceptibility is unknown but it could be due to the presence of inclusion.

© University of Pretoria

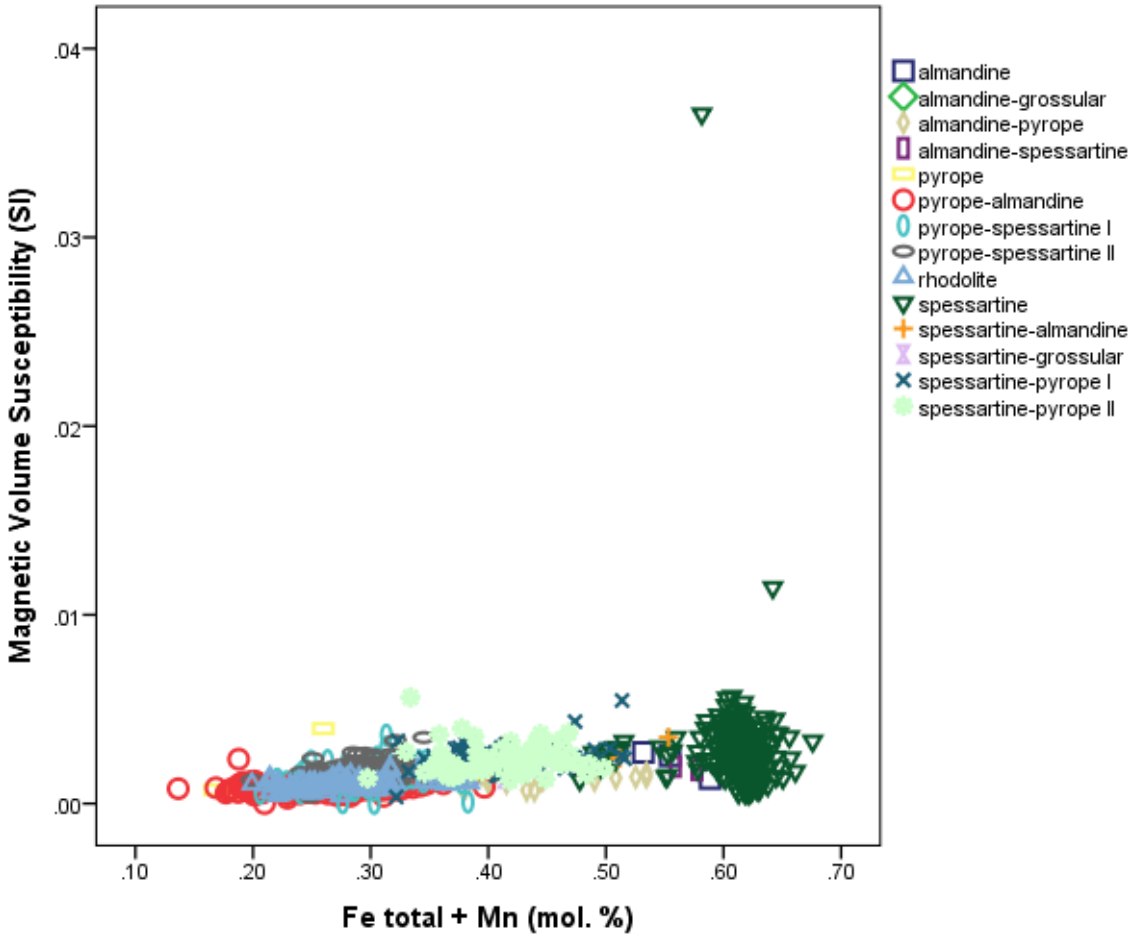

Figure 24. a) Magnetic volume susceptibility vs. Fe_{total} + Mn (mol. %) with the two unusual 'spessartine' samples included. The garnets are only from the pyralspite species.

© University of Pretoria

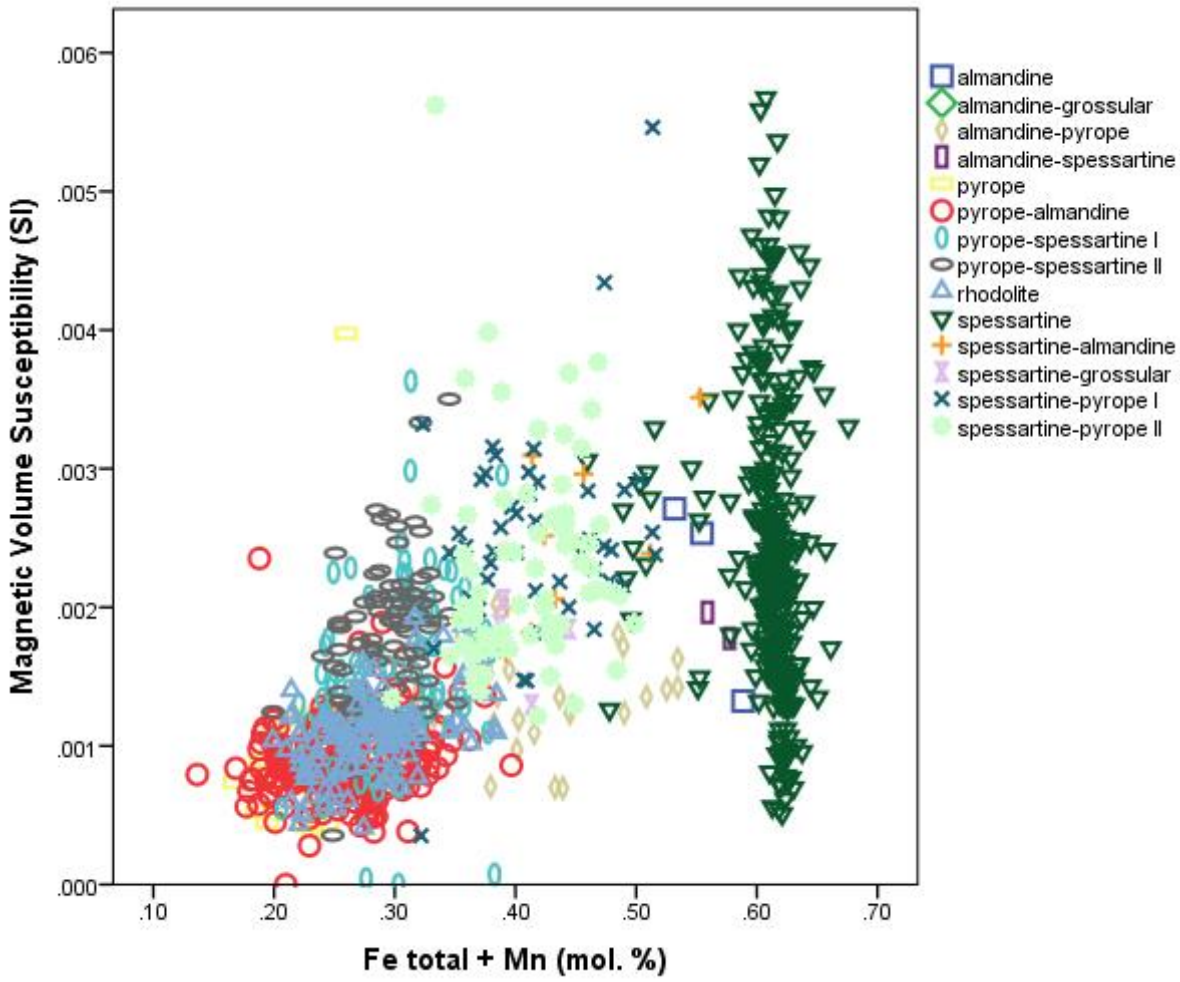

Figure 24. b) Magnetic volume susceptibility vs. Fe_{total} + Mn (mol. %) with the two unusual 'spessartine' samples removed. The garnets are only from the pyralspite species.

Little variation is observed between the two figures (Figure 24a and 24b) with the magnetic volume susceptibility for 'spessartine' showing the same variation in both figures.

The magnetic susceptibility shows a general increase with an increase in Fe_{total} + Mn (mol. %), as expected. However, this trend is not as well defined, as stated in past literature (Hoover and Williams, 2007; Hoover *et al.*, 2008). 'Spessartine' shows the largest range in magnetic susceptibility and some of the highest values. 'Spessartine-grossular' shows lower magnetic susceptibility and lower Fe_{total} + Mn content than spessartine. 'Almandine' has high Fe_{total} + Mn, but its magnetic susceptibilities are relatively low for garnets composed primarily of iron. 'Spessartine-almandine' has higher magnetic susceptibilities than 'almandine-spessartine' despite the latter having a higher Fe_{total} + Mn content. 'Almandine-pyrope' has a higher Fe_{total} + Mn content compared to 'pyrope-almandine', but its magnetic susceptibilities are similar. Looking at the pyrope spessartine solid solution series, 'spessartine-pyrope I' and 'spessartine-pyrope II' display a higher Fe_{total} + Mn content than 'pyrope-spessartine I' and 'pyrope-spessartine II'. The spessartine dominant samples, hence, have a slightly higher

© University of Pretoria

magnetic susceptibility, although this is only evident in a small number of spessartine dominant samples. The 'pyrope-spessartine I and II' and 'spessartine-pyrope I and II' samples show higher magnetic susceptibilities than the 'pyrope-almandine', 'rhodolite' and 'almandine-pyrope' samples. 'Pyrope' shows low magnetic susceptibilities with low Fe_{total} + Mn contents.

4.2.3. Refractive index

The almandine dominant samples have high RI values (except for the one almandine-grossular sample) when compared to the pyrope dominant samples in Figure 25.

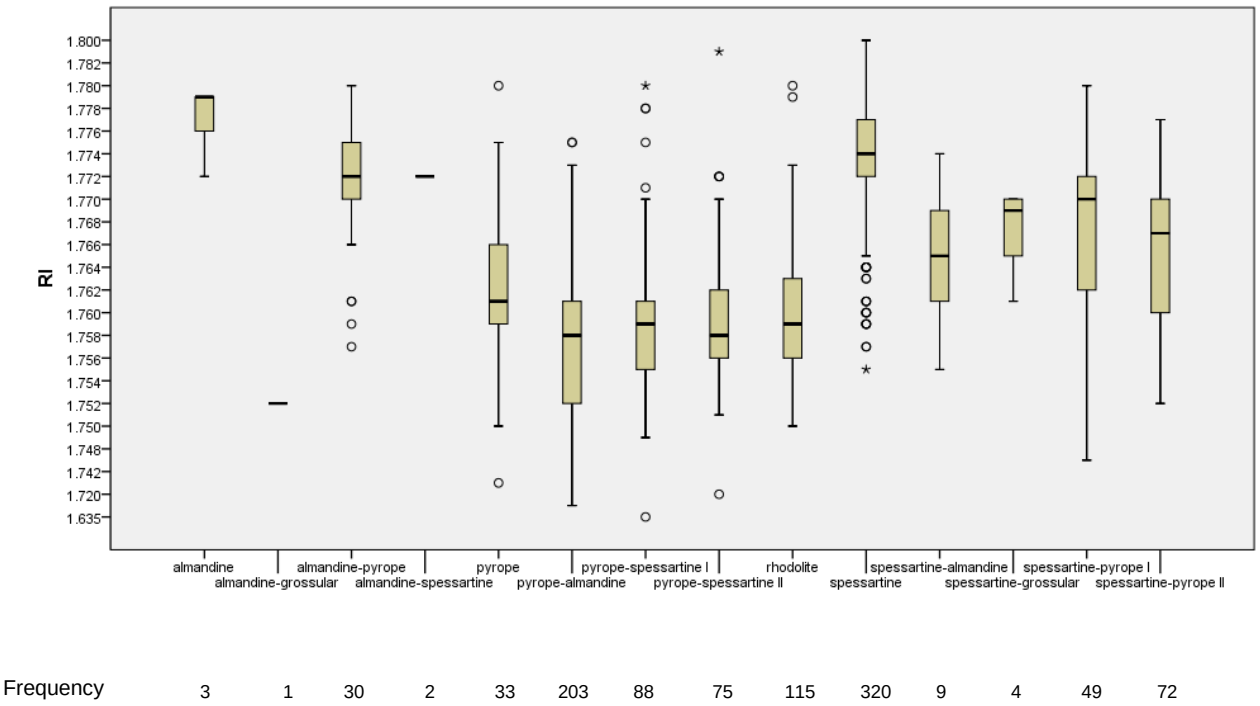

Figure 25. Boxplot showing RI values of the different types of garnets from the pyralspite species. Below the boxplot are the frequencies for the different pyralspite garnets.

Samples with an almost pure spessartine composition also possess high RI values. The RI values of the pyrope spessartine and pyrope almandine solid solution series overlap and cannot be distinguished from each other. 'Pyrope-almandine' and 'rhodolite' possess similar RI values and cannot be distinguished from each other. The spessartine dominant samples in the pyrope spessartine solid solution series have slightly higher RI values than their pyrope dominant counterparts. The 'spessartine-almandine' samples possess RI's similar to the pyrope spessartine solid solution series making distinction between the two difficult. 'Spessartine-grossular' also shows a similar RI range to the 'spessartine-almandine' and the 'spessartine-pyrope I and II' samples.

© University of Pretoria

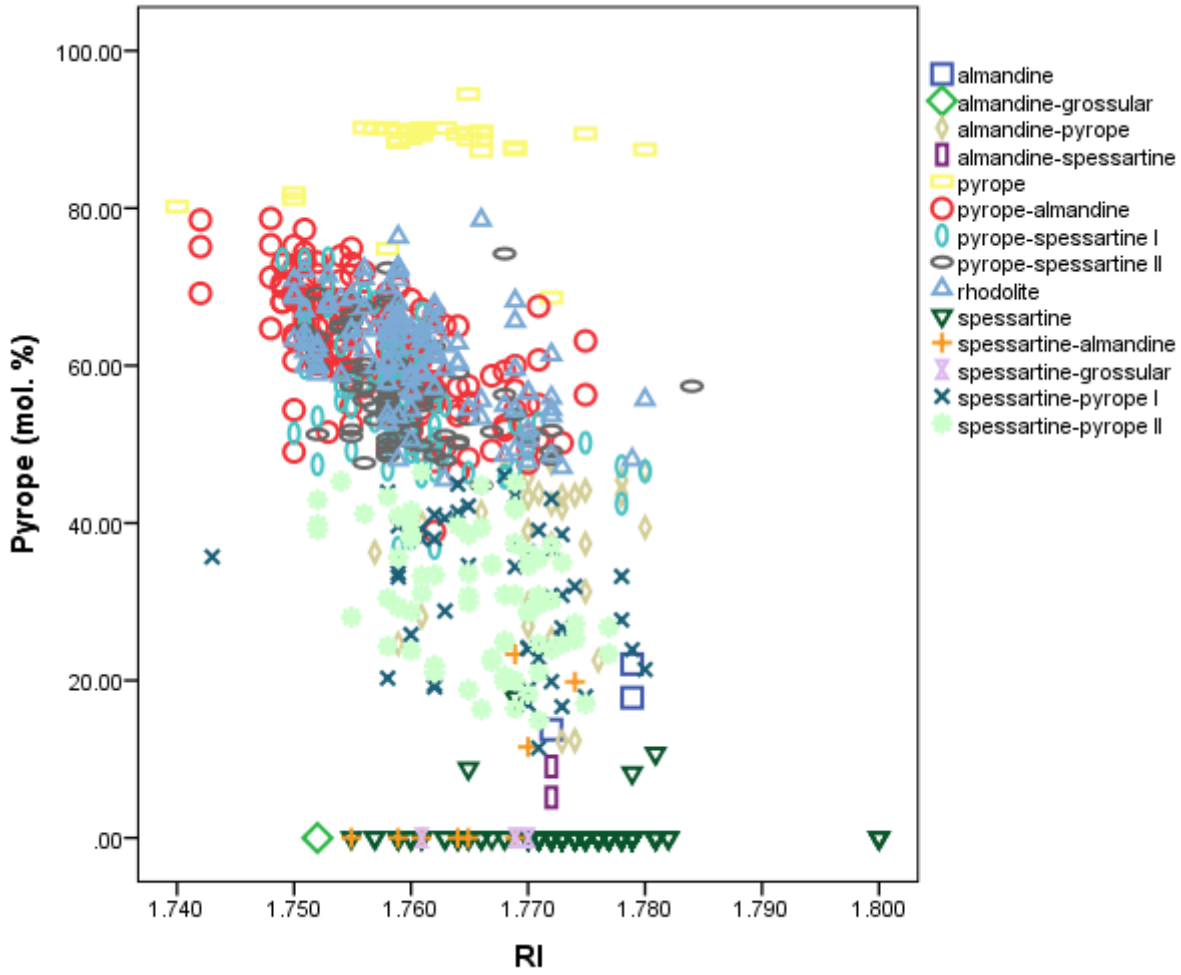

Figure 26. The RI of the different garnets from the pyralspite species plotted against the pyrope component.

Two extreme samples are observed with RI below the accepted range for pyralspite garnets (below 1.74 according to Stockton and Manson (1985)), namely a 'pyrope-spessartine I' with a RI of 1.64 and a 'pyrope-spessartine II' with an RI of 1.73. They were therefore considered as outliers and removed. The 'almandine' samples have RIs that are too low according to Stockton and Manson (1985). 'Almandine-grossular' has a very low RI of 1.752. The 'almandine-pyrope' samples have RIs that conform to the traditional range of 1.742-1.785 (Stockton and Manson, 1985). 'Pyrope-almandine' samples have lower RI's when compared to 'almandine- pyrope' samples. Two of the 'almandine-spessartine' samples have RI's of 1.772 whereas the traditional range is 1.81-1.82 (Stockton and Manson, 1985). The RI of 'spessartine-almandine' is much lower than that of 'almandine-spessartine'. Of the pyrope spessartine solid solution series, most plot within the traditional range of RI's as stated by Stockton and Manson (1985). All of the samples from the pyrope spessartine solid solution series show a slight increase in RI as the pyrope decreases. 'Spessartine' possesses very high RIs, which is to be expected, however, 'spessartine-

© University of Pretoria

grossular' had a much lower RI of 1.761-1.77. This could be due to the presence of grossular.

4.2.4. Colour

4.2.4.1. Orange and red varieties

In Figure 27 below, only the orange and red varieties are plotted, with other colours being excluded for clarity purposes. The majority of the orange and red varieties in Figure 27 are composed predominantly of spessartine with low amounts of almandine.

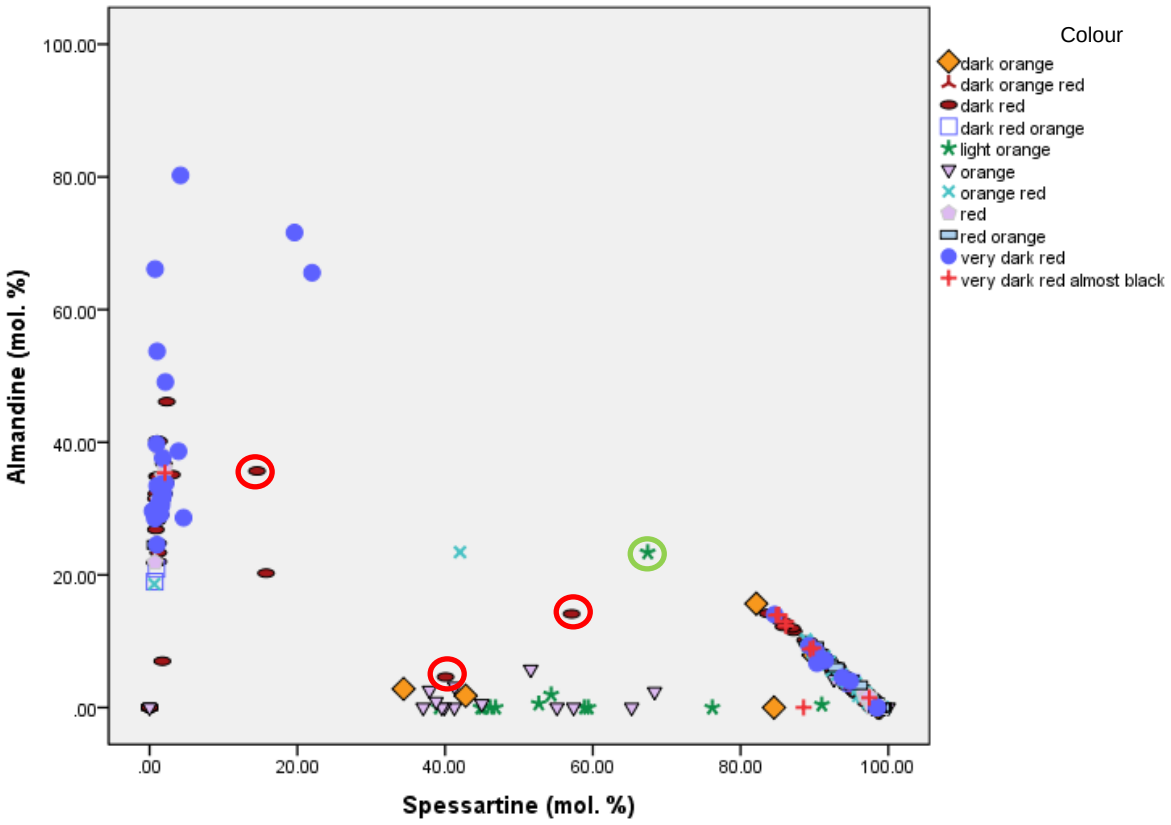

Figure 27. The almandine and spessartine components for the orange and red varieties of the pyralspite garnets. The dark orange red samples are hidden underneath the very dark red and red orange samples. The red circles refer to three dark red samples with high almandine and/or high spessartine. The green circle refers to a light orange 'spessartine-almandine' sample with high almandine.

© University of Pretoria

The compositions of the orange and red varieties are summarised in the table below.

Table 10. Summary of the orange and red varieties and their composition from the pyralspite garnets.

Colour	The common composition observed for that particular colour	The less common composition observed for that particular colour
Dark orange	Spessartine	Pyrope-spessartine I and a spessartine-pyrope I
Dark orange red	Spessartine	None
Dark red	Spessartine	Pyrope-almandine, pyrope, almandine-pyrope, pyrope-spessartine I and spessartine-pyrope II
Dark red orange	Spessartine	Pyrope-almandine
Light orange	Spessartine	Pyrope-spessartine I, spessartine-pyrope I and spessartine-almandine
Orange	Spessartine	Pyrope-spessartine I, spessartine-pyrope I and pyrope
Orange red	Spessartine	Pyrope-almandine and spessartine-almandine
Red	Spessartine	Pyrope-almandine
Red orange	Spessartine	Pyrope-almandine
Very dark red	Spessartine and pyrope-almandine	Almandine-pyrope and almandine
Very dark red almost black	Spessartine	Pyrope-almandine

© University of Pretoria

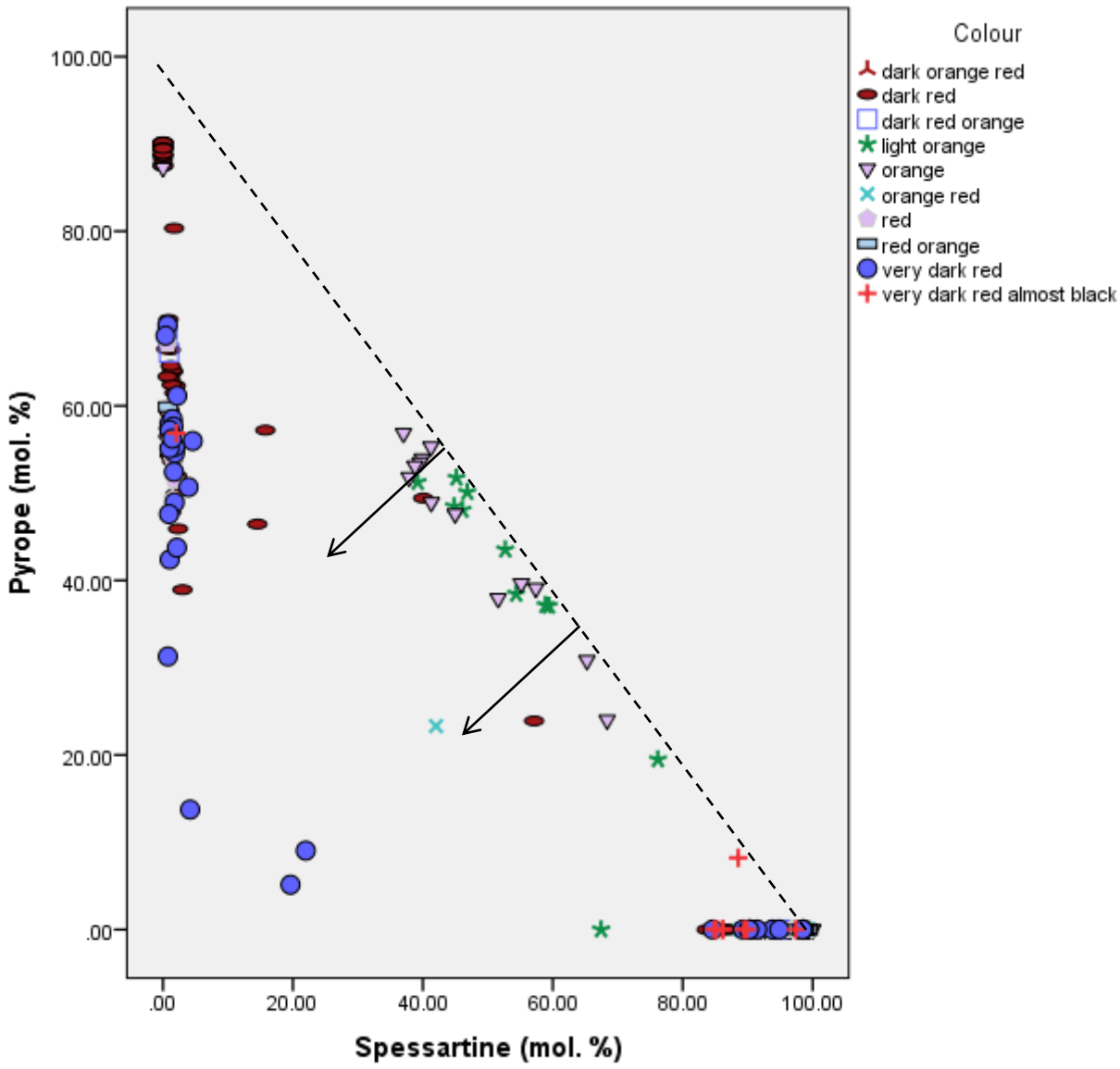

Figure 28. The pyrope and spessartine components of the orange and red samples. The garnets are only from the pyralspite species. The dashed line indicates the solid solution series between pyrope and spessartine. The arrows represent deviation away from the trend line and indicate additional substitutions.

A fair number of the light orange and orange samples plot close to the dashed line in Figure 28 and are ‘pyrope-spessartine l’ and ‘spessartine-pyrope l’ samples as well as two of the dark red samples.

© University of Pretoria

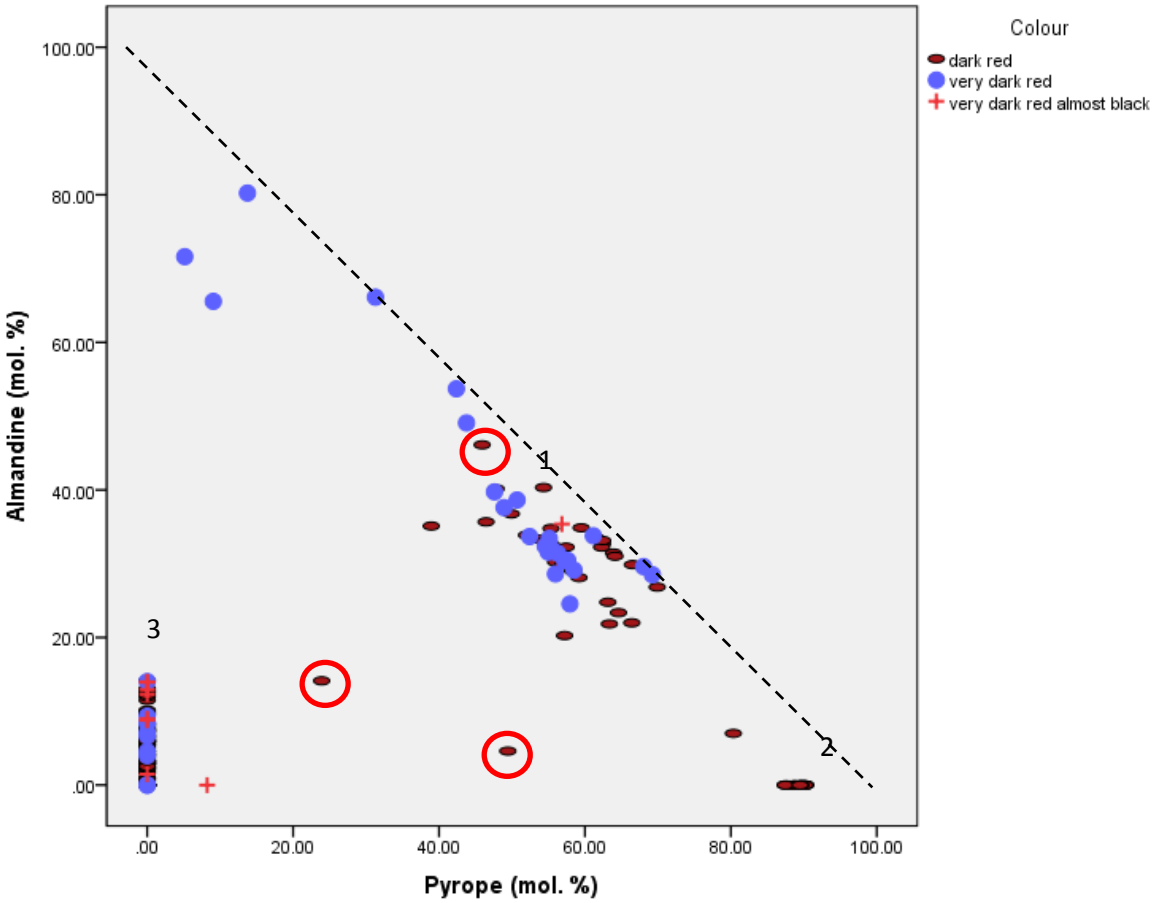

Figure 29. The almandine and pyrope components of the dark red and very dark red samples. The garnets are only from the pyralspite species. The trend line indicates the solid solution series between pyrope and almandine. The red circles refer to the 'almandine- pyrope', 'pyrope-spessartine I' and 'spessartine-pyrope I 'samples mentioned earlier in Figure 27.

The dark red samples plot in '1', '2' and '3' in Figure 29. These are 'pyrope-almandine', 'pyrope' and 'spessartine' respectively.

© University of Pretoria

4.2.4.2. Pink and purple varieties

The pink and purple varieties in Figure 30 have a lower spessartine component than the brown, yellow and orange varieties (Figures 38), with higher almandine.

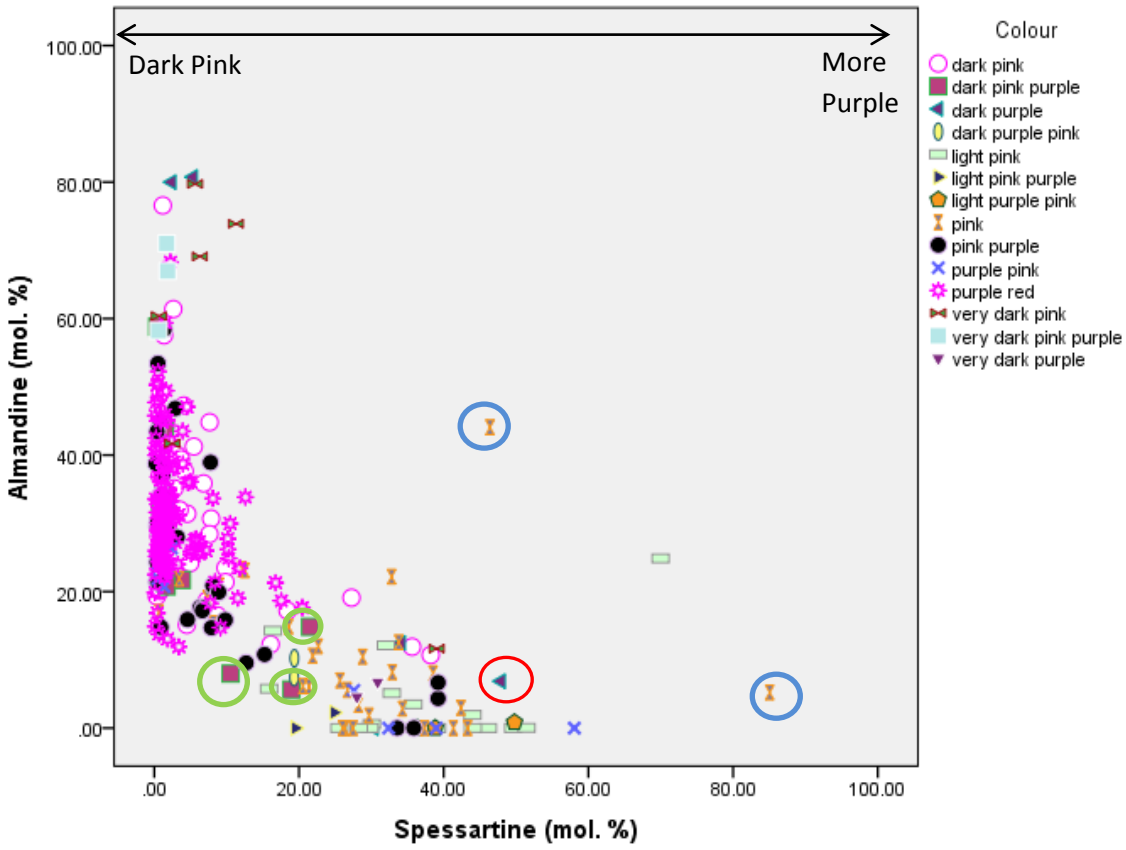

Figure 30. The almandine and spessartine components of the pink and purple samples. The garnets are only from the pyralspite species. The purple red samples are 'rhodolite'. The red circle refers to the dark purple 'spessartine-pyrope II'. The blue circles refer to pink samples with unusual composition ('spessartine-almandine' and 'spessartine'). The green circles refer to dark pink purple samples with odd compositions ('pyrope-spessartine I and II).

The pink colour darkens as spessartine decreases and almandine increases. The very dark pink, very dark pink purple and dark purple (except one as indicated by the red circle) have very high almandine component, which indicates that almandine is responsible for the darkening of these garnets. The lighter coloured samples have lower almandine and higher spessartine content. The purple red samples refer to the 'rhodolite samples'. These samples all plot together with the dark pink, dark pink purple, pink purple and purple pink samples and cannot be differentiated from each other based on chemistry.

© University of Pretoria

The compositions of the purple and pink varieties are summarised in the table below.

Table 11. Summary of the purple and pink varieties and their composition for the pyralspite garnets.

Colour	The common composition observed for that particular colour	The less common composition observed for that particular colour
Dark pink	Pyrope-almandine	Almandine-grossular
Dark pink purple	Pyrope-almandine	Almandine-pyrope, pyrope-spessartine I and II
Dark purple	Almandine and spessartine-pyrope II	None
Dark purple pink	Pyrope-spessartine II	None
Light pink	Pyrope-spessartine I and II	Spessartine-almandine and spessartine-pyrope I and II
Light pink purple	Pyrope-spessartine I and pyrope	None
Light purple pink	Pyrope-spessartine I and II	Spessartine-pyrope II
Pink	Pyrope-spessartine I and II	Pyrope-almandine, spessartine-almandine and spessartine
Pink purple	Pyrope-almandine	Almandine-pyrope and pyrope-spessartine I and III
Purple pink	Pyrope-almandine and pyrope-spessartine I and II	Spessartine-pyrope II
Purple red (rhodolite)	Pyrope-almandine	None
Very dark pink	Almandine-pyrope	Pyrope-almandine
Very dark pink purple	Almandine-pyrope	None
Very dark purple	Pyrope-spessartine I and II	None

© University of Pretoria

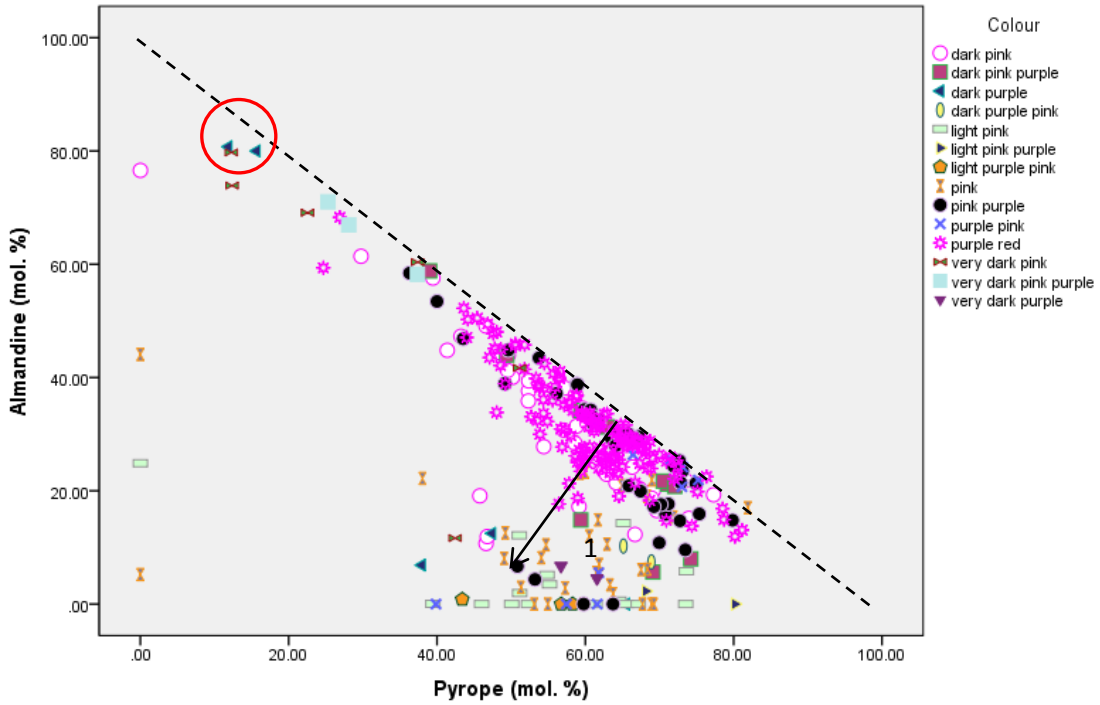

Figure 31. The almandine and pyrope components of the pink and purple samples. The garnets are only from the pyralspite species. The trend line indicates the solid solution series between pyrope and almandine and the arrow indicates additional substitutions. '1' is refers to samples that are pyrope dominant but contain similar amounts of almandine and spessartine.

In Figure 31, the dark purple and very dark purple stones (except for the two dark purple samples in the red circle) contain low almandine (4.55-12.48 mol.%), with high spessartine (28.01-47.91 mol.%) in Figure 30. Where pink is dominant in a sample, this sample plots along the solid solution trend between pyrope and almandine. In the purple dominant samples, the almandine component is lower than in the pink samples and approaches the area indicated by the number '1' (Figure 31). The pink dominant samples have a higher pyrope component than the purple dominant samples, indicating that pink samples have a high pyrope component.

The purple red 'rhodolites' have similar almandine and pyrope components to the other pink samples. All of the rhodolites, and most of the pink samples, close to the trend line in Figure 31.

© University of Pretoria

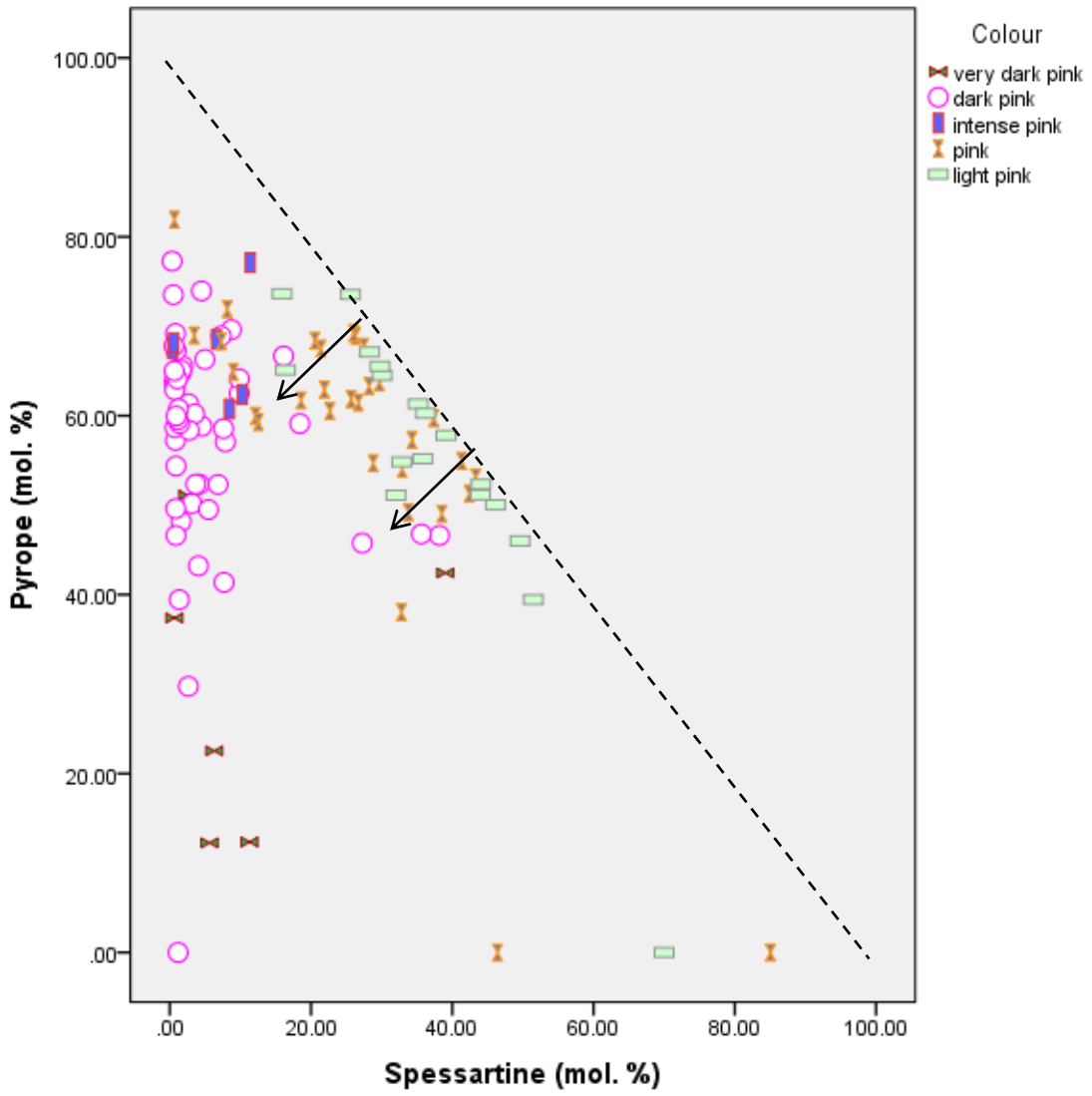

Figure 32. The pyrope and spessartine components of the pink samples. The garnets are only from the pyralspite species. The dashed line represents the solid solution series between pyrope and spessartine. The arrows represent deviation away from the trend line and indicate additional substitutions.

The light pink samples show a higher spessartine and lower pyrope component than the dark pink samples (Figure 32). Darker pink samples contain a lower spessartine component. Pyrope is the dominant component in the pink samples but the spessartine component has increased when compared to the dark pink and very dark pink samples. Pink becomes more dominant and intensifies in samples that are pyrope dominant with lesser amounts of almandine.

© University of Pretoria

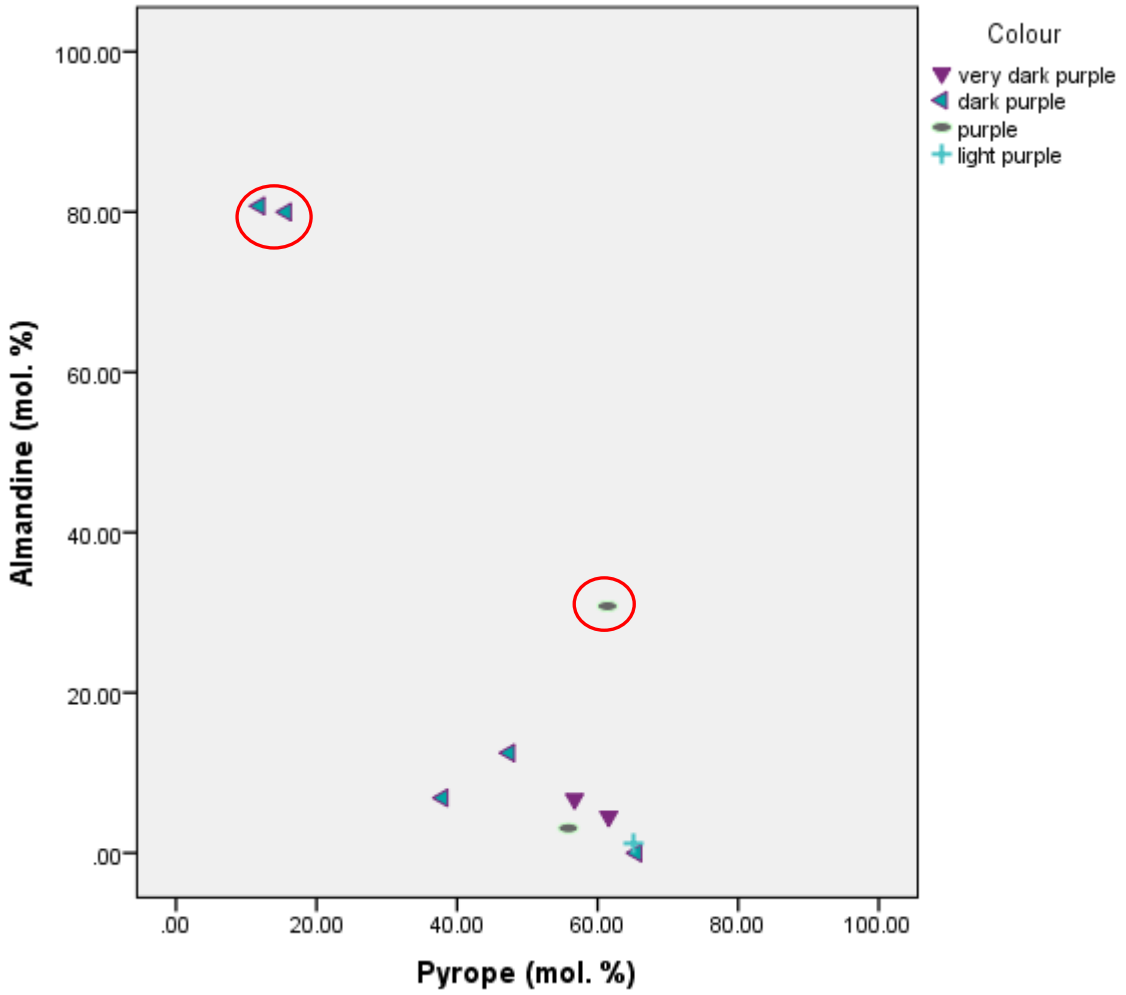

Figure 33. The almandine and pyrope components of the purple samples. The garnets are only from the pyralspite species.

Most of the purple varieties have a low almandine component (excluding the two dark purple and one purple sample in the red circles in Figure 33). This suggests that purple garnet gemstones may contain higher amounts of spessartine than almandine.

© University of Pretoria

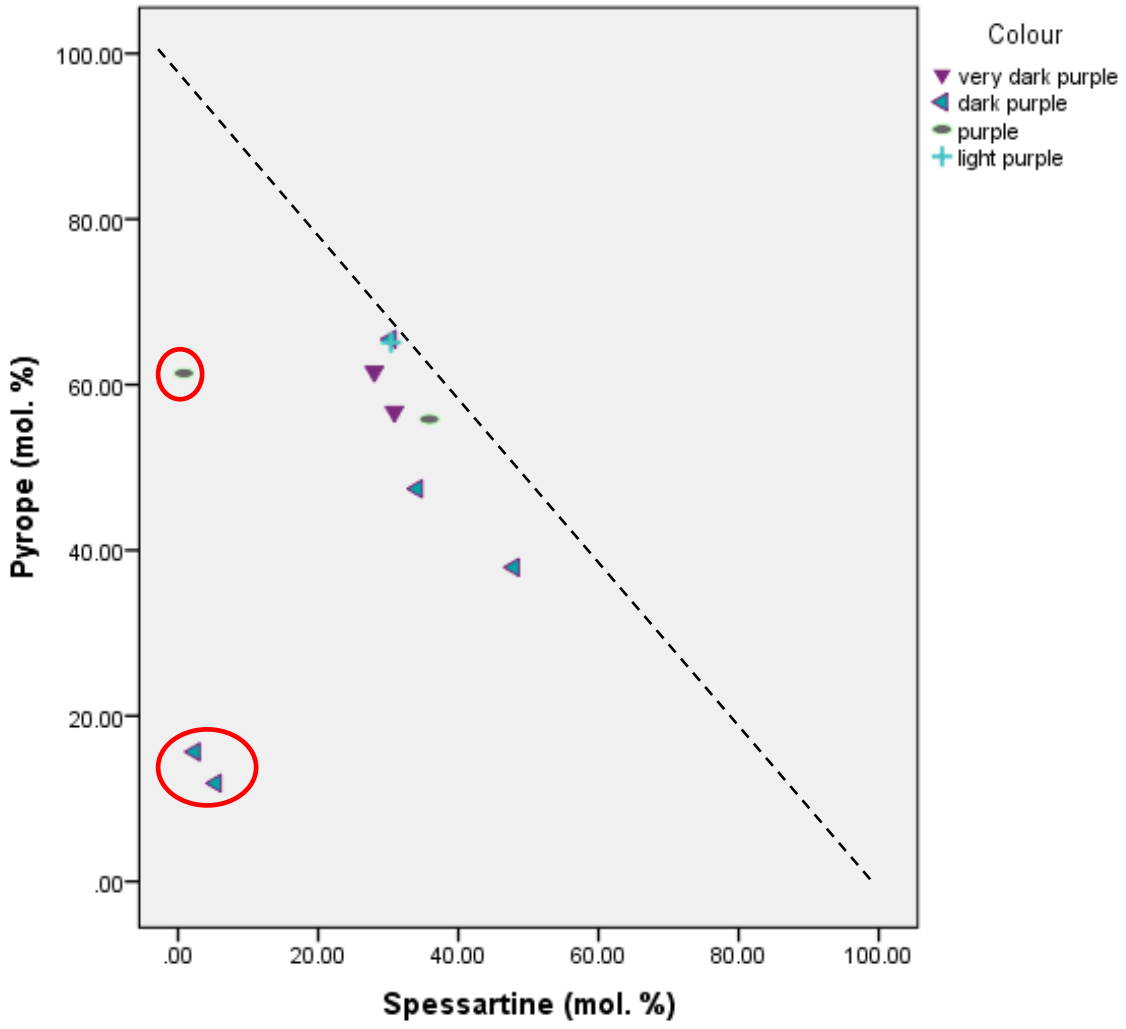

Figure 34. The pyrope and spessartine components of the purple samples. The garnets are only from the pyralspite species. The dashed line represents the solid solution series between pyrope and spessartine.

In Figure 34, most of the purple samples (excluding those in the red circles) contain a relatively high spessartine component.

© University of Pretoria

4.2.4.3. Orange pink varieties

Most of the orange pink varieties in Figure 35 show a lower almandine component and higher spessartine component than those of the dark pink samples. Most of the orange pink varieties are 'pyrope-spessartine I and II' and 'spessartine-pyrope I and II' samples. Only a few of the samples are 'pyrope-almandine' samples.

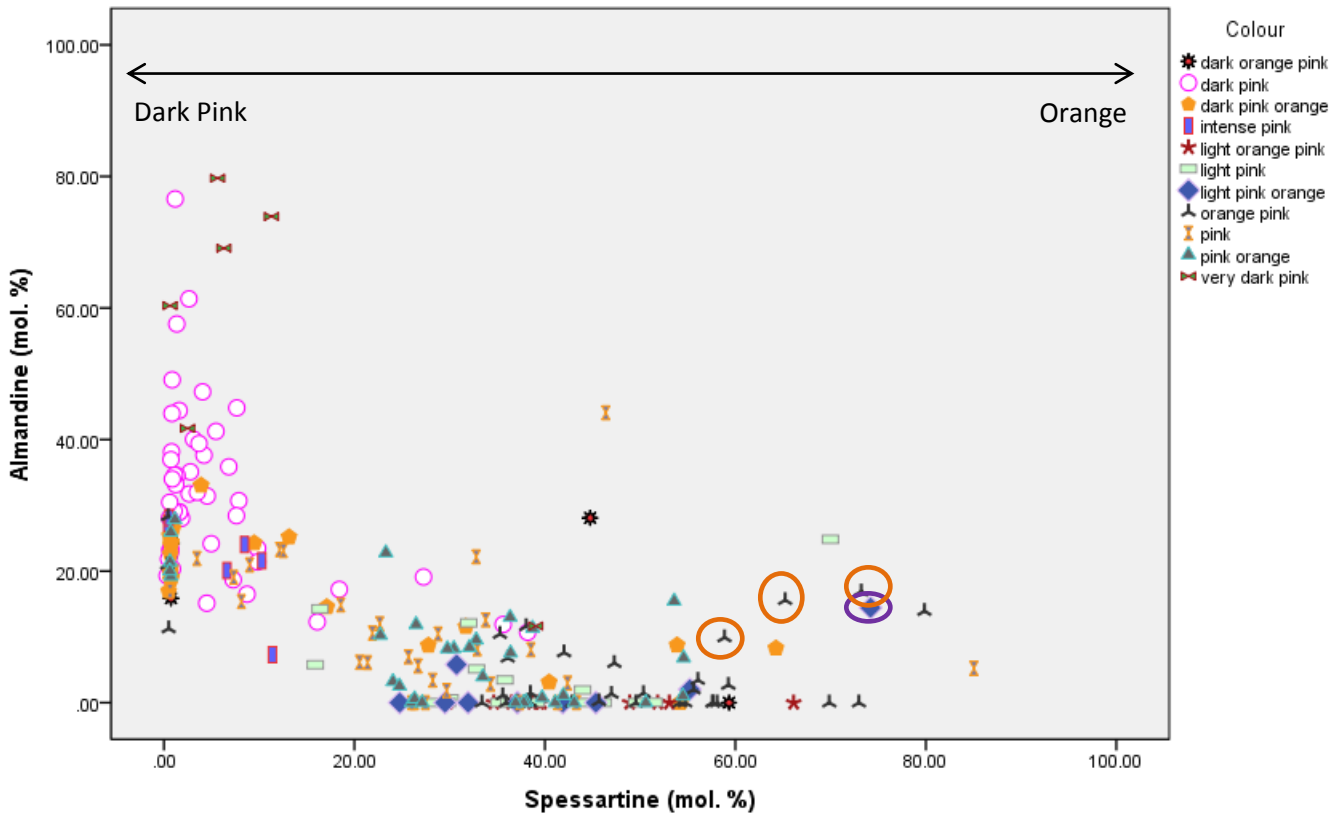

Figure 35. The almandine and spessartine components for dark pink and pink orange samples of the pyralspite garnets. Dark pink and other pink samples were included in this graph to provide a better comparison with the pink orange samples. The purple circle refers to a light pink orange 'spessartine-almandine' sample with high spessartine. The orange circles refer to the three orange pink 'spessartine-almandine' samples.

It can be seen in Figure 35 that the stones become more dark and pink as almandine increases and spessartine decreases. Stones that are a deeper orange show a higher spessartine component than lighter orange stones.

© University of Pretoria

The compositions of the orange pink varieties are summarised in the table below.

Table 12. Summary of the orange pink varieties and their composition for the pyralspite garnets.

Colour	The common composition observed for that particular colour	The less common composition observed for that particular colour
Dark orange pink	None (only 3 samples)	Pyrope-almandine, spessartine-pyrope II and spessartine-almandine
Dark pink orange	Pyrope-almandine	Pyrope-spessartine I and II, and spessartine-pyrope I and II
Light orange pink	Spessartine-pyrope II	Pyrope-spessartine II
Light pink orange	Pyrope-spessartine II and spessartine-pyrope II	Spessartine-almandine
Orange pink	Pyrope-spessartine I and II and spessartine-pyrope II	Pyrope-almandine and spessartine-almandine
Pink orange	Pyrope-spessartine I and II	Pyrope-almandine and spessartine-pyrope I and II

© University of Pretoria

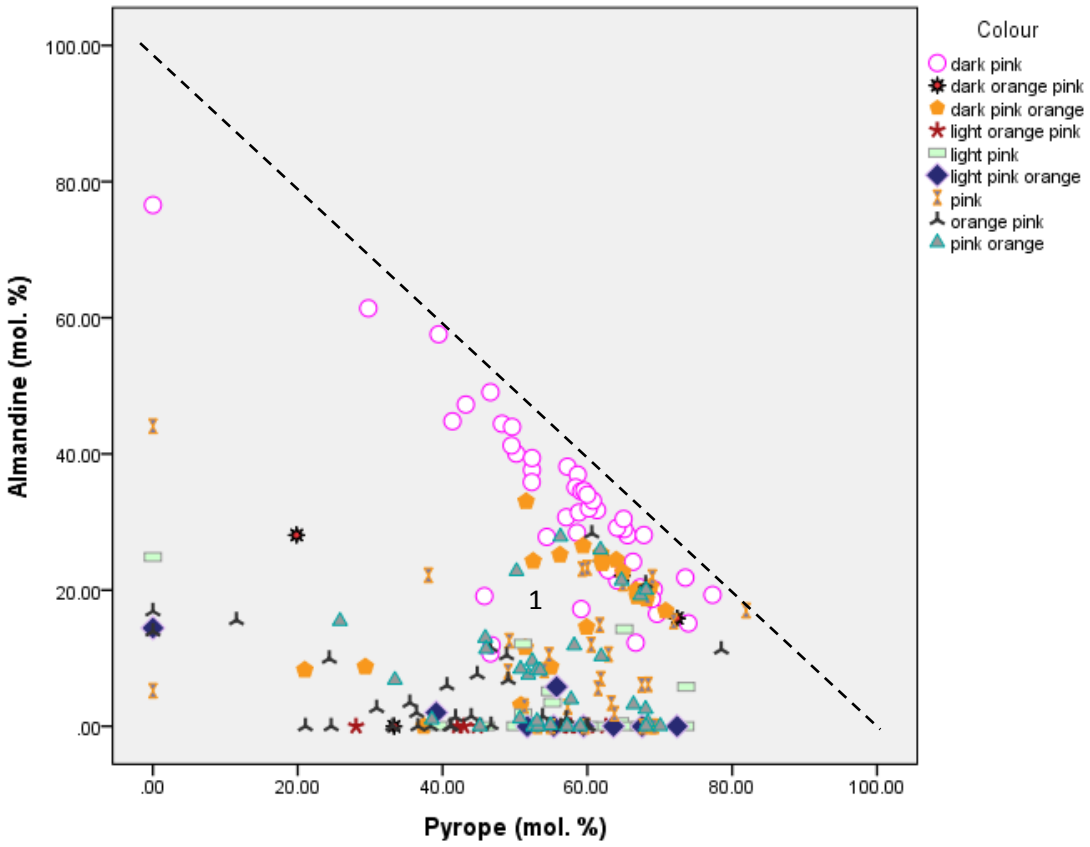

Figure 36. The almandine and pyrope components of the pink orange samples together with the pink varieties. The garnets are only from the pyralspite species. The dashed line represents the solid solution series between almandine and pyrope.

Most of the orange pink samples plot away from the trend line in Figure 36 and have relatively low almandine and pyrope when compared to the dark pink orange and pink orange samples. '1' in Figure 36 refers to samples that are composed predominantly of pyrope with similar amounts of almandine and spessartine. The dark pink orange, pink, and the pink orange samples plot in '1' with all three having high almandine proportions when compared to the light pink, light pink orange, and light orange pink samples. The pink dominant samples contain higher pyrope than the orange dominant samples.

© University of Pretoria

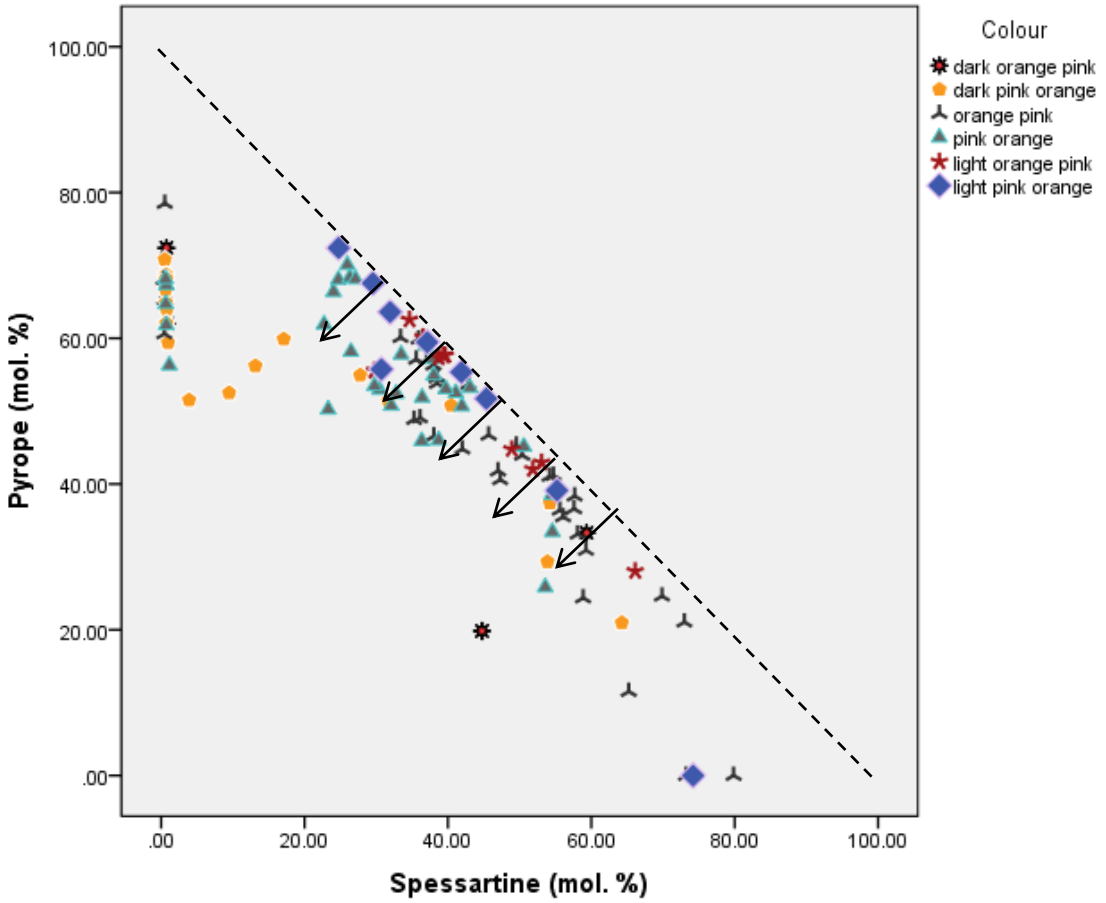

Figure 37. The pyrope and spessartine components of the pink orange samples. The garnets are only from the pyralspite species. The dashed line represents the solid solution series between pyrope and spessartine. The arrows represent deviation away from the trend line and indicate additional substitutions.

All of the light pink orange samples plot close to the trend line in Figure 37. Samples where the orange colour is more dominant have a higher spessartine component. Most of the dark pink orange samples plot away from the trend line and have much lower spessartine than the orange dominant samples. The pink orange samples plot near the trend line but contain lower spessartine than the orange pink and light orange pink samples.

4.2.4.4. Brown and yellow varieties

Most of the brown and yellow varieties in Figure 38 plot along the trend line with most plotting in the spessartine dominant region. Most have a high spessartine component and are ‘spessartine-pyrope I and II’ samples. A few of the samples (circled in yellow in Figure 38) are ‘pyrope-spessartine I and II’. Four brown yellow, one dark yellow brown, and one light brown sample are ‘spessartine’ samples. The samples circled in black in Figure 38 refer to the four ‘spessartine-grossular’ samples with high spessartine component and no pyrope.

© University of Pretoria

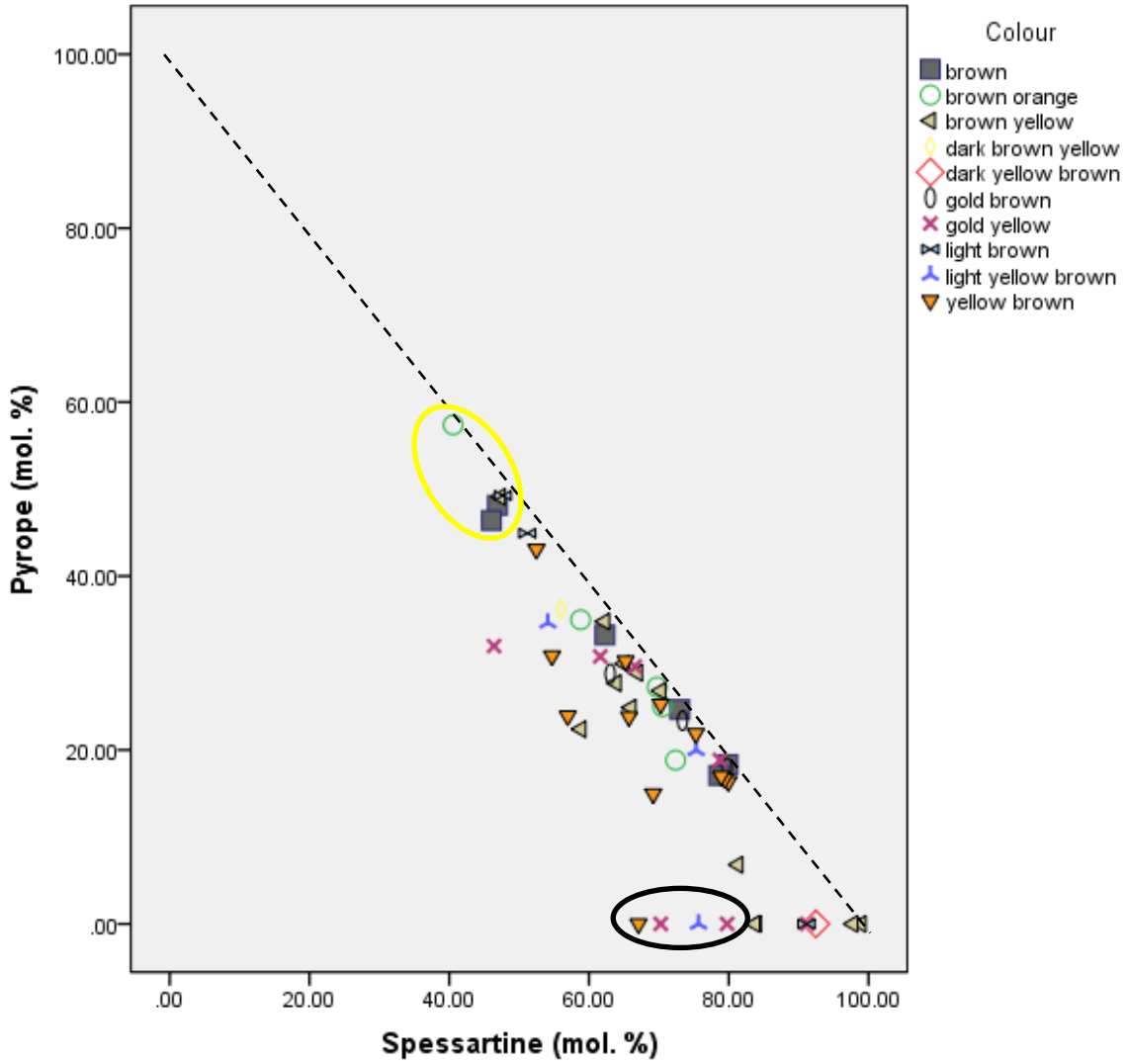

Figure 38. The pyrope and spessartine components of the brown and yellow samples. The garnets are only from the pyralspite species. The dashed line indicates the solid solution series between pyrope and spessartine. The area circled in yellow are the few 'pyrope-spessartine I and II' samples. The samples circled in the black are the four 'spessartine-grossular' samples.

© University of Pretoria

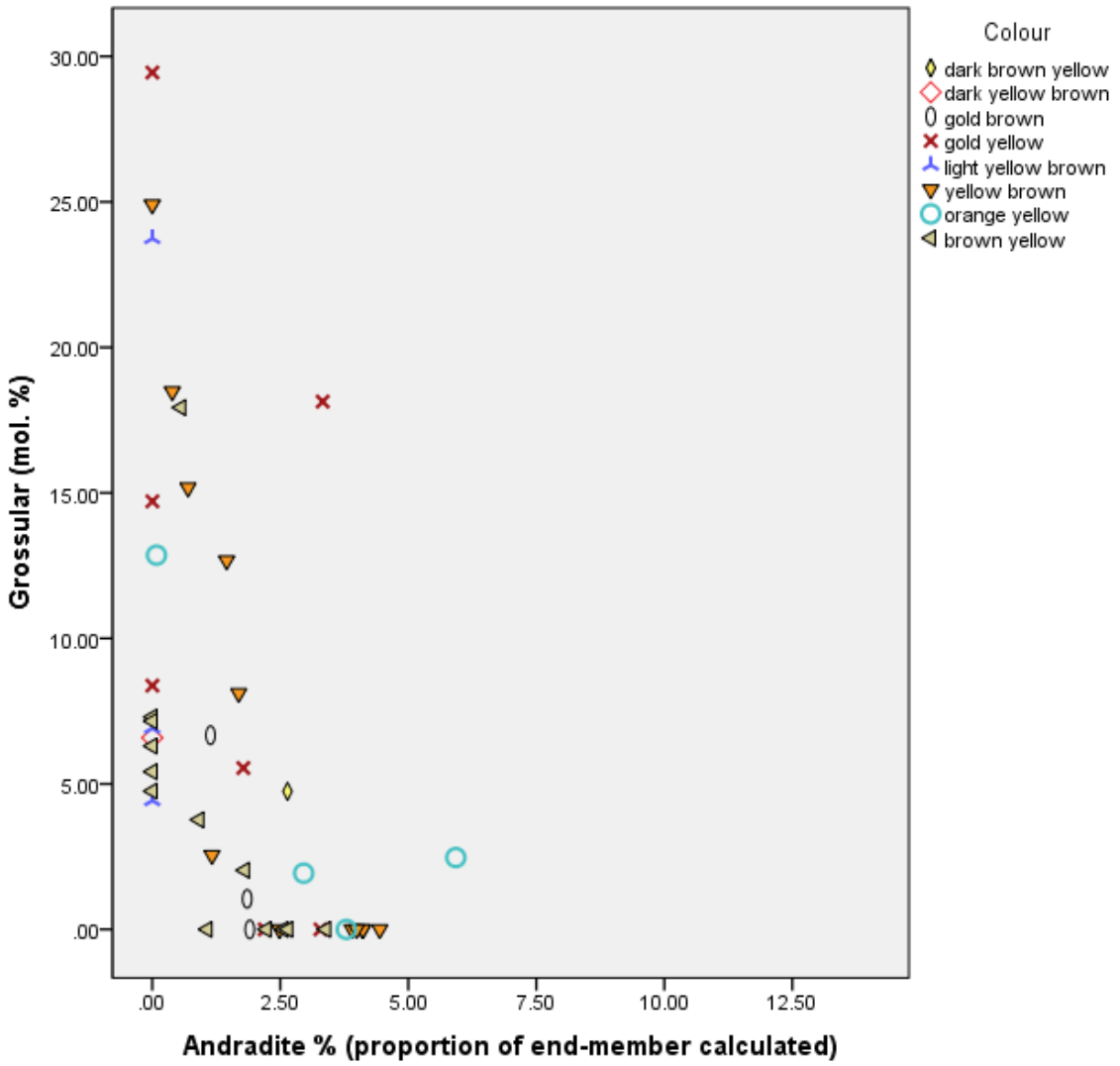

Figure 39. The grossular and andradite components of the yellow and gold garnets from the pyralspite species.

The grossular component in Figure 39 has a wide range with a large number of samples plotting above 5 mol.% grossular. These are some of the highest grossular components observed in the data from the pyralspite species. The other colours from the pyralspite species contain low to no grossular component, with an andradite component below 5 mol.%.

4.2.4.5. Colour change

Samples were referred to as colour change if they displayed a distinct change in colour between daylight and incandescent light. Colour shift refers to samples that display only a slight shift in colour between daylight and incandescent light (see section 3.3. for more details).

© University of Pretoria

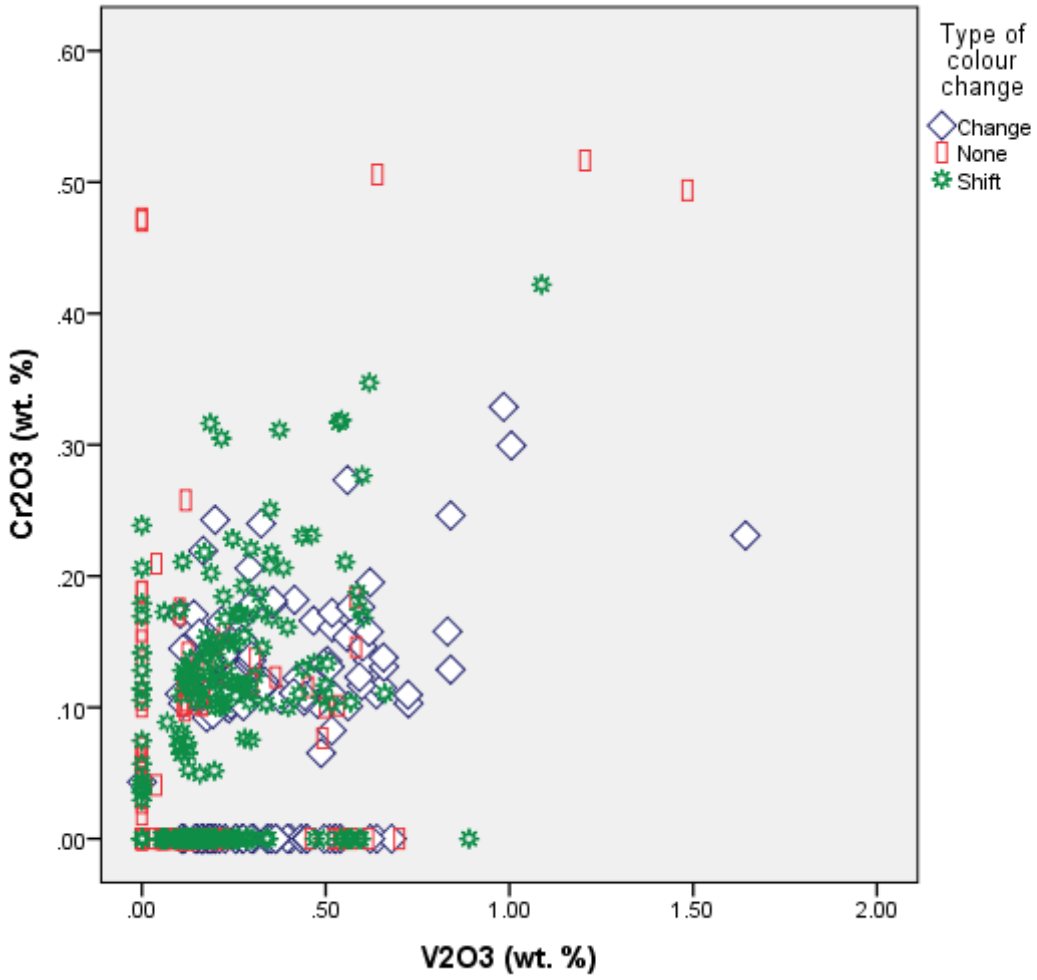

Figure 40. The different types of colour change and the V_2O_3 (wt. %) and Cr_2O_3 (wt. %). The garnets are only from the pyralspite species.

All samples with distinct colour change show either vanadium without chromium or have vanadium and chromium present (Figure 40). There are no colour change samples that possess Cr with no V, hence, all colour change samples possess some V.

© University of Pretoria

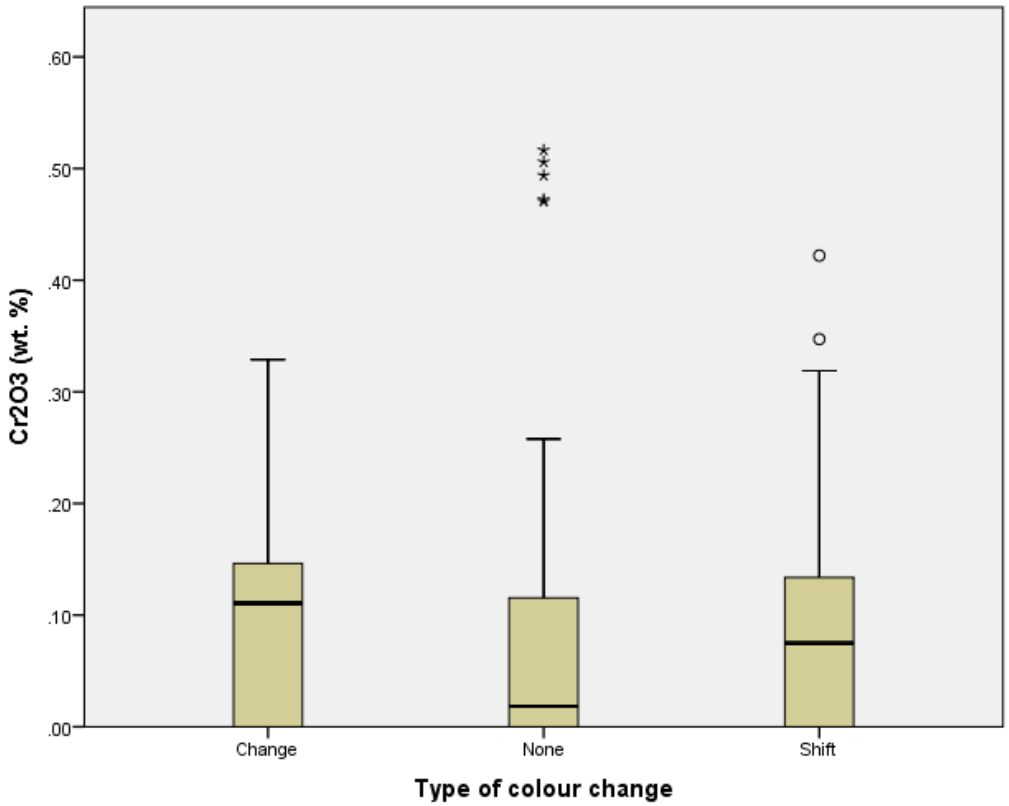

Figure 41. a) Boxplot of Cr_2O_3 content for different types of garnets from the pyralspite species and their colour change behaviour.

The colour change garnets have the largest range of Cr_2O_3 values (Figure 41a), but this is only slightly higher than the colour shift samples. The non-colour change garnets have the lowest range in Cr_2O_3 content except for a few outliers that have the highest Cr_2O_3 content. This suggests that chromium contents alone are not responsible for colour change.

© University of Pretoria

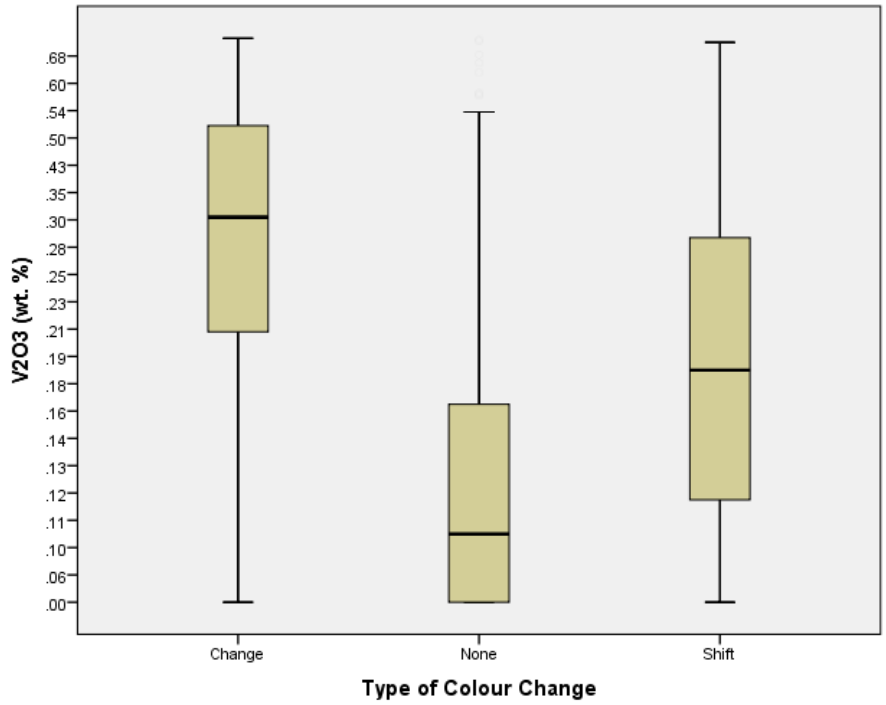

Figure 41. b) Boxplot showing the different types of colour change garnets from the pyralspite species and their V_2O_3 (wt. %) contents.

The colour change samples have the largest range and highest median V_2O_3 values (Figure 41b) while the non-colour change garnets have the lowest. Most of the colour change samples have a V_2O_3 content ranging from 0.21 to 0.53 wt. %, excluding the few samples that have very low and/or very high V_2O_3 values. For the colour shift samples, the majority of the samples have a lower V_2O_3 content than the colour change samples with V_2O_3 ranging from 0.12 to 0.29 wt. %. Again, this excludes those samples that have very low and/or very high V_2O_3 values.

© University of Pretoria

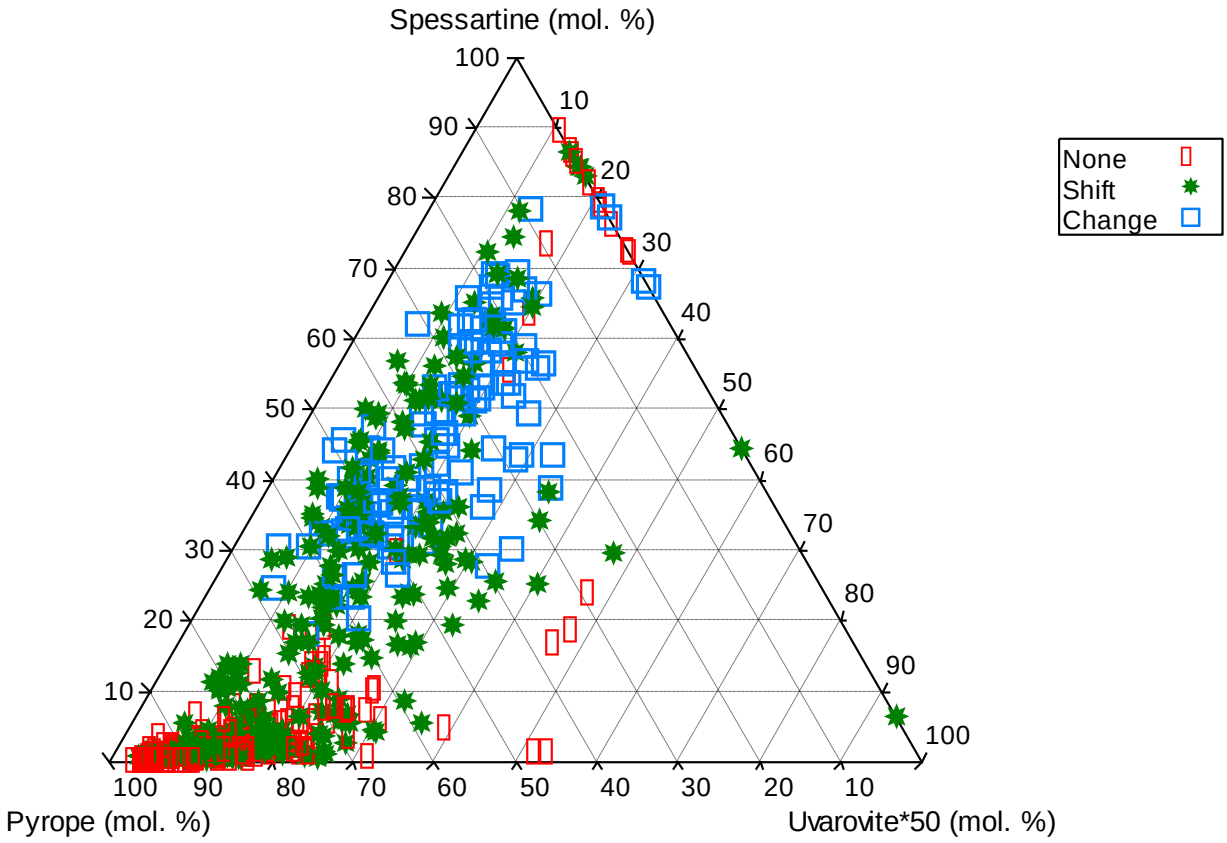

Figure 42. Ternary diagram showing the uvarovite component * 50 for the garnet samples from the pyralspite species based on their type of colour change.

In Figure 42, all of the colour change samples contain some uvarovite. However, these values are not high, and a large number of the colour shift and non-colour change samples show a similar uvarovite component. One of the colour shift samples contains the highest uvarovite component. Chromium does not a cause colour change or shift, but could be a contributing factor.

Most of the colour change samples show a relatively high spessartine component while the colour shift and non-colour change samples are more pyrope dominant.

© University of Pretoria

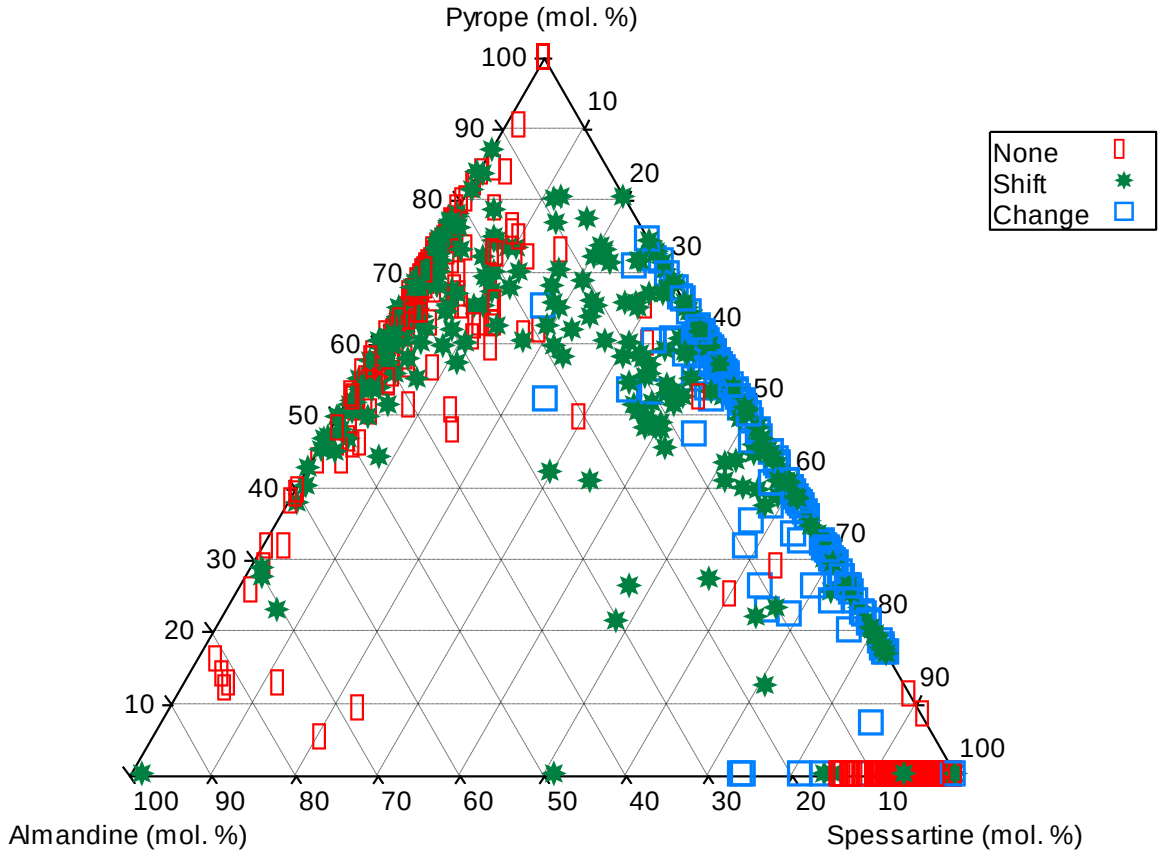

Figure 43. Ternary diagram showing the pyrope, almandine and spessartine components of the pyralspite garnets with their type of colour change.

Most of the colour change samples plot along the solid solution series between pyrope and spessartine (Figure 43). A few of the colour change samples also occur near the spessartine end-member with minor amounts of almandine ('spessartine-almandine' samples). One colour change sample occurs at 100.00 mol.% spessartine and is a 'spessartine' sample. Two colour change samples occur in the centre of Figure 43 (Alm:Sp ≈ 1) and are 'pyrope-spessartine II' samples. The non-colour change samples show a tendency for higher almandine component, when looking at the Alm:Sp ratio, than the colour change samples. Colour change samples are pyrope and spessartine dominant with low amounts of almandine, suggesting that almandine reduces the potential for colour change.

Colour shift samples occur along the solid solution series between pyrope and almandine and the solid solution series between pyrope and spessartine. Towards the almandine-rich region in Figure 43, the number of colour shift samples decreases with only one sample plotting at 100.00 mol.% almandine. A few colour shift samples occur along the solid solution series between spessartine and almandine with spessartine being the dominant end-member.

© University of Pretoria

None of the colour change samples occurs along the solid solution series between pyrope and almandine, and between spessartine and almandine. The non-colour change samples are concentrated near the 100.00 mol.% spessartine corner in Figure 43, with small amounts of almandine. A few occur along the solid solution series between pyrope and spessartine, with small amounts of almandine present.

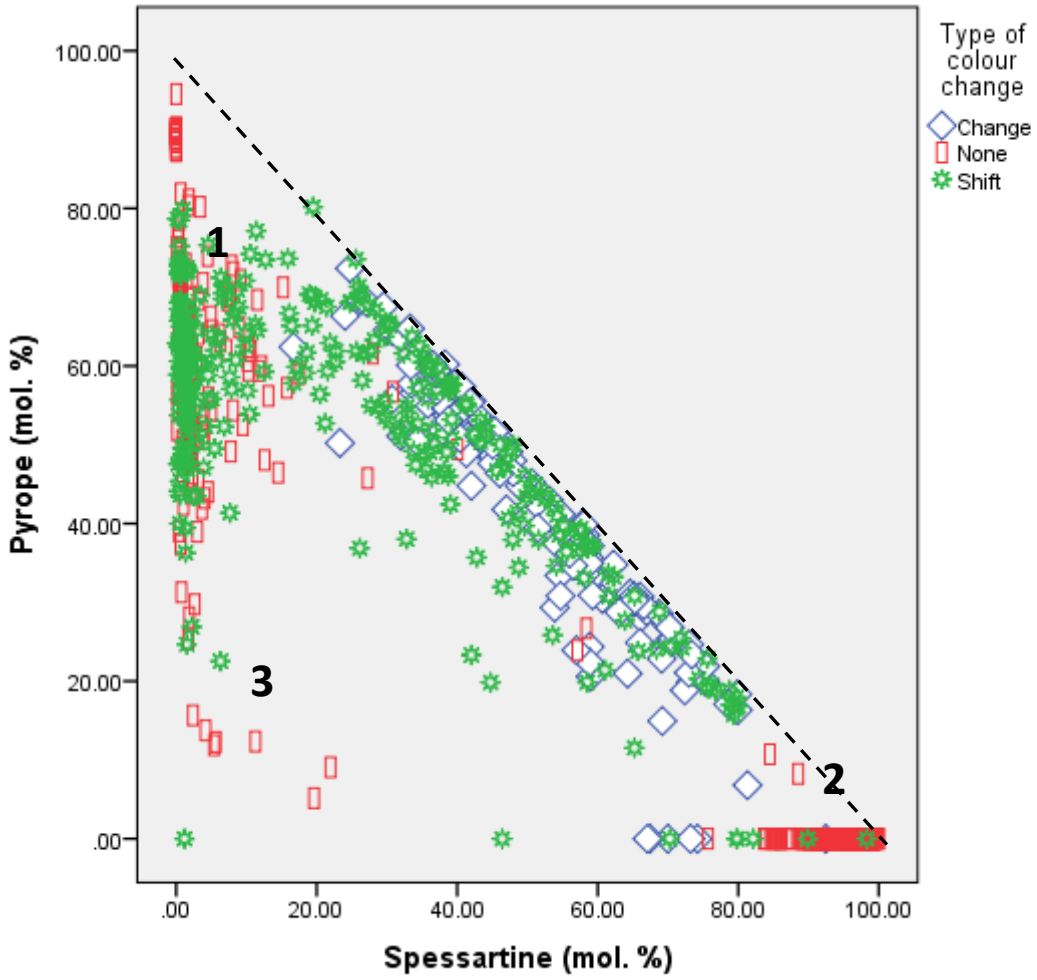

Figure 44. The pyrope and spessartine components of the pyralspite garnets together with the type of colour change. The dashed line indicates the solid solution series between pyrope and spessartine.

Majority of the colour change samples plot along the solid solution series between pyrope and spessartine with a larger number present in the spessartine-rich region (Figure 44). Stones that display a shift in colour occur along the trend line as well as away from the trend line, which indicates additional substitutions of spessartine by almandine. Stones that display no colour change were concentrated in three areas as represented by '1', '2' and '3' in Figure 44. '1' refers to 'pyrope-almandine' and 'rhodolite' samples. '2' refers to the 'spessartine' samples and '3' refers to the 'almandine-pyrope' and 'almandine' samples. A few non-colour change samples also occur close to the trend line in Figure 44.

© University of Pretoria

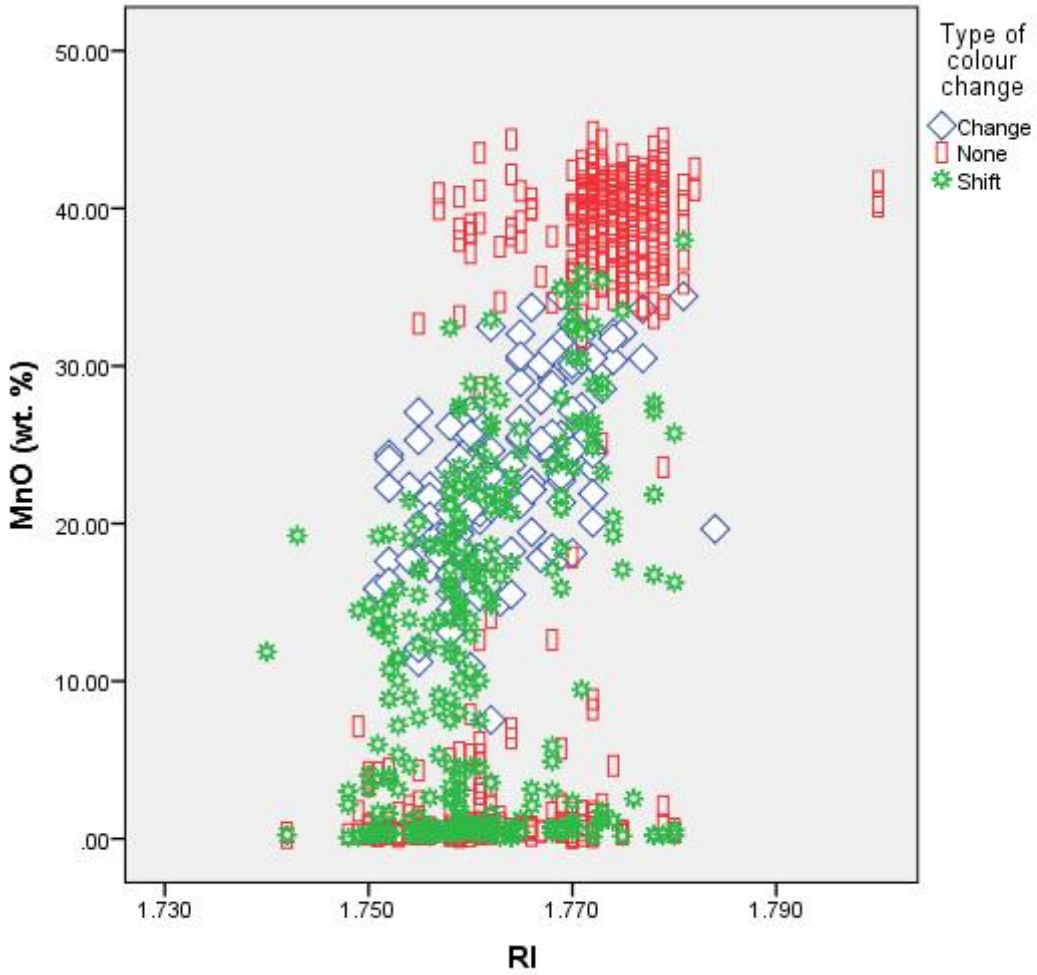

Figure 45. The MnO (wt. %) content and the RI values of the pyralspite garnets together with their type of colour change. For the purpose of clarity, a colour shift sample with an RI of 1.63 was removed.

In Figure 45, the colour change samples occur in the middle region of RI values. The stones that display no form of colour change contain either high amounts of MnO, or very low amounts of MnO. The colour shift samples show variable MnO.

© University of Pretoria

4.3. Ugrandite Species

4.3.1. Chemistry

4.3.1.1. Almandine-grossular

Only one 'almandine-grossular' sample is present in the data, as mentioned earlier. In comparison to the other samples from the uvarovite species, the 'almandine-grossular' sample has relatively high FeO_{total} and a low grossular component (Figures 46 and 47).

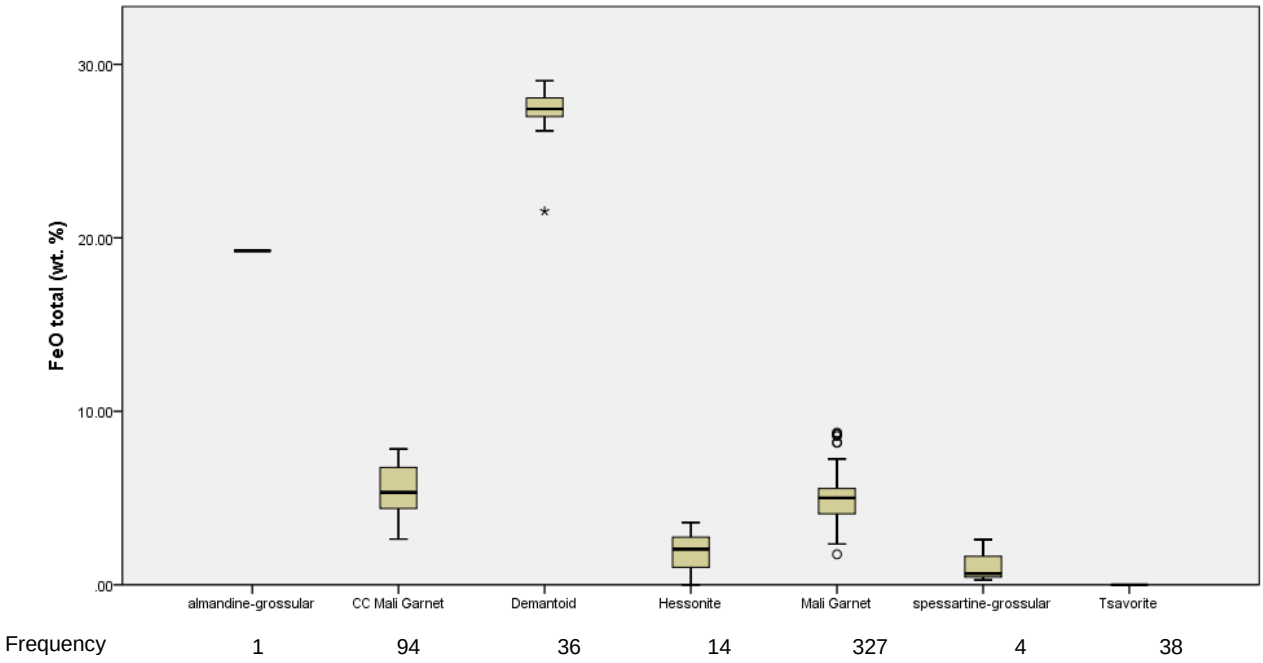

Figure 46. The FeO_{total} (wt. %) content for the ugrandite species. Below the boxplot are the frequencies for the different garnets from the ugrandite species. The 'CC Mali garnets' have a tendency for slightly higher FeO_{total} compared to the Mali garnets.

© University of Pretoria

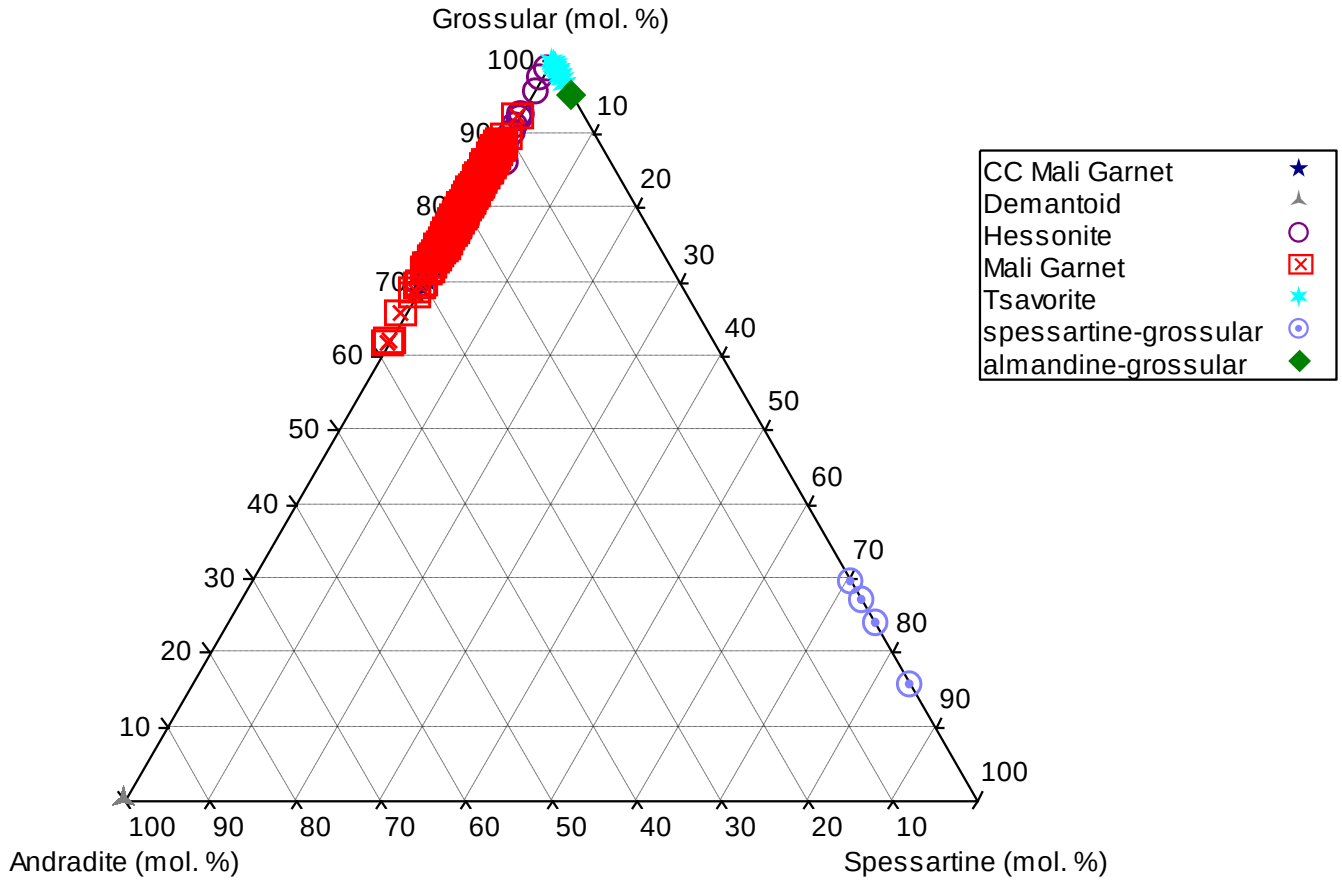

Figure 47. Ternary diagram of the grossular, andradite and spessartine components for the ugrandite species. The 'CC Mali garnets' plot beneath the 'Mali garnets'. The 'tsavorite' samples show a low spessartine component with very high (>90 mol.% grossular). The 'hessonite', 'Mali garnets' and 'CC Mali garnets' form part of the grossular andradite solid solution series.

4.3.1.2. Mali garnet and CC Mali garnet

Three-hundred-and-twenty-seven 'Mali' and 94 'CC Mali garnets' are present in the data. Both types of garnets show similar chemistry with CaO content (29.65-41.02 wt. %) being the highest, followed by FeO_{total} (1.76-8.78 wt. %) (Figures 48 and 46). One 'CC Mali garnet' sample has very low CaO content as shown in Figure 48 (red circle). MgO (0.94-3.35 wt. %) and TiO_2 (0.07-0.40 wt. %) are also present in minor amounts (Figure 49). The MnO content ranges up to 0.16 wt. % (Figure 50). Cr_2O_3 and V_2O_3 were not detected in either the 'Mali' or the 'CC Mali garnets' (Figures 51 and 52). The 'Mali' and 'CC Mali garnets' have some of the highest TiO_2 contents (Figure 49) in the ugrandite species.

© University of Pretoria

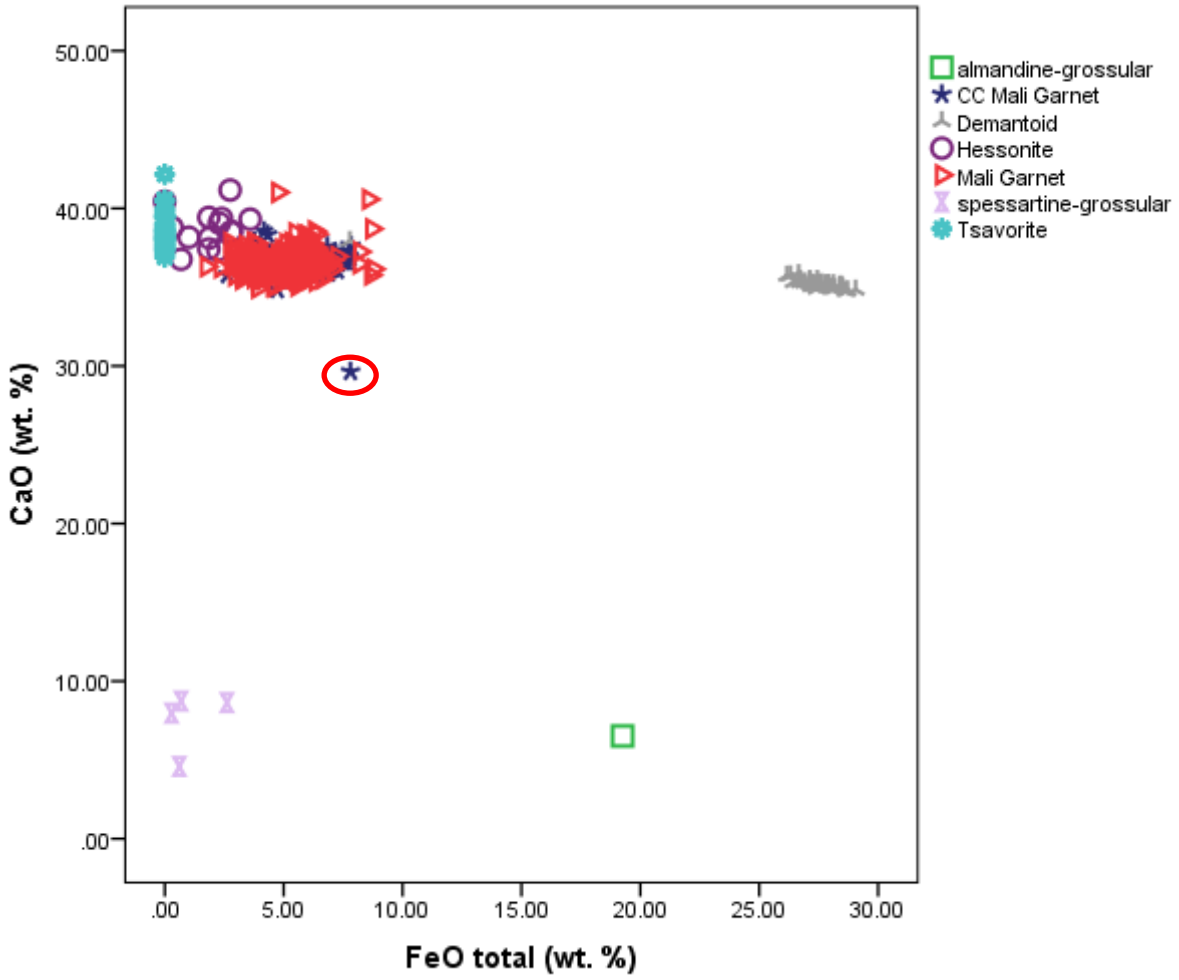

Figure 48. The CaO and FeO_{total} contents in wt. % of the garnets from the ugrandite species. The 'demantoid' samples have the highest FeO_{total} wt.%.

© University of Pretoria

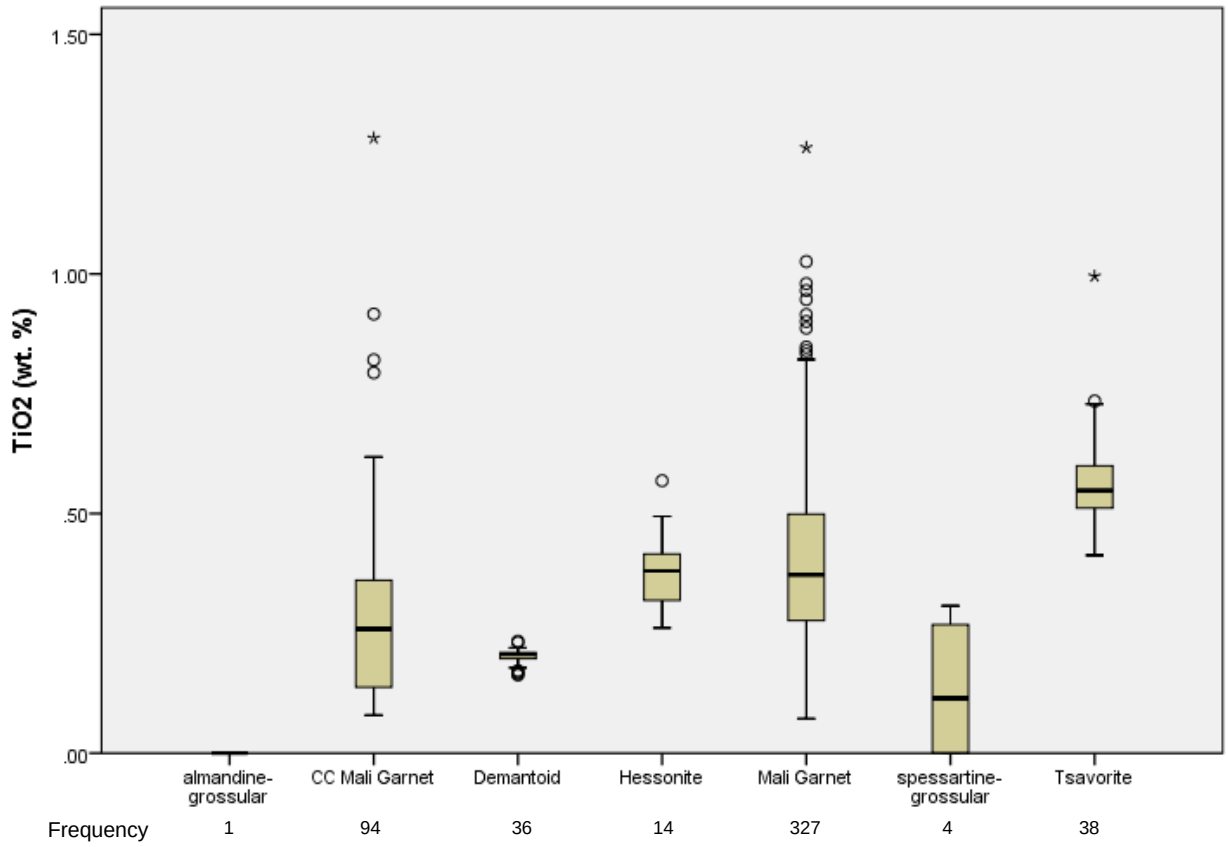

Figure 49. The TiO_2 (wt. %) content for the ugrandite species. Below the boxplot are the frequencies for the different garnets from the ugrandite species. The 'Mali' garnets show the largest range in TiO_2 followed by 'CC Mali garnets'. 'Tsavorite' samples show high TiO_2. 'Demantoid' has the smallest range in TiO2 content. Only 'almandine-grossular' contains no detectable TiO_2.

© University of Pretoria

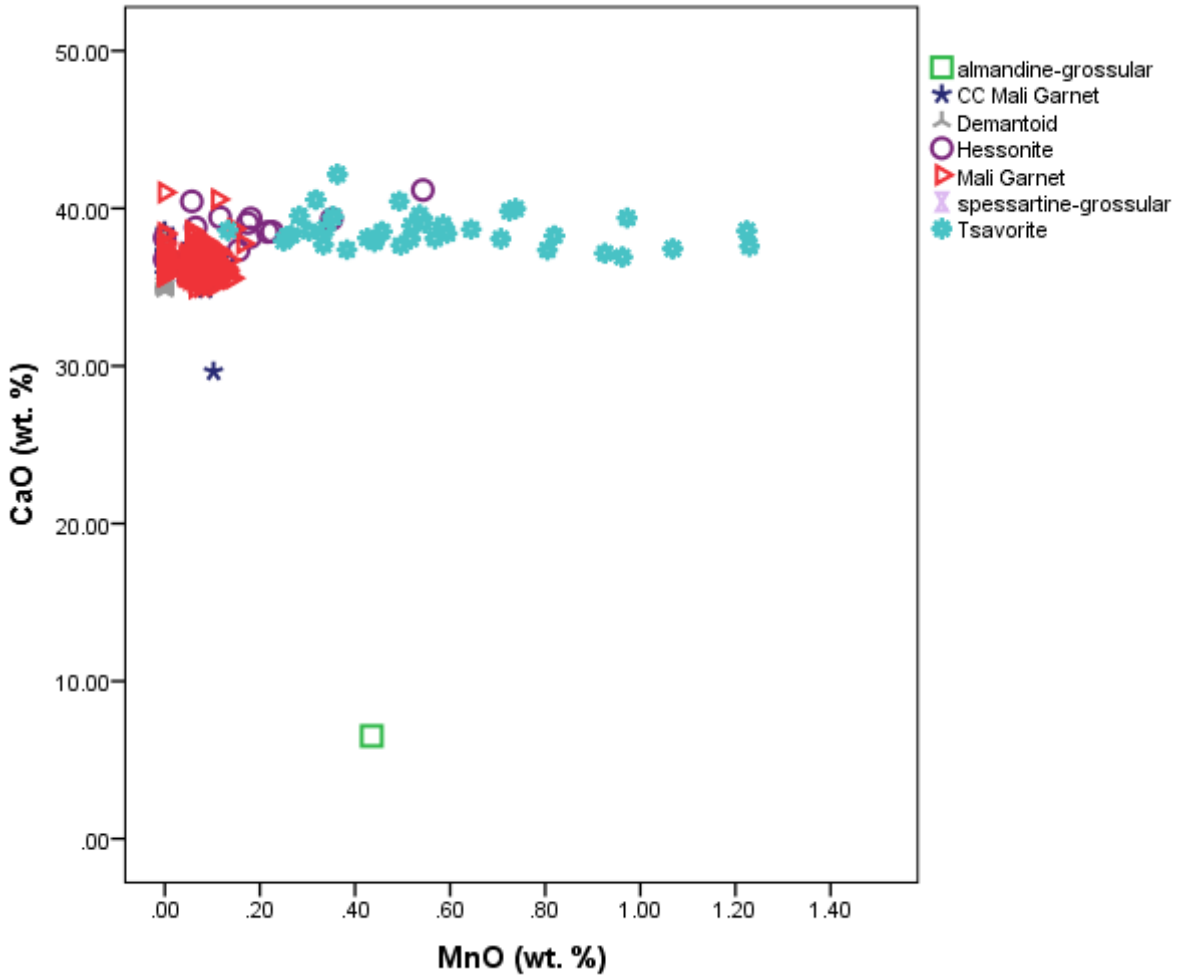

Figure 50. The CaO and MnO contents in wt. % of the garnets from the ugrandite species.

© University of Pretoria

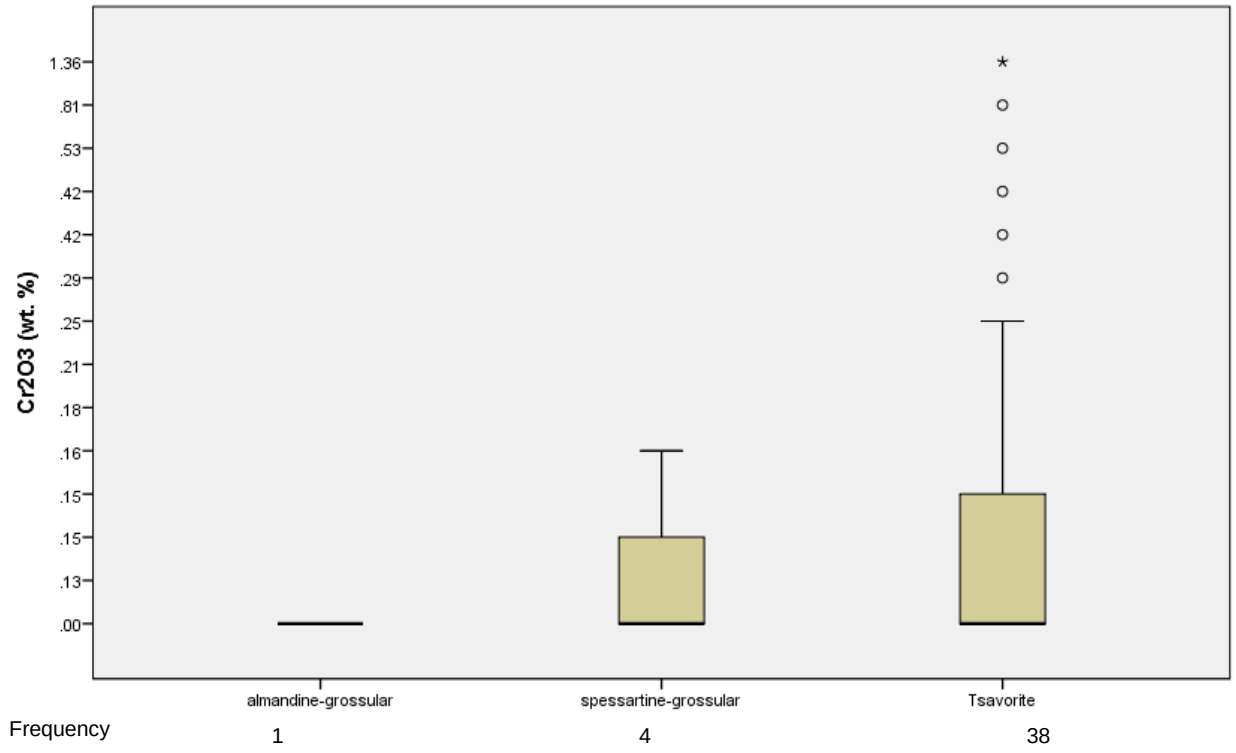

Figure 51. The Cr_2O_3 (wt. %) content for the ugrandite garnets. Below the boxplot are the frequencies for the different ugrandite garnets. For graphical purposes, the 'CC Mali garnet', 'demantoid', 'hessonite' and 'Mali garnet' samples were excluded as they have Cr_2O_3 contents below the detection limit. The tsavorite samples contain the highest Cr_2O_3 contents followed by spessartine-grossular. The one almandine-grossular sample contains very low Cr_2O_3.

© University of Pretoria

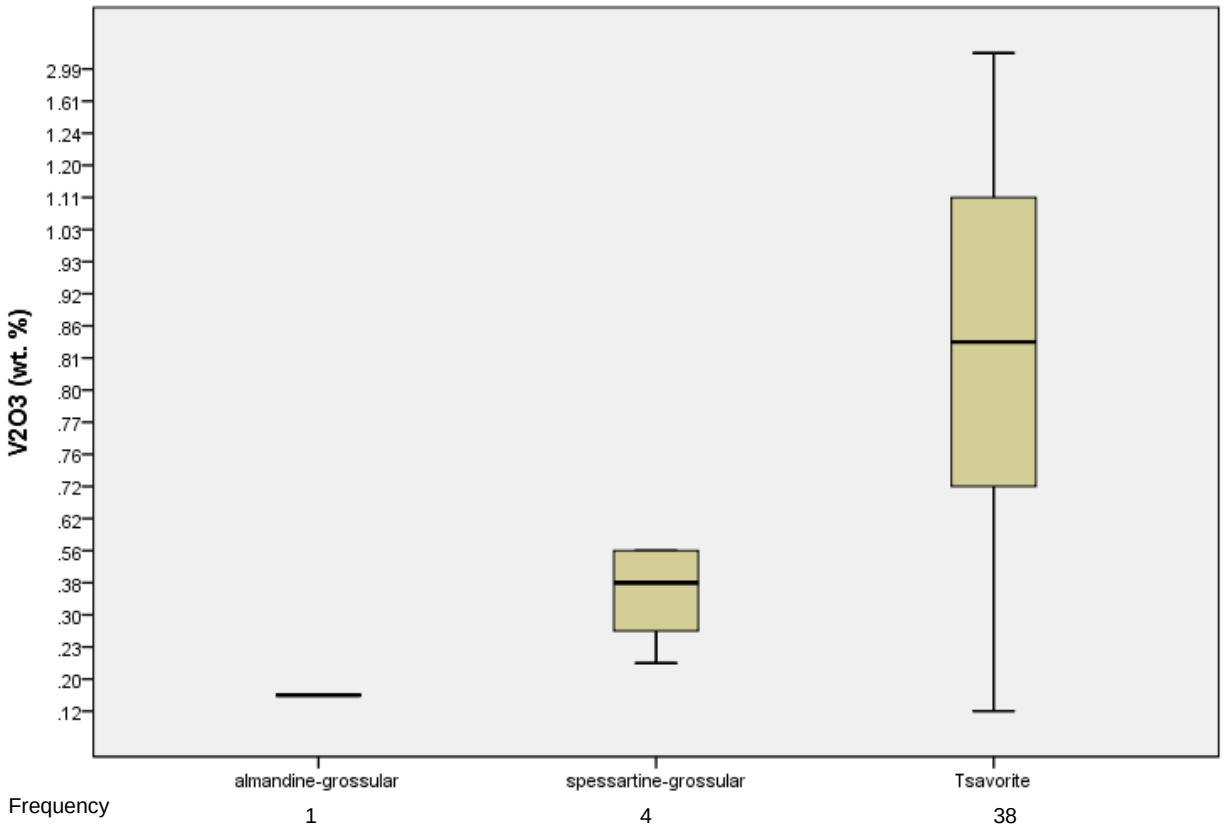

Figure 52. The V_2O_3 (wt. %) content for the ugrandite species. Below the boxplot are the frequencies for the different garnets. For graphical purposes, the 'CC Mali garnet', 'demantoid', 'hessonite' and 'Mali garnet' samples were excluded as they have Cr_2O_3 contents below the detection limit. Both 'tsavorite' and 'spessartine-grossular' samples have the highest V_2O_3 and/or Cr_2O_3 content (Figure 51).

The 'Mali' and 'CC Mali garnets' are composed primarily of grossular (61.07-88.79 mol. %) and andradite (7.02-38.07 mol. %) and form part of the grossular andradite series (Figure 53). This series appears non-continuous, as a large gap (green dashes in Figure 53) exists between the two end-members, where no samples plot. The grossular content of the 'Mali' and 'CC Mali garnets' did not exceed 88.79 mol. % and the andradite content did not exceed 38.07 mol. % (Figures 53). Most of the samples contain no pyrope, but a fair number contains significant proportions of pyrope (≤ 15.41 mol.%) (Figure 53). This is evident in Figure 53, where two distinct groups can be seen in the Mali and CC Mali garnets. Neither the 'Mali' nor the 'CC Mali' garnets contain almandine and vey low uvarovite (≤ 0.23 mol. %) (Figure 54). The spessartine component is also low, ranging up to 0.46 mol. % (Figures 55a and 55b).

© University of Pretoria

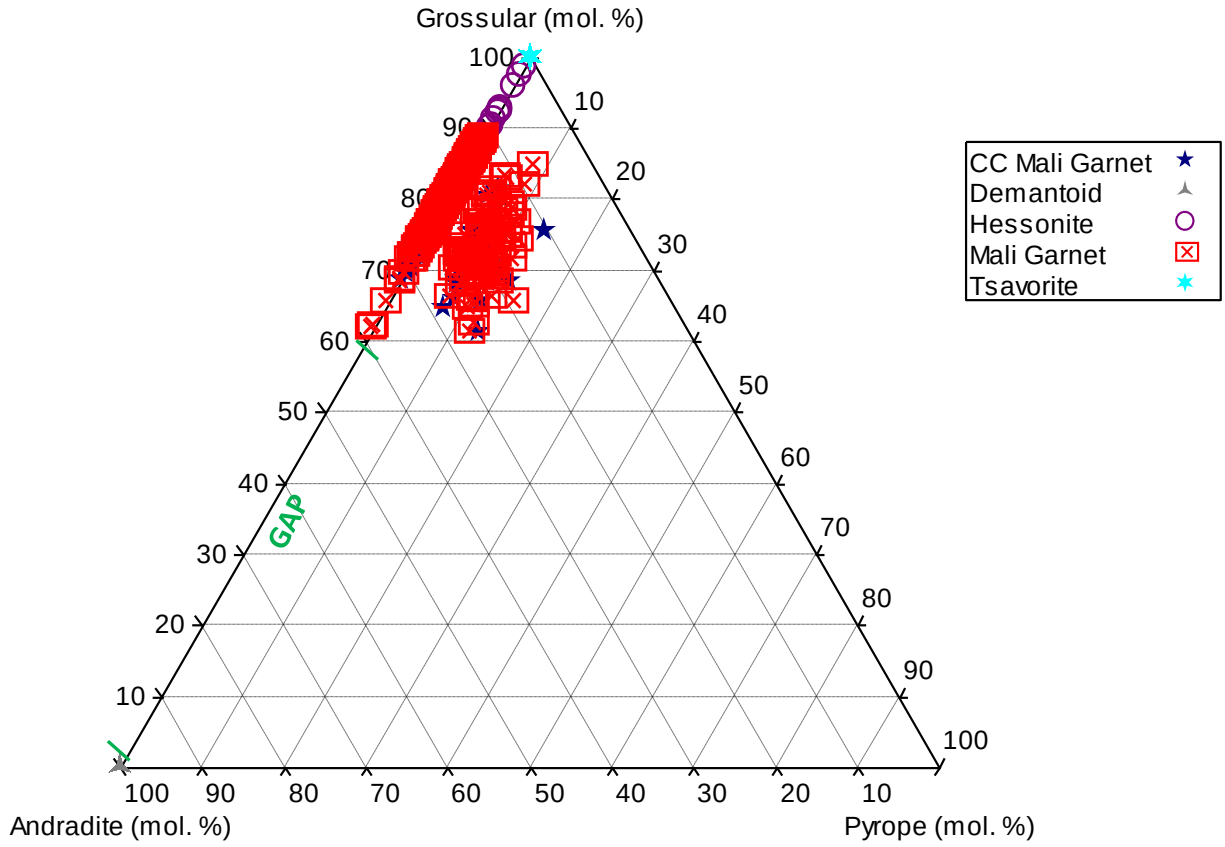

Figure 53. a) Ternary diagram of the grossular, andradite and pyrope components for the ugrandite species. Two groups in the 'Mali and CC Mali garnets' can be seen in the ternary diagram above. The one group has additional substitutions of pyrope and plots away from the grossular-andradite solid solution series. The short green lines indicate the presence of a gap in the series where no samples plot.

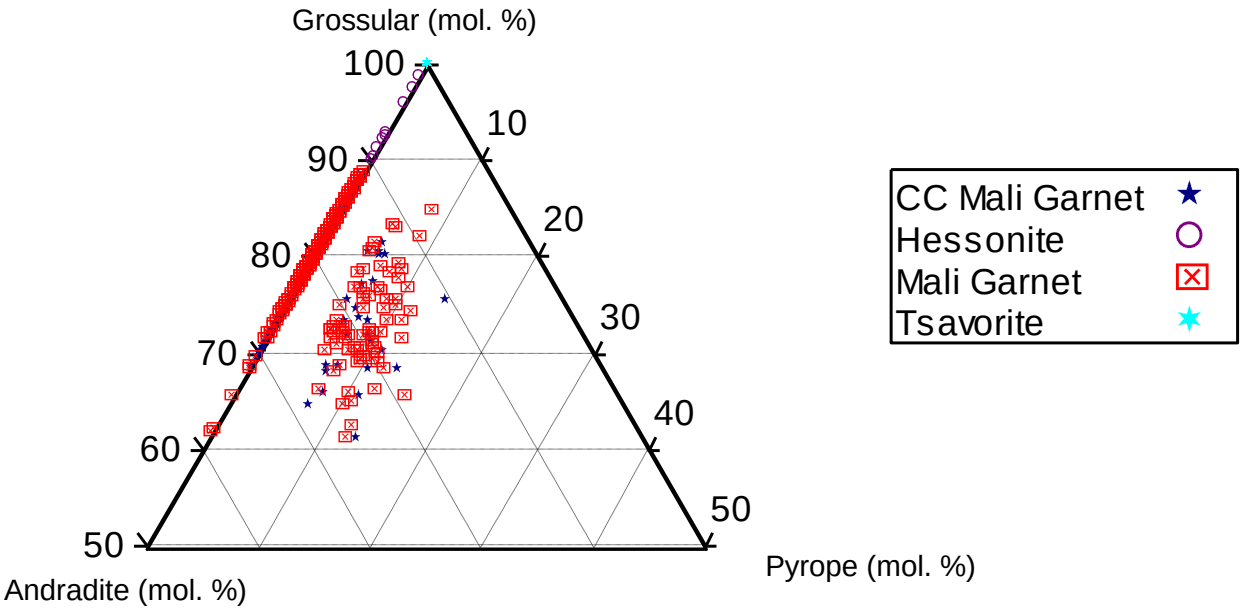

Figure 53. b) An expanded viewo of the ternary diagram in Fiugre 53 a).

© University of Pretoria

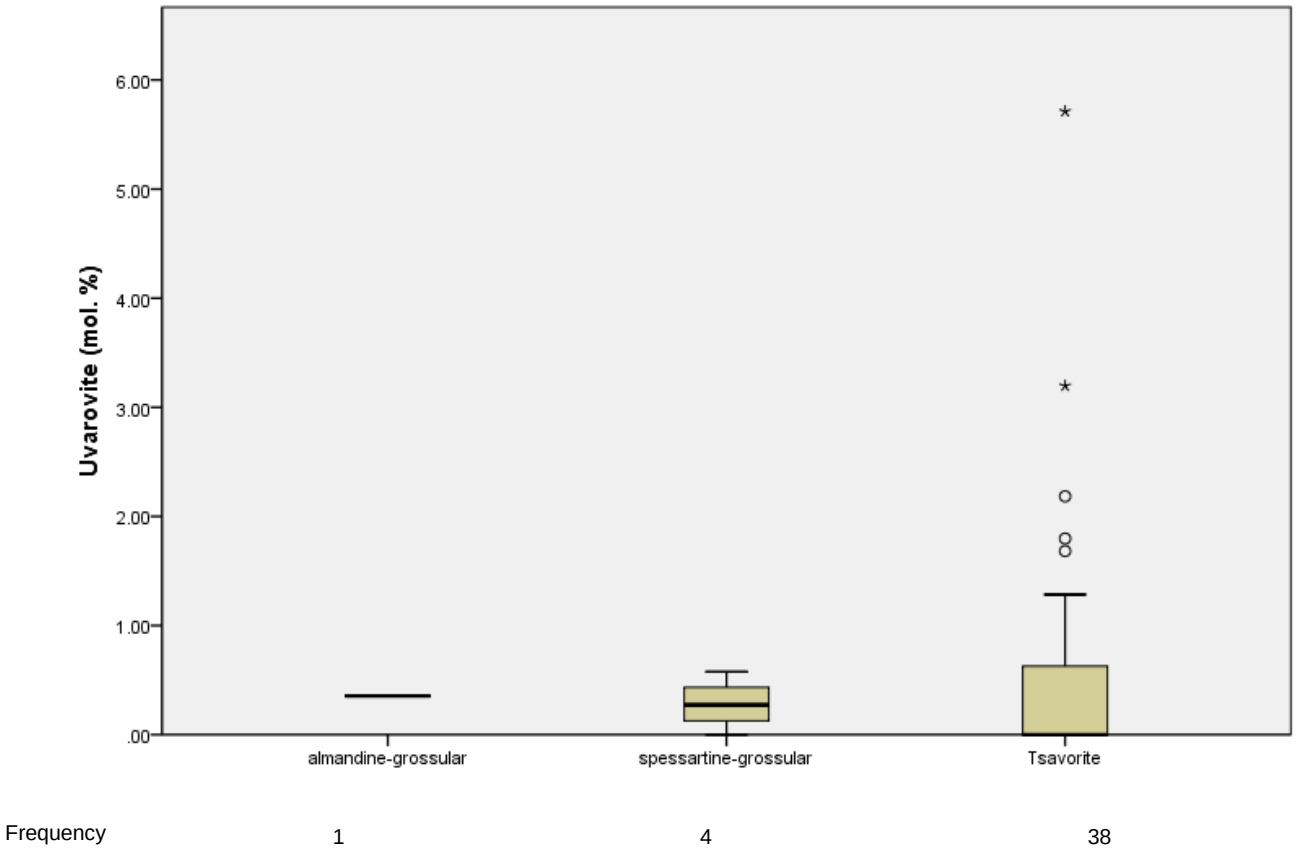

Figure 54. The uvarovite component for the garnets from the ugrandite species. Below the boxplot are the frequencies for the different garnets. For graphical purposes, the 'CC Mali garnet', 'demantoid', 'hessonite' and 'Mali garnet' samples were removed as the uvarovite contents were below the detection limit. The 'tsavorite' samples contain the highest uvarovite component, followed by 'spessartine-grossular'.

4.3.1.3. Demantoid

Thirty-six demantoid samples are found in the data, with the CaO (34.77-37.93 wt. %) and the FeO_{total} (21.54-29.05 wt. %) contents being the highest (Figures 46 and 48). Minor amounts of TiO_2 are present ranging from 0.16 to 0.23 wt. % (Figure 49). No MgO, Al_2O_3, MnO, Cr_2O_3 or V_2O_3 are detected (Figures 50, 51 and 52).

The 'demantoid' samples are composed primarily of andradite (99.88-100.00 mol. %) (Figures 47, 53 and 56). Very little deviation in chemistry is observed in the demantoid garnets and distinct demantoid clusters can be seen in Figures 47 and 48. The 'demantoid' samples plot away from the other garnets in Figure 48, because the FeO_{total} substituted for Al_2O_3. The only other component present in the demantoid samples is uvarovite (≤ 0.12 mol. %) (Figure 54).

© University of Pretoria

4.3.1.4. Hessonite

Fourteen 'hessonite' samples primarily consisting of CaO (36.77-41.17 wt. %) are found (Figure 48). FeO_{total} (≤ 3.59 wt. %) and MnO (≤ 0.54 wt. %) are also present (Figures 46 and 50). TiO_2 was present in trace amounts (0.26-0.57 wt. %) (Figure 49), while MgO, Cr_2O_3 or V_2O_3 were not detected (Figures 53, 51 and 52).

Grossular is the dominant component ranging from 84.39 to 98.55 mol. % (Figures 47 and 53). Andradite is also present in significant amounts, ranging from 1.27 to 14.64 mol. % (Figure 56). The 'hessonite' samples form part of the grossular-andradite solid solution series (Figure 53) and plot as a distinct cluster separate from the 'Mali' and 'CC Mali garnets'. A higher grossular and lower andradite component is observed in the 'hessonite' samples when compared to the 'Mali' and 'CC Mali garnets'. The 'hessonite' garnets contain a low spessartine component (≤ 1.66 mol. %) (Figures 47 and 55a). This spessartine component is higher than the 'Mali' and 'CC Mali garnets'. No almandine, pyrope or uvarovite components are present (Figures 53 and 54).

4.3.1.5. Spessartine-grossular

Four 'spessartine-grossular' samples have been found. In comparison to the ugrandite species, the 'spessartine-grossular' samples contain the highest MnO content (25.08-30.92 wt. %) and very low CaO content (4.59-8.73 wt. %) (Figures 50 and 48). Some samples contain relatively high Cr_2O_3 (up to 0.16 wt. %) and V_2O_3 (0.13-0.22 wt. %) with only the 'tsavorite' samples showing higher chromium and vanadium (Figures 51 and 52). Minor amounts of TiO_2 are present in the samples (≤ 0.31 wt. %) (Figure 49).

The 'spessartine-grossular' samples are composed primarily of spessartine (67.09-79.77 mol. %) and grossular (14.71-29.45 mol. %) (Figures 47 and 55a). A fair amount of almandine is also present in the samples (≤ 8.01 mol. %) when compared to the other garnets from the ugrandite species, which contain no almandine. Minor amounts of uvarovite are present (≤ 0.58vmol. %) (Figure 54).

© University of Pretoria

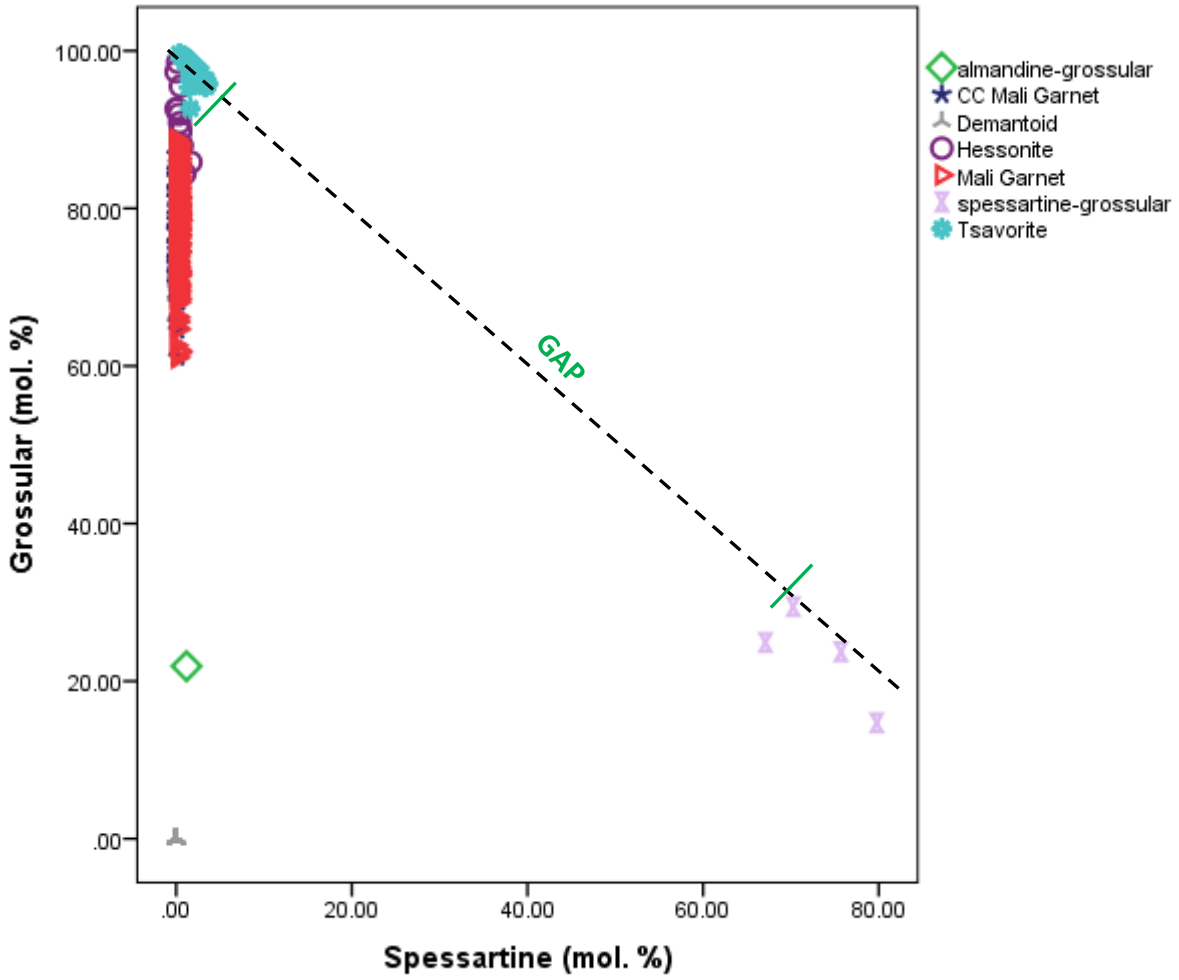

Figure 55. a) The spessartine and grossular components of the ugrandite species. The dashed line represents the solid solution series between grossular and spessartine. The 'spessartine-grossular' samples represent an intermediate composition between these two end-members. The short green lines indicate the gap observed in the grossular spessartine solid solution series. The trend observed in this figure was not observed in Figure 50, as this is an artefact of the end-member calculation process where end-member values might differ slightly from the weight percentages.

4.3.1.6. Tsavorite

Thirty-eight 'tsavorite' samples are found in the data. These samples contain high CaO (36.92-42.16 wt. %) (Figure 48). The Al_2O_3 and SiO_2 contents range from 14.28 to 17.95 wt. % and 39.64 to 43.54 wt. % respectively. The 'tsavorite' samples contain the highest Cr_2O_3 (≤ 1.36 wt. %) and V_2O_3 (0.12-3.40 wt. %) contents in the ugrandite species (Figures 51 and 52).The samples also contain relatively high TiO_2 contents (0.41-1.00 wt. %) (Figure 49). Minor amounts of MnO are present, ranging from 0.13 to 1.23 wt. % (Figure 50).

The 'tsavorite' samples are composed primarily of grossular (92.68-99.63 %) (Figure 47 and 55a). These samples could easily be distinguished from the 'hessonite' samples as

© University of Pretoria

their grossular component is higher and their andradite component is absent. Furthermore, the 'tsavorite' samples show the largest range in the spessartine component (0.37-3.59 %) (Figures 55a and 55b) (with the exception of spessartine-grossular). Minor amounts of uvarovite are present (≤ 5.71 %) (Figure 54).

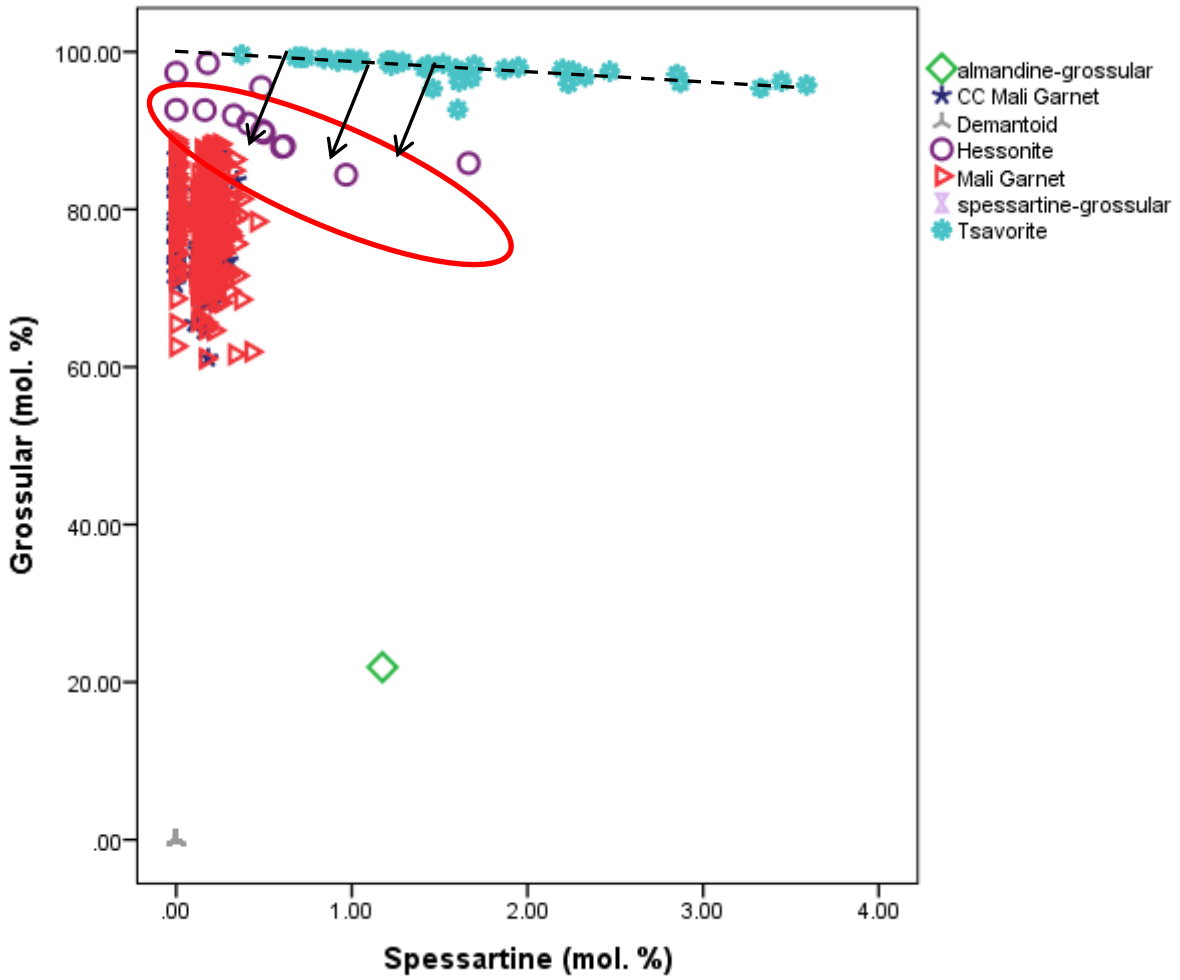

Figure 55. b) Expanded view of Figure 55 a). The dashed line represents the grossular spessartine solid solution series. A closer look at the spessartine and grossular components shows that the hessonite samples (area circled in red) do contain some spessartine, but this is very low. These hessonite samples plot away from the dashed line and suggest additional substitutions (as indicated by the arrows).

© University of Pretoria

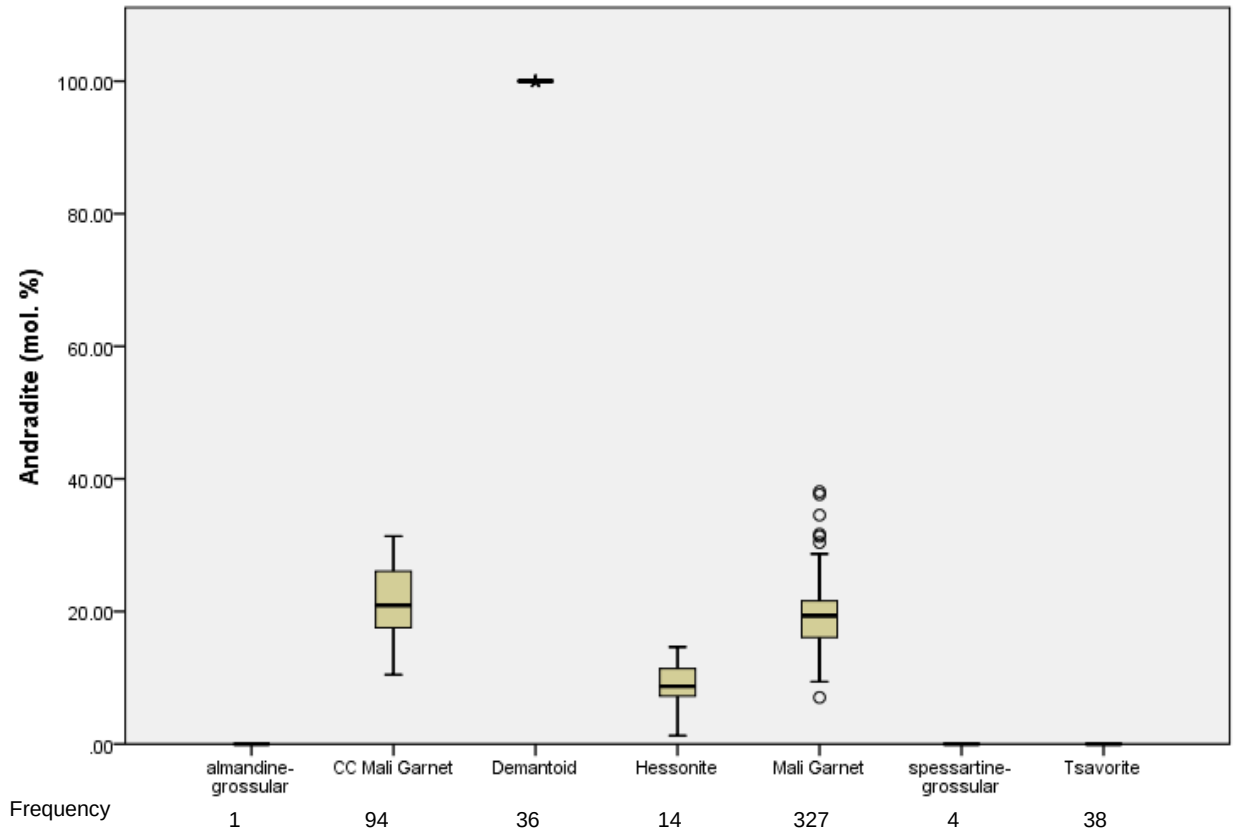

Figure 56. The andradite component for the garnets from the ugrandite species. Below the boxplot are the frequencies for the different garnets.

© University of Pretoria

4.3.2. Magnetic susceptibility

In Figure 57, a tendency is observed where magnetic susceptibility increases with the Fe_{total} + Mn content. The 'demantoid' samples, which are almost 100 mol.% andradite, have the highest magnetic susceptibilities.

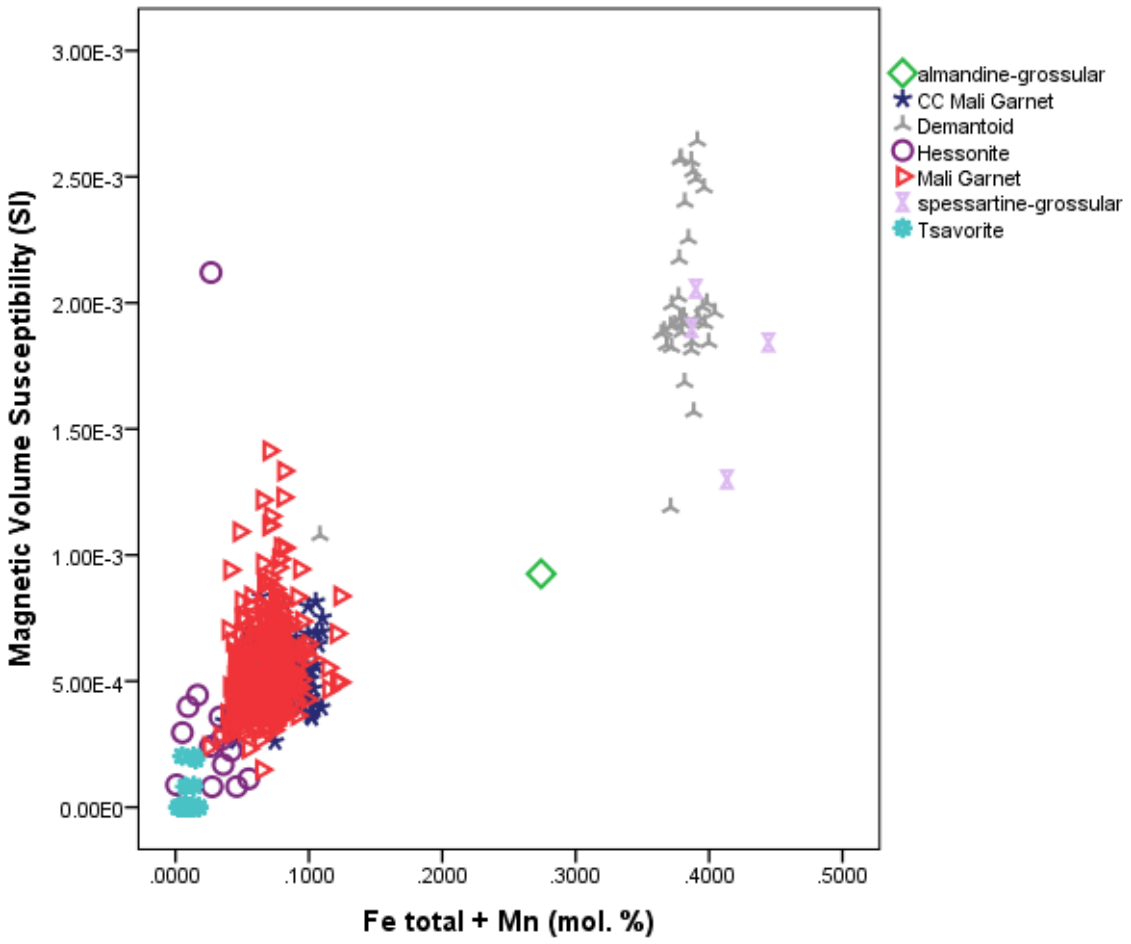

Figure 57. The magnetic susceptibility and Fe $_{total}$ + Mn (mol. %) content for the garnets from the ugrandite species.

The 'spessartine-grossular' samples also have a high magnetic susceptibility.

One 'hessonite' sample has a very high magnetic susceptibility and this could be due to the presence of inclusions in the samples. Some 'Mali' garnets have a higher magnetic susceptibility than expected based on the Fe_{total} + Mn contents.

© University of Pretoria

4.3.3. Refractive Index

The 'spessartine-grossular' samples have the largest range in RI values (Figure 58).

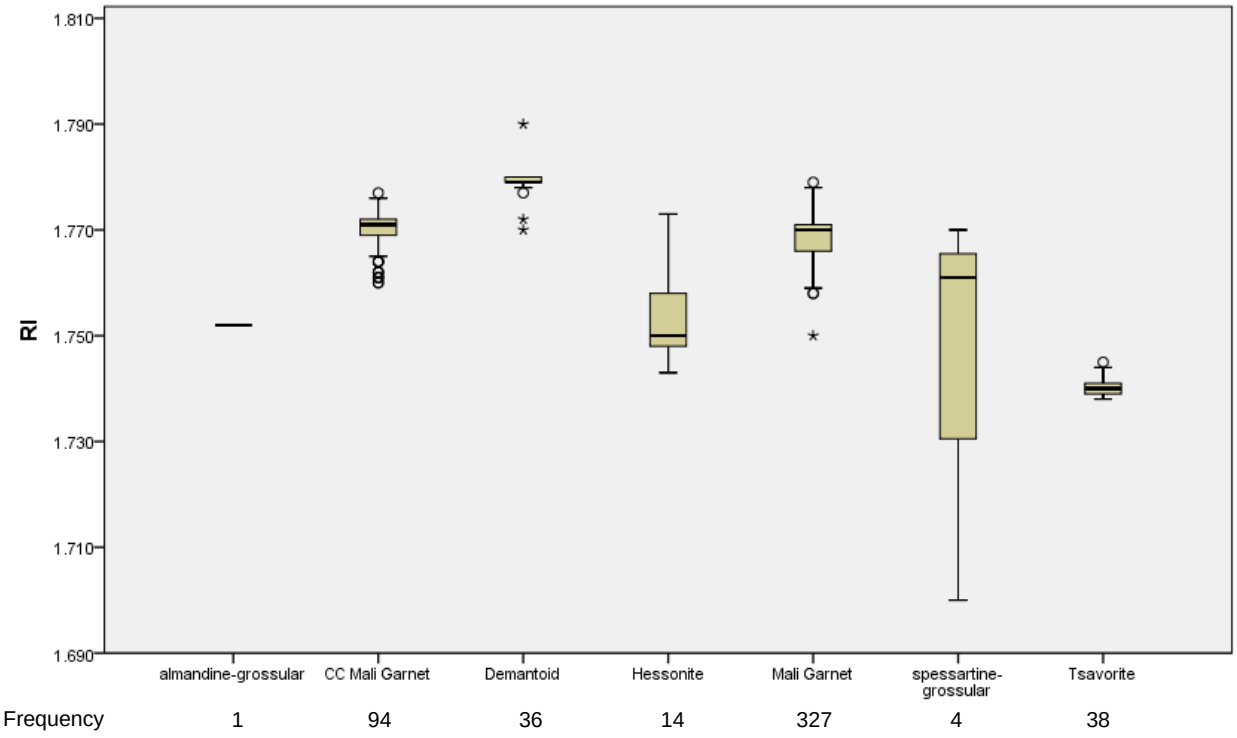

Figure 58. The RI values for the garnets from the ugrandite species. Below the boxplot are the frequencies for the different ugrandite garnets.

Most of the garnets from the ugrandite species have narrow ranges in RI (except for 'spessartine-grossular'). Overlaps occur between the 'spessartine-grossular', 'tsavorite' and 'hessonite' samples. Overlaps also occur between the 'hessonite', 'almandine-grossular', 'CC Mali garnet' and 'Mali garnet' samples. There is also an overlap between the 'demantoid' and 'Mali garnet' samples.

4.3.4. Colour

4.3.4.1. Colour change

No differences can be observed in the chemistry between the 'Mali' and 'CC Mali garnets'. Both garnets have very low uvarovite content and cannot be distinguished from each other.

© University of Pretoria

5. Discussion

5.1. Colour

5.1.1. Pyralspite

- Orange , red orange and orange red

Most of the orange, red orange and orange red samples contain a high spessartine component (most contain > 60 mol. % spessartine). An orange colour in stones indicated the presence of spessartine. The darker hues indicated an increase in spessartine (Figure 27).

- Red

The red (dark red, very dark red and very dark red to almost black) samples plot either as ‘spessartine’, ‘pyrope’, ‘almandine’, ‘almandine-pyrope’ or ‘pyrope-almandine’ (Table 10).

- Pink

Most of the pink samples are composed primarily of pyrope with lesser amounts of almandine and spessartine. The darker pink samples (Figure 30) show a higher almandine component and lower spessartine component. This indicates that the almandine component is responsible for the darkening of a pink stone. The light pink samples contain lower almandine and higher spessartine than the dark pink samples (Figures 30 and 31).

- Purple

The purple samples show a large variability in their chemistry but most are pyrope and spessartine dominant with lesser amounts of almandine (except for two stones with high almandine) (red circles in Figure 34). In Figure 34, the purple samples contain a high spessartine component with most plotting as ‘pyrope-spessartine I and II’ and ‘spessartine-pyrope II’. The purple coloured samples plot everywhere, and cannot be reconciled with a particular composition.

- Pink orange and orange pink

The pink orange and orange pink samples are either part of the pyrope-almandine solid solution series or the pyrope-spessartine solid solution series. Stones that have a dominant orange colour contain a high spessartine component, and stones with a dominant pink colour contain a high pyrope component (Figures 35, 36 and 37). All of the light pink orange and light orange pink samples contain lower almandine (Figure 35) than the darker varieties, showing that almandine causes the darkening of a stone.

- Purple pink and pink purple samples

© University of Pretoria

Most of these samples are part of the pyrope-almandine solid solution series (Figure 30). Pink dominant samples are pyrope dominant with lesser amounts of almandine. The almandine component increases as colour darkens, e.g. towards dark pink purple. Purple dominant samples have lower almandine and higher spessartine.

- Brown and yellow

Most of the brown and yellow samples are part of the pyrope-spessartine solid solution series, with most being ‘spessartine I and II’ samples. The almandine component is low, with a medium to high spessartine component (Figure 38). The gold and yellow samples show variable grossular content, with some containing relatively high grossular (< 29.45 mol.%) (Figure 39). This is in contrast to the other colours from the pyralspite species, which do not contain grossular.

- Purple red

The purple red samples are ‘rhodolite’ and are composed of pyrope with lesser amounts of almandine. The ‘rhodolite’ samples do not form their own separate cluster, but plot with the other different coloured ‘pyrope-almandine’ samples (Figure 30).

The differenct colours and their compositions are plotted in Figure 59 (excluding the red varieties). Different coloured stones can have similar chemistries, and stones with similar compositions can have different colours. The causes are beyond the scope of this thesis. This study can only show that stones with similar compositions can have different colours and vice versa. This means that colour as a means of classification of gem garnets is not reliable.

© University of Pretoria

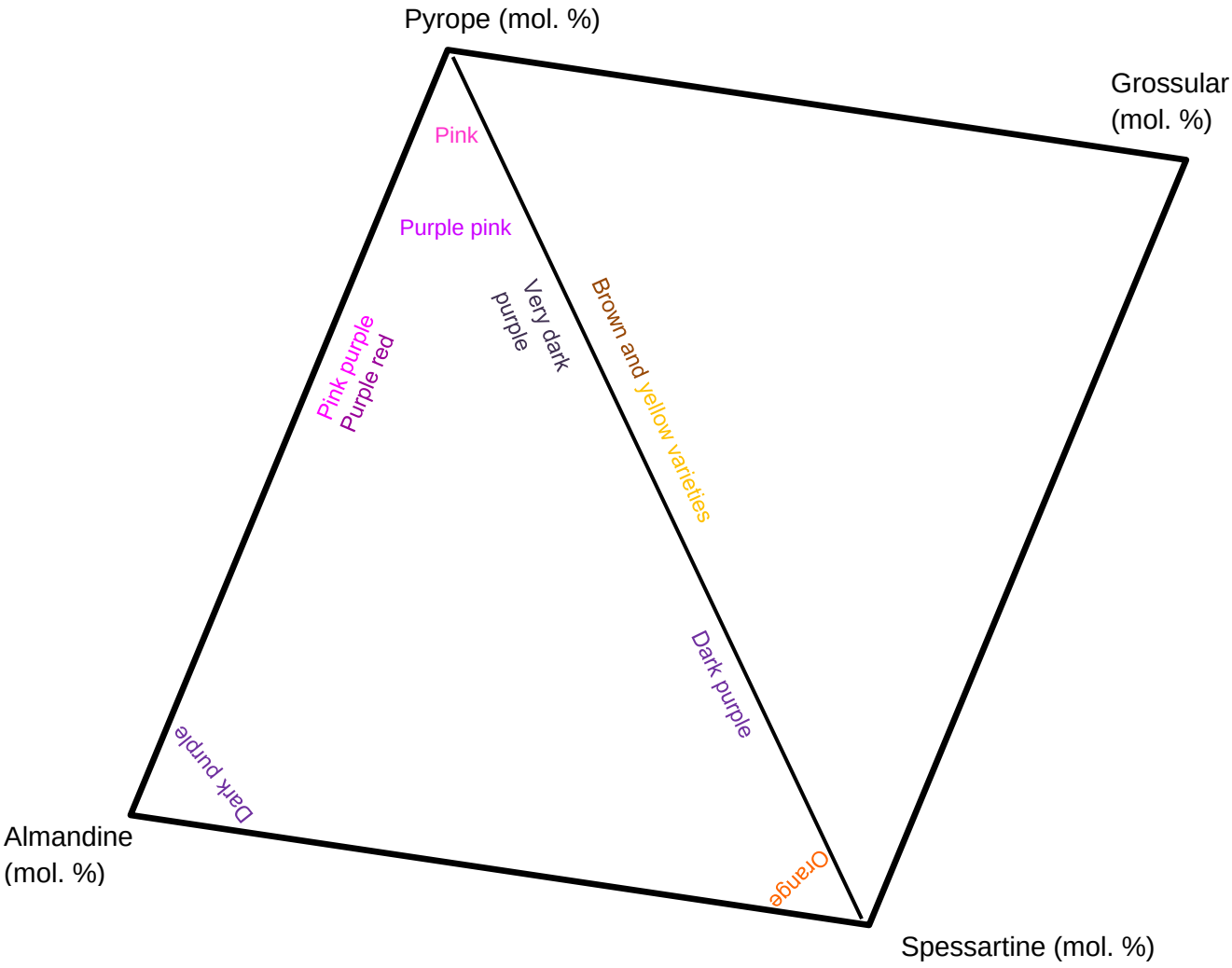

Figure 59. A schematic summary of the composition of the different coloured samples in the pyralspite species excluding the red samples. The red varieties have variable compositions (spessartine, pyrope, almandine, almandine-pyrope and pyrope-almandine). The figure is not quantitative but just a visual representation to show the diverse compositions observed in the different coloured samples.

5.1.2. Ugrandite

The ugrandite samples show no detectable relationship between colour and chemistry, because samples appear very similar to each other despite belonging to different garnet types e.g. the colour green occurs in the ‘demantoid’, ‘tsavorite’, ‘Mali garnet’ and ‘CC Mali garnet’ samples (excluding the brown samples found in the ‘Mali and CC Mali garnets’).

5.2. Colour Change

5.2.1. Pyralspite

© University of Pretoria

Colour change occurs more commonly in the spessartine dominant samples, especially in the case of 'spessartine-almandine' (Figure 8). The 'almandine-spessartine' samples show no colour change.

Those samples approaching a pure end-member in composition show little to no colour change or shift, which indicates that colour change and shift are predominant in the samples of intermediate composition.
In the spessartine-almandine solid solution series, colour change and colour shift occurs only in the spessartine dominant samples and not in the 'almandine-spessartine' samples. This supports the idea that a high almandine component decreases the potential for colour change.

In the pyrope-spessartine solid solution series, colour change and colour shift are common, while colour change occurs more frequently in the 'spessartine-pyrope' samples than in the 'pyrope-spessartine' samples. This contrasts with the observations of Krzemnicki *et al*. (2001), which propose that an increase in the MnO content will reduce the potential for the colour change phenomenon.

5.2.1.1. Colour change chemistry

5.2.1.1.1. Pyralspite

All of the samples from the pyralspite species with distinct colour change contain some vanadium with chromium being present in smaller amounts (Figure 41a or 41b). This suggests that vanadium has a stronger influence on colour change than chromium. This is consistent with Krzemnicki *et al*. (2001), where all (except for one sample) of the colour change samples contain vanadium contents that exceed the chromium contents. However, all of the colour change garnets reported by Krzemnicki *et al*. (2001) contained some chromium (≤ 0.95 wt. %).

Although all of the colour change samples contain some uvarovite component, these values are not high (Figure 42). A large number of the colour shift and non-colour change samples show a similar uvarovite component, which suggests that the presence of uvarovite component alone is the cause of colour change in a gem.

© University of Pretoria

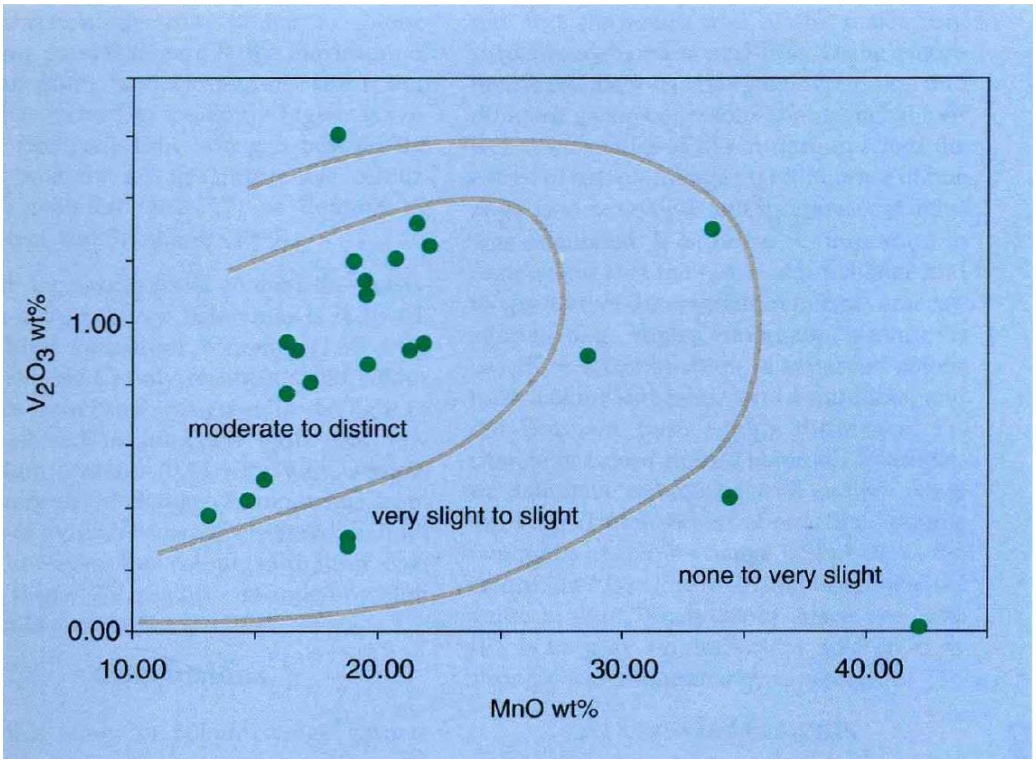

Figure 60. a) The V_2O_3 and MnO contents of the colour change garnets from Krzemnicki *et al*. (2001). Three main fields of colour change strength are indicated. The limits of the fields represent a gradual transition.

© University of Pretoria

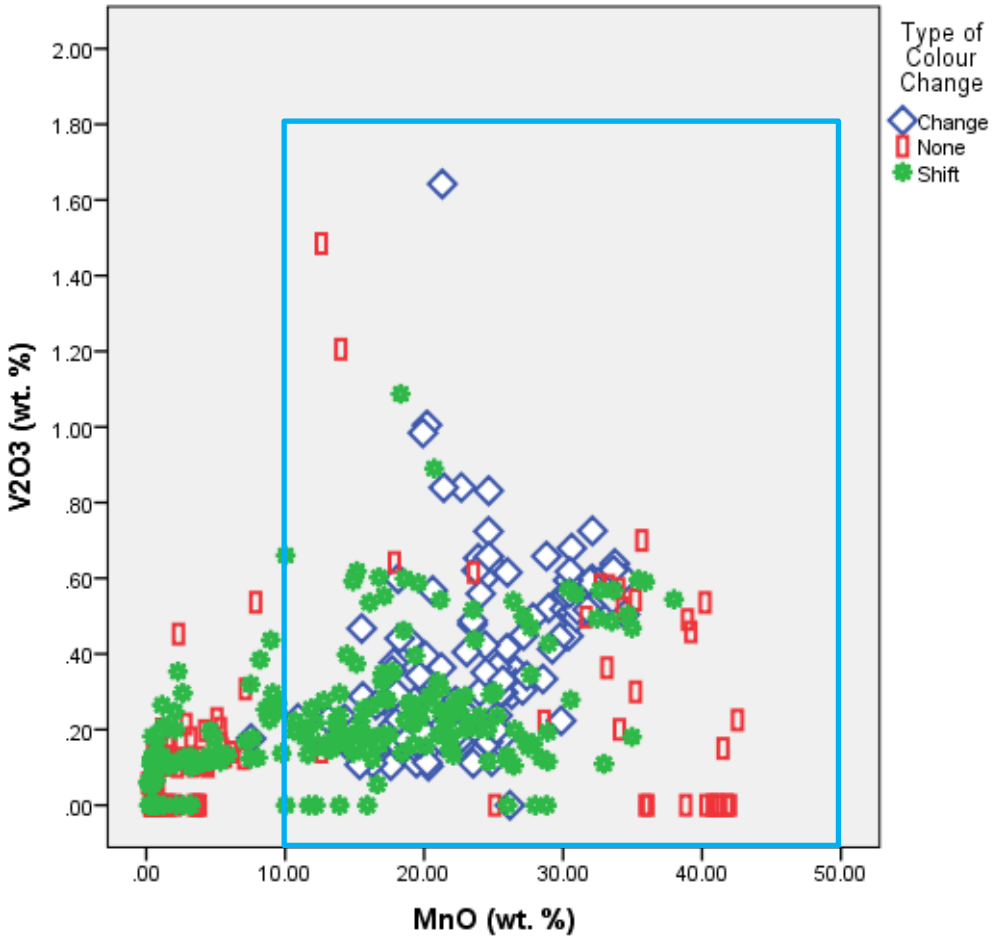

Figure 60. b) The V_2O_3 (wt. %) and MnO (wt. %) content of the pyralspite garnets from this thesis together with their type of colour change. The blue box represents the section depicted by Krzemnicki *et al*. (2001) in Figure 60a.

The colour change garnets from this thesis show much higher MnO contents than those reported by Krzemnicki *et al*. (2001) (Figures 60a and 60b). This suggests that a higher MnO content than that proposed by Krzemnicki *et al*. (2001) does not eliminate the potential for the colour change phenomenon in garnet gems. However, no colour change samples occur at MnO > 34.40 wt. %, indicating that colour change does not occur in samples approaching pure spessartine.

Similar V_2O_3 contents have been observed in the data from this study as in Krzemnicki *et al*. (2001). Schmetzer and Ottemann (1979) and Schmetzer and Bernhardt (1999) propose an upper limit for the vanadium content (1.60 wt. % V_2O_3), where no or only slight colour change is observed when this limit is exceeded. The same has been observed in the data from this thesis. The highest vanadium content observed in the colour change garnets is 1.64 wt. %

© University of Pretoria

5.2.1.1.2. Ugrandite

The 'Mali and CC Mali' garnets cannot be distinguished from each other based on their chemistry. Both show similar grossular, andradite and uvarovite contents. The presence of colour change might be due to trace elements, but this could not be detected in this study.

5.3. Colour Change Terms

The term colour change should only be applied to garnets that display a distinct colour change between daylight and incandescent light, e.g. pink orange to purple. The term colour shift should be used for garnets that show a slight shift between daylight and incandescent light, e.g. purplish red to reddish purple.

5.4. Refractive Index

5.4.1. Pyralspite

Many of the garnets have RI values that lie outside the usual range suggested for that type of garnet, based on the findings of Stockton and Manson (1985) (Figures 6a and 6b).

The use of RI as the sole means of classifying garnets is not reliable. The RI ranges for the different types of garnets overlap with each other (Figure 25). This proves especially true for the pyralspite species such as the spessartine-almandine and pyrope-spessartine solid solution series. Both series possess similar RI ranges, together with similar colour and colour change phenomena.

Three samples have very low RI values that are not typical of garnets (Table 13), all of which are pyrope dominant, with no grossular.

Table 13. Properties of the three 'pyrope-spessartine' samples from the pyralspite species with very low RI when compared to the ranges proposed by Stockton and Manson (1985).

Name	RI	Almandine (mol. %)	Andradite (mol. %)	Grossular (mol. %)	Pyrope (mol. %)	Spessartine (mol. %)	Uvarovite (mol. %)
Pyrope-spessartine I	1.635	14.86	4.42	0	61.71	18.56	0.45
Pyrope-almandine	1.712	14.71	4.11	0	72.75	7.88	0.55
Pyrope-spessartine II	1.720	0.60	4.45	0	64.51	30.06	0.39

5.4.2. Ugrandite

© University of Pretoria

Most of the 'tsavorite', 'hessonite' and 'demantoid' samples have RI values that match the traditional ranges stated by Stockton and Manson (1985). 'Mali and CC Mali' garnets do not apply, as Stockton and Manson (1985) did not have RI ranges for these.

The hessonite samples are the only ones that have a relatively high proportion with RI values that do not fit into the traditional RI scheme for hessonites as founded by Stockton and Manson (1985).

5.5. Magnetic Susceptibility

5.5.1. Pyralspite

There is a general increase in magnetic susceptibility as Fe_{total} +Mn (mol. %) contents increase (Figures 24a and 24b). However, this trend is not as obvious as seen in Hoover (2011), Hoover and Williams (2007), and Hoover *et al*., (2008). Some samples with low Fe_{total} +Mn (mol. %) contents show higher magnetic susceptibilities than the suggested limit. The presence of manganese seems to play a bigger role in magnetic susceptibility than FeO_{total} in the pyralspite species, especially when comparing the pyrope-spessartine solid solution series with the pyrope-almandine solid solution series. The same trend has been observed in the spessartine-almandine solid solution series. Although 'spessartine' did show some of the highest magnetic susceptibilities, it also shows the largest range and some very low magnetic susceptibilities, suggesting that magnetic susceptibility is not a single function of Fe^{2+} and Mn^{2+} content.

The method of classification by magnetic susceptibility, as suggested by Hoover *et al*. (2008) proved to be unreliable for the pyralspite species because a large number of the classifications based on magnetic susceptibility differed from the observations made by Hoover *et al*., (2008) and Gemstone Magnetism (2014). As stated by Gemstone Magnetism (2014), the boundaries set out to distinguish between different gemstones are not as clear-cut as previously stated. Only the 'pyrope' samples show a majority of samples that correlate with the magnetic susceptibility traditionally associated with 'pyropes'. Most of the samples from the pyralspite species have magnetic susceptibilities that fall outside of the range stated by Gemstone Magnetism (2014). It is possible to distinguish between the pyrope-almandine and pyrope-spessartine solid solution series using magnetic susceptibility, but this is not specific enough when dealing with the classification of garnet gemstones. The use of magnetic susceptibility as the sole means of classifying garnets from the pyralspite species is not very reliable and should be used with caution. In addition, the traditional magnetic susceptibility ranges for 'spessartine-grossular', 'almandine-grossular', 'almandine-pyrope',

© University of Pretoria

'pyrope-almandine', 'spessartine-almandine' and 'almandine-spessartine' samples were absent.

5.5.2. Ugrandite

The majority of the samples from the ugrandite species have magnetic susceptibilities that fall within the traditional range as defined by Gemstone Magnetism (2014) (Figures 11a and 11b).

An increase in Fe_{total} + Mn (mol. %) coincides with an increase in magnetic susceptibility (Figure 57). This method of classification, as defined by Hoover *et al*. (2008) and Gemstone Magnetism (2014) is more reliable for the ugrandite species than the pyralspite species.

5.6. Use of Magnetic Susceptibly with RI

Magnetic susceptibility should be used in conjunction with RI, rather than as a sole means. Both methods, together, can be used to distinguish between the ugrandite species and the pyralspite species and can assist, in conjunction with colour, in determining the solid solution series to which that the gem garnet belongs. Determining which solid solution series to which the stone belongs is more reliable than attempting to determine the exact composition or dominant end-member. However, this method should be used with care when attempting to classify stones from the pyralspite species because there is no systematic relationship between magnetic susceptibility, RI and colour.

Another problem with the use of RI and magnetic susceptibility is the lack of RI and magnetic susceptibility ranges for 'spessartine-grossular' and 'almandine-grossular' garnets because stones of these compositions are not common in gemology. However, as this thesis proves, these stones occur and can be easily mistaken for another type of garnet such as the 'Malaya' or 'colour change' garnets.

The spessartine-almandine solid solution series is difficult to distinguish from the pyrope-spessartine solid solution series because samples show similar colour, colour change/shift, RI (1.759-1.774) and magnetic susceptibility (0.0018-0.0035 SI). Also, the traditional range of RI (1.81-1.82) proposed by Stockton and Manson (1985) for 'almandine-spessartine' did not match any of the 'spessartine-almandine' or 'almandine-spessartine' samples in this thesis. The reason for the difference is not known.

© University of Pretoria

5.7. Chemistry of the Pyralspite and Ugrandite Species

5.7.1. Pyralspite

Often, the 'pyrope-almandine', 'rhodolite' and 'pyrope' samples show very similar chemistry making it difficult to differentiate between them. The Cr_2O_3 content (≤ 0.47 wt. %) (Figure 15) is similar for the 'rhodolite' and 'pyrope-almandine' samples, but much lower for the 'pyrope' samples (Cr_2O_3 content ≤ 0.17 wt. %).

The V_2O_3 content (Figure 16) is higher in the 'spessartine-almandine' samples than the 'almandine-spessartine' samples. Because colour change only occurs in the 'spessartine-almandine' samples, this high V_2O_3 content (0.16-0.47 wt. %) is considered the primary cause of colour change in these samples.

It is often difficult to distinguish between the colour change and non-colour change samples from the pyrope-spessartine solid solution series based on their chemistry. Only the V_2O_3 and Cr_2O_3 contents are different between the two. The Cr_2O_3 contents (Figure 15) are different between the colour change and non-colour change 'spessartine-pyrope' samples. In addition, the 'spessartine-pyrope' samples have higher V_2O_3 content (Figure 16) than the 'pyrope-spessartine I and II' samples. This suggests that colour change is more common in spessartine dominant samples from the pyrope-spessartine solid solution series.

5.7.2. Ugrandite

The different garnet types from the ugrandite species can easily be distinguished from each other based on their chemistry. The 'demantoid' samples have the highest FeO_{total} content with only one 'almandine-grossular' sample showing similar FeO_{total} content. The 'demantoid' samples also contain some TiO_2, but this is low. The 'tsavorite' samples have the highest CaO content, followed by 'hessonite'. The two can be differentiated from each other by their MnO and TiO_2 contents, as the 'tsavorite' samples have slightly higher MnO and TiO_2 contents. The 'spessartine-grossular' samples have the highest MnO content with very low CaO content when compared to the other ugrandite samples.

The 'Mali and CC Mali garnets' show the largest range in $FeO_{total.}$ Both the 'Mali and the CC Mali garnets' show very similar CaO and TiO_2 contents. It is difficult to distinguish between the two based on their chemistry.

5.8. End-member Proportions and Variability

5.8.1. Pyralspite

© University of Pretoria

- Pyralspite species chemistry

The pyrope dominant samples show a very large range in the almandine and spessartine components, while samples that are almandine and/or spessartine dominant show less substitutions. This is evident in the pyrope-almandine and pyrope-spessartine solid solution series. As pyrope becomes the more dominant end-member, the potential for substitutions between almandine and spessartine increases. As the almandine or spessartine component increases, the potential for substitutions of almandine or spessartine by pyrope is lowered.

Without chemical analysis, it is impossible to determine the exact composition. The exact difference in physical characteristics between a 'pyrope-almandine' with significant amounts of spessartine and a 'pyrope-spessartine' with significant amounts of almandine cannot be determined. The deviation in colour, RI, and magnetic susceptibility observed in gems of this particular composition is large and no systematic rules can be found to make distinction possible. Hence, the distinctions that have been used in the past are purely arbitrary. There is not scientific data based on chemistry to support the separation of 'rhodolite' from 'pyrope-almandine' and/or 'Malaya' gem garnet. If it is not possible to prove, scientifically, that 'Malaya' or 'rhodolite' have distinct compositions and properties, then the term should be discarded because distinctions are arbitrary and possibly biased.

Gaps that have been observed in the different series are highlighted to be compared with the data from the literature (see section 5.9.).

5.8.2. Ugrandite

- Ugrandite species chemistry

The gem garnets from this species have distinct compositions and can be easily distinguished from each other. The exception to this are the 'CC Mali and Mali garnets'. These garnets are indistinguishable and it is difficult to discriminate between the two using their physical characteristics, apart from the occurrence of colour change. The 'tsavorite' samples contain almost 100 mol.% grossular with variable amounts of spessartine. 'Hessonite' follows with grossular > 90 mol.%, but these samples contain higher andradite than the 'tsavorite' samples. The 'CC Mali and Mali garnets' also have high a grossular content with significantly high andradite. The 'demantoid' samples have almost 100 mol.% andradite and form a distinct cluster that is easily discernible from the other ugrandite garnets. This justifies the distinctions used in classifying these gem garnets from the ugrandite species, as it can be supported by their chemistry.

© University of Pretoria

5.9. Comparison with the Literature

Various examples from the gemological literature were used (Payne; 1981; Bocchio *et al*., 2010; Adamo *et al*.,2011; Stockton and Manson, 1983; Pezzotta *et al*., 2011; Mathavan *et al*., 2000; Johnson *et al*.,1995; Feneyrol *et al*.,2013; Adamo *et al*., 2012; Muije *et al*., 1979; Switzer, 1974, Wang and Liu, 1993; Howie, 1965; Laurs and Knox, 2001; Zwaan, 1974; Hidden and Pratt, 1898; Schmetzer *et al*., 2002; Manson and Stockton, 1984; Schmetzer *et al*., 2001; Guastoni *et al*., 2001; Schlüter and Weitschat, 1991; Hoover, 2011; Krzemnicki *et al*., 2001; and Schmetzer *et al*., 2009). Furthermore, many petrological examples from the literature were also used (Proenza, 1999; Ghosh and Marishita, 2011; Bryhni and Griffin,1971; Carswell and Dawson, 1970; Drahota *et al*., 2005; Zürcher *et al*., 2001; Lu *et al*., 2003; Newberry, 1983; Shimazaki, 1977; Ford, 1915; Pertoldová *et al*., 2009; Kassoli-Fournaraki, 1995; Chauvet *et al*., 1992; Schmädicke and Will, 2003; Operta *et al*., 2011; Zenk and Schulz, 2004; Hariya and Kimura, 1978; Zhang *et al*., 2001; Somarin, 2010; Wan *et al*., 2012; Habaak, 2004; Somarin, 2004; Lingang *et al*., 2010; Fuertes-Fuente *et al*., 2000; Xu and Lin, 2000; Okay, 1993; Glodny *et al*., 2005 and Georoc, 2015). These literary examples were used and compared to those from this thesis. All the pyrope-spessartine and spessartine-pyrope samples reported by Krzemnicki *et al*. (2001), Schmetzer *et al*. (2002) and Schmetzer *et al*. (2009) are colour change samples.

The purpose of comparing the data from this thesis with the literature is to see if there are distinct differences in composition between the data from the thesis and literature. If the data from the literature overlaps with the data from this thesis, then there is nothing unusual about the compositions. However, if the literature data plot in the gaps observed in Sections 4.2.1. (pyralspite chemistry) and 4.3.1. (ugrandite chemistry), then this ‘gap’ is a sampling problem. The data from this thesis that do not plot with any of the literature are circled in red and suggest that garnets of this composition exist but are not represented in the literature presented in this thesis.

5.9.1. Pyralspite

5.9.1.1. Almandine-grossular

In Figure 61, the sample ‘almandine-grossular’ sample plots just below 80 mol. % almandine, together with the samples from the petrological literature and Georoc data. The same can be seen in Figures 63, 64 and 65, where the ‘almandine-grossular’ sample plots together with the data from the petrological and Georoc literature.

© University of Pretoria

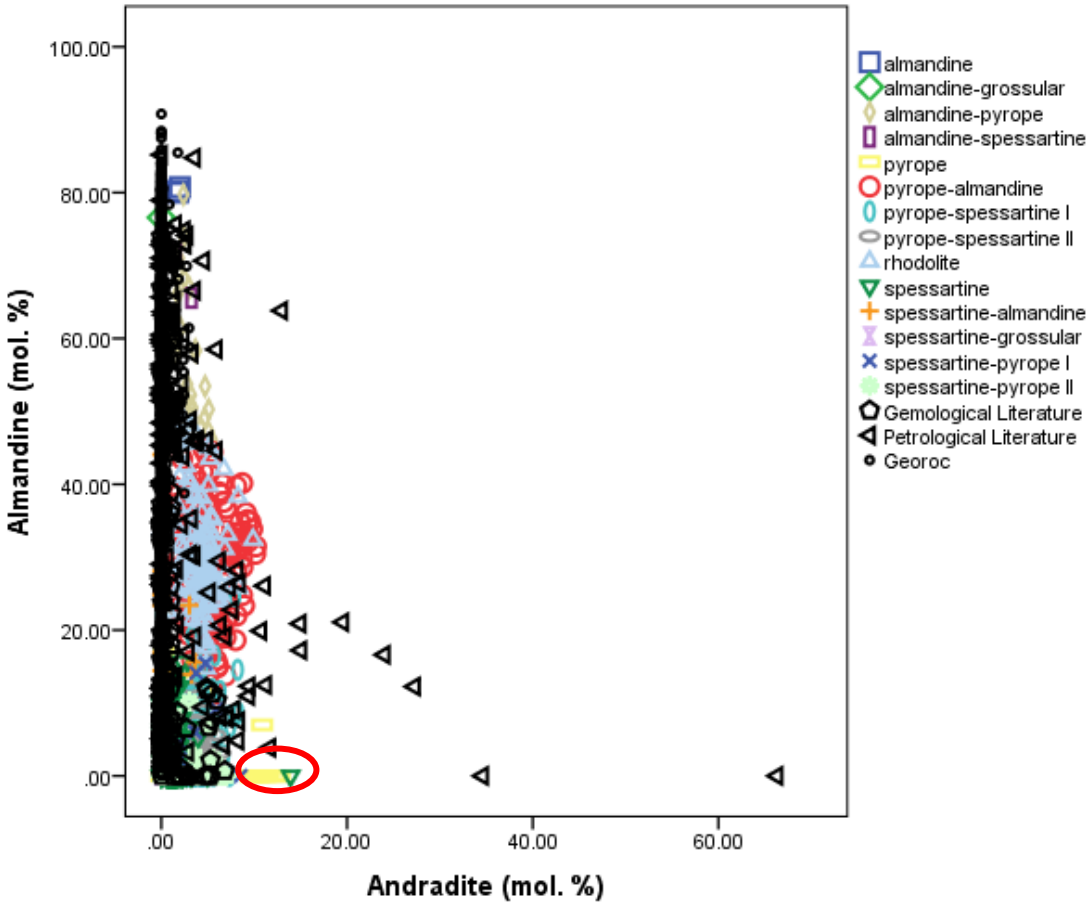

Figure 61. The almandine and andradite components for the garnets from the pyralspite species in this study compared with those from the gemological literature (Wang and Liu, 1993; Howie, 1965; Laurs and Knox, 2001; Zwaan, 1974; Hidden and Pratt, 1898; Schmetzer Schmetzer *et al*., 2002; Manson and Stockton, 1984; Schmetzer *et al*., 2001; Guastoni *et al*., 2001; Schlüter and Weitschat, 1991; Hoover, 2011; Krzemnicki *et al*., 2001 and Schmetzer *et al*., 2009) and petrological literature (Okay, 1993; Glodny *et al*., 2005; Bryhni and Griffin, 1971; Drahota *et al*., 2005; Zürcher *et al*., 2001; Shimazaki, 1977; Ford, 1915; Newberry, 1983; Pertoldová *et al*., 2009; Kassoli-Fournaraki, 1995; Chauvet *et al*., 1992; Schmädicke and Will, 2003; Operta *et al*., 2011; Zenk and Schulz, 2004 ; Carswell and Dawson, 1970 and Georoc, 2015). The red circle represents samples from the thesis that do not plot with the presented literature data.

© University of Pretoria

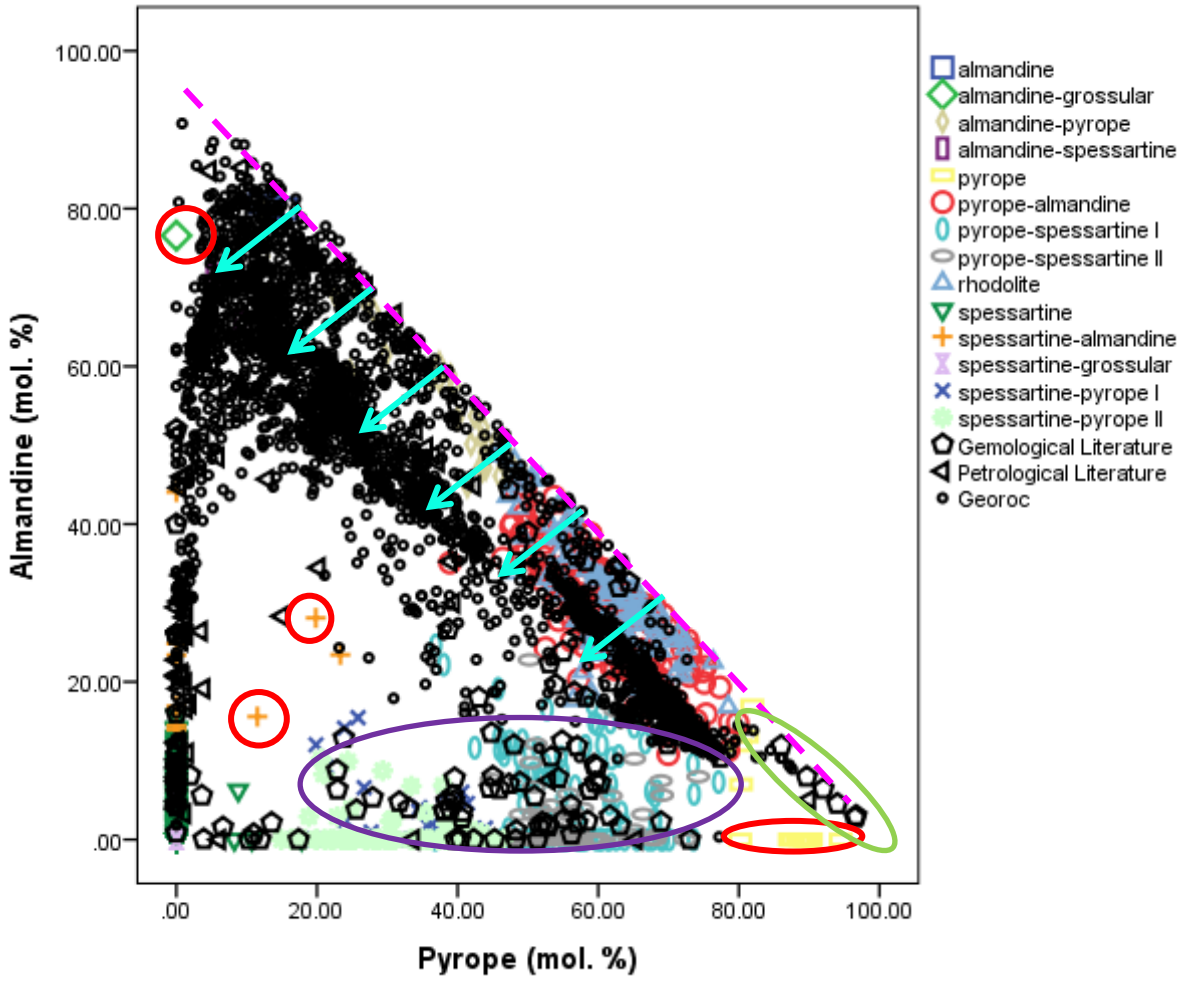

Figure 62. The almandine and pyrope components of the garnets from the pyralspite species in this study compared with those from Georoc (2015) and the gemological and petrological literature. The dashed line represents the solid solution series between almandine and pyrope with the arrows indicating deviation away from the trend line (additional substitutions). The area circled in dark purple indicates where the 'pyrope-spessartine I and II' and 'spessartine-pyrope I and II' samples plot. The area circled in green refers to the samples from the gemological literature (Schlüter and Weitschat, 1991) that fill in the gap present in the data from this thesis. The areas circled in red represent samples from the thesis that do not plot with the presented literature data.

In Figure 62, the 'almandine-grossular' sample plots away from the data gathered from the gemological and petrological literature.

© University of Pretoria

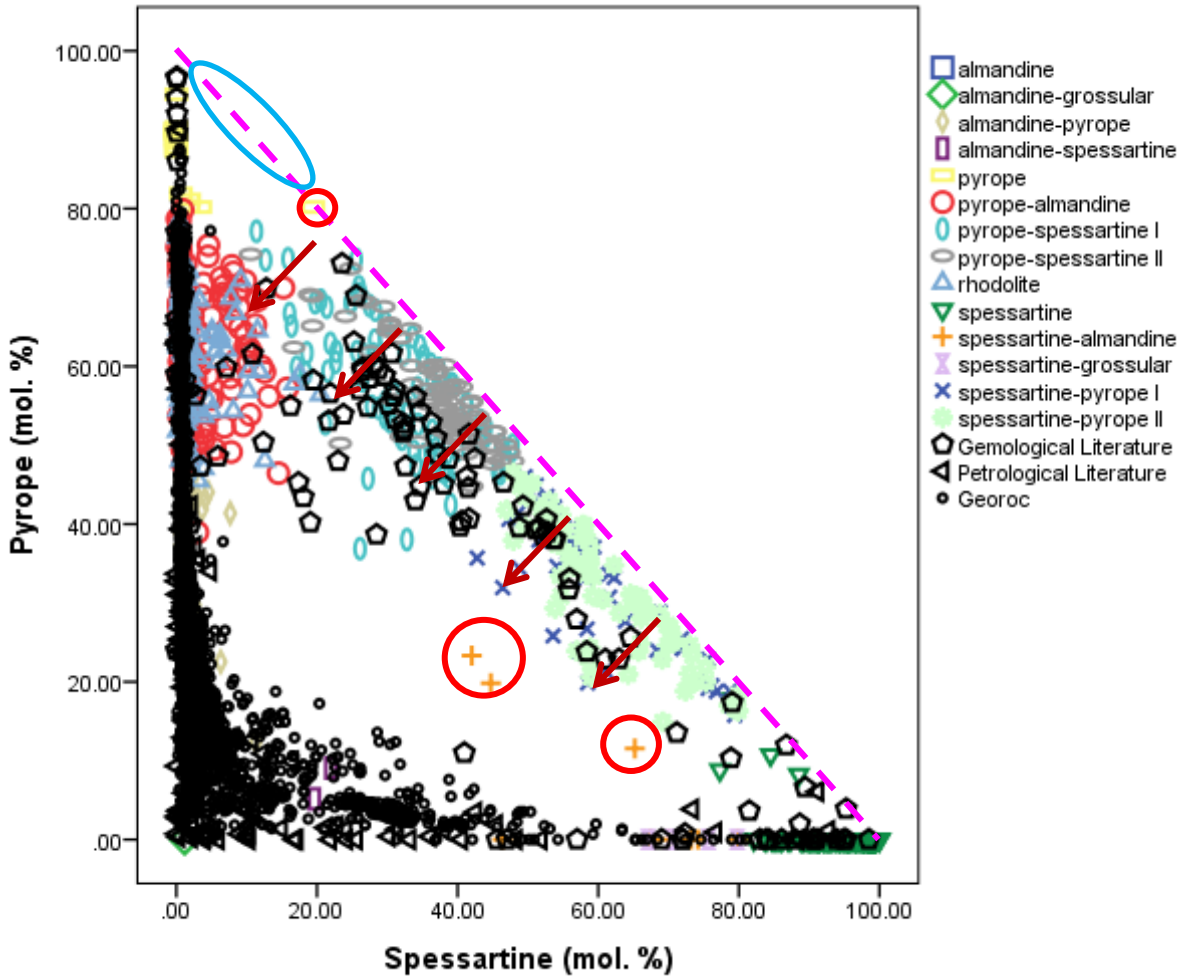

Figure 63. The pyrope and spessartine components of the garnets from the pyralspite species in this study compared with those from Georoc (2015), the gemological and petrological literature. The dashed line represents the solid solution series between pyrope and spessartine with the arrows indicating deviation away from the trend line (additional substitutions). The area circled in blue represents the gap present in the data from both this thesis and the literature where no samples plot. The areas circled in red refer to samples that do not plot with the literature data presented in this thesis.

© University of Pretoria

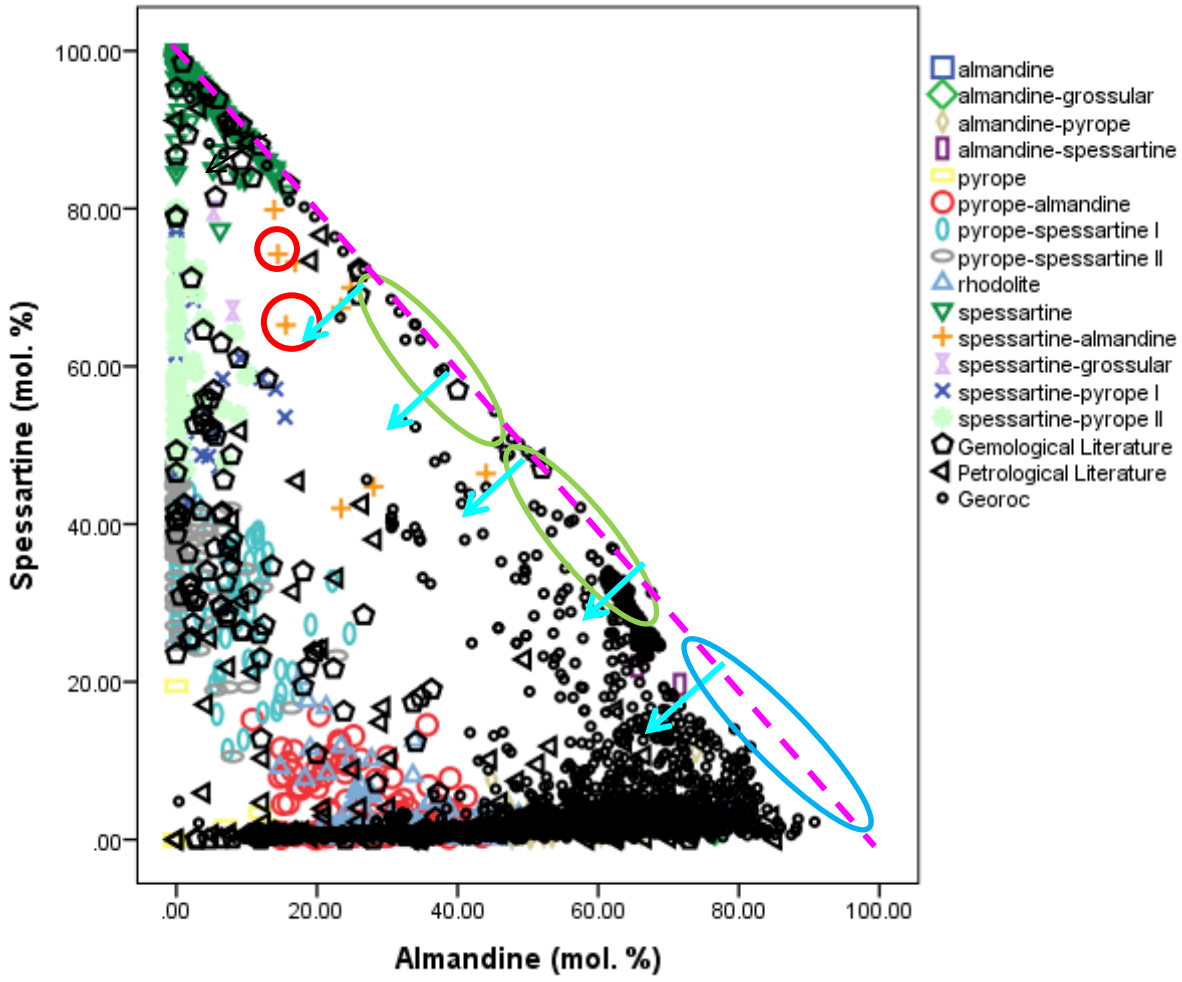

Figure 64. The spessartine and almandine components of the garnets from the pyralspite species in this study compared with those from Georoc (2015), the gemological and petrological literature. The dashed line represents the solid solution series between spessartine and almandine with the arrows indicating deviation away from the trend line (additional substitutions). The areas circled in green refer to the samples from the petrological literature that fills in the gap present in the data from this thesis. The area circled in blue represents the gap present in the data from both this thesis and the literature where no samples plot. The areas circled in red refer to samples that do not plot with the literature data presented in this thesis.

© University of Pretoria

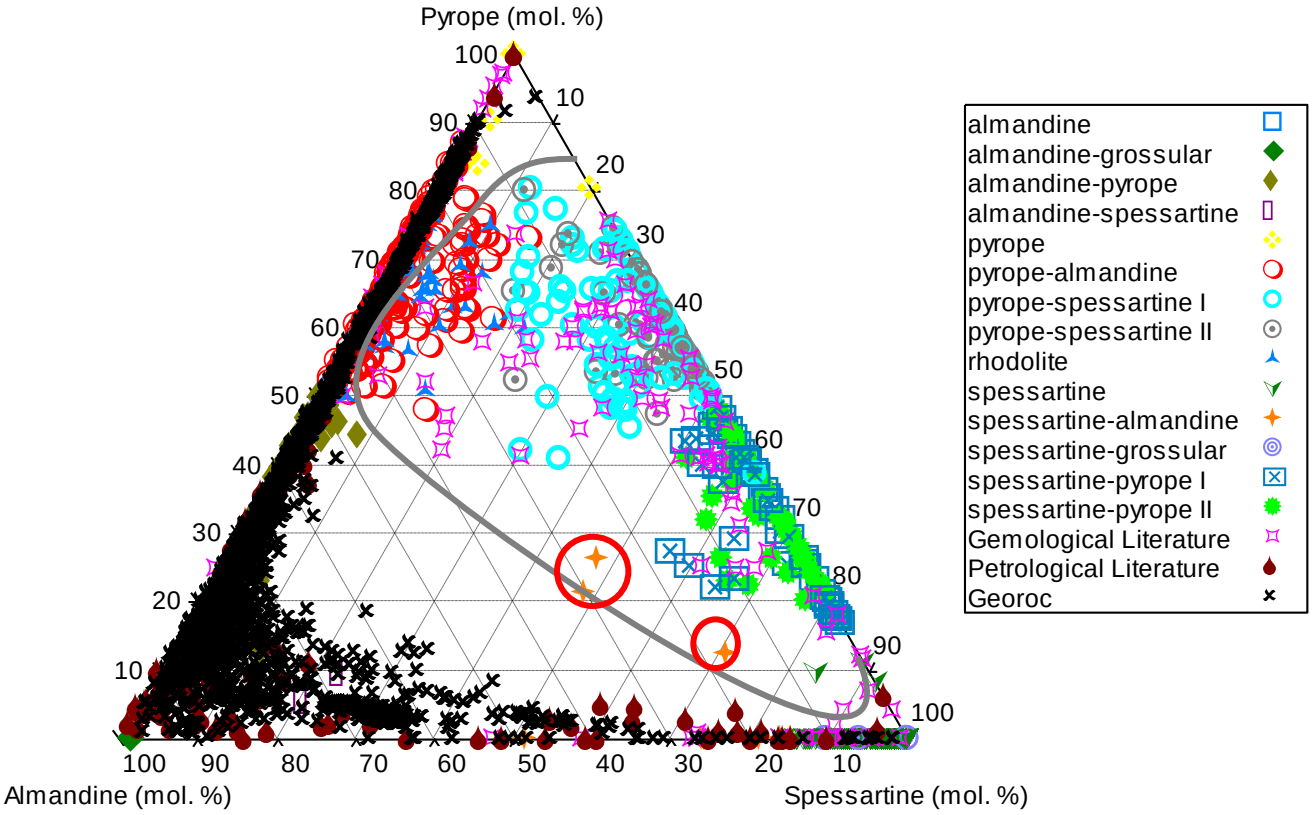

Figure 65. Ternary diagram of the different garnet types from the pyralspite species in this study alongside the data from Georoc (2015), the petrological and the gemological literature. A few of the samples from the gemological literature plot beneath the Georoc (2015) and the petrological literature along the solid solution series between pyrope and almandine. The grey field refers to the area where the data from the petrological literature and Georoc (2015) do not plot. The areas circled in red refer to samples that do not plot with the literature data presented in this thesis.

The large number of 'almandine-grossular' and 'grossular-almandine' samples present in the petrological literature supports the existence of gem quality stones. Their scarcity in the gem market could be either due to them not yet being discovered or a lack of economically viable deposits.

5.9.1.2. Almandine

The 'almandine' samples cluster together with the data from Georoc (2015) and the petrological literature (Figures 61, 62, 63 and 64). Only a few samples from the gemological literature plot near the 'almandine' samples.

© University of Pretoria

5.9.1.3. Almandine-pyrope

The 'almandine-pyrope' samples cluster together with the data from the petrological literature and Georoc (2015) (Figures 61, 62, 63 and 65). Only a few data points from the gemological literature plot together with the 'almandine-pyrope' samples from the thesis.

5.9.1.4. Almandine-spessartine

The 'almandine-spessartine' samples plot together with the samples from Georoc (2015) and the petrological literature (Figures 62, 63, 64 and 65). None of the samples from the gemological literature plot near the 'almandine-spessartine' samples from this thesis because 'almandine-spessartine' is not represented in the gemological literature.

5.9.1.5. Pyrope

Most of the 'pyrope' samples from the thesis plot together with the data from both Georoc (2015) and the petrological, and the gemological literature (Figures 62, 63, 64 and 65). However, a few of the 'pyrope' samples from this thesis are unusual and plot away from the other samples from the literature (as indicated by the areas circled in red in Figures 61, 62, 64).

In Figure 62, some samples from the gemological literature fill in the gap (area circled in green) previously observed in the data from this thesis. These samples are 'pyropes' from Czechoslovakia as reported by Schlüter and Weitschat (1991). This shows that the 'pyropes' with this particular composition exist as gem garnets but are not represented in this thesis.

5.9.1.6. Pyrope-almandine and rhodolite

The 'pyrope-almandine' and 'rhodolite' samples from this thesis cluster together with the samples from Georoc (2015) and the petrological, and the gemological literature (Figures 61, 62, 63, 64 and 65). In Figures 63, 64 and 65, the 'pyrope-almandine' and 'rhodolite' samples, together with those from the gemological literature, show greater variation in chemistry than those from Georoc (2015) and the petrological literature.

5.9.1.7. Spessartine

The 'spessartine' samples from this thesis plot together with those from Georoc (2015) and the petrological, and the gemological literature in Figuees 61, 62, 63 and 64. However, one 'spessartine' sample, as indicated by the area circled in red in Figure 61, plots away from the rest of the data from this thesis and the literature.

© University of Pretoria

In Figure 64, most of the Georoc (2015) samples do not cluster together with the 'spessartine' samples from this thesis. However, the samples from the petrological and the gemological literature cluster together with these 'spessartines' from this research, suggesting that the 'spessartines' of this particular composition are not represented in the Georoc (2015) data.

5.9.1.8. Spessartine-almandine

Most of the 'spessartine-almandine' samples from the thesis cluster together with those from Georoc (2015) and the petrological, and the gemological literature (Figures 61, 62, 63, 64 and 65).

However, three 'spessartine-almandine' samples from this thesis do not plot with the literature data (as indicated by the areas circled in red in Figures 62, 63, 64 and 65). This suggests that garnets of this particular composition are not represented in the literature considered in this thesis.

5.9.1.9. Spessartine-grossular

The 'spessartine-grossular' samples from this study cluster together with those from Georoc (2015) and the petrological and the gemological literature (Figures 61, 62, 63 and 65). However, in Figure 64, the 'spessartine-grossular' samples from the thesis only plot together with those from the gemological literature and not with those from Georoc (2015) and the petrological literature.

The large number of 'spessartine-grossular' samples in the petrological literature and Georoc (2015) suggests that, even though 'spessartine-grossular' is not common amongst gem garnets, it can occur.

5.9.1.10. Pyrope-spessartine (I and II) and spessartine-pyrope (I and II)

The 'pyrope-spessartine I and II' and 'spessartine-pyrope I and II' samples from this thesis only cluster with the samples from the gemological literature (Figures 62, 63, 64 and 65). Only a few of the petrological literature samples plot near the stones from this research in Figures 62 and 64. In Figure 65, none of the samples from the petrological literature plot near the 'pyrope-spessartine I and II', and the 'spessartine-pyrope I and II' samples. This suggests that garnets of this particular composition are not represented in the petrological literature covered in this thesis.

5.9.2. Ugrandite

© University of Pretoria

5.9.2.1. Almandine-grossular

The 'almandine-grossular' sample from this study overlaps with the data from Georoc (2015) and the petrological literature (Figures 66, 67, 68 and 69). No 'grossular-almandine' samples were found in the gemological literature, so no comparison between the two is possible. As mentioned earlier, the large number of 'almandine-grossular' samples present in the petrological research shows that 'almandine-grossular' gem garnets can exist.

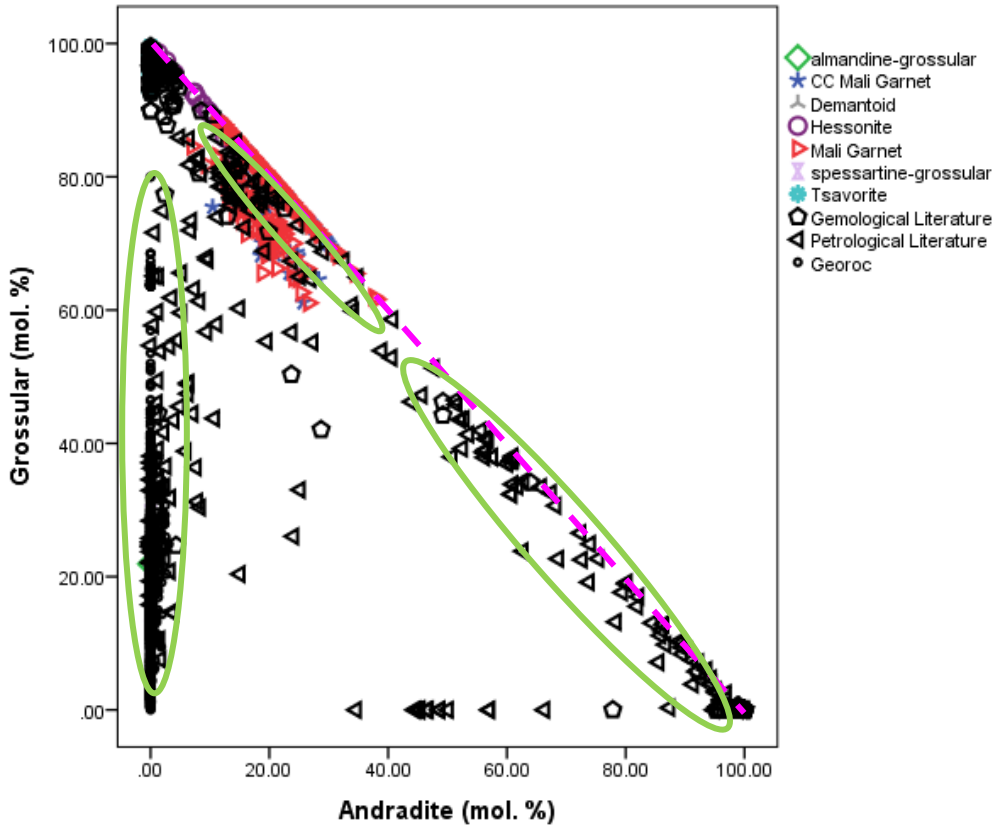

Figure 66. The grossular and andradite components of the samples from the ugrandite species in this study with the data from Georoc (2015), the petrological (Okay, 1993; Glodny *et al*., 2005; Hariya and Kimura, 1978; Zhang *et al*., 2001; Somarin, 2010; Wan *et al*., 2012; Habaak, 2004; Somarin, 2004; Lingang *et al*., 2010; Fuertes-Fuente *et al*., 2000; Xu and Lin, 2000; Proenza *et al*., 1999; Ghosh and Marishita, 2011; Bryhni and Griffin, 1971; Drahota *et al*., 2005; Zürcher *et al*., 2001; Lu *et al*., 2003; Shimazaki, 1977; Ford, 1915; Newberry, 1983; Pertoldová *et al*., 2009; Kassoli-Fournaraki, 1995; Chauvet *et al*., 1992; Schmädicke and Will, 2003; Operta *et al*., 2011; Zenk and Schulz, 2004) and the gemological literature (Payne; 1981; Bocchio *et al*., 2010; Adamo *et al*., 2011; Stockton and Manson, 1983; Pezzotta *et al*., 2011; Mathavan *et al*., 2000; Johnson *et al*., 1995; Feneyrol *et al*., 2013; Adamo *et al*., 2012; Muije *et al*., 1979; Switzer, 1974). The areas circled in green refer to the gaps between the grossular and andradite components that were previously observed in the data from this thesis. The dashed line represents the solid solution series between grossular and andradite. The 'demantoid' and 'tsavorite' samples plot beneath the data from the petrological literature at 100 mol. %, and andradite at 100 mol.% grossular respectively.

© University of Pretoria

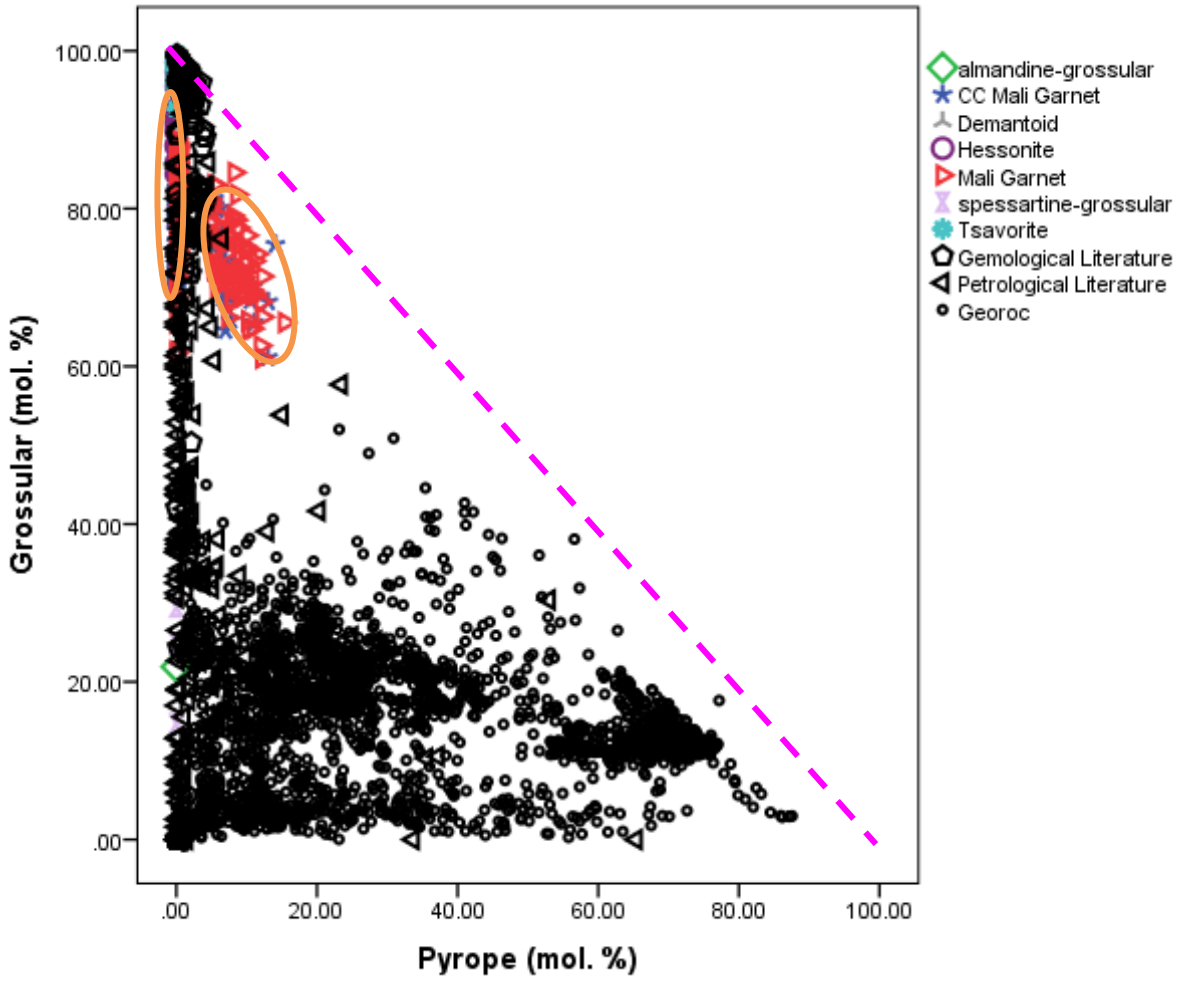

Figure 67. The grossular and pyrope components of the samples from the ugrandite species in this study with the data from Georoc (2015), the petrological and the gemological literature. The dashed line represents the trend observed between grossular and pyrope. The areas circled in orange refer to the two groups observed in the 'Mali and CC Mali garnets' from the thesis.

© University of Pretoria

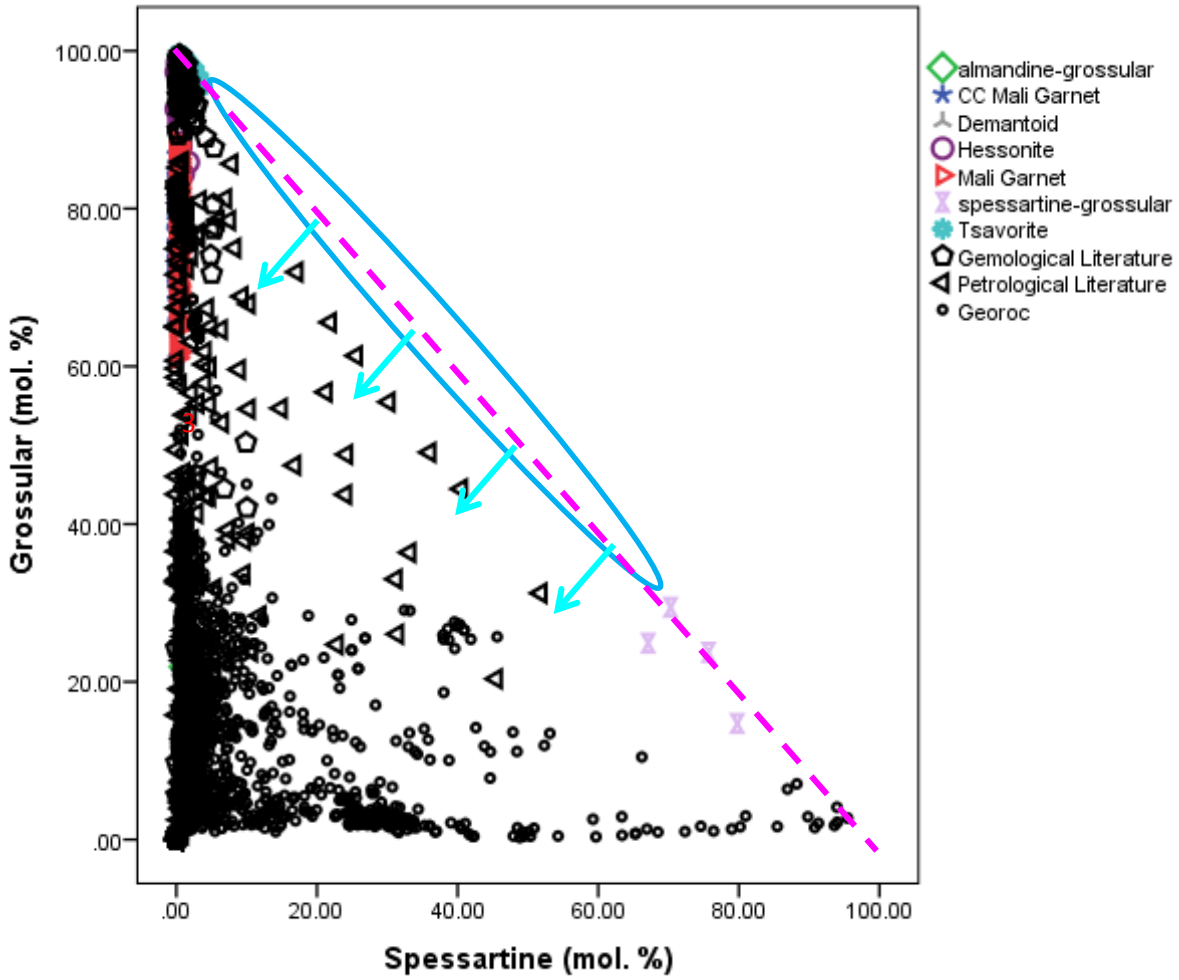

Figure 68. The grossular and spessartine components of the samples from the ugrandite species in this study with the data from Georoc (2015), the petrological and the gemological literature. The dashed line represents the trend observed between grossular and spessartine. The arrows represent deviation from the dashed line and indicate additional substitutions. The area circled in blue refers to the gap observed along the dashed line where no samples plot (the same gap as observed in Figure 55a).

© University of Pretoria

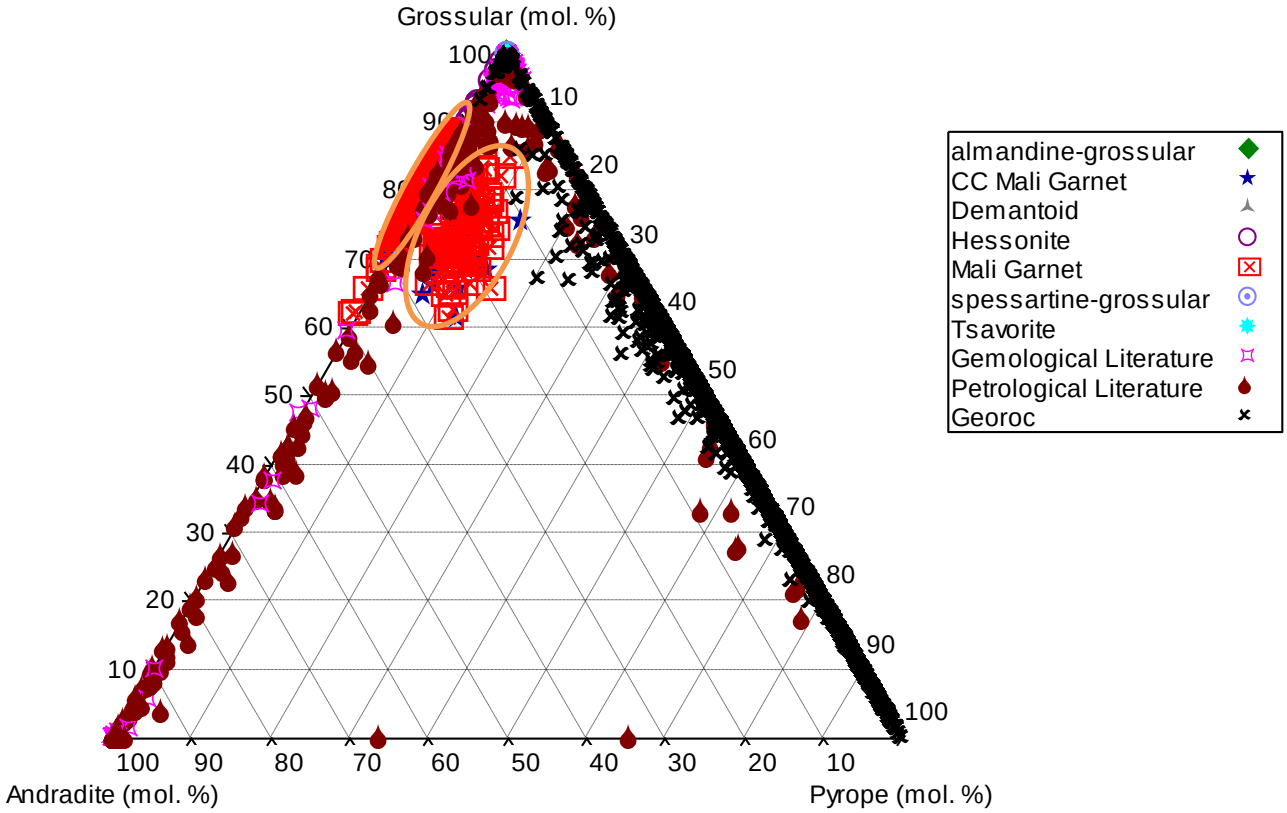

Figure 69. a) The grossular, andradite and pyrope components of the ugrandite species in this study with data from Georoc (2015), the petrological literature and the gemological literature. The areas circled in orange refer to the two groups within the 'Mali and CC Mali garnets'.

© University of Pretoria

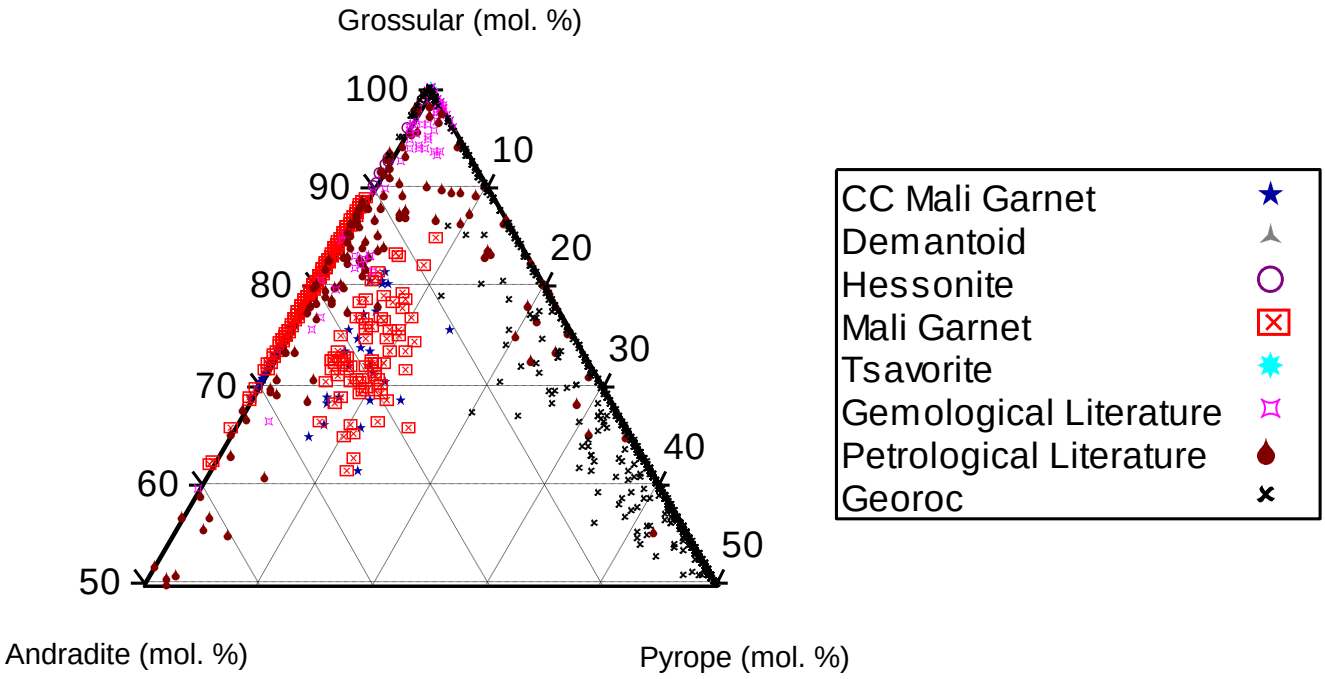

Figure 69. b) An expanded view of Figure 69a. The grossular, andradite and pyrope components of the ugrandite species in this study with data from Georoc (2015), the petrological literature and the gemological literature. The areas circled in orange refer to the two groups within the 'Mali and CC Mali garnets'.

5.9.2.2. CC Mali and Mali garnets

The gemological literature samples plot together with the 'CC Mali and Mali garnets' from this thesis, as well as with the petrological literature samples in Figure 66. The petrological literature samples also fill in the gap observed between the two groups of 'CC Mali and Mali garnets' (Figures 66, 67 and 69) suggesting that gem garnets with this particular composition are possible, but are not represented in the data from this thesis.

In Figure 67 and 69, none of the samples from the literature plot around the one group of 'CC Mali and Mali garnets' from the thesis, which suggests that garnets of this particular composition are not represented in the literature presented in this thesis.

5.9.2.3. Demantoid

The 'demantoid' samples from the thesis cluster together with samples from Georoc (2015) and the gemological and the petrological literature (Figures 66, 67, 68 and 69).

5.9.2.4. Hessonite

The 'hessonite' samples from this study plot together with the data from Georoc (2015) and the petrological and the gemological literature (Figures 66, 67, 68 and 69).

© University of Pretoria

5.9.2.5. Spessartine-grossular

The 'spessartine-grossular' samples from this thesis plot together with the data from Georoc (2015) and the petrological and the gemological literature in Figures 66, 67, 68 and 69).

However, in Figure 68, the 'spessartine-grossular' samples do not overlap with the samples from the literature. These 'spessartine-grossular' samples plot along the dashed line with only a few of the petrological literature samples coming close to the dashed line.

In addition, a gap is evident in Figure 68 (area circled in blue) where none of the samples from the thesis or the literature plot. This indicates that garnets of that particular composition have yet to be discovered or are not represented in the data from both this thesis and the literature.

5.9.2.6. Tsavorite

The 'tsavorite' samples from this research overlap with the samples from Georoc (2015) and the petrological and the gemological literature in Figures 66, 67, 68 and 69).

5.9.3. Garnets of similar composition

The origins of gem garnets can be difficult to determine. If gems are recovered from secondary sources (fluvial deposits), then the original host rock is destroyed. The variability in compositions observed in gem garnets can be attributed to the different geological environments in which they were formed.

Many of the samples from the literature (gemological, petrological and Georoc (2015)) fill in the gaps previously observed in the data from this thesis (the areas circled in green in Figures 62, 64, 66, 67 and 69) suggesting that gem garnets of that particular composition are possible.

However, gaps are still present in Figures 63, 65, 68 and 69 (where none of the samples from this thesis or the literature plot), suggesting that garnets of that particular composition have yet to be discovered or are not represented in the data from both this study or the literature presented.

In Figure 65, none of the petrological literature or Georoc (2015) samples plot in the grey field, with only gem garnets plotting in this region.

© University of Pretoria

There were cases where gem garnet samples from this thesis plotted alone with no (or very few) samples from the literature overlapping them (the areas circled in red in Figures 61, 62, 63, 64 and 65).

Table 14. Summary of the different garnet compositions reported in literature presented in this thesis.

Garnet composition	Similar petrological data reported by	Similar gemological data reported by
Almandine-pyrope, pyrope-almandine and/or rhodolite	Georoc (2015); Okay (1993); Glodny *et al*.(2005); Bryhni and Griffin (1971); Ford (1915); Chauvet *et al*. (1992); Operta *et al*. (2011); Carswell and Dawson (1970)	Schmetzer *et al*. (2001); Hoover (2011); Zwaan (1974); Hidden and Pratt (1898)
Pyrope-spessartine I and II and/or spessartine-pyrope I and II	Ford (1915); Newberry (1983); Chauvet *et al*. (1992)	Schmetzer *et al*. (2002); Hoover (2011); Krzemnicki *et al*. (2001)
Almandine-spessartine and/or spessartine-almandine	Georoc (2015); Ford (1915); Newberry (1983); Chauvet *et al*. (1992)	Hoover (2011)
Mali and/or CC Mali garnets	Hariya and Kimura (1978); Zhang *et al*. (2001); Somarin (2010); Wan *et al*. (2012); Somarin (2004); Lingang *et al*. (2010); Fuertes-Fuente *et al*. (2000); Zürcher *et al*. (2001); Lu *et al*. (2003); Ford (1915); Newberry (1983); Pertoldová *et al*. (2009)	Johnson, *et al*. (1995)
Uvarovite-grossular and/or grossular-uvarovite	Ghosh and Marishita (2011)	N/A
Spessartine	Georoc (2015); Ford (1915)	Wang and Liu (1993); Howie (1965); Laurs and Knox (2001); Schmetzer *et al*. (2002); Schmetzer *et al*. (2001); Hoover (2011); Krzemnicki *et al*. (2001)
Pyrope	Georoc (2015); Carswell and Dawson (1970)	Guastoni *et al*. (2001); Schlüter and Weitschat (1991); Hoover (2011)
Almandine	Georoc (2015); Ford (1915); Chauvet *et al*. (1992)	Hoover (2011)
Andradite	Wan *et al*. (2012); Habaak (2004); Xu and Lin (2000); Ghosh and Marishita (2011); Drahota *et al*. (2005); Ford (1915)	Payne (1981); Bocchio *et al*. (2010); Adamo *et al*. (2011); Stockton and Manson (1983); Pezzotta *et al*. (2011)
Grossular (tsavorite and/or hessonite)	Zhang *et al*. (2001); Somarin (2010); Somarin (2004); Fuertes-Fuente *et al*. (2000); Lu *et al*. (2003); Shimazaki (1977); Ford (1915)	Mathavan *et al*. (2000); Feneyrol *et al*. (2013); Adamo *et al*. (2012); Muije *et al*. (1979); Switzer (1974)

5.9.4. New solid solution series in gem garnets

© University of Pretoria

These solid solution series include pyrope-andradite, grossular-spessartine and grossular-almandine and are not found in gemology. However, these solid solution series are represented in the data from this thesis.

These compositions are uncommon and fall midway between the pyralspite and ugrandite species. Only a few examples of these solid solution series are presented in the gemological literature, which are discussed below.

- Pyrope-andradite solid solution series

A solid solution can exist between pyrope and andradite because the 'pyrope' samples contain pyrope and andradite. The pyrope samples have the highest andradite component in the pyralspite species. The table below summarises their properties.

Table 15. Summary of properties of the 33 'pyrope' samples from the thesis.

Sold as	Type of colour change	Country	Colour	R.I.	Magnetic susceptibility (SI)	Pyrope (mol.%)	Almandine (mol.%)	Grossular (mol.%)	Spessartine (mol.%)	Uvarovite (mol.%)	Andradite (mol.%)
Malaya garnet, CC garnet, spessartine	None	Madagascar, Brazil, Africa, Mozambique, Namibia	Pink, light pink, purple red, dark red, dark orange red, orange	1.74 - 1.80	0.0004-0.0040	80.19-94.51	0.00-17.00	0.00	0.00-19.48	0.00-0.51	0.00-12.70

Two andradite-pyrope samples were reported by Zenk and Schulz (2004) in metabasites from the Barrovian metamorphic zones in Scotland. The compositions of the samples were $An_{66.31}Py_{33.69}$ and $Py_{65.39}An_{34.61}$.

- Grossular-spessartine solid solution series

Four 'spessartine-grossular' samples are represented in the data. The ranges of the various properties of the samples are listed below:

Table 16. Summary of properties of the 'spessartine-grossular' samples from the thesis.

Sample	Sold as	Type of colour change	Country	Colour	Colour under torchlight	R.I.	Magnetic susceptibility (SI)	Almandine (mol. %)	Grossular (mol. %)	Spessartine (mol. %)	Uvarovite (mol. %)	V_2O_3 (wt. %)
645923-4	Malaya garnet	None	Bekily, Madagascar	light yellow brown	no change	1.761	0.0013	0.00	23.74	75.68	0.58	0.22
751656	Colour change garnet	Change	Africa	yellow brown	yellow green	1.770	0.0019	8.01	24.91	67.09	0.00	0.45
860203-3	Colour change garnet	Shift	Unknown	gold yellow	golden yellow	1.769	0.0021	0.00	29.45	70.26	0.29	0.30
860203-6	Colour change garnet	Shift	Unknown	gold yellow	golden yellow	1.768	0.0018	5.27	14.71	79.77	0.26	0.56

© University of Pretoria

In the gemological literature, Howie (1965) reports on spessartine gems with a significant grossular component from Meldon, Okehampton and Devonshire, England. A 'spessartine-grossular' is also reported by Lee *et al*. (1963) from the Victory mine in Nevada, America. The molecular composition of the gems discussed by Howie (1965) is $Sp_{40.0}Gr_{34.5}Py_{8.7}An_{8.6}Al_{8.2}$ and the sample from Lee *et al*. (1963) is $Sp_{42.8}Gr_{41.4}Al_{12.4}An_{3.4}$. Howie (1965) proposes that these 'spessartine-grossular' gems occur in metasomatic calc-silicate assemblages and garnet-quartz rocks. The properties of the gems reported by Howie (1965) and Lee *et al*. (1963) are summarised in the table below.

Table 17. Summary of properties of the gemstones reported by Howie (1965) and Lee *et al*. (1963). Two of the stones are spessartine-pyrope with significant amounts of grossular and two are spessartine-grossular.

Reference	Colour	Country	Almandine (mol.%)	Andradite (mol.%)	Grossular (mol.%)	Pyrope (mol.%)	Spessartine (mol.%)	Uvarovite (mol.%)
Howie (1965)	golden yellow	England	0.00	4.98	5.84	10.32	78.87	0.00
Howie (1965)	brownish red	England	0.70	6.83	40.54	10.98	40.95	0.00
Howie (1965)	yellow brown	England	2.14	5.29	7.87	13.53	71.17	0.00
Lee *et al*. (1963)	peach tan	America	6.72	5.12	42.56	0.00	45.60	0.00

In the petrological literature, 'spessartine-grossular' samples were reported by Shimazaki (1977) and Newberry (1983) in Japan and the Cordillera, America respectively. These 'spessartine-grossular' samples come from scheelite skarns.

Table 18. Summary of 'spessartine-grossular' samples from petrological literature.

Reference	Name	Country	Geology	Almandine (mol.%)	Andradite (mol.%)	Grossular (mol.%)	Pyrope (mol.%)	Spessartine (mol.%)	Uvarovite (mol.%)
Shimazaki (1977)	Spessartine-grossular	Japan	Scheelite skarn	3.86-22.78	6.33-11.69	31.25-78.53	0.00	5.92-51.82	0.00
Newberry (1983)	Spessartine-grossular	Cordillera, America	Scheelite skarn	10.96-19.88	9.40-24.03	20.38-56.73	1.24-1.90	21.25-45.47	0.00-0.52

- Grossular-almandine solid solution series

One 'almandine-grossular' sample is represented in the thesis. This sample comes from Tanzania and appears dark pink in colour. It displays a shift in colour and is dark pinkish red under torchlight. The R.I. is 1.752 and magnetic susceptibility is 0.0009 SI. The molecular composition is $Al_{76.57}Gr_{21.90}Sp_{1.17}Uv_{0.35}$.

Although no 'grossular-almandine' samples are reported in the gemological literature, a few samples are reported in the petrological literature by Okay (1993), Glodney *et al*. (2005), Bryhni and Griffin (1971), Drahota *et al*. (2005), Zürcher *et al*. (2001), Shimazaki (1977), Pertoldová *et al*. (2009), Kassoli-Fournaraki (1995), Chauvet *et al*. (1992),

© University of Pretoria

Schmädicke and Will (2003) and Operta *et al*. (2011). Their compositions and countries of origin are listed below:

Table 19. Summary of the properties of the 'almandine-grossular' and 'grossular-almandine' samples reported in petrological literature.

Reference	Name	Country	Geology	Almandine (mol.%)	Andradite (mol.%)	Grossular (mol.%)	Pyrope (%)	Spessartine (mol.%)	Uvarovite (mol.%)
Okay (1993)	Grossular-almandine	China	Unknown	28.32-53.91	1.27-2.22	33.45-53.86	8.94-20.26	0.96-1.46	0.00-0.09
Glodny *et al*. (2005)	Grossular-almandine	Eastern Alps	Unknown	51.41-63.21	0.22-1.63	21.95-33.63	3.73-11.84	2.55-9.55	0.06-0.22
Bryhni and Griffin (1971)	Grossular-almandine	Norway	Eclogite garnets	48.42-55.89	0.00	24.44-25.76	17.28-24.93	0.89-3.97	0.00
Drahota *et al*. (2005)	Grossular-almandine	Bohemia	Skarn	30.18-65.67	0.00-19.55	28.38-61.85	0.00-6.09	2.95-11.83	0.00-0.64
Zürcher *et al*. (2001)	Grossular-almandine	Mexio	Skarn	33.51	0.66	61.12	0.72	0.00	0.00
Shimazaki (1977)	Grossular-almandine	Japan	Scheelite skarn	12.31-29.48	6.27-9.47	47.45-67.92	0.00	10.31-16.80	0.00
Pertoldová *et al.* (2009)	Grossular-almandine	Bohemia	Skarn	12.45-68.78	0.74-27.27	23.42-73.97	0.20-5.90	0.31-22.84	0.00-0.07
Kassoli-Fournaraki (1995)	Grossular-almandine	Greece	Gneiss, amphibolite, migmatites	58.97-62.73	0.00-2.36	32.73-37.10	2.12-3.86	0.00-1.06	0.00-0.74
Chauvet *et al*. (1992)	Grossular-almandine	Norway	Unknown	63.64-71.03	0.00-0.15	17.15-22.08	5.12-8.40	1.64-4.51	0.00
Schmädicke and Will (2003)	Grossular-almandine	Greece	Blueschist facies	55.19-65.18	1.03-1.43	21.25-34.69	5.11-9.81	1.75-5.47	0.00-0.09
Operta *et al*. (2011)	Grossular-almandine	Bosnia and Herzegovina	Unknown	63.18	0.96	18.33	14.05	3.16	0.32

5.10. Classification Schemes

5.10.1. Traditional gem classification schemes in gemology

The traditional classification scheme for gem garnets designed by Webster (1962) is outdated because it only considers the six end-members (grossular, spessartine, almandine, uvarovite, pyrope and andradite) and the solid solutions between pyrope and almandine, spessartine and almandine, and grossular and andradite. Anderson (1976) goes a step further and provides the RI, SG and traditional colours for the six end-member garnets (Table 3). Stockton and Manson (1985) use a chemical analysis to classify gem garnets and

© University of Pretoria

incorporate many of the recent gem findings, e.g. Malaya, colour change 'pyrope-spessartine' and 'rhodolite'. These garnet types represent intermediate compositions that are not represented in the classification schemes of Webster (1962) and Anderson (1976). Stockton and Manson (1985) also provide the RI and colours for the different gem garnets. However, Stockton and Manson's (1985) classification scheme does not include 'Mali garnets'. The RI values reported by Stockton and Manson (1985) are too narrow because a large number of the samples from this thesis, especially in the pyralspite species, have larger RI ranges.

The classification scheme based on magnetic susceptibility that was designed by Hoover and Williams (2007), Hoover *et al*. (2008), and Gemstone Magnetism (2014) is found to be unreliable for the pyralspite species. The majority of the samples have magnetic susceptibilities outside of the ranges stated by Gemstone Magnetism (2014). The ranges for 'spessartine-grossular' and 'almandine-grossular' are not available because they are not part of this gem garnet classification scheme. Magnetic susceptibility is not a singular function of Fe^{2+} and Mn^{2+}, as stated by Hoover and Williams (2007), Hoover *et al*. (2008) and Gemstone Magnetism (2014). Some of the 'spessartine' samples have very low magnetic susceptibilities, but also the highest spessartine component. However, most of the garnets from the ugrandite species have magnetic susceptibilities that correlate well with those from Gemstone Magnetism (2014).

None of the three classification schemes include properties for the spessartine-grossular and grossular-almandine solid solution series.

5.10.2. Modification of past gem classification schemes

Classification should be based primarily on chemistry with the use of RI, magnetic susceptibility and colour being secondary characteristics. A diverse range of colours was observed in this thesis and these are presented in Table 20.

Stones that display colour change in the pyrope-spessartine solid solution series and the Mali garnets are treated separately from those that do not. Stones from the pyrope-spessartine solid solution series that display a distinct colour change have a 'II' placed at the end of their name, and those that do not have a 'I' placed at the end of their name. The term 'CC' stands for colour change and is only used for Mali garnets that display a distinct change in colour. 'CC' is placed in front of the name, i.e. CC Mali garnet.

© University of Pretoria

Table 20. The colour of the gem garnets from this thesis compared to those from Stockton and Manson (1985). The words in italics represent colours that were not commonly observed in the samples from this thesis.

Name	Description	Description according to Stockton and Manson (1985)
Almandine	Dark purple – very dark red	Orange red through purplish red
Almandine-grossular	Dark pink	
Almandine-pyrope	*Red pink,* dark pink red, very dark red, dark red, very dark pink purple, *pink purple*, very dark pink, dark pink, *purple red*	reddish orange through red-purple
Almandine-spessartine	Very dark red	Reddish orange through orange-red
Pyrope	Pink, purple red, dark red, *dark orange* red with a little purple, *orange, light pink purple*	Purplish red through reddish orange, colourless
Pyrope-almandine	Pink orange, pink, pink purple, *very dark red*, red, dark red, *orange red,* dark pink purple, dark pink, dark pink orange, *dark red orange,*	reddish orange through red-purple
Pyrope-spessartine I	Orange pink, pink, pink orange, dark pink purple, light pink, *pink purple*, very dark purple, dark purple, light pink purple, light purple pink, light orange pink, orange brown, dark orange, light brown, brown, *dark red*, *pink brown,* light orange yellow, dark brown pink, light orange brown,	Greenish yellow through purple
Pyrope-spessartine II	Pink orange, light orange pink, light pink, pink orange, orange pink, light pink orange, light purple, dark purple, *dark purple grey*, light orange, orange, *dark pink purple, dark purple pink, pink purple, dark pink red, pink brown,* orange brown, brown yellow, grey brown, *silver grey*.	Greenish yellow through purple
Rhodolite	Purple red	reddish orange through red-purple
Spessartine	Very dark red, dark red, very dark red (almost black), dark orange, orange red, dark orange red, red orange, red, *light orange*, orange, dark orange, orange brown, *pink*, yellow orange, *light orange yellow, brown yellow, brown grey, gold yellow, dark yellow brown, light brown*	Yellowish orange through reddish orange
Spessartine-almandine	Light pink, orange red, light pink orange, orange pink, pink, dark orange pink, light orange	Reddish orange through orange-red
Spessartine-grossular	Light yellow brown, yellow brown, gold yellow	
Spessartine-pyrope I	Orange pink, pink orange, light orange, *dark red, light pink,* light orange yellow, orange yellow, *yellow brown*, orange, *dark orange*, orange brown, light orange brown, *pink brown, light brown, grey yellow*, *light yellow brown, yellow brown, yellow grey, gold yellow*	Greenish yellow through purple
Spessartine-pyrope II	Light orange pink, orange pink, dark orange pink, light orange, *dark pink orange, pink orange, light pink*, very light orange, *light purple pink, purple pink, pink brown, grey purple*, yellow brown, light yellow brown, brown, brown orange, light orange brown, gold yellow, gold brown	Greenish yellow through purple
CC Mali garnet	Yellow green, green, light green, light yellow, yellow, dark yellow, yellow brown, light brown, brown, *orange yellow, orange brown,*	N/A
Mali garnet	Yellow green, dark yellow green, light yellow green, dark green, green, light green, dark yellow, yellow, light yellow, very light yellow, yellow brown, dark yellow brown, light brown, brown, *dark brown, dark orange, orange brown, dark*	N/A

© University of Pretoria

	brown yellow	
Demantoid	Dark green, green, dark yellow green, *green yellow, dark brown, gold*	Very slightly yellowish green through orangy yellow
Hessonite	Orange brown, *dark orange brown,* orange, light orange, dark orange, *light yellow, dark red, yellow*	Green through reddish-orange, colourless
Tsavorite	Green, intense green, light green, dark green*, very light green*	Green through reddish-orange, colourless

Table 21 summarises a modified classification scheme using RI values and colour, as developed by Stockton and Manson (1985), and magnetic susceptibility values derived from Gemstone Magnetism (2014) combined with the data from this thesis. The original RI and magnetic susceptibility ranges from Stockton and Manson (1985) and Gemstone Magnetism (2014) can be seen in Table 22, along with the molar proportion ranges of end-members for the data from this thesis.

© University of Pretoria

Table 21. A modified classification scheme using RI values and colour from Stockton and Manson (1985) and magnetic susceptibility values from Gemstone Magnetism (2014) combined with data from this thesis. The original RI and magnetic susceptibility values from Stockton and Manson (1985) and Gemstone Magnetism (2014) respectively can be found in Table 22.

Name	Composition	RI (Stockton and Manson (1985)	Magnetic susceptibility (SI) (Gemstone Magnetism, 2014)	Colour
Almandine	> 80.00 almandine	1.772-1.830	0.0010-0.003094	Orange red through purplish red
Almandine-grossular	> 50.00 almandine followed by grossular	1.752	0.0009	Dark pink
Almandine-pyrope	> 50.00 almandine followed by pyrope	1.742-1.785	0.0010-0.0020	Reddish orange through red-purple including pink red, pink, pink purple
Almandine-spessartine	> 50.00 almandine followed by spessartine	1.772-1.820	0.0018-0.0020	Reddish orange through orange-red including red
Pyrope	> 80.00 pyrope	1.714-1.780	0.0000-0.0040	Purplish red through reddish orange, colourless including pink, dark orange red with a purplish tinge, orange
Pyrope-almandine (includes rhodolite)	> 50.00 pyrope followed by almandine	1.712-1.785	0.0000-0.0020	Reddish orange through red-purple including pink orange, pink, pink purple
Pyrope-spessartine I	> 50.00 pyrope followed by spessartine (does not display colour change)	1.635-1.780	0.0000-0.0040	Greenish yellow through purple including orange pink, pink, pink purple, pink brown
Pyrope-spessartine II	> 50.00 pyrope followed by spessartine (displays distinct colour change)	1.720-1.784	0.0000-0.0040	Greenish yellow through purple including pink orange, pink, purple grey, pink purple, pink red, pink brown, grey brown, silver grey
Spessartine	> 80.00 spessartine	1.755-1.810	0.0010-0.0047	Yellowish orange through reddish orange including pink, brown yellow, brown grey
Spessartine-almandine	> 50.00 spessartine followed by almandine	1.755-1.820	0.0020-0.0040	Reddish orange through orange red including pink, pink orange
Spessartine-grossular	> 50.00 spessartine followed by grossular	1.761-1.770	0.0010-0.0020	Yellow brown, gold yellow
Spessartine-pyrope I	> 50.00 spessartine followed by pyrope (does not display colour	1.742-1.780	0.0000-0.0050	Greenish yellow through purple including orange

© University of Pretoria

	change)			pink, pink, pink brown, grey yellow
Spessartine-pyrope II	> 50.00 spessartine followed by pyrope (displays distinct colour change)	1.742-1.780	0.0010-0.0060	Greenish yellow through purple including orange pink, pink, purple pink, pink brown, grey purple
CC Mali garnet	> 50.00 grossular followed by andradite (the grossular component can exceed 80.00 but the andradite component must be the second highest) displays distinct colour change	1.760-1.777	0.003-0.008	Yellow green, green, yellow, yellow brown, brown, orange yellow, orange brown
Mali garnet	> 50.00 grossular followed by andradite (the grossular component can exceed 80.00 but the andradite component must be the second highest) does not display colour change	1.750-1.779	0.0001-0.0014	Yellow green, green, yellow, yellow brown, brown, orange, orange brown, brown yellow
Demantoid	> 80.00 andradite	1.772-1.895	0.0011-0.0028	Very slightly yellowish green through orangy yellow
Hessonite	> 80.00 grossular and appears yellow orange to red (colour is important to distinguish from tsavorite)	1.730-1.773	0.0001-0.0003	Yellow through red
Tsavorite	> 80.00 grossular and appears green (colour is important to distinguish from hessonite)	1.730-1.760	0.0000-0.0003	Green through yellow green

© University of Pretoria

Table 22. Summary of the properties of the different gem garnets with a RI from Stockton and Manson (1985) and magnetic susceptibility from Gemstone Magnetism (2014). The figures in bold represent values that fall outside the traditional ranges observed in Stockton and Manson (1985) and Gemstone Magnetism (2014).

Name	RI	RI (Stockton and Manson, 1985)	Magnetic susceptibility (SI)	Magnetic susceptibility (SI) (Gemstone Magnetism, 2014)	Almandine (mol.%)	Andradite (mol.%)	Grossular (mol.%)	Pyrope (mol.%)	Spessartine (mol.%)	Uvarovite (mol.%)
Almandine	**1.772-1.779**	1.785-1.830	**0.0010**-0.0030	0.001926-0.003094	80.00-80.75	1.77-2.00	0.00-0.00	11.87-15.66	2.38-4.38	0.00-0.19
Almandine-grossular	1.752	N/A	0.0009	N/A	76.57	0.00	21.90	0.00	1.17	0.35
Almandine-pyrope	1.757-1.780	1.742-1.785	0.0010-0.0020	N/A	44.81-79.73	0.00-5.40	0.00-14.22	12.27-47.58	0.27-11.29	0.00-0.42
Almandine-spessartine	**1.772**	1.810-1.820	0.0018-0.0020	N/A	65.56-71.60	1.55-3.24	0.00-1.95	5.15-9.06	19.62-21.98	0.12-0.17
Pyrope	1.740-**1.780**	1.714-1.742	**0.0000-0.0040**	0.001163-0.001971	0.00-17.00	0.00-12.74	0.00	80.18-94.51	0.00-19.48	0.00-0.51
Pyrope-almandine	1.712-1.775	1.742-1.785	0.0000-0.0020	N/A	10.81-44.82	0.30-10.19	0.00-13.70	38.94-79.84	0.09-15.76	0.05-0.78
Pyrope-spessartine I	**1.635-**1.780	1.742-1.780	**0.0000-0.0040**	0.001127-0.003089	0.00-24.62	0.00-8.28	0.00-6.65	36.81-77.13	11.39-58.61	0.00-1.59
Pyrope-spessartine II	1.720-**1.784**	1.742-1.780	**0.0000-0.0040**	0.001127-0.003089	0.00-22.78	1.07-6.67	0.00-7.07	44.79-74.22	10.55-47.83	0.12-1.00
Rhodolite	1.750-1.780	1.742-1.785	**0.0000-0.0020**	0.001007-0.001890	14.74-48.69	0.00-9.87	0.00-9.15	45.49-78.50	0.15-20.46	0.00-1.48
Spessartine	1.755-1.800	1.780-1.810	**0.0010**-0.0370	0.004301-0.004728	0.00-1.80	0.00-13.92	0.00-8.38	0.00-16.82	80.06-100.00	0.00-0.68
Spessartine-almandine	**1.755-1.774**	1.810-1.820	0.0020-0.0040	N/A	13.93-44.07	0.00-3.65	2.66-11.37	0.00-23.32	42.01-79.85	0.00-1.17
Spessartine-grossular	1.761-1.770	N/A	0.0010-0.0020	N/A	0.00-8.01	0.00	14.71-29.45	0.00	67.09-79.77	0.00-0.58
Spessartine-pyrope I	1.743-1.780	1.742-1.780	**0.0000-0.0050**	0.001127-0.003089	18.14-15.46	0.00-8.52	0.00-18.14	15.76-46.01	42.78-79.76	0.00-1.00
Spessartine-pyrope II	1.752-1.777	1.742-1.780	**0.0010-0.0060**	0.001127-0.003089	0.000-10.21	0.00-7.01	0.00-18.48	14.93-46.51	46.99-79.94	0.00-1.55
CC Mali garnet	1.760-1.777	N/A	0.0003-0.0008	0.000234-0.001099	0.00	10.47-31.35	61.14-87.00	0.00-14.07	0.00-0.35	0.00-0.23
Mali garnet	1.750-1.779	N/A	0.0001-0.0014	0.000234-0.001099	0.00	7.02-38.07	61.07-88.79	0.00-15.41	0.00-0.46	0.00-0.14
Demantoid	**1.772-1.790**	1.880-1.895	**0.0011**-0.0026	0.002253-0.002752	0.00	99.88-100.00	0.00	0.00	0.00	0.00-0.12
Hessonite	1.743-**1.773**	1.730-1.760	0.0001-0.0021	0.000091-0.000345	0.00	1.27-14.64	84.39-98.56	0.00	0.00-1.67	0.00
Tsavorite	1.738-1.745	1.730-1.760	**0.0000**-0.0002	0.00002-0.000309	0.00	0.00	92.69-99.63	0.00	0.37-3.59	0.00-5.71

© University of Pretoria

5.11. Concluding Remarks on Chemistry

The chemistry of the gem garnets investigated in this thesis proved to be more diverse than anticipated. Although the ugrandite species has limited chemical variability, the pyralspite species shows such great variation that the classification of gems is difficult without a chemical analysis. Determining the dominant end-member in a stone is difficult without chemical analysis, and it might be more appropriate to label a stone according to the solid solution series to which it belongs.

5.12. Seperation of the Pyralspite and Ugrandite Species

Petrological and gemological examples of the grossular-spessartine and grossular-almandine solid solution series do exist. The scarcity of gem quality deposits could explain its absence in the gem market. These ‘spessartine-grossular’ and ‘almandine-grossular’ samples indicate that the separation of gem garnets into the ugrandite and pyralspite species is too rigid and not justified because there is an overlap between the two species. This suggests the existence of a continuum between the two species.

5.13. Terms

The terms ‘Malaya’, ‘Malaia’ and ‘rhodolite’ are not defendable because these stones do not show distinctive chemistries to warrant a specific name. ‘Malaya’ and/or ‘Malaia’ should be labelled as part of the pyrope-spessartine solid solution series and ‘rhodolite’ as part of the pyrope-almandine solid solution series. The ‘rhodolite’ samples in this thesis display the distinct purple red colour for this type of garnet, but based on chemistry, it cannot be differentiated from the other ‘pyrope-almandine’ samples. The term ‘rhodolite’ is only applied to a stone with the specific purple red colour of the pyrope almandine solid solution series.

The terms ‘tsavorite’, ‘hessonite’, ‘demantoid’ and ‘Mali garnet’ should be kept because these stones have distinctive chemistries that warrant their own names. Each has its own set of physical characteristics that does not overlap with one another.

The term colour change should only be applied to stones that display a distinct change in colour. The term colour shift should be applied to stones that only display a shift in colour under different illuminations. Moreover, the term colour change should be included in the name of the stone e.g. a colour change sample of the pyrope-spessartine solid solution series. This also applies to ‘Mali garnets’ that display colour change.

© University of Pretoria

Colour change is not limited to the pyrope-spessartine solid solution series, but can also occur in the spessartine-almandine and spessartine-grossular solid solution series. The assumption that all colour change samples belong to the pyrope-spessartine solid solution series is incorrect, and this must be remembered when attempting to classify a colour change stone.

5.14. Effect on the Price of Gem Garnets

For the ugrandite species (Figure 9a), the majority of the stones were classified correctly by the seller.

However, many of the garnets from the pyralspite species (Figure 5a and 5b) were incorrectly classified by sellers. Only stones from the pyrope-spessartine solid solution series and the 'spessartine' samples have a majority that is correctly classified by the seller based on RI and colour.

If many garnets are incorrectly classified, this does not bode well for the gemstone business, especially the selling/purchasing of garnets. It is possible to be duped intentionally or unintentionally by the seller when purchasing a stone, depending on the buyers' knowledge of gemstones. Sellers could sell a stone that has been identified incorrectly. This can be avoided by means of a chemical analysis. However, because this method is probably unavailable to the common seller and buyer, it is difficult to actually prove that a garnet, e.g. rhodolite, is what it is claimed to be. This can also be disadvantageous to the seller as the stone he/she sells could be worth more, but due to incorrect classification, it is given a selling price to suit its falsely assumed type. Hence, the buyer actually benefits in this case. Although the opposite can also be true, where a seller has incorrectly classified a garnet to be of more value than what it actually is. In this case, the buyer loses out and purchases something that is not actually worth the price attached to it.

A stone, for example, that is a medium dark red 'Malaya' garnet of 1 ct. will sell for $129.96. However, a 'rhodolite' of the same colour and size will sell for $109.78. Both stones have similar physical characteristics and can easily be mistaken for each other (Gemval, 2015).

The price of gemstones are in constant flux and price differences are larger for bigger stones (e.g. 3 or 5 ct.).

© University of Pretoria

6. Conclusions

Molar proportions of end-member components are used to describe the chemical composition of garnets with 32 end-member species that are recognised, of which only pyrope, almandine, spessartine, andradite, grossular and uvarovite are relevant to gemology (Stockton and Manson 1985; Anderson 1976, Locock, 2008, Grew *et al*. 2013, Rickwood 1968; Webster, 1962).

Gem garnet compositions between these six end-members are more common than pure end-members, resulting in variable compositions and difficulties in gem garnet classification (Stockton and Manson, 1985; Anderson, 1976; Webster, 1962). Care should be taken in deciding which method to use for the recasting of garnet analyses because different methods can produce different results (Locock, 2008; Rickwood, 1968).

Physical characteristics such as colour, refractive index (R.I.) and specific gravity (S.G.) are used to classify gem garnets, but these characteristics often overlap with each other (Stockton and Manson, 1985; Serov *et al*., 2011). Gem garnet classification is made more difficult by the use of trade names that are sometimes not based on any scientific criteria (Stockton and Manson, 1985; Anderson, 1976; Webster, 1962). Traditional gem garnet classification schemes as developed by Webster (1962), Anderson (1976) and Stockton and Manson (1985) are available, but these schemes are inadequate when considering the new gem garnets introduced into the gem market (Seifert and Hyrsl, 1999; Dirlam *et al*., 1992; Crowningshield, 1970; Shigley *et al*., 2000; Schmetzer *et al*., 2001).

By using a non-destructive chemical analysis of 1513 gem garnets, combined with the colour, R.I. and Hoover and Williams' (2007) recently developed method of classification by magnet susceptibility, an evaluation of the reliability of past gem classification schemes is possible.

The Thermo Scientific Niton FXL 959 FM-XRF analyser was used to chemically analyse the gem garnets, and an Excel spreadsheet that follows similar calculation procedures to Rickwood (1968) was used in this thesis. The gem garnets were divided into two species based on their compositions: ugrandite (uvarovite, grossular and andradite) and pyralspite (pyrope, spessartine and almandine) allowing for better and easier management of the data. The allocation of the different gem garnets into the two species is shown in Table 8. The 'almandine-grossular' and 'spessatine-grossular' samples have compositions that overlap between the ugrandite and pyralspite species and are placed in both species in Table 8.

© University of Pretoria

The chemistry of the gem garnets investigated in this thesis is more diverse than expected. The pyralspite species is the most diverse, showing a large range in end-member proportions. Samples in the pyralspite species that approach a pure end-member, e.g. ‘spessartine’, could be identified with relative ease. However, there are a few exceptions such as ‘pyrope’ samples being confused for ‘spessartine’. Additional substitutions in the pyralspite species, specifically the pyrope dominant samples, occur in almost any combination, producing extensive solid solutions between end-members. The garnets from the pyralspite species also display a diverse range of colours, RI and magnetic susceptibilities, with overlaps occurring between them. Some systematic relationships in colour could be observed for the pyralspite species in relation to specific end-member components.

- Orange indicates the presence of spessartine with darker orange corresponding to a higher spessartine component.
- Almandine is responsible for the darkening of a stone with light samples containing very low to no almandine.
- Pink samples are pyrope dominant.
- The purple pink and pink purple samples are composed primarily of pyrope and almandine with variable amounts of spessartine. The spessartine component increases in the purple dominant samples.
- The brown and yellow varieties are composed of predominantly spessartine with lesser amounts of pyrope.

However, there are many exceptions to the above rules, making colour an unreliable means of classification in the pyralspite species. This is most commonly true for stones that are ‘spessartine-almandine’ or ‘almandine-spessartine’. These samples could easily be mistaken for samples from the pyrope-spessartine solid solution series, with both displaying similar colours, colour change phenomena, RI and magnetic susceptibilities. The same is also true, but to a lesser extent, for samples from the pyrope-almandine and pyrope-spessartine solid solution series. No distinction based on RI and magnetic susceptibility can be made in the pyralspite species, meaning that distinctions made in the past are arbitrary.

In the ugrandite species, the use of physical characteristics as a means of classification is appropriate because these characteristics are distinctive and supported by mineral chemistry. However, this excludes the use of colour in the ugrandite species because no relationship between colour and chemistry is observed. e.g. the colour green occurs in ‘demantoid’, ‘tsavorite’, ‘Mali garnet’ and ‘CC Mali garnet’ samples. The ‘Mali and CC Mali’ garnets could not be distinguished from each other based on their chemistry with

© University of Pretoria

the only difference being the presence of colour change in the latter. The distinctive chemistries for the different types of gem garnets in the ugrandite species results in distinctive RI and magnetic susceptibility ranges for each type of garnet. These RI and magnetic susceptibility ranges for the ugrandite species correlate with those from the classification schemes developed by Stockton and Manson (1985) (excluding 'Mali and CC Mali' garnets), Hoover and Williams (2007), Hoover *et al*. (2008), Hoover (2011), and Gemstone Magnetism (2014).

In the colour change samples from the pyralspite species, all the samples contained some V_2O_3, with Cr_2O_3 either being absent or present in smaller amounts. This indicates that vanadium is more influential in the colour change phenomenon than chromium. It is interesting to note that in the spessartine-almandine solid solution series, colour change is only present in the 'spessartine-almandine' samples and not in the 'almandine-spessartine' samples, suggesting that colour change is more prevalent in the former. Colour change is also more dominant in the spessartine dominant samples from the pyralspite species and is present in some 'spessartine-grossular' samples.

When the gem garnets are compared to the data from the literature, similar compositions to those from this thesis are observed in the petrological and gemological literature. However, there are some unique samples from this study that are not covered in the literature presented in this thesis. The 'pyrope' samples in this research contain high a andradite content, suggesting that a extensive solid solution between pyrope and andradite can exist. Four 'spessartine-grossular' samples were also found in this thesis with the only other 'spessartine-grossular' gem garnet being reported by Howie (1965). 'Spessartine-grossular' samples are also reported in the petrological literature by Shimazaki (1977) and Newberry (1983). One 'almandine-grossular' sample occurs in the data collected in this thesis with no gem equivalent reported in any of the gemological literature. 'Almandine-grossular' and 'grossular-almandine' samples are reported in the petrological literature by Okay (1993), Glodney *et al*. (2005), Bryhni and Griffin (1971), Drahota *et al*. (2005), Zürcher *et al*. (2001), Shimazaki (1977), Pertoldová *et al*. (2009), Kassoli-Fournaraki (1995), Chauvet *et al*. (1992), Schmädicke and Will (2003), and Operta *et al*. (2011). These samples with chemistries that fall between the ugrandite and pyralspite species implies the need for a reevaluation of the separation of gem garnets into the two species. The existence of the gem garnets with end-member components from both species suggests a continuum between the two.

Past gem classification schemes are too rigid as the chemical variability is much larger than previously assumed. Based on mineral chemistry alone, some schemes need to

© University of Pretoria

be reworked. An amended classification scheme is provided in section 5.10.2., which is based primarily on chemistry, followed by RI, magnetic susceptibility and colour.

However, because chemical analysis is not usually available to every gemological laboratory, RI, magnetic susceptibility and colour must be used together when classifying gem garnets. These characteristics can be used to distinguish between the ugrandite and pyralspite species. The use of RI alone cannot be applied to the pyralspite species, rather, the use of RI in conjunction with magnetic susceptibility and colour can be used to determine the solid solution series to which the stone belongs. However, these physical characteristics can be misleading with stones having unique characteristics that do not correlate with traditional ranges.

The terms ‘rhodolite’, ‘Malaia’ and ‘Malaya’ should be discarded because these terms are not justifiable as these stones do not show distinctive chemistries to warrant a specific name. ‘Malaia’ and ‘Malaya’ stones should be renamed ‘a garnet from the pyrope-spessartine solid solution series’. ‘Rhodolite’ stones should be renamed ‘a garnet from the pyrope-almandine solid solution series’. The terms ‘tsavorite’, ‘hessonite’, ‘demantoid’ and ‘Mali’ garnets should remain because these stones have distinctive chemistries and physical characteristics that do not overlap with each other.

Colour change should only be applied to gem garnets that display a distinct change in colour between daylight and incandescent light. The abbreviation ‘CC’ should be included in the name of the gem garnet and should be placed in front of the garnet name, e.g. CC Mali garnet or CC pyrope-spessartine. The term ‘colour shift’ should be applied to stones that display a slight shift in colour between daylight and incandescent light, and does not need to be included in the name of the gem garnet.

7. Acknowledgements

The financial assistance of the National Research Foundation (NRF) towards this research is hereby acknowledged. Opinions expressed and conclusions arrived at, are those of the author and are not necessarily to be attributed to the NRF. I would like to thank Prof. Roland K.W. Merkle for supervising my thesis. My thanks also go to Jaco Le Roux from UstechThermo XRF and Ingo Steinhage from United Spectrometer Technologies for the use of the ThermoScientific Niton FXL. Furthermore, I would also like to thank my parents and sister for all their support.

© University of Pretoria

8. References

Adamo, I., Bocchio, R., Diella, V., Pavese, A., Vignola, P., Prosperi, L. and Palanza, V., 2009. Demantoid from Val Malenco, Italy: review and update. *Gems & Gemology,* 45(4), pp. 280-287.

Adamo, I., Diella, V. and Pezzotta, F., 2012. Tsavorite and other grossulars from Itrafo, Madagascar. *Gems & Gemology,* 48(3), pp. 178-187.

Adamo, I., Gataa, G. D., Rotiroti, N., Diella, V. and Pavese, A., 2011. Green andradite stones: gemmological and mineralogical characterisation. *European Journal of Mineralogy,* 23(1), pp. 91-100.

Anderson, B. W., 1976. *Gemstones for every man.* London: Faber and Faber Limited, pp. 182-194.

Anderson, B. W., 1980. *Gem testing.* 9th ed. London: Butterworth, p. 434.

Armbruster, T., Libowitzky, E., Friedrich, A., Miletich, A., Kunz, M., Medenbach, O. and Gutzmer, J., 2001. Structure, compressibility, hydrogen bonding, and dehydrationof the tetragonal Mn3+ hydrogarnet, henritermierite. *American Mineralogist,* 86(1), pp. 147-158.

Berg, R. B. and Cooney, C. F., 2006. Geology of gem deposits: the importance of surface features and adhering material in deciphering the geologic history of alluvial sapphires - an example from Western Montana. *Gems & Gemology,* 47, p. 145.

Bocchio, R., Adamo, I. and Diella, V., 2010. The profile of trace elements, including the REE in gem-quality green andradite from classic localities. *The Canadian Mineralogist,* 48(5), pp. 1205-1206.

Bryhni, I. and Griffin, W. L., 1971. Zoning in eclogite garnets from Nordfjord, West Norway. *Contributions to Mineralogy and Petrology,* 32(2), pp. 112-125.

Carstens, H., 1973. The red-green change in chromium-bearing garnets. *Contributions to Mineralogy and Petrology,* 41(3), pp. 273-273.

Carswell, D. A. and Dawson, J. B., 1970. Garnet peridotite xenoliths in South African kimberlite pipes and their petrogenesis. *Contributions to Mineralogy and Petrology,* 25(3), pp. 163-184.

Chakhmourakian, A. R. and McCammon, C. A., 2005. Schorlomite: a discussion of the crystal chemistry, formula, and inter-species boundaries. *Physics and Chemistry of Minerals,* 32(4), pp. 277-289.

Chauvet, A., Kienast, J. R., Pinardon, J. L. and Brunel, M., 1992. Petrological contraints and PT path of Devonian collapse tectonics within the Scandian mountain belt (Western Gneiss Region, Norway). *Journal of the Geological Society,* 149(3), pp. 383-400.

Crowningshield, R., 1970. A rare alexandrite garnet from Tanzania. *Gems & Gemology,* 13, pp. 174-177.

© University of Pretoria

Deer, W. A., Howie, R. A. and Zussman, J., 1982. *Rock-forming minerals: orthosilicates, Volume 1A.* 2nd ed. New York: Halsted Press, a Divisoin of John Wiley & Sons Inc, pp. 468-701.

Dirlam, D. M., Misiorowski, E. B., Tozer, R., Stark, K. B. and Bassett, A. M., 1992. Gem wealth of Tanzania. *Gems & Gemology,* 28(2), pp. 80-102.

Drahota, P., Pertold, Z. and Pudilova, M., 2005. Three types of skarn in the northern part of the Moldanubian Zone, Bohemian massif - implications for their origin. *Journal of the Czech Geological Society,* 50(1-2), pp. 19-33.

eBay, 2015. *eBay.* [Online]
Available at: http://www.ebay.com/
[Accessed 18 November 2014].

Feneyrol, J., Giuliani, G., Ohnenstetter, D., Fallick, A. E., Martelat, J. E., Monie, P., Dubessy, J., Rollion-Bard, C., Goff, E. L., Malisa, E., Rakotondrazafy, A. F. M., Pardieu, V., Kahn, T., Ichang, D., Venance, E., Voarintsoa, N. R., Ranatsenho, M. M, 2013. New aspects and perspectives on tsavorite deposits. *Ore Geology Reviews,* 53, pp. 1-25.

Feneyrol, J., Giuliani, G., Ohnenstetter, D., Goff, E. L., Malisa, E. P. J., Saul, M., Saul, E., Saul, J. and Pardieu, V., 2010. Lithostratigraphic and structural controls of 'tsavorite' deposits at Lemshuku, Merelani area, Tanzania. *Competus Rendus Geoscience,* 342(10), pp. 778-785.

Ford, W. E., 1915. A study of the relations existing between the chemiscal, optical and other physical properties of the members of the garnet group. *The American Journal of Science,* 235, pp. 33-49.

Fuertes-Fuente, M., Martin-Izard, A., Maldonado, C. and Varela, A., 2000. Preliminary minerlogical and petrological study of the Ortosa Au-Bi-Te ore deposit: a reduced gold skarn in the northern part of the Rio Narcea Gold Belt, Asturias, Spain. *Journal of Geochemical Exploration,* 71(2), pp. 177-190.

Gemstone Magnetism, 2014. *Megnetism in gemstones, an effective tool and method for gem identification.* [Online]
Available at: http://www.gemstonemagnetism.com/
[Accessed 15 July 2014].

Gemval, 2015. *Garnet Malaia: average retail prices, May 2015.* [Online]
Available at: http://www.gemval.com/chart.php?type=29
[Accessed 13 May 2015].

Gemval, 2015. *Rhodolite Garnet (Pyrope-Almandine): average retail prices, May 2015.* [Online]
Available at: http://www.gemval.com/chart.php?type=32
[Accessed 13 May 2015].

Georoc, 2015. *Geochemistry of Rocks of the Oceans and Continents.* [Online]
Available at: http://georoc.mpch-mainz.gwdg.de/georoc/
[Accessed 28 October 2014].

© University of Pretoria

Ghosh, B. and Marishita, T., 2011. Andradite-uvarovite solid solution from hydrothermally altered podiform chromitite, Rutland ophiolite, Andaman, India. *The Canadian Mineralogist,* 49(2), pp. 573-580.

Glodny, J., Ring, U., Kühn, A., Gleissner, P. and Franz, G., 2005. Crystallization and very rapid exhumation of the youngest Alpine eclogites (Tauern Window, Eastern Alps) from Rb/Sr mineral assemblage analysis. *Contributions to Mineralogy and Petrology,* 149(6), pp. 699-712.

Grew, E. S., Locock, A. J., Mills, S. J., Galuskina, I. O., Galuskin, E. V. and Hålenius, U., 2013. Nomenclature of the garnet supergroup. *American Mineralogist,* 98(4), pp. 785-811.

Guastoni, A., Pezzotta, F., Superchi, M. and Demartin, F., 2001. Pyrope from the Dora Maira Massif, Italy. *Gems & Gemology,* 37(3), pp. 198-204.

Gübelin, E. and Schmetzer, K., 1982. Gemstones with alexandrite effect. *Gems & Gemology,* 18(4), pp. 197-203.

Gumpesberger, S., 2006. Magnetic seperation of gemstones. *Gems & Gemology,* 42(3), p. 124.

Habaak, G. H. E., 2004. Pan-African skarn deposits related to banded iron formation, Um Nar area, central Eastern Desert, Egypt. *Journal of African Earth Sciences,* 38(2), pp. 199-221.

Hanneman, W., 2000. *Naming gem garnets.* Ph.D. Thesis. Hanneman Gemological Instruments: Castro Valley, California.

Haralyi, N. L. E., 1993. *Practical methodology for the measurement of the magnetic properties of gemstones.* Paris, 24th International Gemmological Conference, pp. 91-95.

Hariya, Y. and Kimura, M., 1978. Optical anomaly garnet and its stability field at high pressures and temperatures. *Journal of the Faculty of Science, Hokkaido University,* 18(4), pp. 611-624.

Hidden, W. E. and Pratt, J. H., 1898. On Rhodolite, a new variety of garnet. *American Journal of Science,* Volume 28, pp. 294-296.

Hoover, D. B. and Williams, B., 2007. Magnetic susceptibility for gemstone discrimination. *Australian Gemmologist,* Volume 23, pp. 146-159.

Hoover, D. B., Williams, B., Williams, C. and Mitchell, C., 2008. Magnetic susceptibility, a better approach to defining garnets. *Journal of Gemmology,* Volume 31, pp. 91-103.

Hoover, D. B., 2011. Determining garnet composition from magnetic susceptibility and other properties. *Gems & Gemology,* 47(4), pp. 272-285.

Howard, J. W., 1933. Garnets. *Journal of Chemical Education,* 10, pp. 713-716.

Howie, R. A., 1965. Bustamite, rhodonite, spessartine, and tephroite from Medon, Okehampton, Devonshire. *Mineralogical Magazine,* 34, pp. 249-255.

© University of Pretoria

Jan, M. Q., Malik, R. H. and Ahmad, K. S., 1995. Gem garnet in pegmatites from Neelum valley, Azad Kashmir. *Journal of Himalayan Earth Sciences,* 28, pp. 9-14.

Jobbin, E. A., Saul, J. M., Treshman, A. E. and Young, B. R., 1975. Blue colour-change gem garnet from East Africa. *Journal of Gemmology,* 14, pp. 201-208.

Johnson, M. L., Boehm, E., Krupp, H., Zang, J. W. and Kammerling, R. C., 1995. Gem-quality grossular-andradite: a new garnet from Mali. *Gems & Gemology,* 31(3), pp. 152-166.

Kane, R. E., Kampf, A. R. and Krupp, H., 1990. Well-formed tsavorite gem crystals from Tanzania. *Gems & Gemology,* 26(2), pp. 142-148.

Kassoli-Fournaraki, A., 1995. Mineralogy and metamorphic conditions of a garnetiferous lens from the eastern Chalkidiki Peninsula, Northern Greece. *Estudios Geológicos,* 51(3-4), pp. 87-94.

Keller, P. C. and Fuquan, W., 1986. A survey of the gemstone resources in China. *Gems & Gemology,* 22(1), pp. 3-13.

Koivula, J. I. and Fryer, C. W., 1984. Identifying gem-quality synthetic diamonds: and update. *Gems & Gemology,* 20(3), pp. 146-158.

Koller, F., Niedermayr, G., Pintér, Z. and Szabó, C., 2012. The demantoid garnets of the Green Dragon mine (Tubussi, Erongo region, Namibia). *Acta Mineralogica-Petrographica, Abstract Series, University of Szeged,* 7, p. 72.

Krishnan, K. S. and Mookherji, A., 1936. The magnetic anisotropy of copper sulphate pentahydrate, CuSO4.5H2O, in relation to its crystal structure. Part I. *Physical Review,* 50(9), p. 860.

Krzemnicki, M. S., Hanni, H. A. and Reusser, E. , 2001. Colour-change garnets from Madagascar: comparison of colorimetric with chemical data. *Journal of Gemmology,* 27(7), pp. 395-408.

Krzemnicki, M. S., 1999. Diopside needles as inclusions in demantoid garnet from Russia: a Raman microspectrometric study. *Gems & Gemology,* 35(4), pp. 192-195.

Laurs, B. M. and Knox, K., 2001. Spessartine garnet from Ramona, San Diego County, California. *Gems & Gemology,* 37(4), pp. 278-25.

Lee, D. E., Coleman, R. G. and Erd, R. C., 1963. Garnet types from the Cazadero area, California. *Journal of Petrology,* 4(3), pp. 460-492.

Lingang, X., Jingwen, M., Fuquan, Y., Hennig, D. and Jianmin, Z., 2010. Geology, geochemistry and age constraints on the Mengku skarn iron deposit in Xinjiang Altai, NW China. *Journal of Asian Earth Sciences,* 39(5), pp. 423-440.

Locock, A. J., 2008. An Excel spreadsheet to recast analyses of garnet into end-member components, and a synopsis of the crystal chemistry of natural silicate garnets. *Computers & Geosciences,* 34(12), pp. 1769-1780.

© University of Pretoria

Lu, H., Liu, Y., Wang, C., Xu, Y. and Li, H., 2003. Mineralization and fluid inclusion study of the Shizhuyuan W-Sn-Bi-Mo-F skarn deposit, Hunan province, China. *Economic Geology,* 98(5), pp. 955-974.

Manson, D. V. and Stockton, C. M., 1981. Gem garnets in the red-to-violet color range. *Gems & Gemology,* 17(4), pp. 191-204.

Manson, D. V. and Stockton, C. M., 1982. Gem-quality grossular garnets. *Gems & Gemology,* 18(4), pp. 204-213.

Manson, D. V. and Stockton, C. M., 1984. Pyrope-spessartine garnets with unusual color behavior. *Gems & Gemology,* 20(4), pp. 200-207.

Maps of World, 2012. *World garnet producing countries.* [Online]
Available at: http://www.mapsofworld.com/minerals/world-garnet-producers.html#
[Accessed 16 September 2015].

Martin, B. F., 1970. A study of rhodolite garnet. *Journal of Gemmology,* 12, pp. 29-36.

Mathavan, V., Kalubandara, S. T. and Fernando, G. W. A. R., 2000. Occurrences of two new types of gem deposits in Okkampitiya gem field in Sri Lanka. *Journal of Gemmology,* 27 (2), pp. 65-72.

Muhling, J. R. and Griffin, B. J., 1991. On recasting garnet analyses into end-member molecules - revisited. *Computers & Geosciences,* 17(1), pp. 161-170.

Muije, P., Muije, C. and Muije, L. E., 1979. Colorless and green grossularite from Tanzania. *Gems & Gemology,* Volume 16, pp. 162-173.

Newberry, R. J., 1983. The formation of subcalcic garnet in scheelite-bearing skarns. *The Canadian Mineralogist,* 21, pp. 529-544.

Okay, A. I., 1993. Petrology of a diamond and coesite-bearing metamorphic terrain: Dabie Shan, China. *European Journal of Mineralogy,* 5, pp. 659-675.

Olson, D. W., 2015. *United States Geological Survey, garnet statistics and information.* [Online]
Available at: http://minerals.usgs.gov/minerals/pubs/commodity/garnet/garnemyb03.pdf
[Accessed 16 September 2015].

Operta, M., Hyseni, S., Balen, D., Salihović, S. and Durmishaj, B., 2011. Garnet group minerals from the amphibolite facies metamorphic rocks of Krivaja-Konjuh ultramafic massif in Bosnia and Herzegovina. *ARPN Journal of Engineering and Applied Sciences,* 6(7), pp. 20-28.

Payne, T., 1981. The andradites of San Benito County, California. *Gems & Gemology,* 17(3), pp. 157-160.

Pertoldová, J., Týcová, P., Verner, K., Košuličová, M., Pertold, Z., Košler, J., Konopásek, J. and Pudilová, M., 2009. Metamorphic history of skarns, origin of their protolith and implications for genetic interpretation; an example from three units of the Bohemian Massif. *Journal of Geosciences,* 54(2), pp. 101-134.

© University of Pretoria

Pezzotta, F., Adamo, I. and Diella, V., 2011. Demantoid and topazolite from Antetezambato, northern Madagascar: review and new data. *Gems & Gemology,* 47(1), pp. 2-14.

Phillips, W. R. and Talantsev, A. S., 1996. Russian demantoid, Czar of the garnet family. *Gems & Gemology,* 32(2), pp. 100-111.

Pratt, J. H., 1933. Gems and gem minerals of North Carolina. *American Mineralogist,* 18(4), pp. 148-159.

Proenza, J., 1999. Uvarovite in podiform chromitite: the Moa-Baracoa ophiolitic massif, Cuba. *The Canadian Mineralogist,* 37, pp. 679-690.

Rickwood, P. C., 1968. On recasting analyses into end-member molecules. *Contributions to Mineralogy and Petrology,* 18(2), pp. 175-198.

Schlüter, J. and Weitschat, W., 1991. Bohemian garnet - today. *Gems & Gemology,* 27(3), pp. 158-173.

Schmädicke, E. and Will, T. M., 2003. Pressure-temperature evolution of the blueschist facies rocks from Sifnos, Greece, and implications for the exhumation of high-pressure rocks in the Central Aegean. *Journal of Metamorphic Geology,* 21(8), pp. 799-811.

Schmetzer, K. and Bernhardt, H. , 1999. Garnets from Madagascar with a colour change of blue-green to purple. *Gems & Gemology,* 35(4), pp. 196-201.

Schmetzer, K. and Ottemann, J., 1979. Crystal chemistry and colour vanadium-containing garnets. *Journal of Mineralogy and Geochemistry,* 136(2), pp. 146-168.

Schmetzer, K., Bernhardt, H., Bosshart, G. and Hainschwang, T., 2009. Colour-change garnets from Madagascar: variation of chemical, spectroscopic and colorimetric properties. *Journal of Gemmology,* 31(5), pp. 235-282.

Schmetzer, K., Hainschwang, T., Bernhardt, H. and Kiefert, L., 2002. New chromium-and-vandium-bearing garnets from Tranoroa, Madagascar. *Gems & Gemology,* 38(1), pp. 148-155.

Schmetzer, K., Hainschwang, T., Kiefert, L. and Bernhardt, H., 2001. Pink to pinkish orange Malaya garnets from Bekily, Madagascar. *Gems & Gemology,* 37(4), pp. 296-308.

Seifert, A. V. and Hyrsl, J., 1999. Sapphire and garnet from Kalalani, Tanga province, Tanzania. *Gems & Gemology,* 35(2), pp. 108-120.

Serov, R., Shelementiev, Y. and Mashkina, A., 2011. *Identification of the garnet chemical composition and color causes by express Raman and visible spectroscopy,* Moscow: Gemological Center, Moscow State University.

Shigley, J. E., Dirlam, D. M., Laurs, B. M., Boehm, E. W., Bosshart, G. and Larson, W. F., 2000. Gem localities of the 1990s. *Gems & Gemology,* 36(4), pp. 292-335.

Shigley, J. E., Laurs, B. M., Janse, A. J. A., Elen, S. and Dirlam, D. M., 2010. Gem localities of the 2000s. *Gems & Gemology,* 46(3), pp. 188-216.

© University of Pretoria

Shimazaki, H., 1977. Grossular-spessartine-almandine garnets from some Japanese scheelite skarns. *The Canadian Mineralogist,* 15, pp. 74-80.

Somarin, A. K., 2004. Garnet composition as an indicator of Cu mineralization: evidence from skarn deposits of NW Iran. *Journal of Geochemical Exploration,* 81(1), pp. 47-57.

Somarin, A. K., 2010. Garnetization as a ground preparation process for copper mineralization: evidence from the Mazraeh skarn deposit, Iran. *International Journal of Earth Sciences,* 99(2), pp. 343-356.

Stockton, C. M. and Manson, D. V., 1985. A proposed new classification for gem-quality garnets. *Gems & Gemology,* 21(4), pp. 205-218.

Stockton, C. M. and Manson, D. V., 1983. Gem andradite garnets. *Gems & Gemology,* 19(4), pp. 202-208.

Stockton, C. M., 1988. Pastel pyropes. *Gems & Gemology,* 24(2), pp. 104-106.

Suwa, K., Suzuki, K. and Agata, T., 1996. Vanadium grossular from the Mozambique metamorphic rocks, south Kenya. *Journal of Southeast Asian Earth Sciences,* 14(3), pp. 299-308.

Switzer, G. S., 1974. Composition of green garnet from Tanzania and Kenya. *Gems & Gemology,* 14(10), pp. 296-297.

The Open University, 2015. *The Open University.* [Online]
Available at: www.open.ac.uk/earth-research/tindle/AGTWebData/Garnet.xls
[Accessed 30 July 2013].

Thermo Scientific, 2011. *Thermo Fisher Scientific Niton Analyzers FXL Version 8.2.0.* User's Guide (Abridged), Revision A

Wan, B., Xiao, W., Zhang, L. and Han, C., 2012. Iron mineralization associated with a major strike-slip shear zone: Radiometric and oxygen isotope evidence from the Mengku deposit, NW China. *Ore Geology Reviews,* 44, pp. 136-147.

Wang, F. and Liu, Y., 1993. Garnets from Altay, China. *Gems & Gemology,* 29(4), pp. 273-277.

Webster, R., 1962. *Gems; their sourceso, descriptions and identification. Volume 1.* 2nd ed. London: Butterworths, pp.134-148.

Wilson, B. S., 2009. Coloured gemstones from Canada. *Rocks & Minerals,* 85(1), pp. 24-43.

Xu, G. and Lin, X., 2000. Geology and geochemistry of the Changlongshan skarn iron deposit, Anhui Province, China. *Ore Geology Reviews,* 16(1), pp. 91-106.

Zenk, M. and Schulz, B., 2004. Zoned Ca-amphiboles and related P-T evolution in metabasites from classical Barrovian metamorphic zones in Scotland. *Mineralogical Magazine,* 68(5), pp. 769-786.

© University of Pretoria

Zhang, L., Sun, M. and Xu, B., 2001. Phase relations in garnet-bearing metabasites of prehnite-pumpellyite facies from the Darbut-Sartuohai ophiolite, Western Junggar of Xinjiang, China. *Mineralogy and Petrology,* 71(1-2), pp. 67-85.

Zürcher, L., Ruiz, J. and Barton, M. D., 2001. Paragenesis, elemental distribution, and stable isotopes at the Peña Colorada iron skarn, Colima, Mexico. *Economic Geology,* 96(3), pp. 535-557.

Zwaan, P. C., 1974. Garnet, corundum and other gem minerals from Umba, Tanzania. *Scripta Geologica,* 20, pp. 1-41.

Zwaan, P. C., 1982. Sri Lanka: the gem island. *Gems & Gemology,* 18, pp. 62-71.

9. Appendix

9.1. Magnetic susceptibility

Hoover and Williams (2007), and Hoover *et al.*'s (2008) method was used in this thesis to measure magnetic susceptibility. This involves the use of a digital scale to weigh the cut gemstones; a rare earth element magnet; and a device to lift the gemstone slowly towards the magnet to determine the force of attraction between the magnet and the sample. The device was an old microscope stand which provided the means of moving the sample closer towards the magnet. The magnet was a N52 grade neodymium-iron-boron magnet with a diameter of 2.8 cm. The magnet is rated at 54 lbs (24.494 kg). The magnet was suspended by a long thread through the hole in which the objective lens was originally placed (Figure 70b). The digital scale was then placed on the stage, whereafter the sample was then placed on the scale. The stage, with the scale and the sample placed on it, was then incrementally raised, towards the magnet and the change in weight as the sample neared the magnet was recorded. This procedure is discussed in more detail below and can also be seen in the paper by Hoover *et al*. (2008).

© University of Pretoria

Figure 70. Apparatus used to measure magnetic susceptibly. A: the apparatus used by Hoover *et al*. (2008). B: the apparatus used in this thesis.

The determination of magnetic susceptibility involved measuring the weight of the sample and the weight of the sample after the application of a magnet. The difference in weight can then be seen as the 'pull' of the gemstone.

The magnetic volume susceptibility of an unknown gemstone can be given by equation 1:

Equation 1:

$k = C \times Pull$

Where C = k (of standard)/ pull (of standard),

Pull = measured pull of the test stone,

k is expressed as SI and

Pull is expressed as carat (Hoover *et al*., 2008).

© University of Pretoria

Samples were weighed prior to the application of the magnet. A bigger magnet was used in this study as it provided a larger pull for small stones with lower magnetic susceptibilities. The scale is placed on the stage of the microscope stand. To ensure that the scale did not affect the measurements due to its inherent magnetism, a spacer was placed on the scale. The sample was placed in putty with the table of the stone faceup towards the magnet. To ensure that the table was parallel, a press was used for the stone in putty. Once this was done, the scale was turned on and tared. The stage was then incrementally raised towards the magnet and the maximum 'pull' was measured. The magnetic attraction showed as a negative reading on the scale. When the sample came in contact with the magnet, the scale reading became positive. Thus, it is the maximum negative reading that is regarded as the maximum pull. Using the Equation 1, this pull can be converted to magnetic volume susceptibility.

However, Equation 1 was modified marginally. The pull of the standard, i.e. copper sulphate, was not available in carats, but was dimensionless due to it being the gradient of the calibration curve. The gradient is the pull of copper sulphate divided by its weight. Both were measured in carats and the division resulted in a dimensionless answer. Hence, the pull of the gemstone was also divided by its weight to produce a dimensionless answer. This modification also takes into account the size of the sample, which plays a major role in determining magnetic susceptibility. Equation 1 was then altered into Equation 2.

Equation 2:

$k = C \times (Pull_g/Weight_g)$

Where $C = k_s/ [pull_s /weight_s] \rightarrow$ the gradient of the calibration curve (0.255)

Where Pull = measured pull of the samples, subscript g is that of the gemstone and subscript s that of the standard.

k is expressed as SI and Pull is expressed as carat (Hoover *et al*., 2008).

9.1.1. Calibration of magnetic pull using $CuSO_4$. $5H_2O$

A standard was also required to convert the change in weight or 'pull' to the magnetic susceptibility of the gemstone. Copper sulphate ($CuSO_4$. $5H_2O$) was chosen as the standard as it has no measurable anisotropy (Krishnan and Mookherji, 1936). The magnetic susceptibility value for copper sulphate was taken from Hoover and Williams (2007) as 170 X 10^{-6}SI. 29 copper sulphate crystals of varying sizes were grown to produce a calibration

© University of Pretoria

curve (weight of crystals versus average magnetic pull), as seen in Figure 71. Their magnetic pull was determined similarly to the procedure described above to measure magnetic susceptibility of gemstones. A linear regression line was used in the graph. The equation was y = 0.08 + 0.255x with the gradient being used in Equation 2 to calculate magnetic susceptibility.

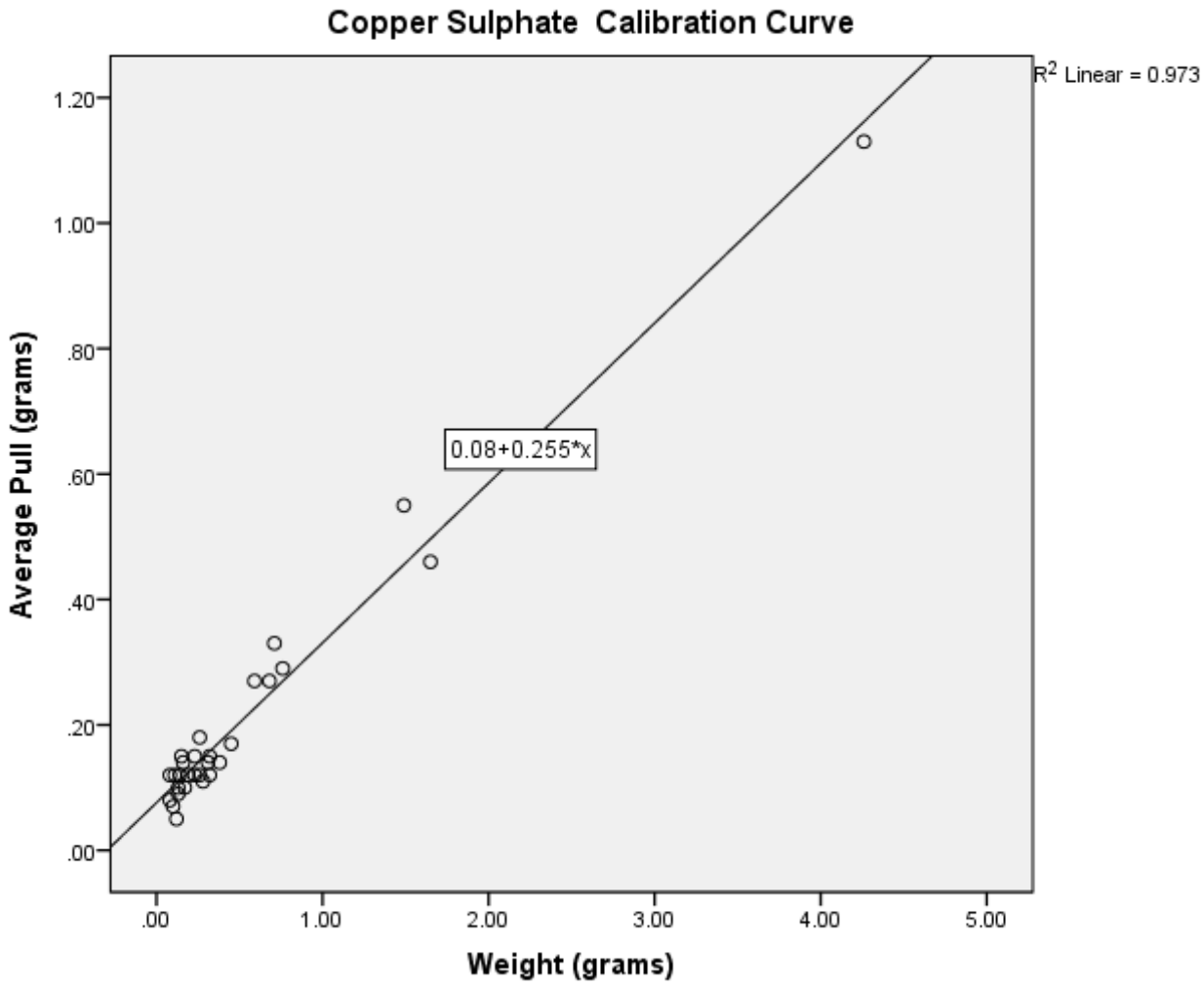

Figure 71. Copper sulphate calibration curve. The white box in the centre shows the calculation for y.

In Table 23, the repeat measurements of the 29 copper sulphate crystals are reported and a graph showing the variability of the magnetic pull of the crystals as standard deviation is plotted in Figure 72. The size of the bubble corresponds to the standard deviation.

© University of Pretoria

Table 23. Repeat measurements of copper sulphate crystals.

Copper Sulphate Crystal	Weight (grams)	Magnetic Pull 1 (grams)	Magnetic Pull 2 (grams)	Magnetic Pull 3 (grams)	Magnetic Pull 4 (grams)	Magnetic Pull 5 (grams)	Magnetic Pull 6 (grams)	Magnetic Pull 7 (grams)	Magnetic Pull 8 (grams)	Magnetic Pull 9 (grams)	Magnetic Pull 10 (grams)	Average Pull (grams)	Standard Deviation
1	0.11	0.11	0.11	0.1	0.13	0.12	0.12	0.11	0.12	0.11	0.13	0.12	0.009165
2	0.08	0.08	0.07	0.07	0.08	0.09	0.08	0.07	0.07	0.08	0.09	0.08	0.007483
3	0.12	0.05	0.04	0.04	0.05	0.04	0.06	0.05	0.05	0.04	0.04	0.05	0.006633
4	0.08	0.11	0.11	0.12	0.12	0.12	0.11	0.12	0.11	0.11	0.12	0.12	0.005
5	0.1	0.06	0.07	0.07	0.07	0.07	0.06	0.06	0.07	0.07	0.07	0.07	0.004583
6	0.13	0.09	0.1	0.08	0.1	0.1	0.1	0.09	0.1	0.1	0.09	0.10	0.006708
7	0.15	0.15	0.13	0.15	0.15	0.16	0.15	0.15	0.13	0.14	0.15	0.15	0.009165
8	0.13	0.08	0.08	0.09	0.1	0.1	0.08	0.09	0.09	0.1	0.09	0.09	0.007746
9	0.16	0.14	0.14	0.15	0.16	0.13	0.14	0.14	0.15	0.13	0.14	0.14	0.008718
10	0.23	0.13	0.15	0.15	0.16	0.14	0.16	0.15	0.13	0.15	0.15	0.15	0.01005
11	0.26	0.17	0.17	0.16	0.18	0.18	0.18	0.19	0.17	0.18	0.19	0.18	0.009
12	0.14	0.11	0.11	0.12	0.11	0.12	0.12	0.12	0.1	0.12	0.12	0.12	0.006708
13	0.17	0.1	0.09	0.08	0.09	0.1	0.11	0.11	0.1	0.1	0.09	0.10	0.009
14	0.19	0.12	0.11	0.11	0.11	0.12	0.13	0.12	0.12	0.11	0.12	0.12	0.006403
15	0.26	0.13	0.12	0.13	0.12	0.12	0.11	0.13	0.12	0.1	0.12	0.12	0.008944
16	0.31	0.14	0.14	0.16	0.16	0.14	0.13	0.14	0.13	0.13	0.14	0.14	0.01044
17	0.32	0.11	0.11	0.13	0.12	0.12	0.12	0.11	0.12	0.13	0.12	0.12	0.007
18	0.32	0.14	0.14	0.14	0.15	0.15	0.14	0.15	0.15	0.15	0.15	0.15	0.004899
19	0.23	0.11	0.11	0.13	0.12	0.12	0.11	0.12	0.13	0.13	0.12	0.12	0.007746
20	0.38	0.15	0.14	0.14	0.14	0.13	0.15	0.15	0.14	0.13	0.14	0.14	0.007
21	0.71	0.33	0.33	0.32	0.33	0.34	0.34	0.33	0.32	0.33	0.34	0.33	0.007
22	0.45	0.18	0.18	0.17	0.18	0.16	0.17	0.16	0.17	0.18	0.17	0.17	0.007483
23	0.68	0.28	0.27	0.27	0.26	0.29	0.27	0.29	0.26	0.27	0.27	0.27	0.01005
24	1.65	0.45	0.44	0.44	0.47	0.46	0.44	0.47	0.46	0.46	0.46	0.46	0.01118
25	4.26	1.12	1.11	1.11	1.13	1.14	1.13	1.13	1.14	1.13	1.12	1.13	0.010198
26	1.49	0.56	0.54	0.54	0.57	0.55	0.54	0.56	0.55	0.55	0.54	0.55	0.01
27	0.76	0.28	0.28	0.28	0.29	0.3	0.3	0.31	0.29	0.28	0.29	0.29	0.01
28	0.59	0.27	0.27	0.27	0.26	0.25	0.28	0.28	0.27	0.26	0.27	0.27	0.008718
29	0.28	0.1	0.1	0.12	0.11	0.11	0.13	0.11	0.1	0.11	0.1	0.11	0.009434

© University of Pretoria

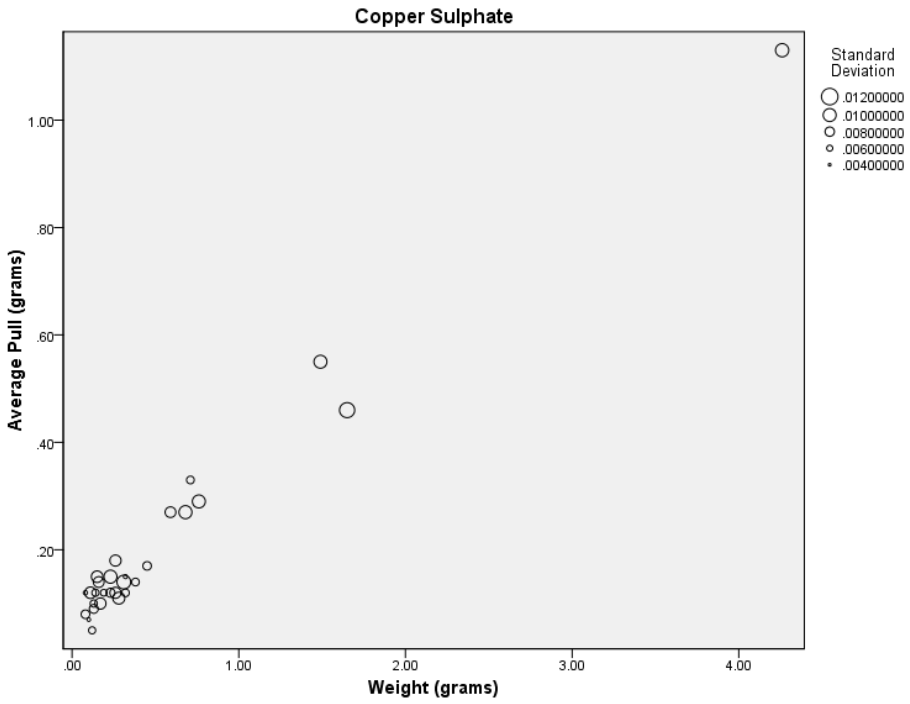

Figure 72. Average pull vs. weight of copper sulphate crystals.

9.2. Chemistry

The Thermo Scientific Niton FXL 959 FM-XRF analyser was used to chemically analyse the stones. Due to the instrument being energy dispersive, the detection limits are not very low. Different filters are available with each designed for a specific range of elements. There are four filters for main, low (V, Ti and Cr), high (Pd through Ba) and light range (Mg, Ca and K) elements. The filter for the main range is the default for the instrument and cannot be excluded. Multi-Range tests involve using more than one filter and are used to excite specific elements for increased sensitivity or to cover a wider range of elements. The Multi-Range test was used for the thesis (Thermo Scientific, 2011).

Several analysis modes are available depending on the nature of the sample. General metal mode is used for samples composed of metal alloys. Electronic metals mode analyses electronic component samples. The Precious Metals mode analyses samples composed of primary metals. The Plastics mode is used for samples composed of plastic, and the Soils mode is used for soil samples. The Mining Cu/Zn mode is used for samples with potential metal ore. The TestAll Geo mode is used for other samples that are not listed above. Initially, TestAll Geo mode was used to analyse the gems, but the results were poor and the Mining Cu/Zn mode was eventually used as this mode proved to be the most accurate out of all the other modes.

© University of Pretoria

When analysing the samples in the Mining Cu/Zn mode, the counting time is 240 s and the error for the measurement was 2.

Once the Mining Cu/Zn mode and the correct filters were chosen, the analyses of a standard were performed. The instrument reports iron as Fe^{2+} and did not report Fe^{3+}. The Fe^{2+} content reported by the instrument can be input into the calculation sequence without the Fe^{3+} content as the calculation sequence calculates the proportions of Fe^{2+} and Fe^{3+} required for charge balance in garnet. The analyses were reported as elemental concentrations and had to be converted to oxide concentrations using the conversion factors provided in the instrument's user guide.

The results from these analyses for the standard were poor with the Fe and Mn measurements showing the greatest discrepancies. This required the instrument to be recalibrated when using the Mining Cu/Zn mode. Recalibration was done using two iron ore standards and a manganese ore standard. The one iron ore standard was a Euro-standard 681.1 from Newham Hall, Middlesbrough, U.K. The other iron ore standard was part of the Canadian Certified Reference Materials Project of the Canada Centre for Mineral and Energy Technology in Ottawa, Ontario, Canada. The manganese ore no. 176/2 was from the British Chemical Standards. The compositions of the standards are summarised in the Tables 24a and 24b.

Table 24. a) Compositions of the iron ore standards from Europe and Canada.

Standard	Fe (wt. %)	Si (wt. %)	Ca (wt. %)	Mg (wt. %)	Al (wt. %)	Ti (wt. %)	Mn (wt. %)	P (wt. %)	S (wt. %)
Fe Euro	33.21	8.32	2.80	0.89	5.62	0.29	0.22	0.88	0.103
Fe Canada	60.73	3.78	0.029	0.020	0.509	0.031	0.777	0.054	0.007

Standard (cont.)	Na (wt. %)	K (wt. %)	F (wt. %)	V (wt. %)	Cr (wt. %)	Ni (wt. %)	C (wt. %)		
Fe Euro	0.068	0.49	0.19	0.077	0.041	0.016	1.80		
Fe Canada									

Tables 24. b) Compositions of manganese ore standard.

Standard	Fe (wt. %)	SiO2 (wt. %)	CaO (wt. %)	MgO (wt. %)	Al2O3 (wt. %)	TiO2 (wt. %)	Mn (wt. %)	P (wt. %)	S (wt. %)
Mn Ore	6.86	2.53	0.09	0.04	5.2	0.30	47.5	0.087	0.015

Standard	Na2O (wt. %)	K2O (wt. %)	BaO (wt. %)	As2O3 (wt. %)					
Mn Ore	0.10	1.30	0.19	0.22					

9.2.1. Recalibration

The graphs in Figures 73a, 73b, 73c and 73d were produced by plotting the percentage of each element as indicated by the standard samples against the percentage of

© University of Pretoria

each element, as reported by the instrument. The linear regression function was then used to calculate the slope and intercept for a straight line drawn through the graph of those points. The slope and intercept from these graphs were then inserted in the instrument as calibration factors for the element (Thermo Scientific, 2011).

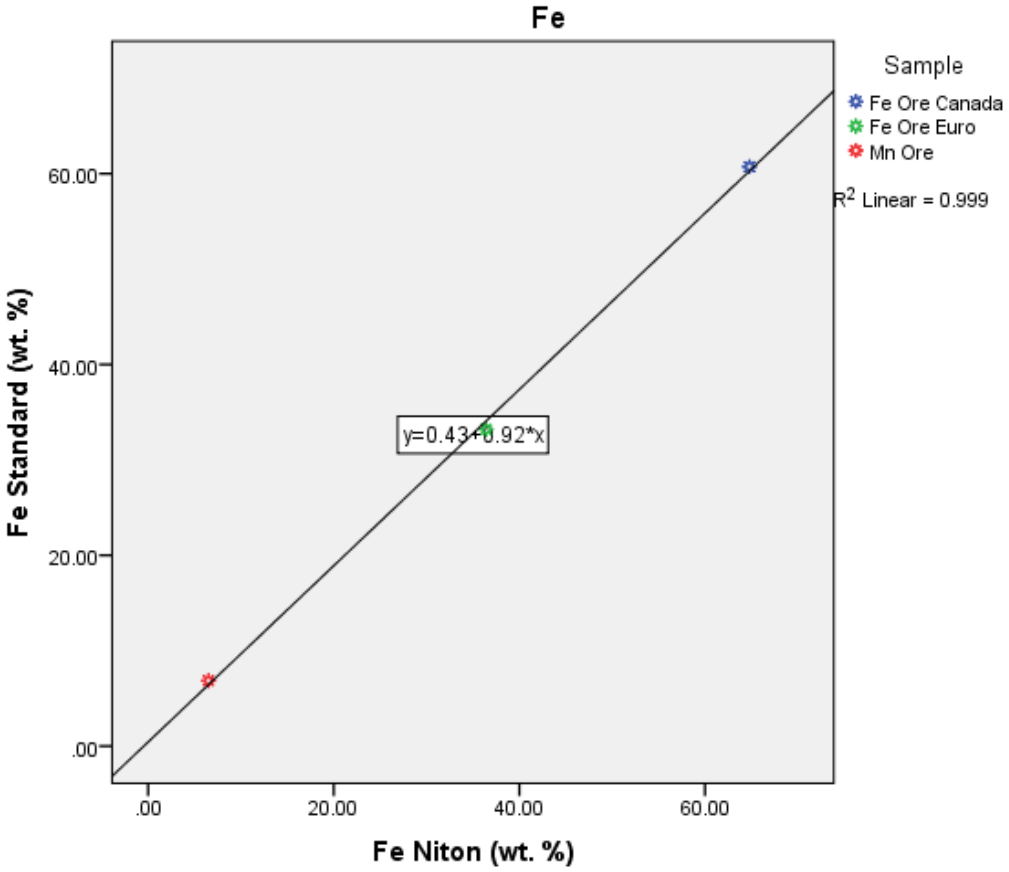

Figure 73. a) Graph on which the calibration is based.

© University of Pretoria

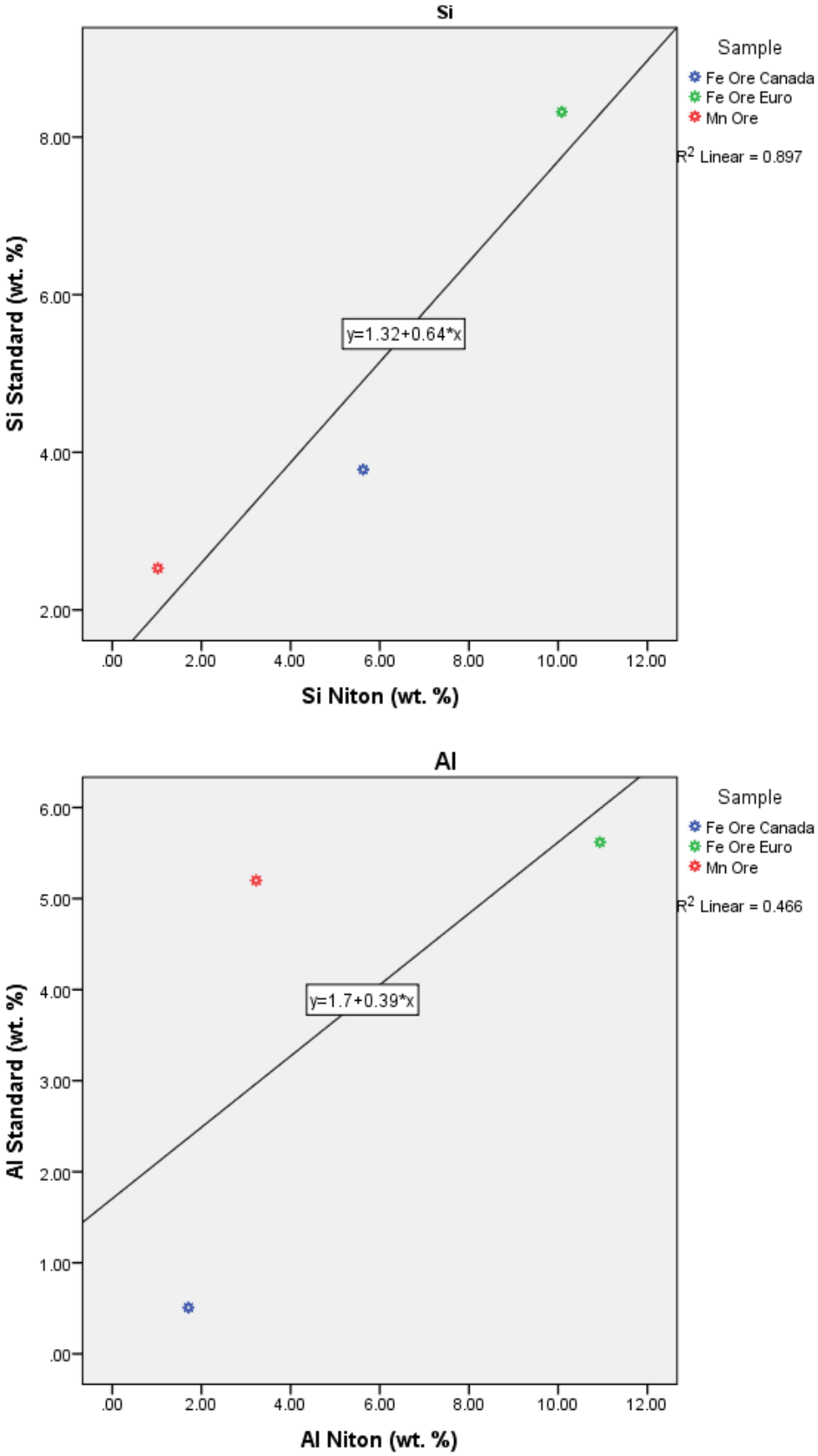

Figure 73. b) Graphs on which the calibration is based.

© University of Pretoria

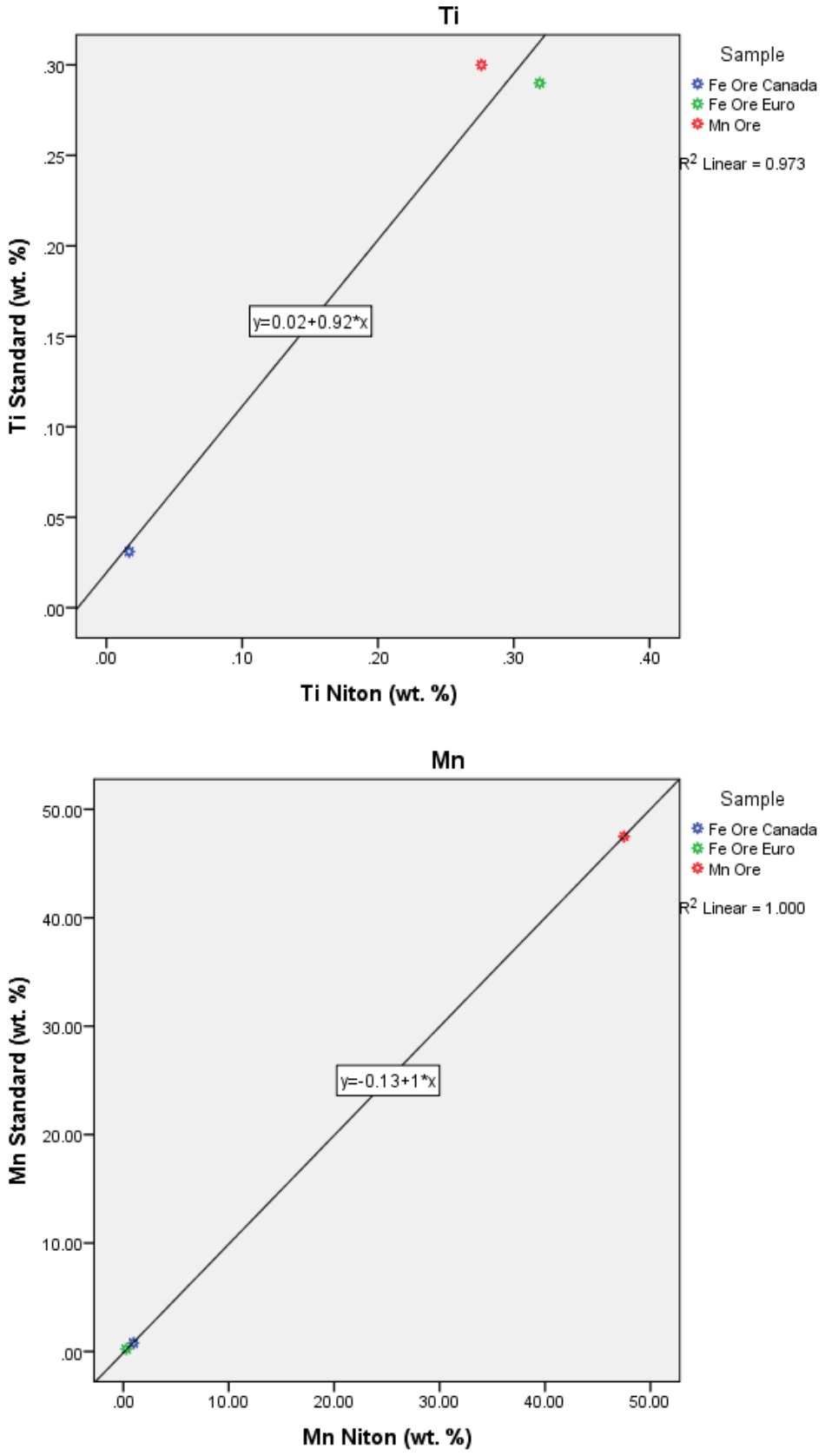

Figure 73. c) Graphs on which the calibration is based.

© University of Pretoria

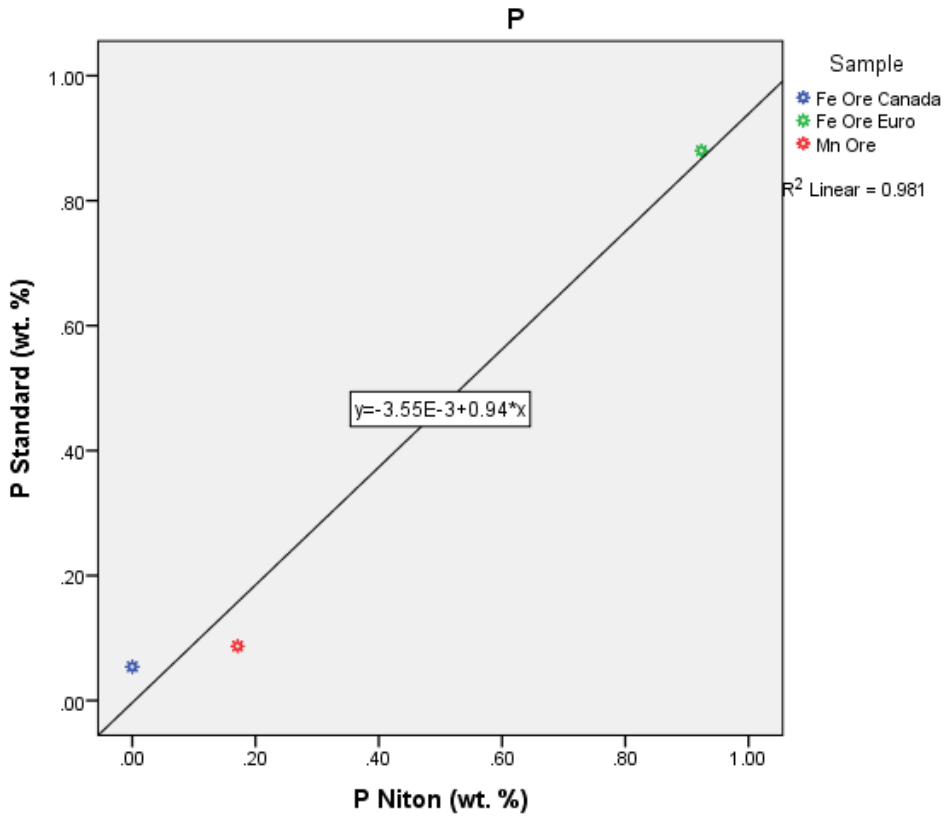

Figure 73. d) Graph on which the calibration is based.

Once the calibration was completed, the analysis of the other standards were performed to ensure that the recalibration of the instrument in the Mining Cu/Zn mode was correct. The results of these analyses produced a strong linear relationship, which was desired. The R^2 values in Figures 74 a, 74b, 74c and 74d are all close to 1 making the recalibration successful.

© University of Pretoria

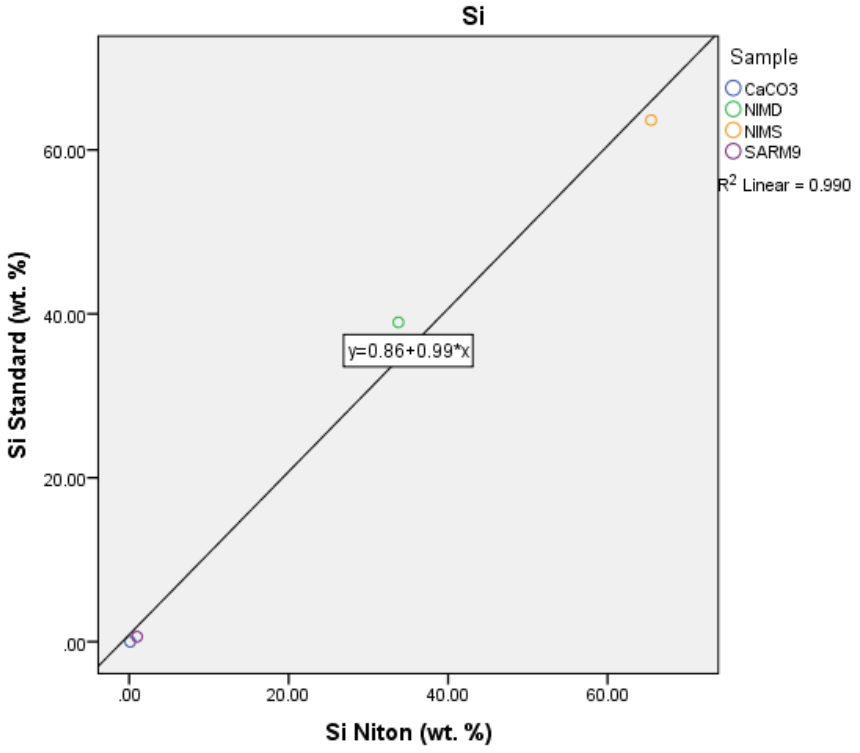

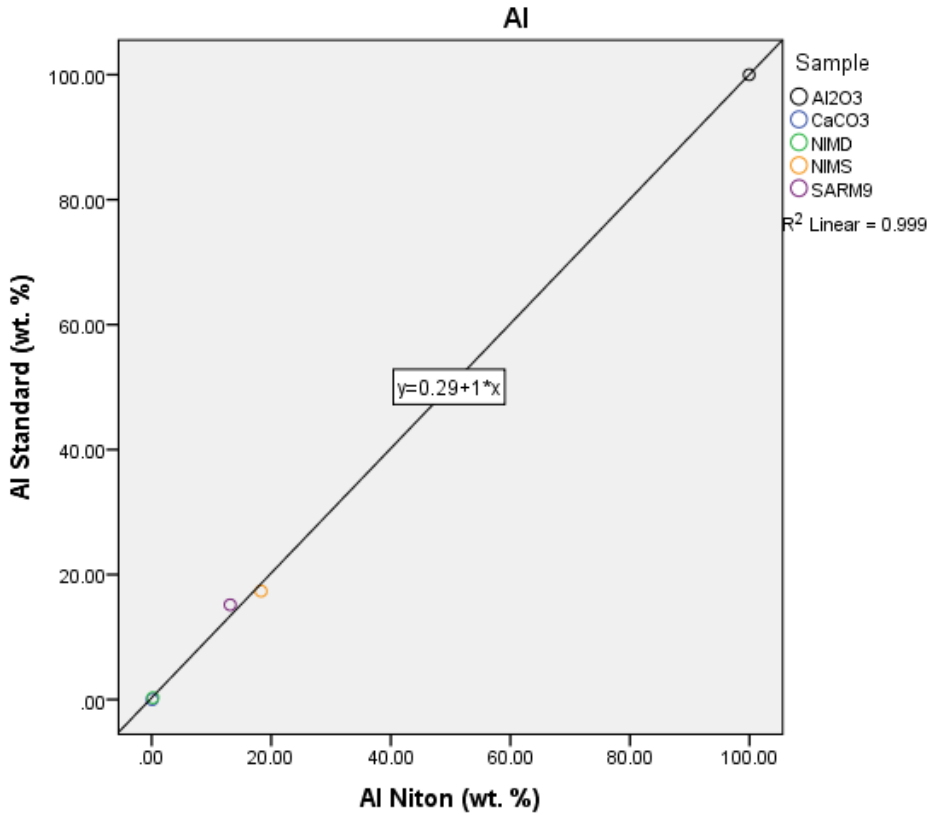

Figure 74. a) Graphs for the various standards after recalibration.

© University of Pretoria

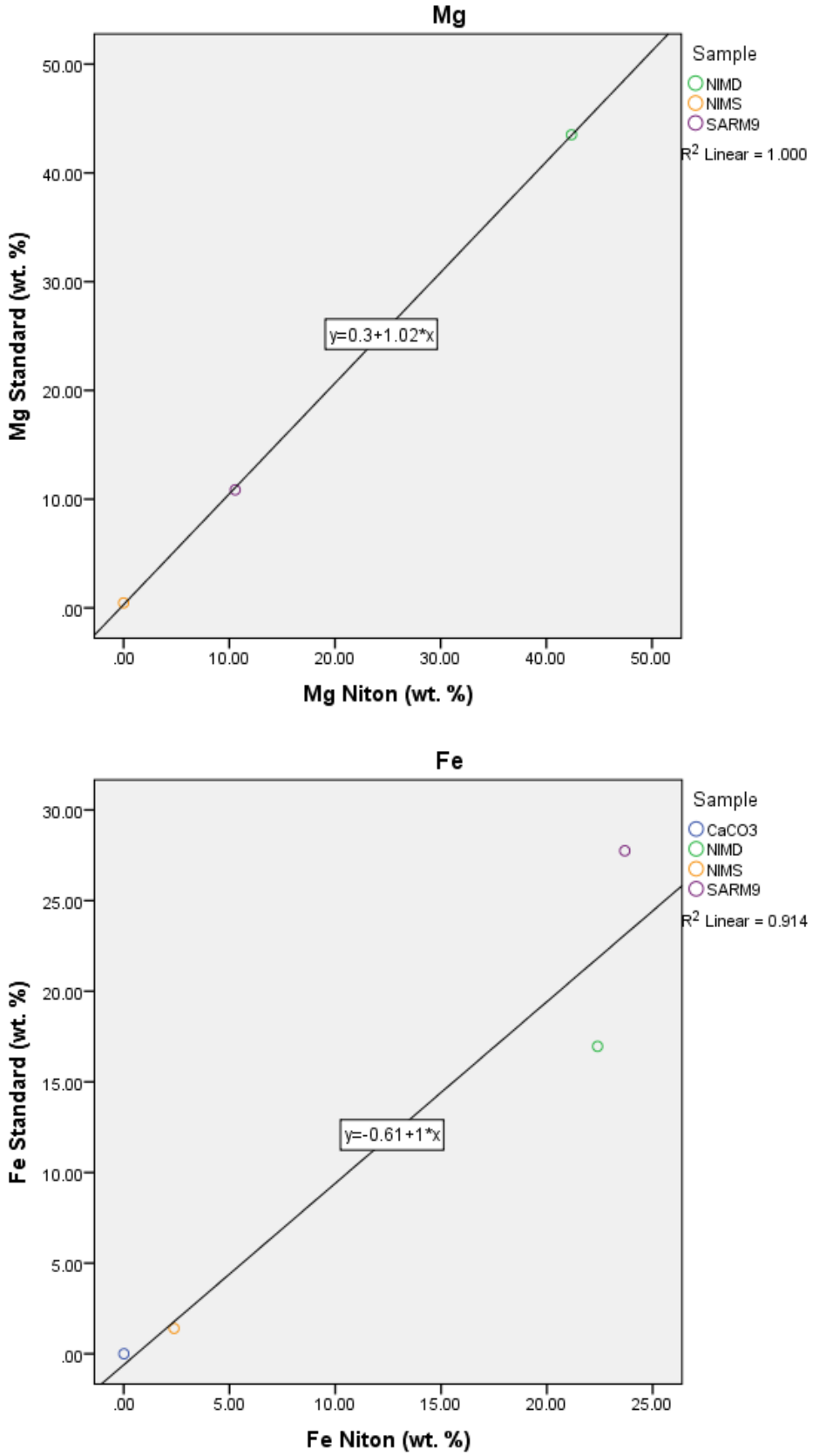

Figure 74. b) Graphs for the various standards after recalibration.

© University of Pretoria

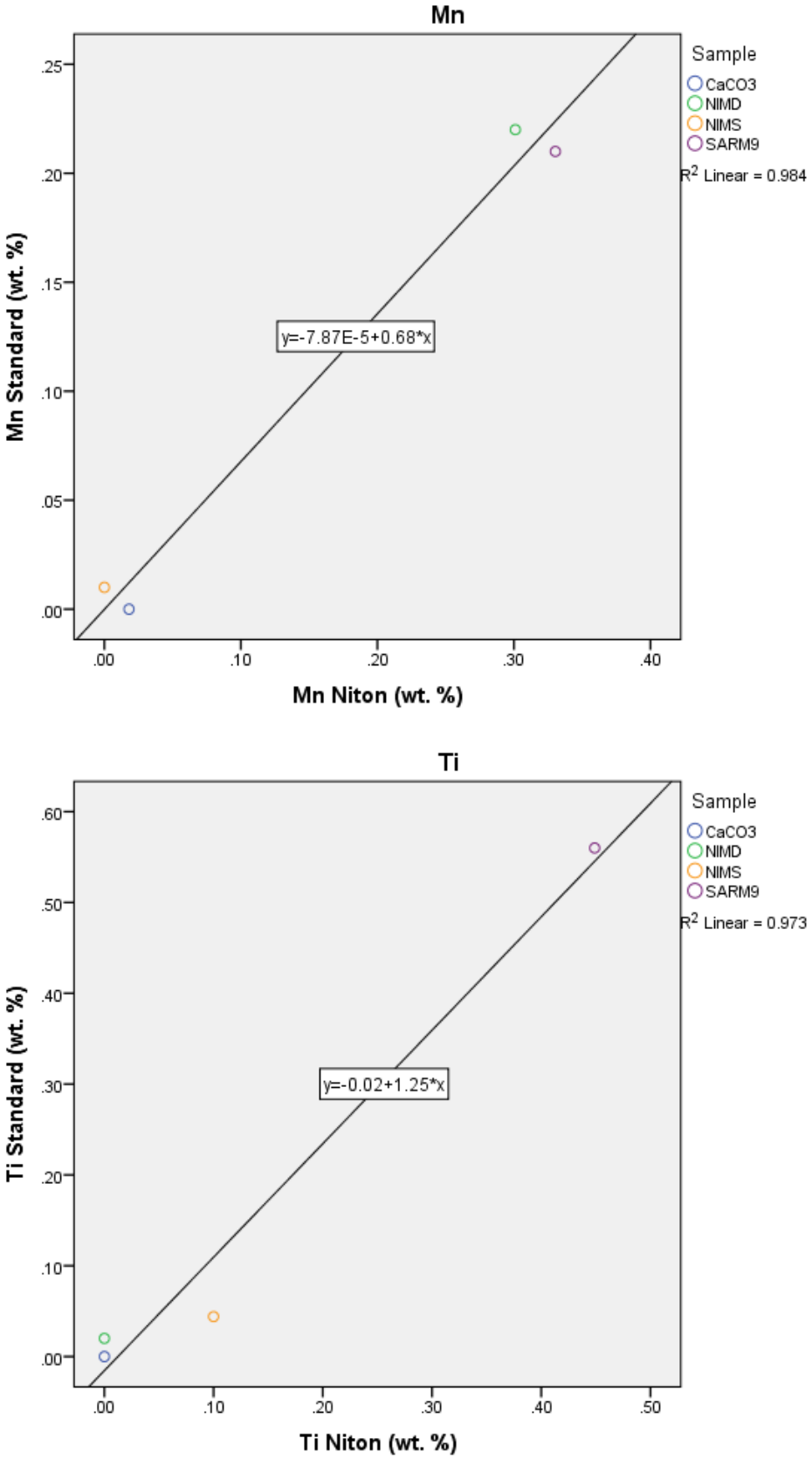

Figure 74. c) Graphs for the various standards after recalibration.

© University of Pretoria

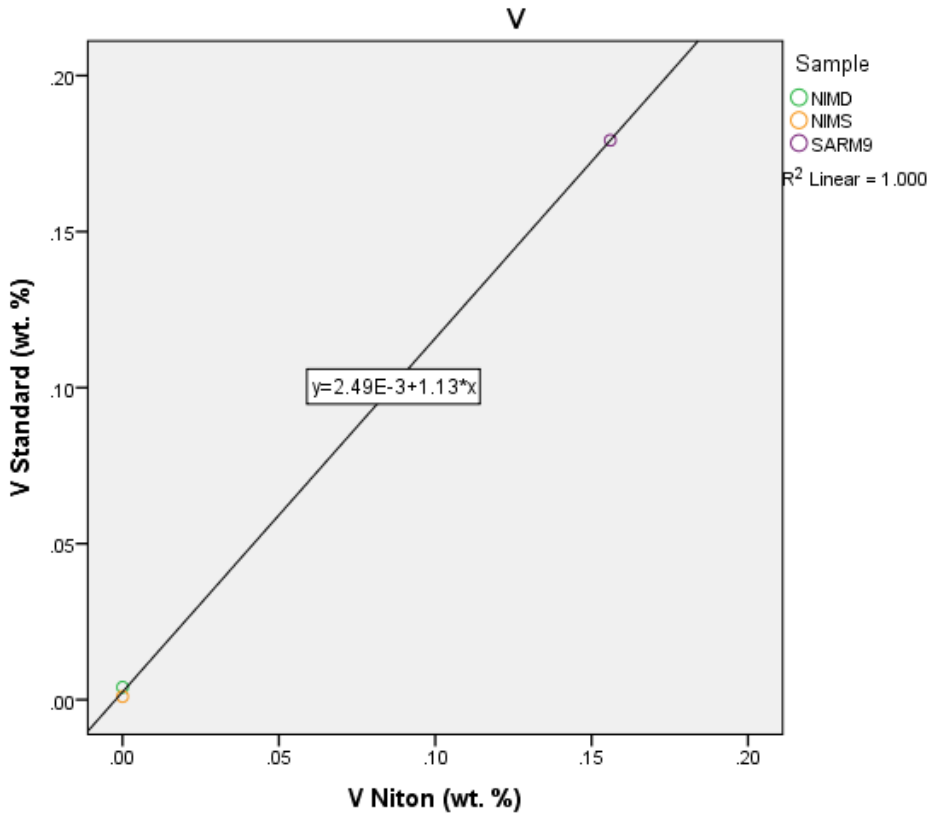

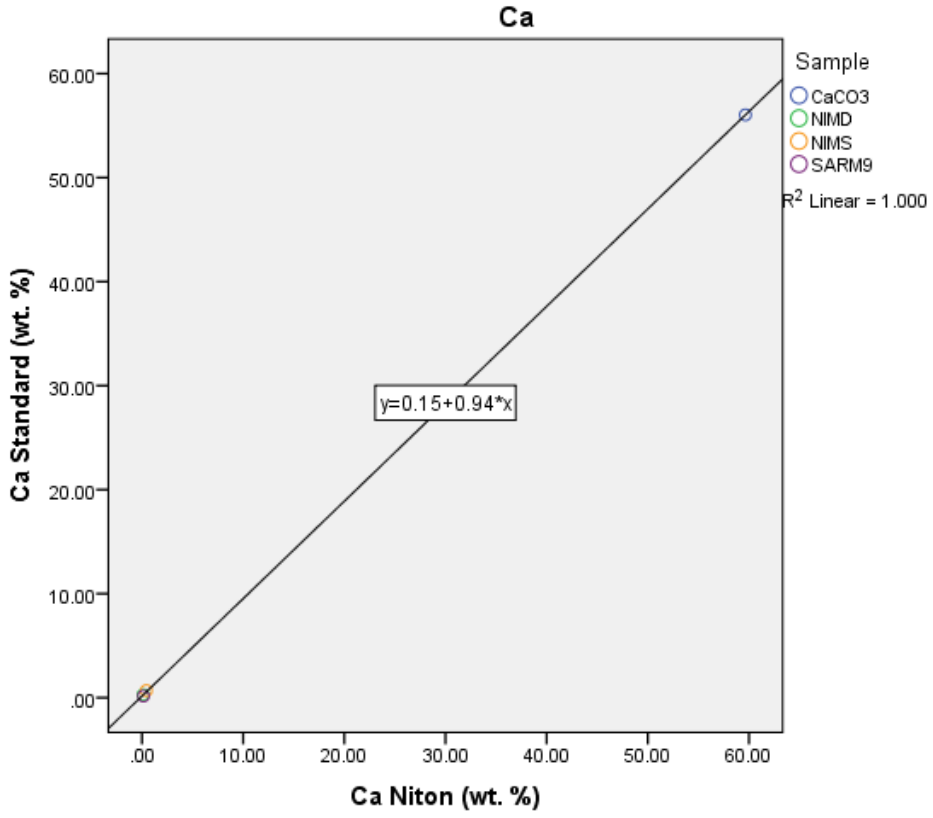

Figure 74. d) Graphs for the various standards after recalibration.

© University of Pretoria

Once the recalibration was completed, the analysis of a known garnet gemstone was carried out. The analysis was converted to oxide concentrations and the wt. % of the various elements was entered into an Excel spreadsheet from The Open University (2015). The spreadsheet calculated Fe^{2+}/Fe^{3+} assuming full site occupancy. The analysis of the garnet gemstone, when entered into the spreadsheet, proved to be a garnet.

9.2.2. Reproducibility

The next step was to test the instrument for consistency. A single garnet gemstone was analysed 11 times at different points on the sample to test whether the analysis was consistent. Little variation was observed in the multiple analyses showing that the instrument is consistent (Table 25). Table 25 is only shows the reproducibility of the instrument, and is not intended for accuracy. The few differences that can be seen could be due to heterogeneity within the sample.

Table 25. The results of the multiple analyses of a garnet gemstone at different points on the sample together with arithmetic mean and standard deviation. BDL stands for below the detection limit.

Sample	mali666702-1	mali666702-2	mal666702-3	mali666702-4	mali666702-5	mali666702-6	mali666702-7	mali666702-8	mali666702-9	mali666702-10	mali666702-11	x	σ
SiO_2 (wt. %)	39.32	39.95	40.06	39.98	39.54	40.64	40.46	40.32	40.57	40.20	40.85	40.17	0.47
Al_2O_3 (wt. %)	10.96	11.94	12.07	12.18	11.83	11.95	12.07	12.04	12.05	12.10	12.13	11.94	0.34
MgO (wt.%)	BDL	BDL	BDL	BDL	BDL	BDL	BDL	BDL	BDL	BDL	BDL		
CaO (wt.%)	42.08	41.47	41.26	41.28	41.48	41.48	41.26	40.98	41.37	41.08	41.03	41.35	0.31
FeO (wt.%)	6.57	5.58	5.53	5.57	5.84	4.89	5.32	5.63	5.10	5.67	5.07	5.52	0.45
MnO (wt.%)	0.14	0.13	0.13	0.12	0.13	0.09	0.11	0.12	0.09	0.12	0.09	0.12	0.02
Cr_2O_3 (wt.%)	BDL	BDL	BDL	BDL	BDL	BDL	BDL	BDL	BDL	BDL	BDL		
V_2O_3 (wt.%)	BDL	BDL	BDL	BDL	BDL	BDL	BDL	BDL	BDL	BDL	BDL		
TiO_2 (wt.%)	0.59	0.64	0.66	0.62	0.71	0.65	0.60	0.59	0.64	0.59	0.63	0.63	0.04
K (wt.%)	BDL	BDL	BDL	BDL	BDL	BDL	BDL	BDL	BDL	BDL	BDL		
Cl (wt.%)	0.32	0.13	0.13	0.10	0.46	0.12	0.12	0.13	0.14	0.19	0.14	0.18	0.11

9.2.3. Limitations of the XRF

There are some interferences and limitations with the XRF that had to be taken into consideration. Errors from counting statistics are the primary source of error in most analyses. Engergy dispersive detection limits are not very low, and the measurement of light elements (Z < 14) is difficult because of the attenuation of low energy x-rays. Elements lighter than the atomic number 14 (Z = 14, silicon) e.g. lithium, beryllium, boron and carbon are not detected. Also, elements lighter than the atomic number 22 (Z = 22, titanium)

© University of Pretoria

e.g.calcium, sulphur, phosphorus, silicon and aluminium are difficult to detect. The minimum detection limits are in parts per million (ppm) range.

The XRF uses a surface and near surface technique and only measures the portion of the sample in front of the windows. This limits the size of gemstones that can be reliably measured.

© University of Pretoria